THE UNIVERSITY OF OKLAHOMA

GRADUATE COLLEGE

CHARACTERIZATION OF CEMENTITIOUSLY STABILIZED SUBGRADES FOR MECHANISTIC-EMPIRICAL PAVEMENT DESIGN

A DISSERTATION

SUBMITTED TO THE GRADUATE FACULTY

in partial fulfillment of the requirements for the

Degree of

DOCTOR OF PHILOSOPHY

By

PRANSHOO SOLANKI
Norman, Oklahoma
2010

CHARACTERIZATION OF CEMENTITIOUSLY STABILIZED SUBGRADES FOR MECHANISTIC-EMPIRICAL PAVEMENT DESIGN

A DISSERTATION APPROVED FOR THE
SCHOOL OF CIVIL ENGINEERING AND ENVIRONMENTAL SCIENCE

BY

Dr. Musharraf M. Zaman, Chair

Dr. Kianoosh Hatami

Dr. Naji Khoury

Dr. Gerald A. Miller

Dr. J. –C. Roegiers

DEDICATION

To my parents and my wife

ACKNOWLEDGMENTS

At first, I want to thank God, The Almighty, for blessing me with the opportunity and ability to complete this work.

I am very happy to have this opportunity to express my deepest appreciation and gratitude from bottom of my heart to my doctoral committee chairman, Professor Musharraf M. Zaman, for his invaluable help, constant support and considerable patience throughout my doctoral studies. It was his guidance and expectations that inspired me to work harder than I thought I could. Without his help and active involvement, this work would not have been possible.

I would like to acknowledge Dr. Naji Khoury, not only for guiding me in the laboratory work, but as a valuable colleague and friend during his stay at the University of Oklahoma. I would like to express my appreciation to Dr. Jean-Claude Roegiers for his valuable comments that helped improve the quality of this work and completion of my dissertation. I would like to thank Dr. Gerald A. Miller for sharing his wealth of knowledge and experience, particularly through his coursework at the University of Oklahoma. I have tremendous respect for Dr. Miller's ability to inspire students to learn. I would also like to express my sincerest gratitude to Dr. Kianoosh Hatami for serving on my dissertation committee. I would also like to thank my committee members and faculty of geotechnical engineering for teaching me some of the basics in geotechnical and rock engineering.

I would like to thank Dr. Joakim G. Laguros for his help and technical guidance. I would also like to thank Dr. Amy Cerato for providing access to the EGME setup and to

Dr. K. K. Muraleetharan for his guidance, support and inputs on the I-35 instrumentation project. I wish to thank the staff of the Engineering Dean's office and School of Civil Engineering and Environmental Science for their help. Specifically, I am thankful to Ms. Audre Carter, Ms. Brenda Finch, Ms. Holly Chronister, Ms. Karen Horne, Ms. Karen Kelly, Ms. Katie Hargrove, Ms. Molly Smith, Ms. Shauna Singleton and Ms. Susan Williams. Also, special thanks and appreciation go to Mr. Mike Schmitz for his valuable assistance in the laboratory. Thanks are extended to Ashish, Charbel, Chunyang, Dharamveer, Diana, Karim, Kazmee, Kunal, Marc, Nur, Rajul, Rajah, Ravi, Rouzbeh, Roy, Selva, Son, Wasi and Zahid for being nice colleagues in the laboratories and offices. I also thank my other friends who helped me in numerous ways during my student life at the University of Oklahoma. I am indebted to Dr. Preston Larson for performing all the scanning electron microscopy and energy dispersive spectroscopy tests. In addition, the help provided by Mr. Tim Rawlsky to perform the X-ray fluorescence studies at Lafarge North America is acknowledged.

Special thanks go to the suppliers of the stabilizing agents namely, Lafarge North America and Texas Lime Company. The financial support from the Oklahoma Department of Transportation, the Oklahoma Transportation Center and the Federal Highway Administration is highly appreciated and acknowledged. Thanks are also extended to Mr. Jeff Dean, Mr. Vincent Reidenbach and Mr. Chris Clarke from the Oklahoma Department of Transportation for guiding and helping me in the sampling of soils.

I would like to thank my undergraduate advisors Dr. A. B. Gupta and Dr. Sudhir Kumar from Malviya National Institute of Technology for motivating me to pursue

graduate studies. Special thanks to my Master thesis advisor Dr. K. G. Sharma for his guidance and continuous support with my decision to study abroad. Also, I would like to thank professors Dr. K. S. Rao, Dr. A. Varadarajan, Dr. G. V. Rao, and Dr. J. T. Shahu from my masters program for guiding me during my stay at Indian Institute of Technology, Delhi.

I would also like to thank my mother (Rajesh Solanki), my father (Vir Bhadra Solanki), my elder sister (Divyanshi) and my lovely brother (Vibhashit) for their encouragements and for giving me the fortitude and perseverance to finish this study. Last, but not least, I would like to thank my beloved wife, Preeti, for standing by me no matter how rough the sea and the journey has been. She is the only one that can attest to all sacrifices we both had to make, so that this manuscript can become a reality.

TABLE OF CONTENTS

LIST OF TABLES

LIST OF FIGURES

ABSTRACT

Pavements are vulnerable to subgrade layer performance because it acts as a foundation. Due to increase in the truck traffic, pavement engineers are challenged to build more strong and long-lasting pavements. To increase the load-bearing capacity of pavements, subgrade layer is often stabilized with cementitious additives. Thus, an overall characterization of stabilized subgrade layer is important for enhanced short- and long-term pavement performance.

In this study, the effect of type and amount of additive on the short-term performance in terms of material properties recommended by the new Mechanistic-Empirical Pavement Design Guide (MEPDG) is examined. A total of four soils commonly encountered as subgrades in Oklahoma are utilized. Cylindrical specimens stabilized with lime (3%, 6% and 9%), class C fly ash (CFA) (5%, 10% and 15%) and cement kiln dust (CKD) (5%, 10% and 15%) are molded, cured for 28 days, and then subjected to different stress sequences to study the resilient modulus (M_r) followed by modulus of elasticity (M_E) and unconfined compressive strength (UCS) test. Results show that the changes in the M_r, M_E and UCS values stabilized specimens depend on the soil type and properties of additives.

The long-term performance (or durability) of stabilized soil specimens is investigated by conducting freeze-thaw (F-T) cycling, vacuum saturation and tube suction tests on 7-day cured P-, K- and C-soil specimens stabilized with 6% lime, 10% CFA and 10% CKD. Also, specimens are capillary-soaked for 60 days and tested for M_r, as an additional indicator for evaluating long-term performance. This study is motivated by the fact that during the service life of pavement stabilized layers are subjected to F-T

cycles and moisture variations. It is found that that UCS value of all the stabilized specimens decreased with increase in the number of F-T cycles. A strong correlation was observed between UCS values retained after vacuum saturation and F-T cycles indicating that vacuum saturation could be used as a time-efficient and inexpensive method for evaluating durability of stabilized soils. Among other benefits, this study helps enrich the database on the durability of stabilized subgrade soils. Also, improved understanding of different procedures for evaluation of durability is needed to enable a more objective selection of test method(s) by design engineers and to facilitate a more meaningful comparison of data obtained from different additives and different evaluation procedures.

Over the past few decades, detrimental effects of stabilization of sulfate bearing soil with calcium-based additives have surfaced around the world. In the past, emphasis has been placed on using sulfate resistant additives for stabilizing sulfate bearing soils which are not readily available and are also expensive. In this study, short- and long-term observations from stabilization of sulfate bearing soil with locally available low (CFA), moderate (CKD) and high (lime) calcium-based stabilizers are determined to evaluate and compare the effect of additive type on the phenomenon of sulfate-induced heave. The impact of different factors on the development of the ettringite, responsible for sulfate-induced heaving, is also discussed.

For Level 2 design of pavements, a total of four stress-based statistical models and two feed-forward-type artificial neural network (ANN) models, are evaluated for predicting resilient modulus of 28-day cured stabilized specimens. Specifically, one semi-log stress-based, three log-log stress-based, one Multi-Layer Perceptrons Network (MLPN), and one Radial Basis Function Network (RBFN) are developed. Overall, semi-

log stress-based and MLPN neural network are found to show best acceptable performance for the present evaluation and validation datasets. Further, correlations are presented for stress-based models to correlate M_r with compacted specimen characteristics and soil/additive properties. The models and correlations developed in this study could be refined using an enriched database.

Additionally, the effect of type of additive on indirect tensile and fatigue characteristics of selected stabilized P- and V-soil is evaluated. This study is based on the fact that stabilized layer is subjected to tensile stresses under wheel loading. Thus, the resilient modulus in tension (M_{rt}), fatigue life and strength in tension (σ_t) or flexure (represented by modulus of rupture, MOR) becomes another important design parameter within the mechanistic framework. Cylindrical specimens are prepared, cured for 28 days and subjected to different stress sequences in indirect tension to study the M_{rt}. On the other hand, stabilized beam specimens are compacted using a Linear Kneading Compactor and subjected to repeated cycles of reloading-unloading after 28 days of curing in a four-point beam fatigue apparatus for evaluating fatigue life and flexural stiffness. It is found that all three additives improved the M_{rt}, σ_t and MOR values; however, degree of improvement varied with the type of additive and soil. The magnitude of resilient modulus in tension is found lower than it is in compression. Findings from this study shed light on the differences in properties of cementitiously stabilized soil in indirect tension, flexure and compression. The fatigue life values and model of stabilized specimens is expected to provide a better understanding of performance of cementitiously stabilized layers in mechanistic sense.

The design of pavement structure has evolved from the empirical method, namely the AASHTO 1993 design guide, to the mechanistic-empirical approach (AASHTO 2002 Mechanistic-Empirical Pavement Design Guide, MEPDG). In the past, few studies evaluated conventional flexible pavement section (without stabilized layer) using both AASHTO 1993 and MEPDG. But to the author's knowledge, no effort has been directed towards design of *semi-rigid* type (with stabilized layer and no aggregate base) flexible pavements using both AASHTO 1993 and new MEPDG. Since the new MEPDG is intended to replace previously existing AASHTO 1993 pavement design based on empirical methods, it is important to evaluate and compare *semi-rigid* pavement designs using both AASHTO 1993 and MEPDG. To this end, this study encompasses the differences in the design of semi-rigid pavements developed using AASHTO 1993 and AASHTO 2002 MEPDG methodologies. Further, the design curves for fatigue performance prediction of stabilized layers are developed for different stabilized pavement sections. It is found that the design thickness is influenced by the type of soil, additive, selection of material property and design method. Cost comparisons of sections stabilized with different percentage and type of additives is also made. Knowledge gained from the parametric analysis of different sections using AASHTO 1993 and MEPDG is expected to be useful to pavement designers and others in implementation of the new MEPDG for future pavement design.

CHAPTER 1

INTRODUCTION

1.1 Background and Needs

According to the recent report by AASHTO/TRIP, only half of the nation's major roads are in good condition (AASHTO, 2009). The report found that major urban centers have the roughest roads – some with more than 60% of roads in poor condition. Weak subgrade soils are a leading factor in this regard. Driving roads in need of repairs threaten public safety and add $335 annually to typical vehicle operation costs by an average driver. In urban areas with high concentrations of rough roads, extra vehicle operating costs can be as high as $746 annually (AASHTO, 2009; ODOT, 2007). In the last few decades, pavement engineers have been challenged to build, repair and maintain pavement systems with enhanced longevity and reduced costs. Specifically, efforts have been made to improve the design methodology (AASHTO, 2004) and to establish techniques for modification of highway pavement materials. Cementitious stabilization is considered one of these techniques; it enhances the engineering properties of subgrade soils, which is essential for structurally sound pavements.

Cementitious stabilization is widely used in Oklahoma and elsewhere as a remedial method to ameliorate subgrade soil properties such as strength, stiffness, swell potential, workability and durability through the addition of cementitious additives. It consists of mixing stabilizing agents (or additives) such as lime, class C fly ash (CFA) and cement kiln dust (CKD) with soil. In the presence of water, these agents react with soil particles to form cementing compounds that are responsible for the enhancement in the aforementioned engineering properties. However, the degree of enhancement is

influenced by many factors such as stabilizing agent type, type of soil to be stabilized, curing time, cost, and seasonal factors (AFJMAN, 1994; Parsons et al., 2004; Khoury, 2005).

With the movement toward implementation of the new Mechanistic-Empirical Pavement Design Guide (MEPDG) (AASHTO, 2004), new material properties required for short- and long-term critical performance prediction of cementitiously stabilized layers are recommended. These material properties include: 28-day elastic (M_E) (for lean concrete, cement treated material, soil cement, and lime-cement-flyash), 28-day resilient modulus (M_r) (for lime-stabilized soil), unconfined compressive strength (UCS) (7-day for cement-stabilization, and 28-day for lime and lime-cement-flyash-stabilization), and 28-day flexural strength. The evaluation of these input parameters is required to pursue a Level 1 (most accurate) design under the hierarchical scheme. For a Level 2 (intermediate) design, however, design inputs are user selected, possibly from an agency database or from a limited testing program or could be estimated through correlations (AASHTO, 2004). Level 3, which is the least accurate, requires only the default values and is generally not recommended. This approach provides the designer with a great deal of flexibility to obtain the inputs for a project based on the importance of that project and available resources. The hierarchical approach is employed with regard to traffic, materials, and condition of existing pavement inputs (Von Quintus and Moulthrop, 2007).

Although several studies have been conducted in the past to evaluate the performance of stabilized materials in pavement construction (see e.g., McManis and Arman, 1989; Baghdadi, 1990; Zaman et al., 1992; Puppala et al., 1996; Misra, 1998; Little, 2000; Miller and Zaman, 2000; Senol et al., 2002; Kim and Siddiki, 2004; Khoury

and Zaman, 2007; Camargo et al., 2009; Gomez 2009; Prozzi and Aguiar-Moya, 2010), only a few studies have established some of the required short- and long-term inputs of stabilized soils that are suitable for the new MEPDG (Kim and Siddiki, 2004; Camargo et al., 2009; Gomez, 2009; Prozzi and Aguiar-Moya, 2010) when designing a new pavement. However, no studies to the author's knowledge evaluated all the required short- and long-term parameters of cementitiously stabilized subgrade.

Consequently, the primary objective of this study is to evaluate M_r, M_E, UCS, and flexural strength of subgrade soils stabilized with different cementitious additives, namely, lime, CFA, and CKD. The new MEPDG does not consider the durability of cementitiously stabilized materials for modeling purposes (AASHTO, 2004). However, the testing of durability of stabilized subgrade layer is of utmost importance due to the loss of strength and stiffness in long-term climate changes inducing freeze-thaw (F-T) and wet-dry (W-D) cycles (Little and Nair, 2009; Saxena et al., 2010). Thus, the effect of additive type on long-term performance (or durability) is examined in this study using three different methods namely, F-T cycling, vacuum saturation and tube suction tests. Also, specimens were capillary-soaked and tested for M_r, as an additional indicator for evaluating durability. The short- and long-term performance characteristics and mechanisms are explained by using the scanning electron microscopy and X-ray diffraction data. Additionally, the energy dispersive spectroscopy micrographs are used to identify the elements in the cementitious products due to stabilization.

Knowledge gained from the experimental program illustrating the effect of type of additive and soil on the short- and long-term performance of stabilized soil specimens is expected to be useful to pavement designers and others in future pavement design and

maintenance projects. Also, improved understanding of different procedures for evaluation of durability is needed to enable a more objective selection of test method(s) by design engineers and to facilitate a more meaningful comparison of data obtained from different additives and different evaluation procedures.

For design of new pavement, M_r for stabilized soil specimens is generally determined by conducting repeated load triaxial tests in the laboratory on 28-day cured specimens according to the AASHTO T-307-99 test method (AASHTO, 2004). The AASHTO T-307-99 test method, however, is a complex, time consuming and expensive test method and not particularly well suited for small projects. Hence, in the present study selected stress-based statistical and artificial neural network models are evaluated and validated. Also, correlations of M_r with the characteristics of molded stabilized specimen as well as soil/additive properties are developed. The results from this study could be used for both the currently used AASHTO 1993 Design Guide and the Level 2 and Level 3 recommendations of the AASHTO 2002 MEPDG.

Stabilized subgrade layers may be used to provide support for either flexible or rigid pavements, but are more frequently used with flexible pavements (FHWA, 2009). In a conventional flexible pavement section (AASHTO, 2004) with a granular base course, stress analysis indicates that the radial stress or strain is maximum at the bottom of the asphalt concrete layer directly under the center of the wheel load (Huang, 2004; Papagiannakis and Masad, 2007) (Figure 1.1 a). However, some studies (e.g., AASHTO 2004, Adaska and Luhr, 2004, Kuennen, 2006; Lav et al., 2006; Molenaar and Pu, 2008; Agostinacchio et al., 2008) showed that when the same cross-section is analyzed with the granular course replaced by a stabilized layer (Figure 1.1 b), the location of the critical

tensile stress shifts to bottom of the stabilized subgrade and, hence, the performance of the flexible pavement, from a mechanistic standpoint. The type of flexible pavement with a cementitiously stabilized layer below asphalt concrete is classified as *semi-rigid* type flexible pavement by the new MEPDG (AASHTO, 2004). A *semi-rigid* pavement would require evaluation of additional engineering properties such as flexural strength, modulus in flexure and fatigue life of stabilized subgrade layer. However, due to difficulties associated with preparing and handling of a beam specimen, several studies recommend using indirect diametrical tensile test method (or Brazilian test), as a possible alternative to the flexural beam test (see e.g., Foley et al., 2001; Khattak and Alrashidi, 2006; Gnanendran and Piratheepan, 2008). Hence, this study further examines this proposition and investigates the strength and modulus determined by both flexural beam and indirect diametrical testing tests.

Several developments over recent decades have offered an opportunity for more rational and rigorous pavement design procedures (Carvalho and Schwartz, 2006). The design procedures developed in the AASHTO 1993 guide for new pavement are based on the algorithms originally developed from the AASHO road test (Mulandi et al., 2006). Some newer concepts such as the resilient modulus for pavement material characterization were introduced in this version (AASHTO, 1986; AASHTO, 1993). On the other hand, the new MEPDG (AASHTO, 2004) adopted a mechanistic-empirical approach to the damage analysis of flexible pavements. This involves computing the pavement structural responses to load (i.e., stresses/strains), translating them into damage, and accumulating the damage into distresses that are responsible for reduced pavement performance over time (Papagiannakis and Masad, 2007). Very little attention,

to the author's knowledge, has previously been focused on differences in the pavement designs developed using AASHTO 1993 and AASHTO 2002 design guides.

In the present research, a parametric study of structural designs for a typical *semi-rigid* type flexible pavement section with a stabilized subgrade layer is conducted using both the AASHTO 1993 design guide and the new MEPDG. Such work is expected to contribute towards the comparative merits and demerits of the pavement designs developed by using AASHTO 1993 and mechanistic-based AASHTO 2002 pavement design guides.

1.2 Objectives of the Research

The final goal of this research work is to characterize and design cementitiously stabilized subgrade layer as structural component of a pavement system in the light of the new MEPDG. In order to carry out this research, there is an obvious necessity to study the behavior and characteristics of stabilized subgrade recommended by the new MEPDG. The specific objectives of this study are noted below:

(1) Determine the effect of various stabilizing agents, namely, lime, CFA, and CKD, by conducting M_r in compression, M_E and UCS, representing short-term performance.

(2) Evaluate the long-term performance (or durability) of stabilized subgrades by conducting freeze-thaw cycling, vacuum saturation, tube suction and M_r (60-day capillary-soaked specimens) tests.

(3) Determine the effect of lime, CFA and CKD on flexural strength and fatigue life of specimens prepared by using selected soils. Also, evaluate strength and resilient modulus in indirect tension.

(4) Determine and compare the magnitude of sulfate-induced heaving of sulfate bearing soil stabilized with various cementitious additives, namely, lime, CFA and CKD.

(5) Identify the micro-structural developments in the matrix of stabilized soil specimens by conducting mineralogical studies such as scanning electron microscopy and energy dispersive spectroscopy.

(6) Develop statistical and artificial neural network (ANN) based models to predict resilient modulus of stabilized subgrade soils as a function of factors that are used in the development of the statistical models.

(7) Conduct statistical analyses to develop correlations of M_r with compacted specimen characteristics and soil/additive properties.

(8) Compare and analyze the design of a *semi-rigid* type flexible pavement by using both the AASHTO 1993 design guide and the new MEPDG design guidelines.

1.3 Organization of the Dissertation

Following the introduction presented in Chapter 1, Chapter 2 entitled "*Influences of Various Cementitious Additives on the Short-Term Performance of Stabilized Subgrades*" addresses the effect of different additives on the evaluation of MEPDG inputs representing short-term performance of soils stabilized with different cementitious additives, namely, lime, class C fly ash (CFA) and cement kiln dust (CKD) (Solanki et al., 2009b). Cylindrical specimens were compacted and cured for 28 days in a humidity room having a constant temperature and controlled humidity. At the end of the curing period, specimens were tested for M_r, M_E, and UCS representing short-term performance. This study is also directed to evaluating the effect of different chemical and physical properties of soils and additives on the improvement in M_r values.

Chapter 3 entitled "*Influences of Various Cementitious Additives on the Durability of Stabilized Subgrades*" examines the long-term performance (or durability) of stabilized soil specimens (Solanki and Zaman, 2010). Cylindrical specimens were molded, cured for 28 days, and then tested for durability by conducting F-T cycling, vacuum saturation and tube suction tests. Also, specimens were capillary-soaked for 60 days and tested for M_r, as an additional indicator for long-term performance. The effect of F-T cycles on the strength of stabilized specimens was evaluated. Also, durability evaluated by using two time-efficient and inexpensive laboratory procedures was compared with conventional durability test.

The study presented in Chapter 4 entitled "*Influences of Various Cementitious Additives on the Laboratory Performance of Sulfate Bearing Soil*" was undertaken to evaluate natural sulfate bearing lean clay from northwestern Oklahoma for the effect of type and amount of additive on the short- and long-term performance by evaluating material properties, as recommended by the new MEPDG (Solanki et al., 2009a). Lean clay specimens stabilized with lime, CFA, and CKD were molded, cured for 28 days, and then subjected to different stress sequences to study the M_r. The same specimens were then tested for M_E and UCS or 3-D swell. Specimens tested for 3-D swell were further tested for M_r, M_E, and UCS, after 120 days of capillary soaking. Further, results were supported by conducting scanning electron microscopy (SEM) tests in conjunction with X-ray diffraction (XRD) analyses.

Chapter 5 entitled "*Statistical and Artificial Neural Network Modeling*" is related to statistical and artificial neural network (ANN) modeling of M_r for Level-2 pavement design applications (Solanki et al., 2010). A total of three stress-based statistical models

and two ANN models were developed using a dataset containing M_r test results of 160 specimens. The strengths and the weaknesses of the developed models were examined using additional M_r test results that were not used in the development of these models. Further, possible correlations of M_r with compacted specimen characteristics and soil/additive properties were also investigated.

Chapter 6 entitled "*Behavior of Cementitiously Stabilized Subgrade Soils Under Tension and Flexure*" is devoted to examining the influence of cementitious additives on indirect tensile and flexural characteristics of selected soils stabilized with lime, CFA and CKD. Cylindrical specimens were compacted using a Superpave gyratory compactor and cured for 28 days, prior to subjecting them to cycles of unloading-reloading cycles for determining resilient modulus in tension (M_{rt}). Additionally, beam specimens were compacted and cured for evaluating effect of additive type on flexural characteristics namely, flexural stiffness (M_{rf}) and fatigue life. The cylinders and beams were also tested for determining indirect tensile and flexural strength, respectively.

Chapter 7 entitled "*Design of Semi-Rigid Type of Flexible Pavement*" includes a parametric study of structural designs of a typical *semi-rigid* type flexible pavement section using both the AASHTO 1993 design guide and the new MEPDG. Also, design curves for predicting the performance of stabilized layers are presented. Finally, economic differences between a pavement section constructed using different additives is also discussed.

In Chapter 8, the summary of this dissertation and recommendations for future research are presented.

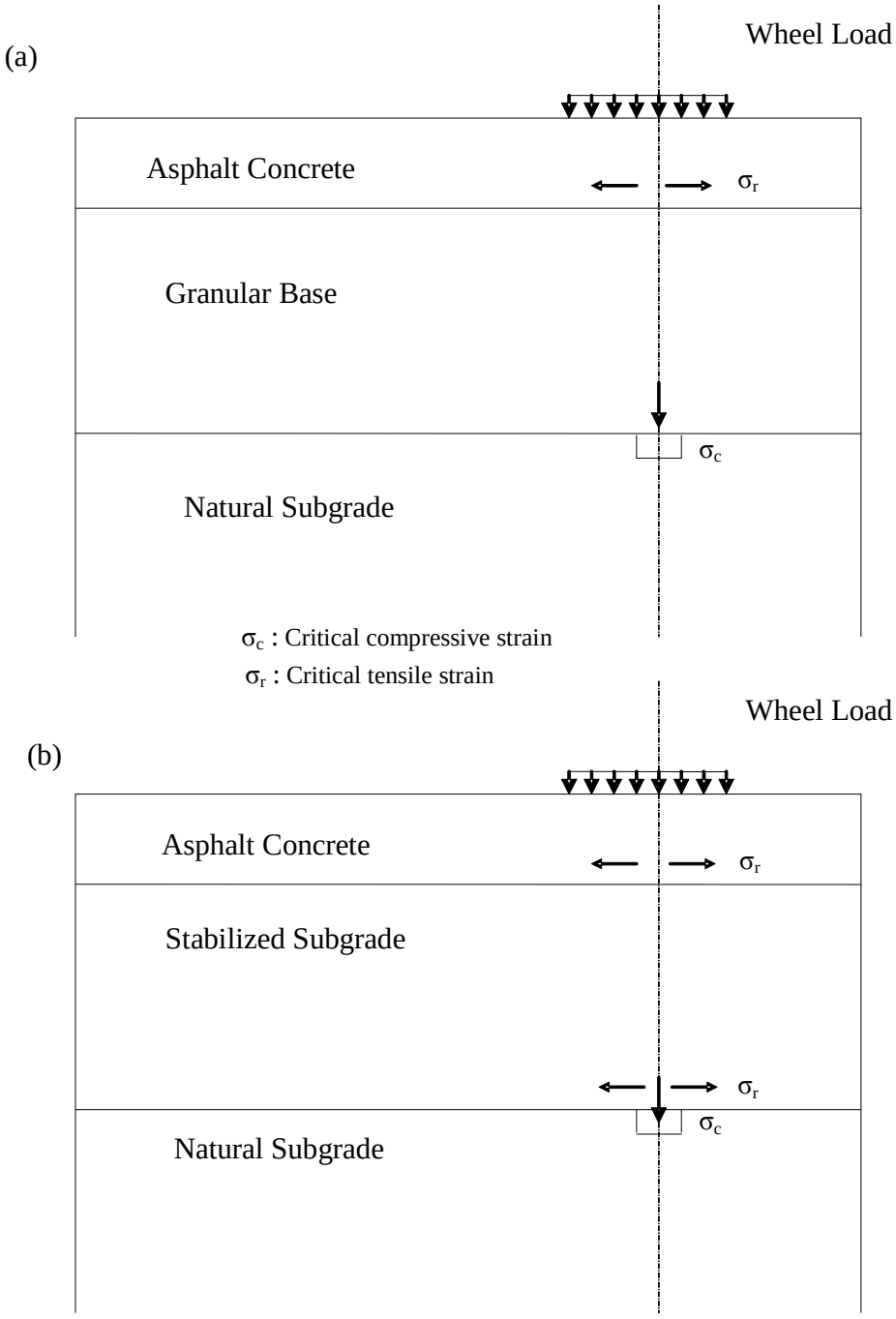

Figure 1.1 Typical Flexible Pavement Section (a) Conventional Flexible and (b) Stabilized Subgrade Showing Locations of Critical Compressive and Tensile Strains

CHAPTER 2

INFLUENCES OF VARIOUS CEMENTITIOUS ADDITIVES ON THE SHORT-TERM PERFORMANCE OF STABILIZED SUBGRADES

2.1 Introduction

The efficacy of cementitious stabilization depends on the composition of soils and the stabilization parameters such as property and percentage of additive (AFJMAN, 1994; Little et al., 2000; Al-Rawas et al., 2002; Parsons et al., 2004; Evangelos, 2006). The degree of improvement achieved by cementitious stabilization can be evaluated by different engineering properties. For pavement application, however, the new Mechanistic-Empirical Pavement Design Guide (MEPDG) (AASHTO, 2004) recommends new materials properties for critical short-term performance prediction. These properties include resilient modulus (M_r) or elastic modulus (M_E), and unconfined compressive strength (UCS) representing short-term performance of pavement. The evaluation of these inputs is required to pursue a Level 1 (most accurate) design under the hierarchical scheme. For a Level 2 (intermediate) design, however, design inputs are user selected possibly from an agency database or from a limited testing program or could be estimated through correlations (AASHTO, 2004). Level 3, which is the least accurate, requires only the default values and is generally not recommended.

Consequently, the primary objective of the study presented herein is to evaluate M_r, M_E, and UCS of four commonly encountered subgrade soils in Oklahoma stabilized with locally available cementitious additives, namely, lime, class C fly ash (CFA) and cement kiln dust (CKD). This study is also directed to evaluate the effect of different chemical and physical properties of soils and additives on the improvement in M_r values. Further, mineralogical studies such as scanning electron microscopy and energy

dispersive spectroscopy were also used to verify research findings observed from the macro test results.

2.2 Literature Review

Several pertinent studies have previously been undertaken to evaluate the engineering properties of soils stabilized using different cementitious additives. A summary of different studies is presented in the Table 2.1. Chang (1995) investigated the resilient properties and microstructure of a fine grained soil (Lateritic soil) stabilized with CFA and lime. Strength was evaluated after a 7-day curing period by performing UCS tests. Specimens were compacted at near optimum moisture content (OMC) in a mold with a diameter of 38 mm (1.5 in) and a height of 100 mm (4 in). The resilient modulus tests were performed in accordance with the AASHTO T 274-82 test method. Results showed that the M_r values varied between 125 to 250 MPa (18 to 36 ksi). But, no attempt was made to study the M_E of specimens, as recommended by the new MEPDG.

Little (2000) reported that the effect of lime stabilization induces a 1,000 percent or more increase in M_r over that of the untreated soil. The AASHTO T 294 method was used to determine the M_r values. Values of back-calculated (from field falling weight deflectometer testing) M_r typically falls within a range of 210 and 3,500 MPa (30 and 508 ksi). The strength values determined for lime-stabilized soil was reported as high as 7,000 to 10,000 kPa (1,016 to 1,451 psi). However, this study was limited to lime-stabilized subgrade soils and no attempt was made to compare with other additives.

Qubain et al. (2000) determined the effect of lime stabilization on pavement design having medium to stiff clayey soils. The AASHTO TP 46-94 test method was used to determine the M_r values on 1-hour cured cylindrical specimens. Each test

consisted of 16 stress stages with deviatoric stress ranging from 12 to 62 kPa (2 to 9 psi). The average UCS at 5% lime content was 620 kPa (90 psi), with a M_r value of 250 MPa (36 ksi). In a similar laboratory study, Ramakrishna (2002) evaluated M_r values of lean clay specimens stabilized with cement and fly ash and cement mix. The percentage of additive used was 8% cement, 15% fly ash with 5% cement and 20% slag. The M_r values were reported to be 600 to 1200 MPa (87 to 174 psi) for clays stabilized with cement, 350 to 700 MPa (51 to 102 ksi) for clays stabilized with fly ash and cement mix and 325 to 570 MPa (47 to 83 ksi) for clays stabilized with slag.

Further, Parsons and Milburn (2003) conducted a series of tests, namely UCS and modulus of elasticity to evaluate the relative performance of lime, cement, CFA and an enzymatic stabilizer. These stabilizers were combined with a total of seven different soils having Unified Soil Classification System (USCS) classifications of CH, CL, ML and SM. Lime- and cement-stabilized soils showed the most improvement in performance for multiple soils, with CFA-stabilized soils showing substantial improvement. The results also showed that for many soils, more than one stabilization options may be effective for the construction of subgrade. No attempt was made to examine the M_r values.

Further in comparative studies, Kim and Siddiki (2004) conducted a series of laboratory tests to evaluate the performance of fine grained soils encountered in Indiana and stabilized them with lime and lime kiln dust (LKD). These tests include UCS, California Bearing Ratio (CBR), and M_r. Findings from the study indicate that LKD may be viable, cost effective in enhancing the strength of fine grained soils, compared to hydrated lime. Their study addressed most of the properties that will be evaluated in the proposed study. Also, their study addressed the design inputs for the MEPDG. However,

it was carried out on predominantly fine grained soils, namely, A-4, A-6, and A-7-6 encountered in Indiana. It is also important to note that the mineralogical and textural characteristics of soils in Oklahoma are different than those in Indiana, and thus those results may not be directly used for design of pavements in Oklahoma at Level 1 or Level 2.

In a recent study, Camargo et al. (2009) conducted California Bearing Ratio (CBR), M_r, UCS, and durability (freeze-thaw) tests for evaluating the effects of adding CFA to the recycled pavement material and a road surface gravel to enhance their mechanical properties. It was reported that M_r and UCS values of stabilized material increased significantly. Freeze-thaw cycling had a small effect on the M_r and UCS of the recycled materials. A strong relationship was found between M_r and UCS of recycled materials blended with fly ash. However, this study was limited to aggregate base and no subgrade soils were considered.

In another recent study, Gomez (2009) evaluated the M_r values of soil specimens stabilized with two additives, namely, CFA and CKD. In this study, five project sites were selected in Oklahoma. Both stabilized and raw soils were collected, mixed, compacted, cured under controlled conditions, and tested for M_r at specific times of curing. The five test soils included clayey and silty sands (SC and SM), a low plasticity silty soil (ML), and two low plasticity clayey soils (CL). It was found that CKD treated samples gave larger improvement rates than CFA treated samples for low plastic and non-plastic soils when compared to the efficiency of lime and CFA as soil stabilizers. Although larger improvements were reported for the CKD-stabilized specimens, no consistent correlations were found when related to the soil parameters. The M_r values

obtained from field mixed samples showed lower improvement parameters when compared to lab mixed specimens. Ultimate field-mixed specimen improvements were found to be 1.5 to 6 times lower than lab-mixed improvements. As expected, additive content generally showed a direct relationship with improved M_r values.

2.3 Materials and Sources

In the present study, a total of four soils and three cementitious additives are used. This section describes the fundamental properties including grain size distribution, index properties and chemical compositions of the soils and additives.

2.3.1 Native Soils

The following soils are used in the present study: (1) Port series (P-soil); (2) Kingfisher series (K-soil); (3) Vernon series (V-soil); and (4) Carnasaw series (C-soil). A summary of the soil properties determined in the laboratory and the corresponding standard testing identification are presented in Table 2.2. According to the USCS, P-soil is classified as CL-ML (silty clay with sand) with a liquid limit of approximately 27 and a plasticity index (PI) of approximately 5. K-soil is classified as CL (lean clay), according to the UCSS with an average liquid limit of approximately 39% and a PI of approximately 21. As per the USCS, V-soil is a sulfate-bearing soil (Sulfate content ≈ 15,400 ppm) and classified as lean clay (CL), with an average liquid limit of approximately 37 and a PI of approximately 11. C-soil is classified as fat clay (CH) according to USCS with a PI value of 29. A summary of physical and chemical properties of soils is presented in Table 2.3.

2.3.2 Cementitious Additives

As noted earlier, three different cementitious additives, namely, hydrated lime, class C fly ash (CFA), and cement kiln dust (CKD) were used. Hydrated lime was supplied by the Texas Lime Company, Cleburne, Texas. It is a dry powder manufactured by treating quicklime (calcium oxide) with sufficient water to satisfy its chemical affinity with water, thereby converting the oxides to hydroxides. CFA from Lafarge North America (Tulsa, Oklahoma) was brought in well-sealed plastic buckets. It was produced in a coal-fired electric utility plant. CKD used was provided by Lafarge North America located in Tulsa, Oklahoma. It is an industrial waste collected during the production of Portland cement. The physical and chemical properties of the stabilizing agents are presented in Table 2.4. The XRF analysis was conducted using a Panalytical 2403 spectrometer on specimens obtained by using fused bead preparation method. The fused bead preparation technique consists of dissolving the specimen in a solvent called a flux at high temperature (>1000°C) in a platinum crucible and to cast it in a casting-dish. It is evident from Table 2.4 that the calcium oxide content in hydrated lime is 68.6%. This can be explained using the stoichiometry of the chemical reaction taking place during the specimen preparation for XRD.

$$Ca(OH)_2 \xrightarrow{T = 512^oC} CaO + H_2O$$

$$(74)=40x1+16x2+1x2 \qquad (56)=40x1+16x1 \qquad (18)=1x2+16x1$$

Using above chemical equation, it can be shown that 95.9% of $Ca(OH)_2$ (reactant) will produce approximately 72% of CaO (product). Further, the free lime content (i.e., any lime not bound up in glassy phase compounds such as tricalcium silicate and tricalcium aluminate) was determined in accordance with ASTM C 114 (Alternate Test

Method B, ammonium acetate titration). Although CFA is having very low lime content (0.2%), specimens stabilized with CFA showed enhancement in strength and modulus values (see Sections 2.7 and 2.8). It is speculated that during the reaction process some lime is liberated from the bound state which takes part in the cementitious reactions and thus, producing increase in strength and modulus values.

2.4 Factors Affecting Cementitious Stabilization

The effectiveness of cementitious stabilization depends on properties of both soil and additive (AFJMAN, 1994, Al-Rawas et al., 2002, Parsons et al., 2004, Evangelos, 2006). A description of pertinent factors intrinsic to the soils and additives which influences the efficiency of cementitious stabilization is presented herein.

2.4.1 Soil Properties

2.4.1.1 Gradation and Plasticity Index

Several researchers (e.g., Diamond and Kinter, 1964; Haston and Wohlgemuth, 1985; Prusinski and Bhattacharja, 1999; Little, 2000; Qubain et al., 2000; Kim and Siddiki, 2004; Mallela et al., 2004; Puppala et al., 2006; Consoli et al., 2009) recommended use of lime with fine-grained soils. However, CFA (see e.g., McManis and Arman, 1989; Chang, 1995; Misra, 1998; Zia and Fox, 2000; Puppala et al., 2003; Bin-Shafique et al., 2004; Phanikumar and Sharma, 2004; Nalbantoglu, 2004; Camargo et al., 2009; Li et al., 2009) and CKD (e.g., McCoy and Kriner, 1971; Napierala, 1983; Baghdadi and Rahman, 1990; Zaman et al., 1992; Sayah, 1993; Miller and Azad, 2000; Miller and Zaman, 2000; Parsons and Kneebone, 2004; Sreekrishnavilasam et al., 2007; Peethamparan et al., 2008; Gomez, 2009) is used successfully with both fine- and coarse-

grained soils. Lower effectiveness of lime with coarse-grained soil can be attributed to scarcity of pozzolana (silicious and aluminacious material) in coarse-grained soils which is required for pozzolanic (or cementitious) reactions. Little (2000) and Mallela et al. (2004) recommend a soil with a minimum clay content (< 0.002 mm) of 10% and a plasticity index of 10 for lime-stabilization. In this study, only K-, V- and C-soil fulfils this requirement with C-soil having highest clay content of 48%. However, mineralogical analysis conducted using X-ray fluorescence spectroscopy (XRF) revealed that all the fours soils used in this study are having high (> 70%) amount of pozzolana, as presented in Table 2.3.

2.4.1.2 Cation Exchange Capacity

Cation Exchange Capacity (CEC) is the quantity of exchangeable cations required to balance the charge deficiency on the surface of the clay particles (Mitchell, 1993). During ion-exchange reaction of soil with cementitious additive, cation of soil (e.g., Na^{+}, K^{+}) is replaced by cation of additive (Ca^{2+}) and the thickness of double diffused layer is reduced. Hence, the replacement of cations results in increase in workability and strength of soil-additive mixture. The rate of exchange depends on clay type, solution concentrations and temperature (Gomez, 2009). In soil stabilization studies, CEC values have been used to a limited extent to explain the effectiveness of soil stabilization (Nalbantoglu and Tuncer, 2001; Al-Rawas et al., 2002; Nalbantoglu, 2004; Gomez, 2009).

In this study, CEC was measured by sodium acetate method in accordance with EPA 9081 test method (Chapman, 1965). As evident from Table 2.3, K-soil and C-soil showed highest and lowest CEC values of 21.7 and 5.2 meq/100 gm, respectively. On the

other hand, P- and V-soil produced a CEC value of 11.5 and 19.9 meq/100 gm, respectively.

2.4.1.3 Sulfate Content

Primary "sulfate-induced heaving" problems arise when natural sulfate rich soils are stabilized with calcium-based additives (Puppala et al., 2004), also known as "sulfate attack." This heave is known to severely affect the performance of pavements, and other geotechnical engineering structures built on sulfate rich soils stabilized with calcium-based additive (Hunter, 1988; Mitchell and Dermatas, 1990; Petry and Little, 1992; Rajendran and Lytton, 1997; Rollings et al., 1999; Puppala et al., 2004). According to current understanding, "low to moderate" and high sulfate soils are those with sulfate less than 2,000 ppm and more than 2,000 ppm, respectively (Kota et al., 1996; Mitchell and Dermatas, 1990; Puppala et al., 2002; Rao and Shivananda, 2005). In this study, soluble sulfate content in the soils were measured using the Oklahoma Department of Transportation procedure for determining soluble sulfate content: OHD L-49 (ODOT, 2006). Only V-soil was found to have high sulfate content of 15,400 ppm (>10,000 ppm) which may have the potential to cause serious damage due to calcium-based additive. This issue has been further discussed in Chapter 4.

2.4.1.4 Specific Surface Area

Surface phenomena have an important influence on the behavior of fine-grained soils; they affect many physical and chemical properties (Cerato and Lutenegger, 2002). The specific surface area (SSA), refers to the area per unit mass of soil, may be a dominant factor in controlling the fundamental behavior of many fine-grained soils

(Gomez, 2009). The mineralogy of fine-grained soils is the dominant factor in determining the effect of SSA. For this study, only total SSA measurement was conducted using the polar liquid Ethylene Glycol Monoethyl Ether (EGME) method (Cerato and Lutenegger, 2002) and results are presented in Table 2.3. C-soil had the highest SSA value of 118.5 m^2/gm, P-soil, on the other hand, had the lowest SSA of 51.0 m^2/g.

2.4.1.5 Silica Sesquoxide Ratio

Many properties of soils are related with the silica sesquioxide ratio (SSR) (Winterkorn and Baver, 1934; Fang, 1997; Mallela et al., 2004). Hence, in this study it was decided to evaluate SSR of soils. It is defined as:

$$SSR = \frac{\frac{x}{A}}{\frac{y}{B} + \frac{z}{C}} \tag{2.1}$$

where, x is the percent of SiO_2, y is the percent of Al_2O_3, z is the percent of Fe_2O_3, A is the molecular weight of SiO_2 (60.1), B is the molecular weight of Al_2O_3 (102.0), and C is the molecular weight of Fe_2O_3 (159.6). From the results presented in Table 2.3 it is clear that P-soil is having highest SSR value of 14.9 while C-soil is having lowest SSR value of 3.9.

2.4.2 Additive Properties

2.4.2.1 Free-Lime Content

In calcium-based stabilizers (e.g., Portland cement, CFA, CKD) most of the lime (CaO) is bound up in compounds such as tricalcium silicate and tricalcium aluminate.

The unreacted lime that is not combined in any of these compounds is called free-lime, which is expected to play a major role in stabilization (Collins and Emery, 1983; Misra, 1998; Zaman et al., 1998; Ferguson and Levorson, 1999; Miller and Azad, 2000; Miller and Zaman, 2000; Sezer et al., 2006; Khoury and Zaman, 2007; Peethamparan and Olek, 2008). Free-lime content was determined by conducting titration in accordance with ASTM C 114 alternative test method B and results are presented in Table 2.4. It is clear that lime is having highest free-lime content of 46.7% followed by 6.7% for CKD and 0.2% for CFA.

2.4.2.2 Specific Surface Area

The specific surface area (SSA) of additives, as measured by using the ethylene glycol monoethyl ether (EGME) method (Cerato and Lutenegger, 2002), were 17.0, 6.0, and 12.0 m^2/gm, respectively, for lime, CFA and CKD. It can be seen that lime and CFA had the highest and the lowest SSA values, respectively. A higher SSA indicates more reactivity of additive (Nalbantoglu and Tuncer, 2001; Sreekrishnavilasam et al., 2007).

2.4.2.3 Loss on Ignition

A higher loss on ignition (LOI) value indicates high carbonates for CFA/CKD and high hydroxides for lime. Some researchers reported that high LOI indicates low free-lime content for CKDs, making CKDs less reactive, and therefore lower improvements (Bhatty et al., 1996; Miller and Azad, 2000). In the laboratory, LOI was evaluated by igniting additive inside a muffle furnace at a temperature of 950^{o}C (1742^{o}F) in accordance with ASTM C 114 test method for hydraulic cements. As evident from results presented in Table 2.4, lime and CFA produced highest and lowest LOI values of 31.8%

and 1.2%, respectively. On the other hand, approximately 27% of CKD is lost on ignition.

2.4.2.4 Percent Passing No. 325 Sieve

Several researchers noticed increased reactivity of additive with increase in amount of additive passing No. 325 (45 µm) sieve (NCHRP, 1976; Bhatty et al., 1996; Zaman et al., 1998; Zheng and Qin, 2003; Khoury, 2005). The percentage of passing No. 325 sieve for lime, CFA and CKD determined in accordance with ASTM C 430 test method are 98.4, 85.8 and 94.2, respectively. It is clear that lime is finer among all the additives used in this study.

2.4.2.5 pH and pH Response

The elevated pH level of soil-lime mixture is important because it provides an adequate alkaline environment for ion-exchange reactions (Little, 2000). In the laboratory, pH is determined using the method recommended by ASTM D 6276 for lime-stabilization, which involves mixing the solids with de-ionized (DI) water, periodically shaking samples, and then testing with a pH meter after 1 h. The procedure specifies that enough lime must be added to a soil-water system to maintain a pH of 12.4 after 1 h. This ensures that adequate lime is provided to sustain the saturation during the 1-h period (Prusinski and Bhattacharja, 1999).

Several researchers (e.g., Haston and Wohlgemuth, 1985; Prusinski and Bhattacharja, 1999; IRC, 2000; Little, 2000; Qubain et al., 2000; Mallela et al., 2004; Puppala et al., 2006; Consoli et al., 2009) used pH values on soil-lime mixture as an indicator of reactivity of lime. However, only limited studies (see e.g., Miller and Azad,

2000; Parsons et al., 2004; Peethamparan and Olek, 2008; Gomez, 2009) evaluated pH response of soil-CFA or soil-CKD mixtures. Hence, the pH values of soil-additive mixtures were determined to investigate whether pH would reflect the effectiveness soil stabilization with lime, CFA or CKD.

The pH results of raw soil, raw additive and soil-additive mixtures are presented in Table 2.5 and are used as the primary guide for determining the amount of additive required to stabilize each soil. It is clear that raw P-, V- and K-soil are alkaline with a pH value greater than 8.0. On other hand, C-soil is acidic with a pH value approximately 4.17. Also, it was found that raw lime, CFA and CKD had a pH value of 12.58, 11.83 and 12.55, respectively. The pH values of raw CFA and CKD are consistent with the results reported by other researchers (e.g., Miller and Azad, 2000; Sear, 2001; Parsons et al., 2004; Peethamparan and Olek, 2008; Gomez, 2009). The pH trend of raw additives is similar to the trend of available free-lime content in additive, as shown in Table 2.4.

For all the soil-additive mixtures, pH values increase with the increase in the percentage of additive and show an asymptotic behavior after a certain percentage. In the current study, an increase of less than 1% in pH percent increase with respect to raw soil is assumed as starting point of asymptotic behavior. As evident from Table 2.5, pH values started showing an asymptotic behavior with 3% lime for P-, K- and V-soil. With CFA and CKD, P-, K- and V-soil showed asymptotic behavior at an additive content of 10%. However, C-soil, due to acidic nature, attained asymptotic behavior at a higher lime content of 5%. Additionally, C-soil never attained an asymptotic behavior with CFA and CKD contents up to 17.5%. This can be attributed to the acidic behavior of C-soil which requires higher amount of moderately basic CFA and CKD for neutralization. Based on

the aforementioned observations, it was decided to select 3%, 6% and 9% lime for laboratory performance evaluation. On the other hand, 5% 10% and 15% were selected for CFA- and CKD-stabilization.

2.4.2.6 Silica Sesquoxide Ratio

As noted earlier, SSR values of additives were evaluated using Eqn. 2.1 and results are presented in Table 2.4. From Table 2.4, SSR values of lime, CFA and CKD are 1.9, 3.0 and 6.0, respectively. Further, SSR values of additives and soils were added together, called as combined SSR value, and correlated with improvement in M_r values, as will be discussed later in Section 2.9.

2.5 Moisture-Density Test

In the laboratory soil was mixed manually with stabilizer for determining moisture-density relationship of soil-additive mixtures. The procedure consists of adding specific amount of additive, namely, lime (3%, 6% or 9%) or CFA (5%, 10% or 15%) or CKD (5%, 10% or 15%) to the processed soil. The amount of additive was added based on the dry weight of soil. The additive and soil were mixed manually to uniformity, and tested for moisture-density relationships by conducting Proctor test in accordance with ASTM D 698 test method.

2.5.1 P-soil and Additive Mixtures

The moisture-density test results (i.e., OMCs and maximum dry density, MDDs) for P-soil are presented in Table 2.6. The moisture content was determined by oven-drying the soil-additive mixture. The OMC and MDD of raw soil was found to be 13.1% and 17.8 kN/m^3 (108.7 pcf), respectively. In the present study, laboratory experiments

showed an increase in OMC with increasing percentage of lime and CKD. On the other hand, a decrease in the MDDs with increasing percent of lime and CKD is observed from Table 2.6. Other researchers (e.g., Haston and Wohlegemuth, 1985; Zaman et al., 1992; Miller and Azad, 2000; Sreekrishnavilasam et al., 2007) also observed effects similar to those in the current study. One of the reasons for such behavior can be attributed to the increased number of fines in the mix due to the addition of lime and CKD.

A higher MDD was obtained by increasing the CFA content. However, the MDD increase diminished with the increase in CFA beyond 10%. Conversely, the OMC showed an increase for 5% CFA and then it generally decreased with increasing CFA content. These observations were similar to those reported by McManis and Arman (1989) for sandy silty soil and by Misra (1998) for clays.

2.5.2 K-soil and Additive Mixtures

The moisture-density test results for K-soil are presented in Table 2.7. The OMC and MDD of raw soil was found to be 16.5% and 17.4 kN/m^3 (110.6 pcf), respectively. In the present study, laboratory experiments showed an increase in OMC with increasing percentage of lime. On the other hand, a decrease in the MDDs with increasing percent of lime is observed from Table 2.7. This is consistent with the results reported by Nagaraj (1964), Haston and Wohlegemuth (1985), Ali (1992) and Little (1996). Little (1996) believed that OMC increased with increasing lime content because more water was needed for the soil-lime chemical reactions. Nagaraj (1964) suggested that the decrease in MDD of the lime-treated soil is reflective of increased resistance offered by the flocculated soil structure to the compactive effort.

For CFA stabilization, MDD increased with increase in CFA content. On the other hand, OMC decreased for 5 percent CFA mix and then increased for 10 and decreased again for 15 percent of fly ash mix. A similar observation was reported by McManis and Arman (1989), Misra (1998) and Solanki et al. (2007a). Misra (1998) reported that the increase in MDD can be attributed to the packing of finer fly ash particles (smaller than a No. 200 sieve) in voids between larger soil particles. This behavior of OMC was attributed to progressive hydration of soil and fly ash mixtures and increased number of finer particles (specific surface) in the soil-fly ash mixtures.

CKD-stabilized soil showed the same trends like lime-stabilized soil. An increase in OMC and a decrease in MDD with increase in the percentage of additive was observed. Other researchers (e.g., Zaman et al., 1992; Miller and Azad, 2000) also observed effects similar to those in the current study. Similar statements as mentioned for lime-stabilization can be used to rationalize the compaction behavior of CKD-stabilized soils.

2.5.3 V-soil and Additive Mixtures

The moisture-density test results for V-soil mixed with different percentages of additives are summarized in Table 2.8. The Proctor tests conducted on raw V-soil showed an OMC and MDD value of 23.0% and 16.0 kN/m^3 (101.9 pcf), respectively. Similar to P- and K-soil-lime/CKD mixtures, OMC-MDD essentially showed the same trend. Hence, reasons as mentioned in the preceding section can be used to justify the observed trends in OMC and MDD values.

For CFA stabilization, the moisture-density results were more complex. Laboratory experiments showed that MDD decreased with 5 percent CFA, and then

increased with increase in the percentage of additive. On the other hand, OMC decreased with the increase in the amount of CFA, as evident from Table 2.8.

2.5.4 C-soil and Additive Mixtures

The OMC was found to be 20.3% for the raw C-soil. For lime- and CKD-stabilized soil samples, it was evident that OMC increased and MDD decreased with increasing percentage of lime as illustrated in Table 2.9. For CFA stabilization, Proctor results showed that MDD decreases for 5 percent of CFA, increases for 10 percent and then again decreases for 15 percent CFA as shown in Table 2.9. On the other hand, OMC decreased with the increase in the percentage of CFA. Since moisture-density results of C-soil and additive mixtures showed similar trends to other soil-additive mixtures used in this study, similar reasons as mentioned in the preceding Section 2.5.1 can be used to justify the observed OMC-MDD trends.

2.6 Specimen Preparation

In this study, a total of 160 specimens were prepared according to the method described by Solanki et al. (2009a) and Solanki et al. (2009b). The mixture for each specimen consists of raw soil mixed with specific amount of additive. The amount of additive (3%, 6%, or 9% for lime and 5%, 10%, or 15% for CFA and CKD) was added based on the dry weight of the soil. The additive and soil were mixed manually for uniformity. After the blending process, a desired amount of water was added based on the OMC. Then, the mixture was compacted in a mold having a diameter of 101.6 mm (4.0 in) and a height of 203.2 mm (8.0 in) to reach a dry density of between 95%-100% of the maximum dry density (MDD) (Tables 2.6 through 2.9). After compaction, specimens

were cured at a temperature of 23.0 ± 1.7°C (73.4 ± 3.1°F) and a relative humidity of approximately 96% for 28 days; 28-day curing period is recommended by the new MEPDG (AASHTO, 2004).

2.7 Experimental Methodology

2.7.1 Resilient Modulus, Modulus of Elasticity and Unconfined Compressive Strength

The resilient modulus (M_r) tests were performed in accordance with the AASHTO T 307 test method. The test procedure consisted of applying 15 stress sequences using a cyclic haversine-shaped load pulse with duration of 0.1 seconds and rest period of 0.9 seconds. The sample was loaded following the sequences shown in Table 2.10. For each sequence, the applied load and the vertical displacement for the last five cycles were recorded and used to determine the M_r. A 2.23 kN (500 lb) load cell was used to apply the required load level. Two linear variable differential transformers (LVDTs) were used to measure the resilient vertical deformation. These LVDTs were attached to two aluminum clamps that were mounted on the specimen at a distance of approximately 50.8 mm (2.0 in) from both ends of the specimen. The LVDTs had a maximum stroke length of 5.08 mm (0.2 in). Figure 2.1 shows a photographic view of the LVDTs mounted on a sample. A power supply was used to excite and amplify the LVDT signals. This is consistent with Barksdale et al. (1997) that measuring relative displacement between two points on the specimen eliminates the extraneous deformations occurring past the ends of the specimens. A complete setup of M_r testing on stabilized subgrade soil specimen is shown in Figure 2.2.

To generate the desired haversine-shaped load and to read the load and displacement signals, a program was written using Material Testing System (MTS) Flex

Test SE Automation software, as shown in Figure 2.3. The load-deformation response was recorded for last 5 cycles of each stress sequence by using a computer-controlled Flex Test SE Test Controller (see Figure 2.3). The Flex Test SE digital servo-controller from MTS is made up of a powerful array of reliable, flexible and easy-to-use controllers designed to address the full spectrum of material and component testing needs. Basic capabilities include station configuration, auto-zeroing, control mode switching with hydraulics on, and adaptive control. The controller provides a self-contained single-channel control, and can be linked to other controllers for multi-channel testing. All the data were collected and stored in an MS Excel file and a macro program in Excel was written to process these data and evaluate the resilient modulus. The M_r for each sequence was calculated from the average recoverable strain and average load from last five cycles by using the following expression:

$$M_r = \frac{\sigma_d}{\varepsilon_r} \tag{2.2}$$

where, σ_d = repeated cyclic deviatoric stress, and ε_r = recoverable strain (or resilient strain). Further, details of the apparatus and the noise reduction method used are given by Solanki et al. (2009b).

The new MEPDG recommends the use of Mixture Design and Testing Protocol (MDTP) developed by Little (2000) in conjunction with the AASHTO T 307 test protocol for determining the M_r of soils stabilized with lime. The PDG also requires M_E as one of the design inputs for soil-cement, cement-treated materials, lime-cement-fly ash mixtures and lean concrete. Since no specific parameters were recommended for CFA and CKD stabilization, it was decided to evaluate the modulus of elasticity (M_E) and

unconfined compressive strength (UCS) as an additional indicator of the mechanical behavior of CFA- and CKD-stabilized specimens.

M_E and UCS tests were conducted in accordance with the ASTM D 1633 test method. Specimens were loaded in a MTS frame at a constant strain rate of 0.63% (of sample height) per minute, which is equivalent to 1.27 mm (0.05 in.) per minute for the specimen configuration used here. Deformation values were recorded during the test using LVDTs fixed to opposite sides of and equidistant from piston rod with a maximum stroke length of ±12.7 mm (±0.5 in). The load values were obtained from a load cell having a capacity of 22.7 kN (5,000 lb). Each specimen was subjected to two unloading-reloading cycles before loading it to failure. Straight lines were drawn through the first two unloading-reloading curves (secant modulus) and the average slope of these lines is the M_E of the stabilized clay specimen.

2.7.2 Mineralogical Studies

To facilitate the macro-behavior comparison and explanation, the mineralogical study techniques such as Scanning Electron Microscopy (SEM) and Energy Dispersive Spectroscopy (EDS) were employed to qualitatively identify the micro-structural developments in the matrix of the stabilized soil specimens.

The Scanning Electron Microscopy (SEM) technique was employed using a JEOL JSM 880 microscope to qualitatively identify the micro-structural developments in the matrix of the stabilized soil specimens. After the UCS test on specimens, broken mix was air-dried for approximately four days. Three representative tiny pieces were mounted on stubs (1 cm, i.e., 0.4 in. wide discs that have a pin-mount on the base of the disc). The samples were not electrically conductive; therefore, they were initially coated by Iridium

to maintain conductivity. The quality of images was not satisfactory, so it was decided to use gold-palladium alloy for the process instead of Iridium coating. Hence, pieces were coated with a thin layer (≈ 5 nm) of an alloy of gold-palladium by sputter coating technique to provide surface conductivity. A JEOL JSM 880 scanning electron microscope operating at 15 kV was used to visually observe the coated specimens. The JEOL JSM 880 was fitted with an energy-dispersive X-ray spectrometer (EDS). The EDS was used to analyze chemical compositions of the specimen. In this technique, electrons are bombarded in the area of desired elemental composition; the elements present will emit characteristic X-rays, which are then recorded on a detector. The micrographs were taken using EDS2000 software. It must be noted that SEM study allows only a tiny area of raw and stabilized specimen to be examined (unlike engineering laboratory specimens). However, it is believed to be representative of the reaction process of stabilized specimens.

2.8 Presentation and Discussion of M_r Results

The M_r test results of the four soils namely, P-, K-, V-, and C-soil stabilized with lime, CFA and CKD are shown in Tables 2.11 to 2.22. Each M_r value listed in Tables 2.11 to 2.22 is an average of M_r tests conducted on four specimens. One way to observe the effect of different percentages of additives on the resilient properties is to compare the average M_r at a particular stress level (Elliot and Thornton, 1988; Drumm et al., 1997; Ping et al., 2001). For example, Strategic Highway Research Program (SHRP) Protocol P-46 (1989) suggests reporting M_r values of subgrade at a deviatoric stress of 28 kPa (4.0 psi) and a confining pressure of 41 kPa (6 psi). However, to the author's knowledge, there is no such recommendation for stabilized subgrades. It is also important to note that

the actual stress level (i.e., deviatoric and confining stress) can be estimated by calculating the in-situ stress using a multi-layer elastic program (e.g., KENLAYER); however, stress level may change depending on the pavement configuration. So for comparison purposes, it was decided to use experimental M_r values determined at a stress level closest to the level recommended by SHRP P-46 (1989). Therefore, mean M_r at a deviatoric stress of 25 kPa (3.6 psi) and a confining pressure of 41 kPa (6.0 psi) were selected for comparison, as shown in Figure 2.4. Additionally, to study the comparative effectiveness of lime, CFA and CKD on the four soils, graphs of percent improvement in M_r values (deviatoric stress = 25 kPa, i.e., 3.6 psi and confining pressure = 41 kPa, i.e., 6.0 psi) versus percentage of additive were plotted (Figures 2.4 – 2.7).

2.8.1 Effect of Lime Content

It is clear from Tables 2.11 through 2.14 that mean M_r values increased due to stabilization. This increase, however, depends on the type of soil. For example, 3% lime provided an increase of approximately 459%, 1,261%, 647% and 115% with P-, K-, V- and C-soil, respectively (Figures 2.4 – 2.7). This improvement is maximum with K-soil, however, a reduction in M_r values was observed beyond a certain percent (Figure 2.5). For example, K-soil specimens stabilized with 9% lime showed 33 percent decrease in M_r values as compared to specimens stabilized with 6% lime. This is consistent with other studies (Haston and Wohlgemuth, 1985; Petry and Wohlgemuth, 1988; Arora and Aydilek, 2005; Osinubi and Nwaiwu, 2006) that an increase in lime beyond 5% results in lower strength values. One explanation is that excess lime behaved as low strength filler, effectively weakening the lime-soil mixture (Osinubi and Nwaiwu, 2006). It is also worth noticing that the new MEPDG recommends M_r value range between 207 – 413 MPa (30

– 60 psi) for lime-stabilized soils. This range is similar to the range of M_r values obtained in this study for C-soil specimens (213 – 573 MPa, i.e., 31 – 83 psi). However, P-, V- and K-soil specimens stabilized with lime showed higher range of M_r values (> 500 MPa, i.e., 73 ksi).

2.8.2 Effect of CFA Content

From Tables 2.15 through 2.18, one can see that the average M_r value increased with amount of CFA with a range of M_r values between 150 – 2,500 MPa (22 – 363 ksi). The increase in M_r values with increased amount of CFA is consistent with the studies conducted by other researchers such as McManis and Arman (1989), Chang (1995), Misra (1998), Senol et al. (2002), Mir (2004), and Arora and Aydilek (2005). It is evident from Figures 2.4 – 2.7 that for the percentages used in this study, 15% CFA-stabilized specimens showed a maximum increase in M_r values of approximately 1,305%, 1,078%, 894%, and 174% for P-, K-, V- and C-soil specimens, respectively, as compared to raw soil. For 5% and 10% CFA, K-soil specimens showed highest improvements of approximately 498% and 983%, respectively.

2.8.3 Effect of CKD Content

Tables 2.19 through 2.22 summarized the effect of CKD on M_r. Results showed that M_r increased with the increased percentage of additive with a range of M_r values between 150 – 2,700 MPa (22 – 392 ksi); this is consistent with Zhu (1998), Parsons et al. (2004), Khoury (2005), and Gomez (2009). For example, the M_r values of 15% CKD-stabilized specimens increased as much as 1,608%, 2,277%, 1,473%, and 565% for P-, K-, V- and C-soil, respectively. As depicted in Figure 2.4, a large increase in average M_r

can be observed when the CKD content is increased from 0 to 5%, 5 to 10% and 10 to 15%. This rate of increase in M_r values is the highest between 5% and 10% CKD. For example, this increase is 174%, 219%, 193% and 51% for P-, K-, V- and C-soil, respectively. In the present study, CKD treatment (>10%) resulted in the highest M_r values (Figures 2.4 – 2.7).

2.8.4 Effect of Stress Level

To analyze the effect of stress level (deviatoric stress, σ_d and confining pressure, σ_3), selected plots were drawn between stress ratio (σ_d/UCS) and M_r values of raw and stabilized P- and K-soil specimens (Figures 2.8 – 2.11). In general, it is clear from Figures 2.8 to 2.11 that the M_r values of raw and stabilized soil specimens increases with increase in confining pressure and with decreasing deviatoric stress. However, the percentage of increase in modulus is relatively small for stabilized soil specimens compared to untreated specimens. For example, at a deviatoric stress of 37 kPa (5.4 psi), increase in confining pressure from 14 to 41 kPa (2 to 6 psi) increases M_r value by approximately 30%, 23%, 3% and 4% for raw, 9% lime-, 15% CFA-, and 15% CKD-stabilized specimens, respectively, of P-soil. At similar stress level, K-soil specimens showed approximately 8%, 4%, 2% and 3% enhancement in M_r values with 0%, 9% lime, 15% CFA and 15% CKD, respectively. Similar observations were reported by Achampong (1996), Achampong et al. (1997) and Ramakrishna (2002) for cement- and lime-stabilized soil. The lower sensitivity of stabilized soil specimens towards change in stress level could be attributed to higher strength of stabilized soil specimens. For example, raw P-soil specimens are subjected to load range inducing stresses between 5 to

30% of UCS. On the other hand, P-soil specimens stabilized with 15% CKD are subjected to load range inducing stresses between 1 to 5% of UCS.

2.9 Presentation and Discussion of M_E and UCS Results

The variation of modulus of elasticity (M_E) and UCS values with the additive content is shown graphically in Figures 2.12 and 2.13, respectively. The UCS values were found to be 224, 191, 168 and 207 kPa, i.e., 33, 28, 24 and 30 psi for the raw P-, K-, V- and C-soil, respectively. In general, the trend of the behavior of M_E and UCS values for different percentages of additives is the same as that observed for M_r values.

2.9.1 Effect of Lime Content

As depicted in Figure 2.12, in lime-stabilized specimens an increase of approximately 186%, 516%, 436% and 72% in M_E values was observed for 3% lime-stabilized P-, K-, V- and C-soil specimens, respectively. Similarly, addition of 3% lime increased the UCS values by 67%, 138%, 297% and 21% for P-, K-, V- and C-soil, respectively. It is clear that K- and V-soil showed the highest improvement with lime. On the other hand, C-soil with the lowest pH and CEC value showed the lowest enhancements in both M_E and UCS values. Also, all the soils and percentages of lime used in this study were having strength lower than 1,723 kPa (250 psi), as recommended by MEPDG for stabilized soil layer in a flexible pavement.

2.9.2 Effect of CFA Content

It is evident from Figures 2.12 and 2.13 that there is a significant increase in M_E and UCS with increasing CFA content in the treated soils. A maximum increase of 367%, 586%, 616%, and 95% was observed in M_E values for 15% CFA stabilized P-, K-, V- and

C-soil, respectively. Correspondingly, these different stabilized soil specimens showed an increase in UCS values by 278%, 250%, 396%, and 99%. Clearly, V-soil specimens stabilized with CFA showed better performance, as compared to other soils used in this study. Similar to lime, all the UCS values were lower than 1,723 kPa (250 psi) for CFA-stabilized specimens.

2.9.3 Effect of CKD Content

It is evident that there is significant increase in the M_E with increasing amount of CKD content in the stabilized soils (Figure 2.12). The M_E values in all soils exhibited an increase with the amount of CKD. As depicted in Figure 2.13, in P-soil specimens the maximum increase (about 638%) in M_E values was observed by adding 15% CKD. Similarly, 15% CKD-stabilized K-, V- and C-soil specimens exhibited the maximum increase of approximately 1,061%, 1,042% and 194%, respectively, compared to the raw soil. The variation of UCS values with the CKD content is illustrated in Figure 2.13. It is observed that UCS values of all the soils used in this study increases as the amount of CKD increases. For example, the UCS values increased by 529%, 505%, 705%, and 154% for the P-, K-, V-, and C-soil specimens, respectively, when stabilized with 15% CKD. This observation is consistent with that of Miller and Azad (2000), Sreekrishnavilasam et al. (2007), Peethamparan and Olek (2008) and Peethamparan et al. (2009). Again, CKD-stabilization was not able to provide minimum strength of 1,723 kPa (250 psi), as recommended by the new MEPDG.

2.10 Effect of Soil and Additive Type

From the aforementioned results it is obvious that the resilient modulus, modulus of elasticity and unconfined compressive strength of stabilized specimens is influenced by the type of soil and additive. Since the trend of improvement in M_r, M_E and UCS values is similar, as discussed earlier, only M_r values are used herein to discuss the effect of soil and additive type.

For all the four soils used in this study, it is clear, in general, that at lower application rates (3% to 6%), the lime-stabilized soil specimens showed the highest improvement in the M_r values. At higher application rates (> 10%), however, the CKD treatment provided the maximum enhancements (Figures 2.4 – 2.7). Overall, 15% CKD-stabilized specimens showed the highest improvement for all the four soils. In addition, stabilization of K-soil resulted in the maximum enhancement in M_r values (Figure 2.5). On the other hand, C-soil specimens showed much lower improvements in M_r values, as shown in Figure 2.7. One of the explanations for lowest improvement in M_r values of C-soil could be acidic nature of C-soil (pH = 4.17), as discussed earlier. It is also observed that the normalized percent increase in M_r (NM_r = % Increase in M_r value/% Additive) values is influenced by CEC of soil. This behavior is graphically presented in Figure 2.14. C-soil having lowest CEC value (5.2 meq/100 gm) produced lowest NM_r of 38% with 3% lime. On the other hand, K-soil having highest CEC value (21.7 meq/100 gm) enhanced NM_r by 420% with 3% lime. Similar trend is observed for P-, K-, V- and C-soils stabilized with 10% CFA and 10% CKD (Figure 2.14). No specific trend was observed for the variation of M_r with gradation, plasticity index and specific surface area of soil. For example, C-soil specimens with higher plasticity index (29) and clay content

(48%) stabilized with 6% lime had NM_r values lower than P-soil (plasticity index = 5, clay content = 11%).

Attempts were made to observe the effect of additive properties, namely, free-lime content, alkali content, loss on ignition, specific surface area, pH, passing No. 325 sieve, and SSR ratio. The effect of free-lime content is depicted in Figure 2.15. It is clear that the NM_r value increases with the free-lime content; however, the percent increase varied from one soil to another. For example, the NM_r of P-soil specimens increased from 121 to 153% as the free-lime content increased from 6.7 to 46.1%. C-soil specimens, on the other hand, exhibited an increase of approximately 22 to 38% as the free-lime content increased from 6.7 to 46.1%. Figures 2.16 and 2.17 show the variation of NM_r values of 3% lime-, 10% CFA- and 10% CKD-stabilized P-, K-, V- and C-soil specimens with the alkali content and loss on ignition value of additive, respectively. A decrease in NM_r values with alkali content can be observed; however, increase in NM_r values with loss on ignition was observed. This trend is contrary to the behavior reported by other researchers for different type of CKDs (e.g., Bhatty et al., 1996; Miller and Azad, 2000; Peethamparan and Olek, 2008). For example, Bhatty et al. (1996) reported that CKDs containing less than 6% alkalis and low LOI values are reactive and produces higher strength. This difference in behavior could be attributed to other factors such as free-lime content that might have influenced in enhancing the effectiveness of the additives. Although CFA had higher alkali content and lower LOI than lime, it also had lower free-lime content (0.2% for CFA versus 46.1% for lime).

Figure 2.18 shows a plot between percent passing No. 325 sieve of additives and NM_r values. It is clear from Figure 2.18 that percent passing No. 325 sieve influences the

M_r values. An increase in percent passing No. 325 sieve from 85.8% (CFA) to 98.4% (lime) increased the NM_r values from 32 to 153 for P-soil. This can be attributed to increase in fine contents in the soil and thus increased surface area for pozzolanic reactivity. Normalized percent increase in M_r values versus specific surface area of additive are shown in Figure 2.19. All curves in Figure 2.19 show clear correlation between the NM_r values with SSA. For example, P-soil specimens showed an increase in NM_r values (32 to 153%) with an increase in SSA value of additive from 6.0 to 17.0 m^2/gm. For similar magnitude of SSA values, K-soil specimens showed an increase in NM_r from 98 to 420%. The fact that the additive particles have a larger surface to interact with the soil can explain this behavior. Larger SSA values imply more available surface for soil-additive interaction resulting in more cementitious products and thus higher gain in modulus values. The pH value of additive also plays an important role in enhancing the M_r values, as evident from Figure 2.20. An increase in NM_r values with pH can be observed from Figure 2.20. Lime-stabilized specimens having highest pH value of 12.58 produced highest modulus value followed by CKD- (pH = 12.55) and CFA- (pH = 11.83) stabilized specimens. As discussed earlier, high pH value causes silica from the clay minerals to dissolve and, in combination with Ca^{2+} form calcium silicate and calcium aluminate hydrate (Eades, 1962; Diamond and Kinter, 1964).

Further, an attempt was made to correlate the SSR value of soil-additive mix with variation in M_r values. Figure 2.21 depicts the change in NM_r values of stabilized specimens with SSR. It is clear from Figure 2.21 that the NM_r values exhibited an increase with the SSR values; however, a reduction in NM_r values was observed beyond a certain percentage of SSR value (between 7 – 13%). This is an indication that the

amount of SSR up to a certain percentage (7 – 13%) would contribute to the increase in pozzolanic reactivity, which is responsible for the modulus increase.

2.11 Microstructure Characteristics

As noted earlier, mineralogical studies such as SEM and EDS were conducted on all the raw soils, raw additives and 28-day cured stabilized C-soil specimens to study the influence of stabilization on microstructure characteristics.

2.11.1 Raw Soils and Additives

Figure 2.22 shows SEM micrographs of raw soil samples at high magnification (10,000 times). It is clear that the raw soil has a discontinuous structure, where the voids are more visible because of the absence of hydration products. The raw additives used in this study were also studied using SEM/EDS methods. Figures 2.23 (a), (b) and (c) show SEM/EDS of raw lime, CFA and CKD powder, respectively. As evident from Figure 2.23 (a), raw lime is an amorphous powder consisting mainly of calcium compounds. This is in agreement with the XRF results reported in Table 2.4. On the other hand, CFA and CKD are more complex compounds. EDS results indicated presence of calcium, aluminum, silicon, iron, sulfur, phosphorous, titanium, and magnesium minerals in CFA. Whereas EDS results of CKD indicated presence of calcium, silicon, magnesium, sulfur, and potassium minerals. The SEM micrographs of raw CFA showed that CFA is composed of different size spherical particles (or cenosphere); however, CKD micrographs showed particles with poorly defined shapes.

2.11.2 C-Soil with 9% Lime

To study the microstructure of 9% lime-stabilized C-soil specimens, 28-day UCS tested specimens were examined using SEM micrographs. Figure 2.24 (a) shows the microstructure at a magnification level of 10,000 times, which when compared with the raw soil micrograph of Figure 2.22 (d) shows marked change in morphology. From Figure 2.24 (a), it is clear the raw soil structure has transformed from a particle based form to a more integrated composition due to cementitious reactions. At a higher magnification (x 25,000 times), the cementing phases could clearly be seen. Further, EDS pattern was used as a basis to monitor the changes occurring in the chemical composition at selected locations within the C-soil after stabilization with 9% lime. As evident from Figure 2.24 (a), analysis on the cementing phases showed presence of calcium (Ca) and silicon (Si), which is an indication of the presence of C-S-H (Calcium-Silicate-Hydrate, $x\text{CaO}.y\text{SiO}_2.z\text{H}_2\text{O}$). It should be noted that the other two peaks not marked in Figure 2.24 (a) belongs to gold-palladium coating used for making specimens electrically conductive. The cementing phases, due to gradual crystallization of the new secondary minerals, caused an increase in the strength of the stabilized soil, as discussed in Section 2.8. Similar observations were reported by other researchers (see e.g., Locat et al., 1996; Ghosh and Subbarao, 2001; Nalbantoglu, 2006; Kavak and Akyarh, 2007). Figure 2.24 (b) shows micrograph of same specimen at a magnification level of 5,000 times taken from a different location. A flower-like structure of calcium hydroxide crystals is evident which indicates presence of un-reacted hydrated lime in the stabilized specimen. This is consistent with the observations reported in Section 2.7.1 that excess lime acts as filler resulting in decreased strength.

2.11.3 C-Soil with 15% CFA

The SEM micrographs of C-soil stabilized with 15% CFA are presented in Figures 2.25 (a) through (c). Figure 2.25 (a) reveals the formation of cementing products, with lamellar form, adjacent to the fly ash particles. The EDS analysis showed presence of Ca and Si indicating presence of C-S-H, the main cementing product responsible for strength gain (Choquette et al., 1987; Lav and Lav, 2000). Also, two additional peaks of gold and palladium appeared because specimens were sputter coated with alloy of gold-palladium. In viewing these samples, one would notice that the spherical particles of fly ash are joined strongly to the clay particles in its surrounding (Chang, 1995). It was also apparent that the fly ash particles served as nucleation sites for the growth of the hydration products (or coatings), as shown in Figure 2.25 (b). Formation of ettringite, $Ca_6[Al(OH)_6]_2.(SO_4)_3.26H_2O$, was also observed in the form of heaps of rod-like crystals (Figure 2.25 c). This observation was further confirmed by conducting EDS analysis which suggested presence of Ca, Al (aluminum) and S (sulfur) with traces of Si and Ti (titanium) as impurities. No areas were found showing normal ettringite spectra without traces of Si and Ti. Similar structure, as shown in Figure 2.25 (c), was reported as ettringite by other researchers (e.g., Mitchell and Dermatas, 1992; Intharasombat, 2003). Further, SEM micrographs revealed that most of the fly ash particles were covered with a reaction shell as seen in Figure 2.25 (d). The approximate chemical composition of the outer shell was determined at location 1 and 3 by the EDS analysis and a typical composition is presented in pattern marked as point and 1 and 3. The composition of the shell was slightly different from that of the un-reacted inner fly ash surface which is shown in spectrum 2. The higher calcium peak in 1 and 3 compared to spectrum 2

suggests the initiation of reaction products (e.g., C-A-S-H) formation on the surface of fly ash particle. It should be noted that the exact quantitative composition cannot be obtained using the EDS analysis of the stabilized specimens.

2.11.4 C-Soil with 15% CKD

SEM micrographs as illustrated in Figures 2.26 (a) and (b) show significant changes in the microstructure of raw soil when mixed with CKD and cured for 28 days. It could be observed that flat clay structure surfaces observed in Figure 2.22 (d) is covered with cementitious reaction products, as shown in Figure 2.26 (a). Figure 2.26 (a) show the C-A-S-H (Calcium-Alumino-Silicate-Hydrate, $x\text{CaO}.y\text{Al}_2\text{O}_3.z\text{SiO}_2.w\text{H}_2\text{O}$) phase development which contains distinct peaks of Ca, Si and Al elements based on the EDS analysis, consistent with observation reported by Chaunsali and Peethamparan (2010). Figure 2.26 (b) shows micrographs of hydration coatings and bonds developed in 15% CKD-stabilized C-soil. Another prominent feature of the microstructure of 15% CKD-stabilized C-soil was the presence of needle-shaped ettringite crystals (Figure 2.26 c). The presence of ettringite crystals in CKD-stabilized soil is consistent with the observations reported by Peethamparan et al. (2008), Moon et al. (2009), and Chaunsali and Peethamparan (2010). Hence, improved strength and stiffness exhibited by CKD-stabilized soil specimens after curing could be attributed to aforementioned reaction products.

2.12 Concluding Remarks

This study was undertaken to evaluate four soils from Oklahoma for the effect of type and amount of additive on the material properties as recommended by new MEPDG

for critical performance prediction. Subgrade clay specimens stabilized with lime (3%, 6% and 9%), CFA (5%, 10% and 15%) and CKD (5%, 10% and 15%) were molded, cured for 28 days, and then subjected to different stress sequences to study the M_r followed by M_E and UCS test. Based on the study presented in this chapter the following conclusions can be derived:

1. All three additives improved the M_r, M_E and UCS values of P-, K-, V- and C-soil specimens; however, degree of improvement varied with the type of additive and soil.
2. The results from pH tests showed that 3% lime, 10% CFA and 10% CKD provide an asymptotic behavior (less than 1% increase in pH w.r.t raw soil pH) in P-, K- and V-soil-additive mixtures. No such asymptotic behavior was observed for C-soil stabilized with 10% CFA and 10% CKD.
3. The range of M_r values (213 – 573 MPa, i.e., 31 – 83 ksi) of lime-stabilized fat clay specimens is similar to the range of M_r values recommended by MEPDG for lime-stabilized specimens; however, silty clay and lean clays showed higher range of M_r values (> 500 MPa, i.e. 73 ksi).
4. For the different percentage of CFA used in this study, the range of M_r values were 150 – 2,500 MPa (22 – 363 ksi) for silty clay, 300 – 1,300 MPa (44 – 189 ksi) for lean clays and 150 – 400 MPa (22 – 58 ksi) for fat clay. On the other hand, CKD-stabilization provided M_r values ranging between 400 – 2,600 MPa (58 – 377 ksi) for silty clay, 250 – 2,000 MPa (36 – 290 ksi) for lean clays and 150 – 900 MPa (22 – 131 ksi) for fat clay.
5. For CFA- and CKD-stabilization, the amount of improvement increases with increase in the additive content; however, a reduction in M_r, M_E and UCS values was observed

beyond a certain percentage of lime content (between 6 – 9% for K- and C-soil, between 3 – 6% for V-soil).

6. In general, lime-stabilization produced highest M_r values with K-soil (918 – 1,382 MPa, i.e., 133 – 201 ksi). On the other hand, CFA- and CKD-stabilization produced highest M_r values with P-soil (1,037 – 2,435 MPa for CFA, i.e., 151 – 353 ksi; 2,333 – 2,613 MPa for CKD, i.e., 339 – 379 ksi).
7. At lower application rates (3% to 6%), lime showed highest improvement in the M_r values. At higher application rates (> 10%), CKD provided maximum enhancements.
8. The M_r values of raw and stabilized soil specimens increases with increasing confining pressure and with decreasing deviatoric stress. However, the percentage of increase in modulus is relatively less pronounced for stabilized soil specimens compared to untreated specimens. The lower sensitivity of stabilized soil specimens towards change in stress level could be attributed to higher strength of stabilized soil specimens.
9. None of the additive percentages used in this study was able to provide minimum strength of 1,723 kPa (250 psi), as recommended by new MEPDG for stabilized base layer in a flexible pavement. However, M_r values were higher or similar than the values recommended by MEPDG for lime-stabilized soil specimens; no recommendations are available for CFA- and CKD-stabilized soils, hence no comparisons were made.
10. The percentage of increase in M_r values is better correlated with soil properties – cation exchange capacity; additive properties – free-lime content, alkali content, loss

on ignition, percent passing No. 325 sieve, specific surface area, pH; and soil-additive mixture properties – silica sesquioxide ratio.

11. Microscopic analysis confirms that the addition of lime or CFA or CKD to soil induces beneficial reactions and significant improvements in strength and stiffness. Also, it could be concluded that the formation of reaction products such as C-S-H, C-A-S-H and ettringite contributed to strength development of stabilized soil.

Table 2.1 A Summary of Relevant Laboratory Studies on Soils Stabilized with Different Additives

Reference	Type of soil[a]	Type of additive	Parameters/Tests[b]
Haston and Wohlgemuth (1985)	CL	Lime	UCS
McManis and Arman (1989)	A-3, A-2-4	FA	UCS, R
Baghdadi (1990)	Kaolinite clay	CKD	UCS
Zaman et al. (1992)	Clays	CKD	UCS
Chang (1995)	Lateritic soil	FA, Lime	UCS, M_r
Achampong (1996)	CL, CH	PC, Lime	UCS, M_r
Misra (1998)	Clays	FA	UCS
Prusinski and Bhattacharja (1999)	Clays	PC, Lime	UCS, CBR (No)
Little (2000)	Fine grained soils	Lime	UCS, M_r
Miller and Azad (2000)	CH, CL, ML	CKD	UCS
Miller and Zaman (2000)	Shale, Sand	CKD	CBR, UCS
Qubain et al. (2000)	CL	Lime	UCS, M_r
Zia And Fox (2000)	Loess	FA	UCS, CBR
Senol et al. (2002)	Clays	FA	UCS, CBR, M_r
Parsons and Milburn (2003)	CH, CL, ML, SM	Lime, PC, CFA, Enzymatic stabilizer	UCS, Modulus
Kim and Siddiki (2004)	A-4, A-6, A-7-6	Lime, LKD	UCS, CBR, M_r
Prabakar et al. (2004)	CL, OL, MH	FA	UCS, CBR, Shear strength parameters
Arora and Aydilek (2005)	SM	FA	UCS, CBR, M_r
Barbu and McManis (2005)	CL, ML	Lime, PC	UCS, Cyclic Triaxial test
Hillbrich and Scullion (2006)	A-3	PC	M_r, Seismic Modulus
Osinubi and Nwaiwu (2006)	CL	Lime	UCS
Puppala et al. (2006)	CH	Lime with polypropylene fiber	UCS
Ling et al. (2008)	Silty clay	Lime, PC	M_r
Gomez (2009)	SC, SM, ML, CL	FA, CKD	M_r

[a] Soils according to USCS and AASHTO classification; [b] pH, Compaction and Atterberg limit tests are not included in the list

M_r: Resilient modulus test; CBR: California Bearing Ratio; R: Soil support resistance value; FA: Fly ash; PC: Portland cement; CKD: Cement kiln dust; LKD: Lime kiln dust

Table 2.2 Testing Designation and Soil Properties

Method	Parameter/Units	P-soil	K-soil	V-soil	C-soil
ASTM D 2487	USCS Symbol	CL-ML	CL	CL	CH
AASHTO M 145	AASHTO Designation	A-4	A-6	A-6	A-7-6
ASTM D 2487	USCS Name	Silty clay with sand	Lean clay	Lean clay	Fat clay
ASTM D 2487	% finer than 0.075 mm	83	97	100	94
ASTM C 430	% finer than 0.045 mm	54	89	95	87
ASTM D 422	% finer than 0.002 mm (clay content)	11	45	39	48
ASTM D 4318	Liquid limit	27	39	37	58
ASTM D 4318	Plastic limit	21	18	26	29
ASTM D 4318	Plasticity index	5	21	11	29
…	Activity	0.24	0.47	0.28	0.69
ASTM D 854	Specific gravity	2.65	2.71	2.61	2.64
ASTM D 698	Optimum moisture content (%)	13.1	16.5	23.0	20.3
ASTM D 698	Max. dry unit weight (kN/m^3)	17.8	17.4	16.0	16.3

USCS: Unified Soil Classification System

Table 2.3 Chemical and Physical Properties of Soils used in this Study

Chemical compound/Property	Percentage by weight, (%)			
	P-soil	K-soil	V-soil	C-soil
Silica (SiO_2)[a]	77.7	65.8	54.0	63.4
Alumina (Al_2O_3)[a]	7.4	13.0	17.6	21.5
Ferric oxide (Fe_2O_3)[a]	2.3	4.8	7.2	9.1
Silica/Sesquioxide ratio (SSR) $SiO_2/(Al_2O_3+Fe_2O_3)$	14.9	7.0	4.1	3.9
Calcium oxide (CaO)[a]	3.1	3.6	3.8	0.1
Magnesium oxide (MgO)[a]	1.9	3.5	5.0	1.2
Sulfur trioxide (SO_3)[a]	0.0	0.1	1.8	0.0
Alkali content ($Na_2O + K_2O$)[a]	2.4	3.2	5.8	3.0
Percentage passing No. 325[b]	54.0	88.8	94.8	87.2
pH (pure material)[c]	8.91	8.82	8.14	4.17
Sulfate content (ppm)[d]	< 40	< 40	15,400	267
Specific surface area (m^2/gm)[e]	51.0	92.5	116.5	118.5
Cation exchange capacity (meq/100 gm)[f]	11.5	21.7	19.9	5.2
28-day UCS (kPa)	224	191	168	207

[a]X-ray Fluorescence analysis; [b]ASTM C 430; [c]ASTM D 6276; [d]OHD L-49 test method; [e]Ethylene glycol monoethyl ether method (Cerato and Lutenegger 2001); [f]EPA 9081 test method; No. 325: 0.045mm

Table 2.4 Chemical and Physical Properties of Stabilizers used in this Study

Chemical compound/Property	Percentage by weight, (%)		
	Lime	CFA	CKD
Silica (SiO_2)[a]	0.6	37.7	14.1
Alumina (Al_2O_3)[a]	0.4	17.3	3.1
Ferric oxide (Fe_2O_3)[a]	0.3	5.8	1.4
Silica/Sesquioxide ratio (SSR) $SiO_2/(Al_2O_3+Fe_2O_3)$	1.9	3.0	6.0
Calcium oxide (CaO)[a]	68.6	24.4	47
Calcium hydroxide ($Ca(OH)_2$)[a]	95.9**	…	…
Magnesium oxide (MgO)[a]	0.7	5.1	1.7
Sulfur trioxide (SO_3)[a]	0.1	1.2	4.4
Alkali content ($Na_2O + K_2O$)[a]	0.1	2.2	1.7
Loss on ignition[b]	31.8*	1.2	27
Free lime[b]	46.1	0.2	6.7
Percentage passing No. 325[c]	98.4	85.8	94.2
pH (pure material)[d]	12.58	11.83	12.55
Specific surface area (m^2/gm)[e]	17.0	6.0	12.0
28-day UCS (kPa)	…	708	17

[a]X-ray Fluorescence analysis; [b]ASTM C 114; [c]ASTM C 430; [d]ASTM D 6276; [e]Ethylene glycol monoethyl ether method (Cerato and Lutenegger 2001); UCS: Unconfined compressive strength; *$Ca(OH)_2$ decomposes at 512^{o}C; **Before ignition

Table 2.5 Variation of pH Values with Soil and Additive Type

Type of Additive	Additive Content (%)	P-soil		K-soil		V-soil		C-soil	
		pH value	% Increase[a]	pH value	% Increase[a]	pH value	% Increase[a]	pH value	% Increase[a]
Lime	0	8.91	---	8.82	---	8.14	---	4.17	---
	1	12.24	37.4	12.04	36.5	11.67	43.4	9.22	121.1
	3[b]	**12.43**	**39.5**	**12.49**	**41.6**	**12.41**	**52.5**	12.23	193.3
	5	12.45	39.7	12.50	41.7	12.49	53.4	**12.54**	**200.7**
	6	12.45	39.7	12.54	42.2	12.52	53.8	12.55	201.0
	7	12.46	39.8	12.57	42.5	12.52	53.8	12.55	201.0
	9	12.47	40.0	12.57	42.5	12.52	53.8	12.57	201.4
	100	12.58	41.2	12.58	42.6	12.58	54.5	12.58	201.7
CFA	0	8.91	---	8.82	---	8.14	---	4.17	---
	2.5	10.97	23.1	10.03	13.7	10.40	27.8	5.19	24.5
	5	11.30	26.8	10.83	22.8	10.85	33.3	5.93	42.2
	7.5	11.39	27.9	11.28	27.9	11.05	35.7	6.55	57.1
	10[b]	**11.50**	**29.1**	**11.42**	**29.5**	**11.14**	**36.8**	7.79	86.8
	12.5	11.59	30.0	11.50	30.4	11.15	37.0	8.32	99.5
	15	11.6	30.2	11.57	31.2	11.19	37.5	8.86	112.5
	17.5	11.62	30.4	11.61	31.6	11.38	39.8	9.47	127.1
	100	11.83	32.8	11.83	34.1	11.83	45.3	11.83	183.7
CKD	0	8.91	---	8.82	---	8.14	---	4.17	---
	2.5	11.35	27.4	11.11	26.0	10.99	35.0	7.05	69.1
	5	11.88	33.3	11.73	33.0	11.59	42.4	8.8	111.0
	7.5	12.09	35.7	12	36.1	11.79	44.8	10.11	142.4
	10[b]	**12.22**	**37.1**	**12.15**	**37.8**	**12.14**	**49.1**	10.88	160.9
	12.5	12.3	38.0	12.23	38.7	12.21	50.0	11.28	170.5
	15	12.36	38.7	12.3	39.5	12.31	51.2	11.62	178.7
	17.5	12.38	38.9	12.36	40.1	12.38	52.1	11.98	187.3
	100	12.55	40.9	12.55	42.3	12.55	54.2	12.55	201.0

[a]Increase in pH w.r.t. pH value of raw soil; [b]Bold values represent minimum additive content providing asymptotic behavior (< 1% increase)

Table 2.6 A Summary of OMC-MDD of Lime-, CFA- and CKD-P-soil Mixtures

Type of additive	Percentage of additive	OMC (%)	Maximum dry density	
			kN/m^3	pcf
Raw	0	13.1	17.8	113.4
Lime	3	14.7	17.1	108.7
	6	15.9	16.9	107.2
	9	16.5	16.6	105.9
CFA	5	14.0	17.8	113.5
	10	12.8	18.1	114.9
	15	11.7	18.0	114.7
CKD	5	14.8	17.4	110.5
	10	15.2	17.2	109.3
	15	15.3	17.1	108.6

1 pcf = 0.1572 kN/m^3; OMC: optimum moisture content; MDD: maximum dry density; CFA: class C fly ash; CKD: cement kiln dust

Table 2.7 A Summary of OMC-MDD of Lime-, CFA- and CKD-K-Soil Mixtures

Type of additive	Percentage of additive	OMC (%)	Maximum dry density	
			kN/m^3	pcf
Raw	0	16.5	17.4	110.6
Lime	3	16.1	17.0	108.4
	6	16.5	16.8	106.6
	9	18.5	16.3	103.8
CFA	5	13.0	17.4	110.8
	10	15.3	17.4	111.0
	15	15.1	17.5	111.5
CKD	5	16.9	17.3	110.2
	10	17.3	17.1	108.6
	15	17.6	16.9	107.8

1 pcf = 0.1572 kN/m^3; OMC: optimum moisture content; MDD: maximum dry density; CFA: class C fly ash; CKD: cement kiln dust

Table 2.8 A Summary of OMC-MDD of Lime-, CFA- and CKD-V-Soil Mixtures

Type of additive	Percentage of additive	OMC (%)	Maximum dry density	
			kN/m^3	pcf
Raw	0	23.0	16.0	101.9
Lime	3	25.4	15.6	99.5
	6	25.9	15.3	97.4
	9	26.8	14.9	95.0
CFA	5	22.6	16.0	101.6
	10	21.7	16.1	102.5
	15	21.2	16.2	102.9
CKD	5	24.1	15.7	100.1
	10	23.5	15.8	100.3
	15	23.1	15.8	100.7

1 pcf = 0.1572 kN/m^3; OMC: optimum moisture content; MDD: maximum dry density; CFA: class C fly ash; CKD: cement kiln dust

Table 2.9 A Summary of OMC-MDD of Lime-, CFA- and CKD-C-Soil Mixtures

Type of additive	Percentage of additive	OMC (%)	Maximum dry density	
			kN/m^3	pcf
Raw	0	20.3	16.3	103.7
Lime	3	22.0	16.0	101.5
	6	22.7	15.6	99.0
	9	23.8	15.3	97.3
CFA	5	20.0	16.3	103.5
	10	18.6	16.6	105.3
	15	16.6	16.4	104.1
CKD	5	21.6	16.1	102.3
	10	21.7	16.0	101.8
	15	21.9	15.9	101.4

1 pcf = 0.1572 kN/m^3; OMC: optimum moisture content; MDD: maximum dry density; CFA: class C fly ash; CKD: cement kiln dust

Table 2.10 Testing Sequence used for Resilient Modulus Test

Sequence Number	Confining Pressure (kPa)	Maximum Axial Stress (kPa)	Cyclic Stress (kPa)	Constant Stress (kPa)	No. of Load Applications
Conditioning	41	28	25	3	500
1	41	14	12	1	100
2	41	28	25	3	100
3	41	41	37	4	100
4	41	55	50	6	100
5	41	69	62	7	100
6	28	14	12	1	100
7	28	28	25	3	100
8	28	41	37	4	100
9	28	55	50	6	100
10	28	69	62	7	100
11	14	14	12	1	100
12	14	28	25	3	100
13	14	41	37	4	100
14	14	55	50	6	100
15	14	69	62	7	100

Table 2.11 A Summary of Resilient Modulus Values of Lime-Stabilized P-soil Specimens

σ_3	σ_d	M_r (MPa)											
(kPa)	(kPa)	Raw	SD	CV	3% Lime	SD	CV	6% Lime	SD	CV	9% Lime	SD	CV
41	12	181	4	2	1,104	91	8	1,298	95	7	1,388	121	9
41	25	153	3	2	856	65	8	1,091	90	8	1,120	102	9
41	37	137	2	2	694	78	11	815	64	8	860	92	11
41	50	127	2	2	615	78	13	708	48	7	737	71	10
41	62	120	2	2	550	69	13	637	33	5	650	45	7
28	12	161	3	2	1,176	60	5	808	80	10	1,255	131	10
28	25	133	2	2	799	72	9	934	71	8	882	125	14
28	37	120	2	1	647	76	12	679	29	4	706	102	14
28	50	114	2	1	570	73	13	625	26	4	642	65	10
28	62	110	2	2	533	66	12	592	27	5	613	47	8
14	12	146	3	2	1,092	80	7	981	18	2	1,261	187	15
14	25	116	2	2	740	58	8	990	3	0	844	102	12
14	37	105	2	2	597	69	12	695	1	0	698	98	14
14	50	99	2	2	532	66	12	629	3	0	614	69	11
14	62	96	1	2	504	62	12	627	10	2	585	49	8

1 psi = 6.89 kPa; 1 ksi = 6.89 MPa; SD: standard deviation; CV: coefficient of variation (%)

σ_d : deviator stress; σ_3 : confining pressure; M_r : resilient modulus (using internal LVDTs)

* Deformations are out of the measuring range of LVDTs

Table 2.12 A Summary of Resilient Modulus Values of Lime-Stabilized K-soil Specimens

σ_3	σ_d	M_r (MPa)											
(kPa)	(kPa)	Raw	SD	CV	3% Lime	SD	CV	6% Lime	SD	CV	9% Lime	SD	CV
41	12	97	1	1	1,174	41	4	1,382	128	9	929	27	3
41	25	83	1	2	1,130	36	3	1,206	44	4	813	12	1
41	37	68	1	2	1,101	42	4	1,063	34	3	755	10	1
41	50	57	1	3	1,069	56	5	987	19	2	725	2	0
41	62	50	2	3	1,027	59	6	926	15	2	680	8	1
28	12	92	1	1	1,107	18	2	1,254	109	9	828	28	3
28	25	77	2	2	1,117	29	3	1,108	34	3	770	28	4
28	37	65	2	3	1,055	43	4	990	21	2	736	4	1
28	50	57	2	3	1,029	61	6	958	18	2	700	9	1
28	62	51	1	3	1,034	65	6	922	17	2	677	11	2
14	12	90	1	1	1,179	48	4	1,209	96	8	832	49	6
14	25	75	2	3	1,090	42	4	1,115	50	4	772	21	3
14	37	63	2	3	1,062	58	5	1,006	23	2	723	8	1
14	50	55	2	4	1,040	58	6	941	19	2	699	9	1
14	62	50	2	4	1,042	62	6	918	15	2	667	11	2

1 psi = 6.89 kPa; 1 ksi = 6.89 MPa; SD: standard deviation; CV: coefficient of variation (%)

σ_d : deviator stress; σ_3 : confining pressure; M_r : resilient modulus (using internal LVDTs)

* Deformations are out of the measuring range of LVDTs

Table 2.13 A Summary of Resilient Modulus Values of Lime-Stabilized V-soil Specimens

σ_3	σ_d	M_r (MPa)											
(kPa)	(kPa)	Raw	SD	CV	3% Lime	SD	CV	6% Lime	SD	CV	9% Lime	SD	CV
41	12	145	8	6	958	68	7	821	25	3	745	22	3
41	25	126	1	1	941	41	4	772	23	3	706	14	2
41	37	108	1	1	916	7	1	740	20	3	700	19	3
41	50	94	2	2	911	4	0	710	12	2	682	22	3
41	62	83	2	3	876	11	1	717	8	1	651	20	3
28	12	127	6	5	1,049	63	6	843	18	2	719	23	3
28	25	103	0	0	922	15	2	750	15	2	698	22	3
28	37	90	2	2	909	4	0	729	16	2	676	19	3
28	50	83	3	3	896	8	1	703	14	2	662	26	4
28	62	77	3	3	869	6	1	678	13	2	645	21	3
14	12	119	6	5	1,010	32	3	820	26	3	710	44	6
14	25	95	0	0	939	7	1	756	14	2	683	20	3
14	37	83	2	2	898	9	1	724	17	2	668	22	3
14	50	75	3	3	883	14	2	699	15	2	650	24	4
14	62	71	3	4	868	10	1	684	10	1	643	29	5

1 psi = 6.89 kPa; 1 ksi = 6.89 MPa; SD: standard deviation; CV: coefficient of variation (%)

σ_d : deviator stress; σ_3 : confining pressure; M_r : resilient modulus (using internal LVDTs)

* Deformations are out of the measuring range of LVDTs

Table 2.14 A Summary of Resilient Modulus Values of Lime-Stabilized C-soil Specimens

σ_3	σ_d	M_r (MPa)											
(kPa)	(kPa)	Raw	SD	CV	3% Lime	SD	CV	6% Lime	SD	CV	9% Lime	SD	CV
41	12	137	1	1	293	7	2	573	67	12	421	20	5
41	25	129	1	1	277	5	2	502	36	7	388	11	3
41	37	117	1	1	257	5	2	472	32	7	360	7	2
41	50	106	1	1	237	4	2	445	28	6	334	5	2
41	62	96	1	1	220	4	2	422	27	6	310	5	2
28	12	130	1	1	288	4	2	555	51	9	409	10	2
28	25	123	1	1	261	5	2	491	31	6	375	5	1
28	37	115	1	1	242	5	2	461	28	6	339	7	2
28	50	104	1	1	226	4	2	435	27	6	326	5	2
28	62	96	1	1	217	4	2	423	27	6	307	5	2
14	12	117	1	1	283	10	3	519	34	7	400	12	3
14	25	114	2	1	258	5	2	473	28	6	359	8	2
14	37	106	2	2	237	4	2	448	27	6	334	6	2
14	50	99	2	2	223	5	2	431	29	7	319	6	2
14	62	91	1	1	213	5	2	418	28	7	298	7	2

1 psi = 6.89 kPa; 1 ksi = 6.89 MPa; SD: standard deviation; CV: coefficient of variation (%)

σ_d : deviator stress; σ_3 : confining pressure; M_r : resilient modulus (using internal LVDTs)

* Deformations are out of the measuring range of LVDTs

Table 2.15 A Summary of Resilient Modulus Values of CFA-Stabilized P-soil Specimens

σ_3	σ_d	M_r (MPa)											
(kPa)	(kPa)	Raw	SD	CV	5% CFA	SD	CV	10% CFA	SD	CV	15% CFA	SD	CV
41	12	181	4	2	280	7	2	818	83	10	2,435	234	10
41	25	153	3	2	255	6	2	642	28	4	2,150	151	7
41	37	137	2	2	230	6	2	587	17	3	1,394	127	9
41	50	127	2	2	212	5	3	553	11	2	1,155	16	1
41	62	120	2	2	197	5	2	520	9	2	1,038	17	2
28	12	161	3	2	246	7	3	746	85	11	2,221	198	9
28	25	133	2	2	209	5	3	580	24	4	1,756	187	11
28	37	120	2	1	190	5	3	539	17	3	1,348	120	9
28	50	114	2	1	181	5	3	520	14	3	1,148	115	10
28	62	110	2	2	178	5	3	503	11	2	1,038	116	11
14	12	146	3	2	214	5	2	730	98	13	1,961	176	9
14	25	116	2	2	177	4	2	567	34	6	1,923	142	7
14	37	105	2	2	162	4	2	517	21	4	1,359	31	2
14	50	99	2	2	155	4	2	493	14	3	1,131	25	2
14	62	96	1	2	154	4	3	484	12	2	1,037	17	2

1 psi = 6.89 kPa; 1 ksi = 6.89 MPa; SD: standard deviation; CV: coefficient of variation (%)

σ_d : deviator stress; σ_3 : confining pressure; M_r : resilient modulus (using internal LVDTs)

* Deformations are out of the measuring range of LVDTs

Table 2.16 A Summary of Resilient Modulus Values of CFA-Stabilized K-soil Specimens

σ_3	σ_d	M_r (MPa)											
(kPa)	(kPa)	Raw	SD	CV	5% CFA	SD	CV	10% CFA	SD	CV	15% CFA	SD	CV
41	12	97	1	1	605	54	9	1,003	49	5	1,086	35	3
41	25	83	1	2	496	11	2	899	22	2	978	31	3
41	37	68	1	2	450	11	3	876	20	2	954	35	4
41	50	57	1	3	416	13	3	851	15	2	949	33	3
41	62	50	2	3	389	13	3	846	11	1	924	29	3
28	12	92	1	1	540	29	5	889	10	1	1,034	44	4
28	25	77	2	2	431	10	2	882	14	2	975	34	3
28	37	65	2	3	397	14	3	854	7	1	952	30	3
28	50	57	2	3	373	14	4	847	17	2	917	28	3
28	62	51	1	3	366	13	4	842	9	1	924	26	3
14	12	90	1	1	498	29	6	926	39	4	967	35	4
14	25	75	2	3	412	11	3	898	10	1	970	32	3
14	37	63	2	3	373	14	4	879	10	1	931	28	3
14	50	55	2	4	352	15	4	857	13	1	919	22	2
14	62	50	2	4	340	16	5	843	13	2	945	9	1

1 psi = 6.89 kPa; 1 ksi = 6.89 MPa; SD: standard deviation; CV: coefficient of variation (%)

σ_d : deviator stress; σ_3 : confining pressure; M_r : resilient modulus (using internal LVDTs)

* Deformations are out of the measuring range of LVDTs

Table 2.17 A Summary of Resilient Modulus Values of CFA-Stabilized V-soil Specimens

σ_3	σ_d	M_r (MPa)											
(kPa)	(kPa)	Raw	SD	CV	5% CFA	SD	CV	10% CFA	SD	CV	15% CFA	SD	CV
41	12	145	8	6	750	72	10	1,092	64	6	1,255	66	5
41	25	126	1	1	629	24	4	1,013	29	3	1,253	62	5
41	37	108	1	1	586	16	3	995	26	3	1,169	20	2
41	50	94	2	2	549	13	2	957	23	2	1,180	10	1
41	62	83	2	3	527	10	2	935	24	3	1,145	23	2
28	12	127	6	5	719	70	10	1,104	70	6	1,212	89	7
28	25	103	0	0	588	19	3	1,004	42	4	1,168	4	0
28	37	90	2	2	558	15	3	964	28	3	1,148	16	1
28	50	83	3	3	532	11	2	934	27	3	1,142	16	1
28	62	77	3	3	514	9	2	931	26	3	1,151	4	0
14	12	119	6	5	661	53	8	1,183	86	7	1,203	139	12
14	25	95	0	0	572	19	3	996	46	5	1,145	53	5
14	37	83	2	2	545	13	2	957	34	4	1,150	22	2
14	50	75	3	3	525	10	2	940	27	3	1,141	25	2
14	62	71	3	4	510	9	2	920	28	3	1,136	14	1

1 psi = 6.89 kPa; 1 ksi = 6.89 MPa; SD: standard deviation; CV: coefficient of variation (%)

σ_d : deviator stress; σ_3 : confining pressure; M_r : resilient modulus (using internal LVDTs)

* Deformations are out of the measuring range of LVDTs

Table 2.18 A Summary of Resilient Modulus Values of CFA-Stabilized C-soil Specimens

σ_3	σ_d	M_r (MPa)											
(kPa)	(kPa)	Raw	SD	CV	5% CFA	SD	CV	10% CFA	SD	CV	15% CFA	SD	CV
41	12	137	1	1	241	10	4	290	12	4	359	11	3
41	25	129	1	1	225	11	5	274	10	4	354	11	3
41	37	117	1	1	205	11	5	256	10	4	331	9	3
41	50	106	1	1	190	10	5	240	9	4	313	9	3
41	62	96	1	1	176	10	6	228	10	4	295	7	2
28	12	130	1	1	229	12	5	276	10	4	331	15	5
28	25	123	1	1	206	11	5	252	10	4	311	10	3
28	37	115	1	1	189	11	6	236	11	5	295	7	2
28	50	104	1	1	177	10	6	223	11	5	285	7	2
28	62	96	1	1	168	10	6	215	10	5	276	6	2
14	12	117	1	1	218	13	6	267	15	6	307	9	3
14	25	114	2	1	195	11	6	238	12	5	293	9	3
14	37	106	2	2	180	12	6	222	12	6	275	5	2
14	50	99	2	2	168	11	7	212	13	6	263	4	2
14	62	91	1	1	160	11	7	205	12	6	258	4	2

1 psi = 6.89 kPa; 1 ksi = 6.89 MPa; SD: standard deviation; CV: coefficient of variation (%)

σ_d : deviator stress; σ_3 : confining pressure; M_r : resilient modulus (using internal LVDTs)

* Deformations are out of the measuring range of LVDTs

Table 2.19 A Summary of Resilient Modulus Values of CKD-Stabilized P-soil Specimens

σ_3	σ_d	M_r (MPa)											
(kPa)	(kPa)	Raw	SD	CV	5% CKD	SD	CV	10% CKD	SD	CV	15% CKD	SD	CV
41	12	181	4	2	666	52	8	*	*	*	*	*	*
41	25	153	3	2	734	21	3	2,010	359	18	2,613	365	14
41	37	137	2	2	531	14	3	1,784	202	11	2,563	229	9
41	50	127	2	2	456	11	2	1,627	236	14	2,428	204	8
41	62	120	2	2	409	8	2	1,495	147	10	2,389	136	6
28	12	161	3	2	673	49	7	*	*	*	*	*	*
28	25	133	2	2	601	18	3	1,969	257	13	2,549	344	14
28	37	120	2	1	477	12	2	1,840	199	11	2,511	175	7
28	50	114	2	1	425	10	2	1,619	132	8	2,400	170	7
28	62	110	2	2	400	8	2	1,493	157	10	2,328	165	7
14	12	146	3	2	662	52	8	*	*	*	*	*	*
14	25	116	2	2	617	19	3	1,916	232	12	2,532	357	14
14	37	105	2	2	465	11	2	1,747	148	8	2,502	253	10
14	50	99	2	2	418	10	2	1,543	126	8	2,337	193	8
14	62	96	1	2	391	8	2	1,488	125	8	2,333	161	7

1 psi = 6.89 kPa; 1 ksi = 6.89 MPa; SD: standard deviation; CV: coefficient of variation (%)

σ_d : deviator stress; σ_3 : confining pressure; M_r : resilient modulus (using internal LVDTs)

* Deformations are out of the measuring range of LVDTs

Table 2.20 A Summary of Resilient Modulus Values of CKD-Stabilized K-soil Specimens

σ_3	σ_d	M_r (MPa)											
(kPa)	(kPa)	Raw	SD	CV	5% CKD	SD	CV	10% CKD	SD	CV	15% CKD	SD	CV
41	12	97	1	1	355	36	10	1,264	93	7	*	*	*
41	25	83	1	2	344	29	9	1,096	51	5	1,973	239	12
41	37	68	1	2	322	25	8	1,118	50	4	1,926	156	8
41	50	57	1	3	303	23	7	1,095	41	4	1,894	59	3
41	62	50	2	3	285	20	7	1,076	64	6	1,885	55	3
28	12	92	1	1	341	24	7	1,226	89	7	*	*	*
28	25	77	2	2	332	24	7	1,132	53	5	1,944	134	7
28	37	65	2	3	309	23	7	1,111	30	3	1,910	147	8
28	50	57	2	3	293	20	7	1,070	39	4	1,854	40	2
28	62	51	1	3	283	21	7	1,080	47	4	1,829	61	3
14	12	90	1	1	339	32	9	1,201	99	8	*	*	*
14	25	75	2	3	323	23	7	1,180	28	2	1,928	280	15
14	37	63	2	3	306	21	7	1,084	22	2	1,862	269	14
14	50	55	2	4	290	20	7	1,073	34	3	1,845	133	7
14	62	50	2	4	281	21	7	1,086	39	4	1,827	50	3

1 psi = 6.89 kPa; 1 ksi = 6.89 MPa; SD: standard deviation; CV: coefficient of variation (%)

σ_d : deviator stress; σ_3 : confining pressure; M_r : resilient modulus (using internal LVDTs)

* Deformations are out of the measuring range of LVDTs

Table 2.21 A Summary of Resilient Modulus Values of CKD-Stabilized V-soil Specimens

σ_3	σ_d	M_r (MPa)											
(kPa)	(kPa)	Raw	SD	CV	5% CKD	SD	CV	10% CKD	SD	CV	15% CKD	SD	CV
41	12	145	8	6	462	18	4	2151	213	10	*	*	*
41	25	126	1	1	427	17	4	1660	158	10	1982	208	10
41	37	108	1	1	389	16	4	1633	172	11	1962	202	10
41	50	94	2	2	356	16	5	1551	110	7	1934	198	10
41	62	83	2	3	326	16	5	1547	127	8	1881	182	10
28	12	127	6	5	413	18	4	2140	192	9	*	*	*
28	25	103	0	0	378	17	5	1635	177	11	1925	77	4
28	37	90	2	2	354	18	5	1554	113	7	1839	197	11
28	50	83	3	3	335	17	5	1569	149	9	1825	133	7
28	62	77	3	3	318	17	5	1552	127	8	1800	180	10
14	12	119	6	5	400	19	5	2065	178	9	*	*	*
14	25	95	0	0	376	21	6	1608	146	9	1892	29	2
14	37	83	2	2	346	19	6	1577	170	11	1869	194	10
14	50	75	3	3	324	19	6	1572	122	8	1821	202	11
14	62	71	3	4	310	18	6	1545	132	9	1793	197	11

1 psi = 6.89 kPa; 1 ksi = 6.89 MPa; SD: standard deviation; CV: coefficient of variation (%)

σ_d : deviator stress; σ_3 : confining pressure; M_r : resilient modulus (using internal LVDTs)

* Deformations are out of the measuring range of LVDTs

Table 2.22 A Summary of Resilient Modulus Values of CKD-Stabilized C-soil Specimens

σ_3	σ_d	M_r (MPa)											
(kPa)	(kPa)	Raw	SD	CV	5% CKD	SD	CV	10% CKD	SD	CV	15% CKD	SD	CV
41	12	137	1	1	251	19	7	434	38	9	901	120	13
41	25	129	1	1	230	17	7	417	34	8	858	55	6
41	37	117	1	1	205	17	8	395	36	9	844	33	4
41	50	106	1	1	186	15	8	376	36	10	814	31	4
41	62	96	1	1	169	13	7	355	35	10	798	26	3
28	12	130	1	1	238	20	8	412	35	8	933	98	11
28	25	123	1	1	208	16	8	391	34	9	897	47	5
28	37	115	1	1	189	15	8	376	36	10	841	44	5
28	50	104	1	1	173	15	9	361	37	10	826	31	4
28	62	96	1	1	162	14	9	348	36	10	804	28	3
14	12	117	1	1	226	19	8	413	31	7	927	74	8
14	25	114	2	1	201	19	9	386	38	10	899	73	8
14	37	106	2	2	179	17	9	370	38	10	874	61	7
14	50	99	2	2	165	16	10	355	38	11	848	45	5
14	62	91	1	1	154	15	10	344	38	11	822	44	5

1 psi = 6.89 kPa; 1 ksi = 6.89 MPa; SD: standard deviation; CV: coefficient of variation (%)

σ_d : deviator stress; σ_3 : confining pressure; M_r : resilient modulus (using internal LVDTs)

* Deformations are out of the measuring range of LVDTs

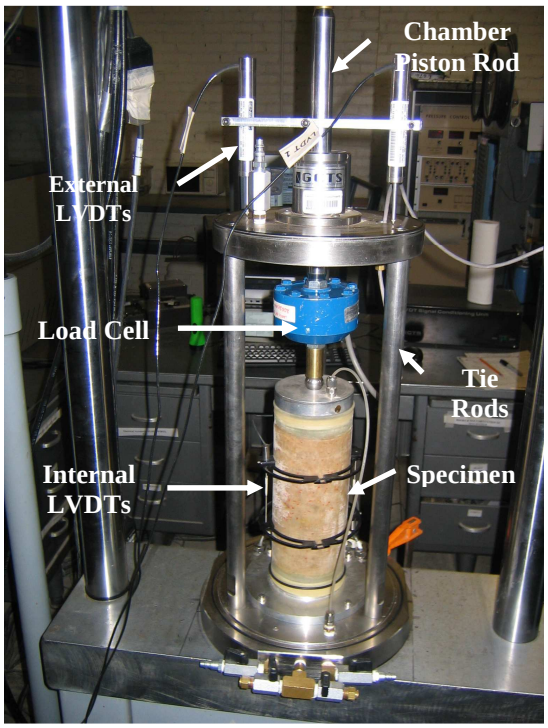

Figure 2.1 Setup for Resilient Modulus Test (Without Pressure Chamber)

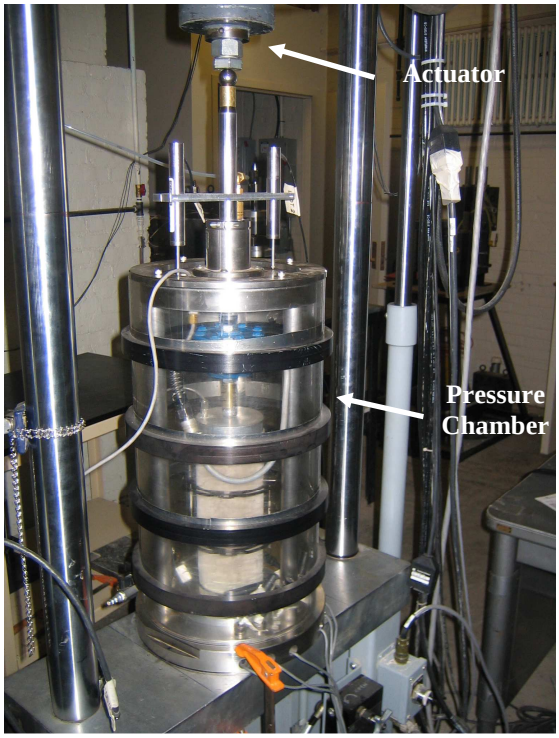

Figure 2.2 Setup for Resilient Modulus Test (With Pressure Chamber)

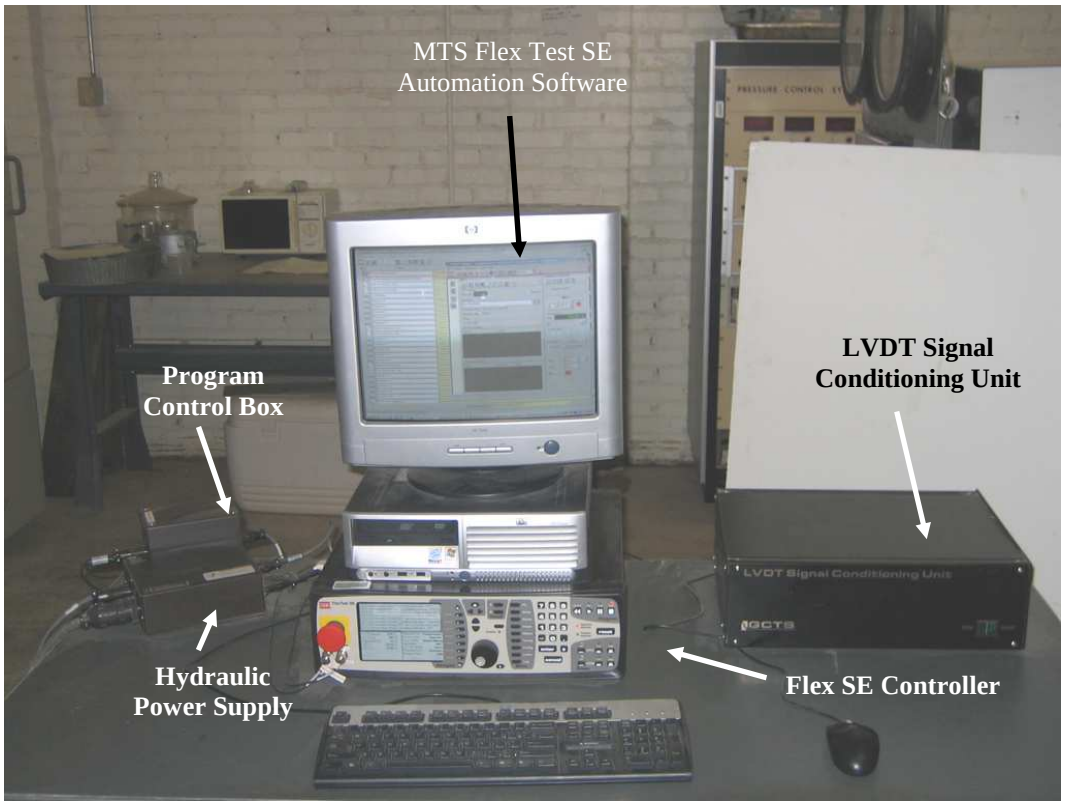

Figure 2.3 MTS Digital Control System and Computer

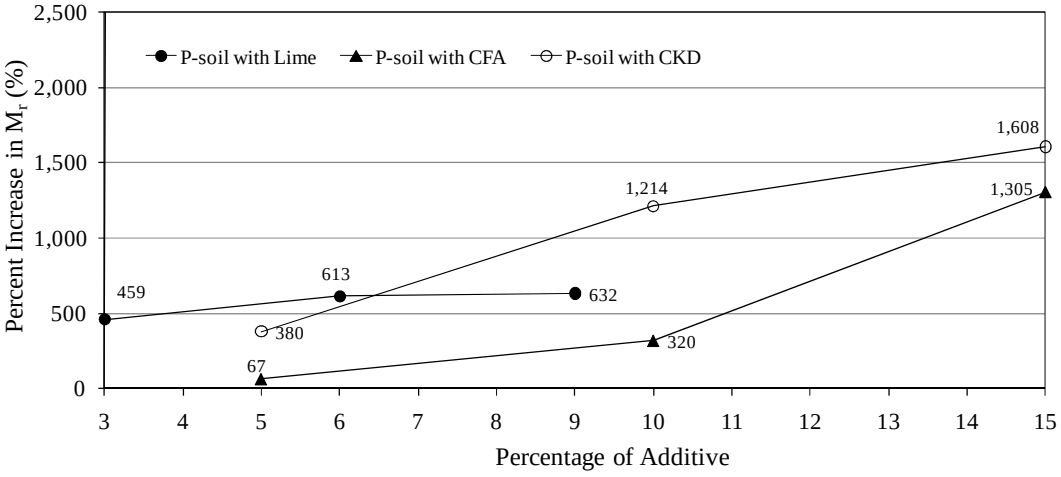

Figure 2.4 Improvement of M_r Values for P-soil

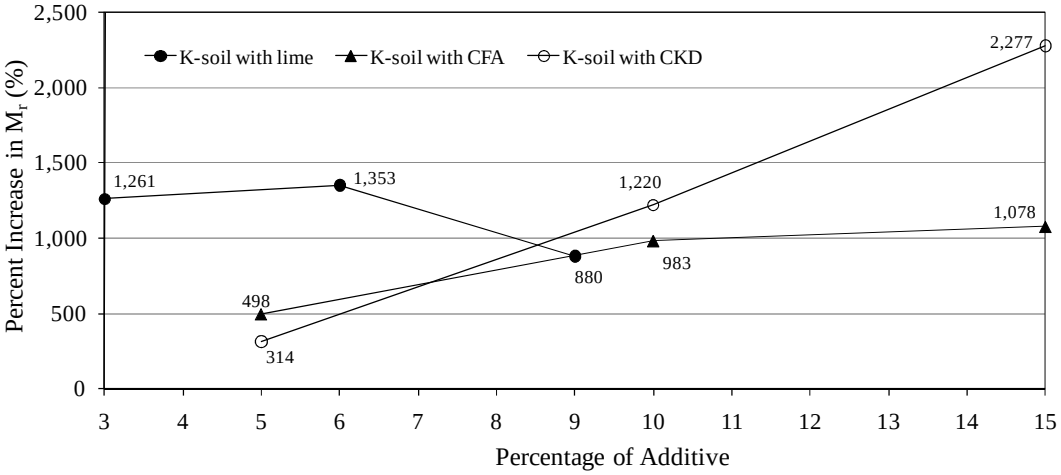

Figure 2.5 Improvement of M_r Values for K-soil

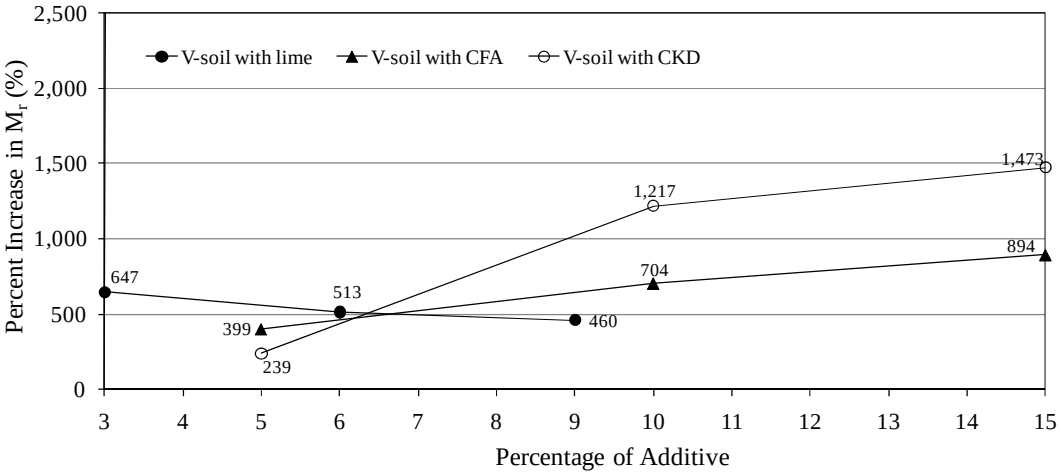

Figure 2.6 Improvement of M_r Values for V-soil

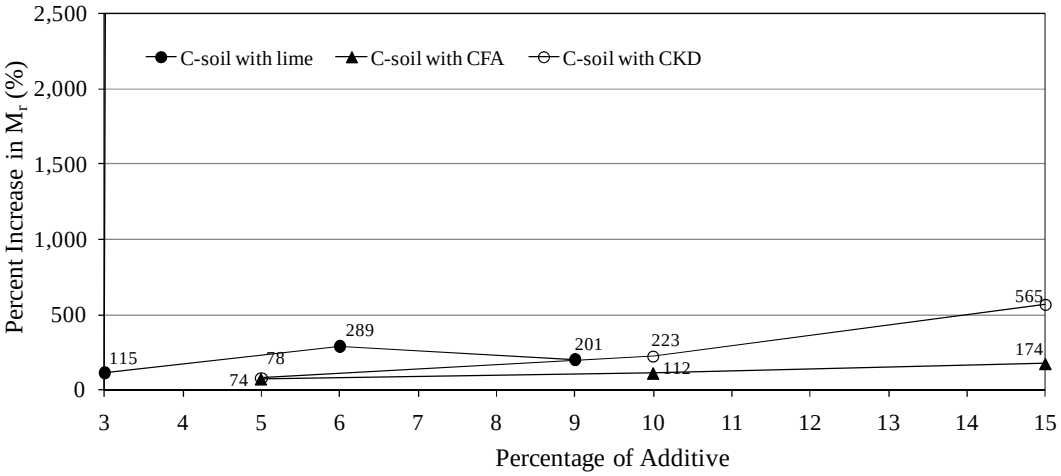

Figure 2.7 Improvement of M_r Values for C-soil

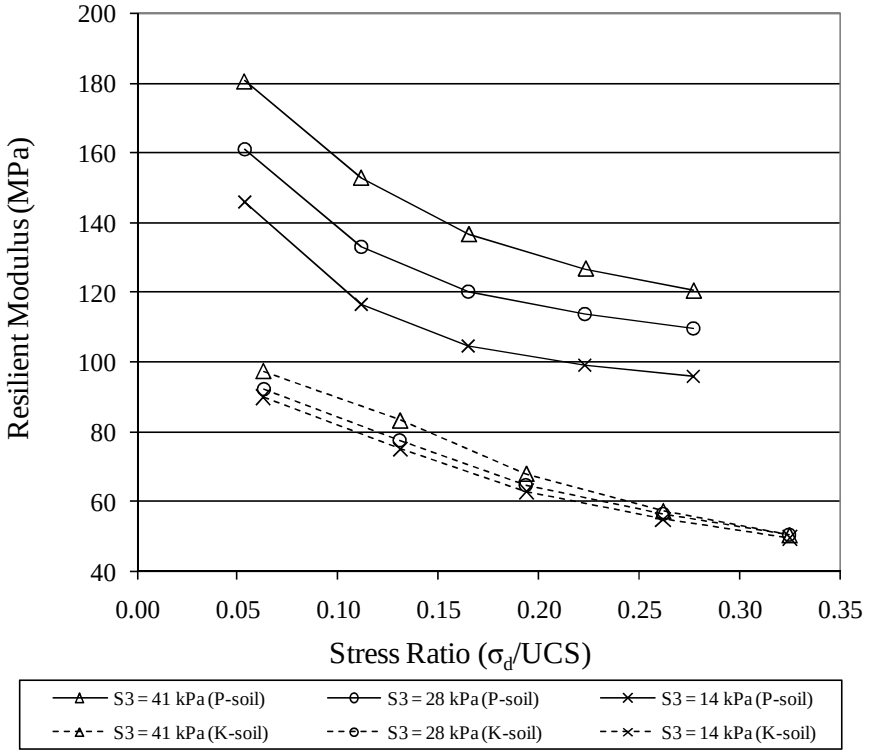

Figure 2.8 Effect of Stress Level on M_r Values of Raw Soil

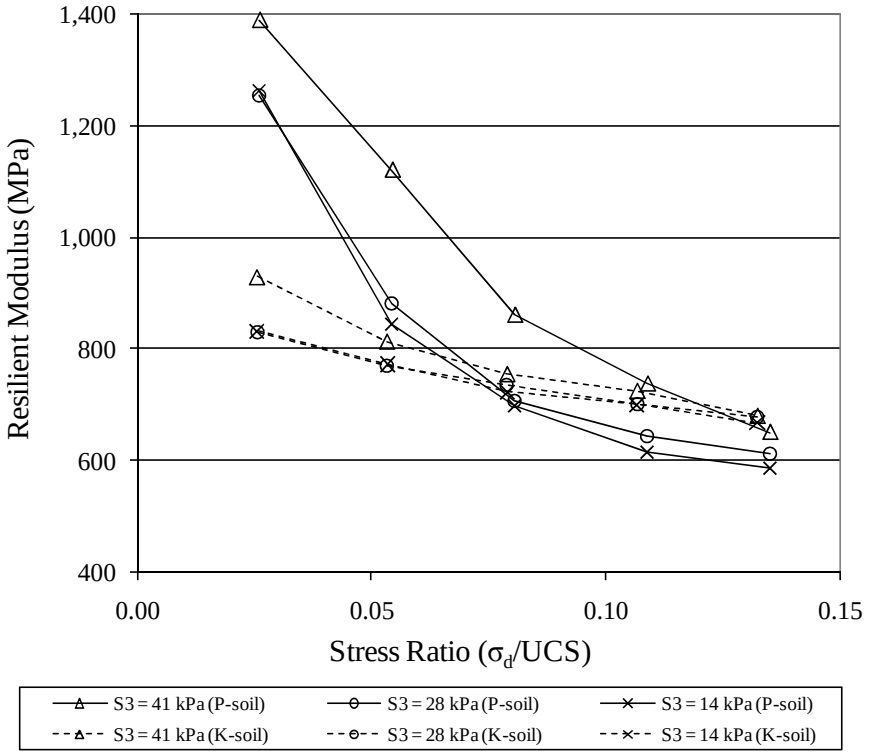

Figure 2.9 Effect of Stress Level on M_r Values of 9% Lime-Stabilized Soil

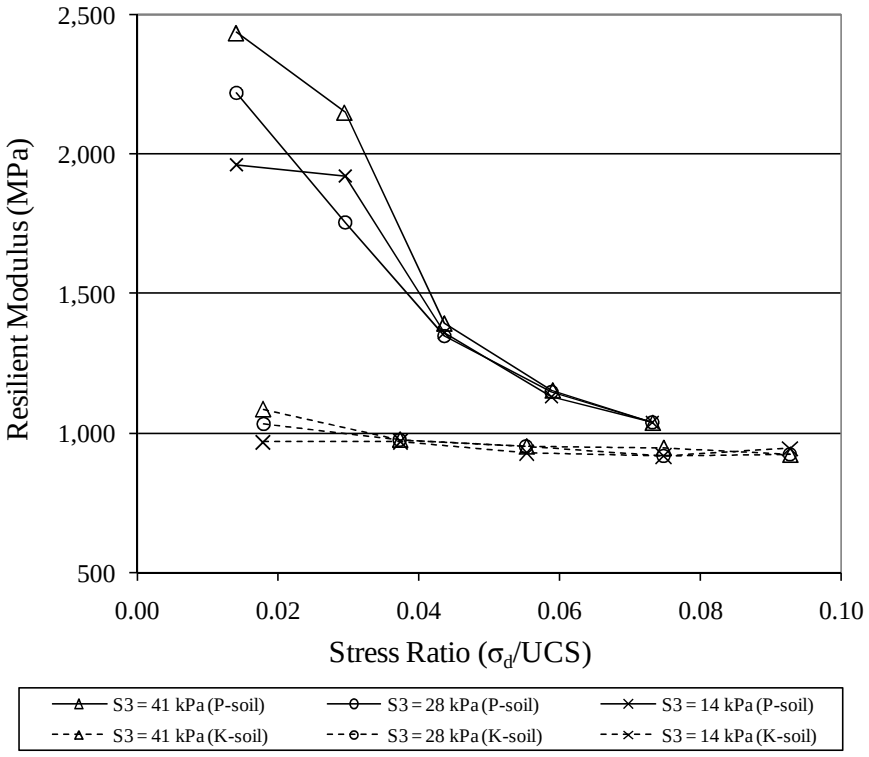

Figure 2.10 Effect of Stress Level on M_r Values of 15% CFA-Stabilized Soil

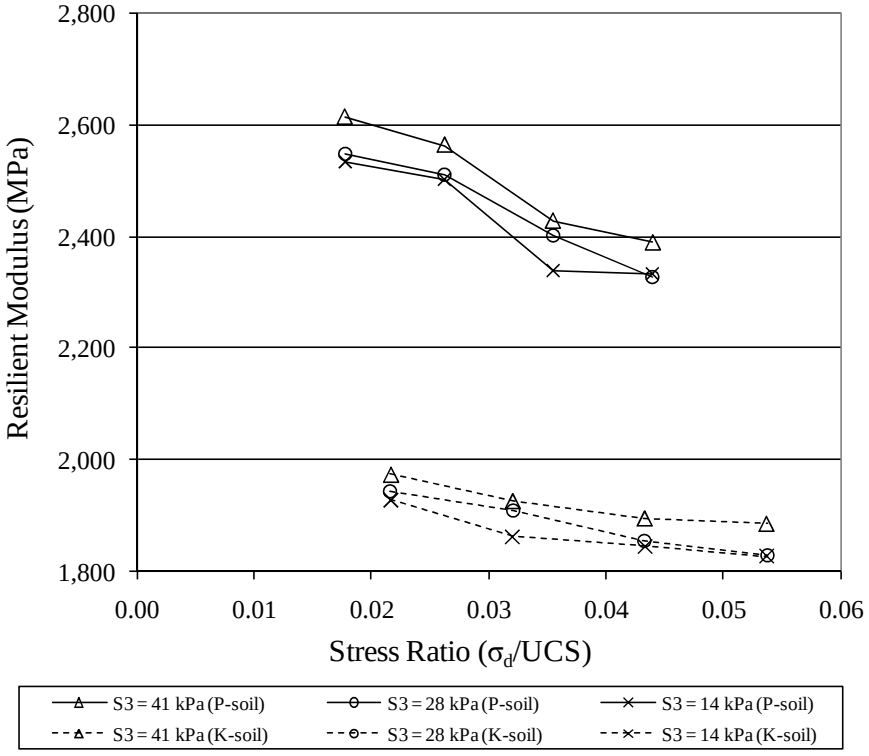

Figure 2.11 Effect of Stress Level on M_r Values of 15% CKD-Stabilized Soil

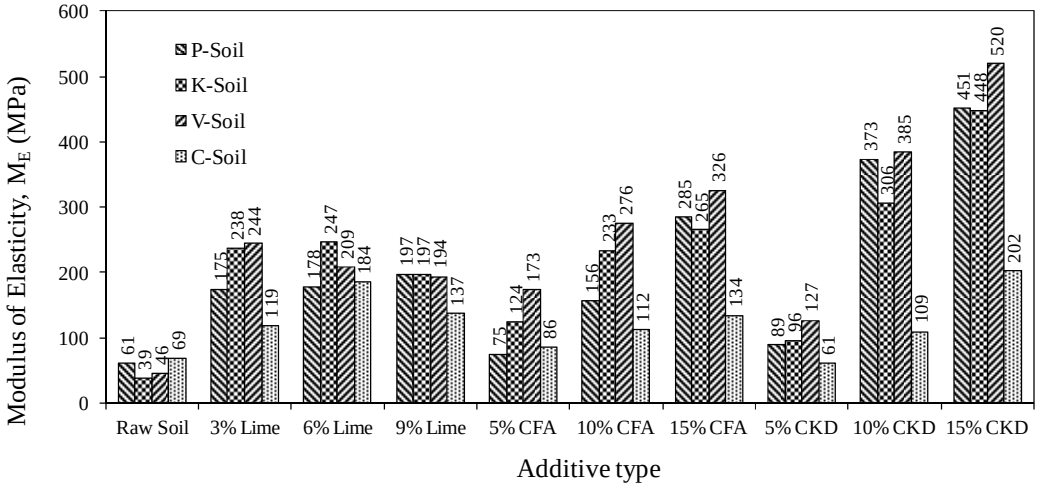

Figure 2.12 Variation of M_E Values with Soil and Additive Type

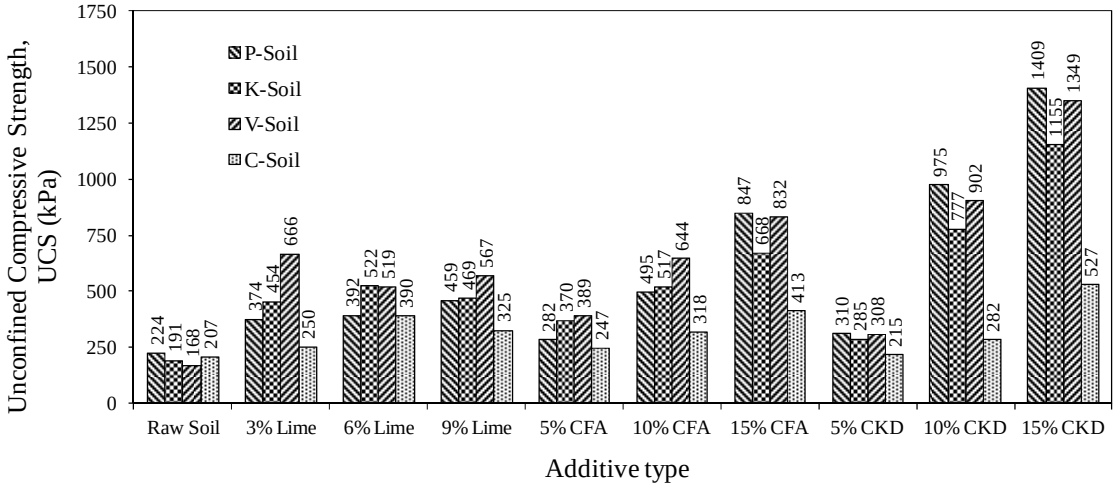

Figure 2.13 Variation of UCS Values with Soil and Additive Type

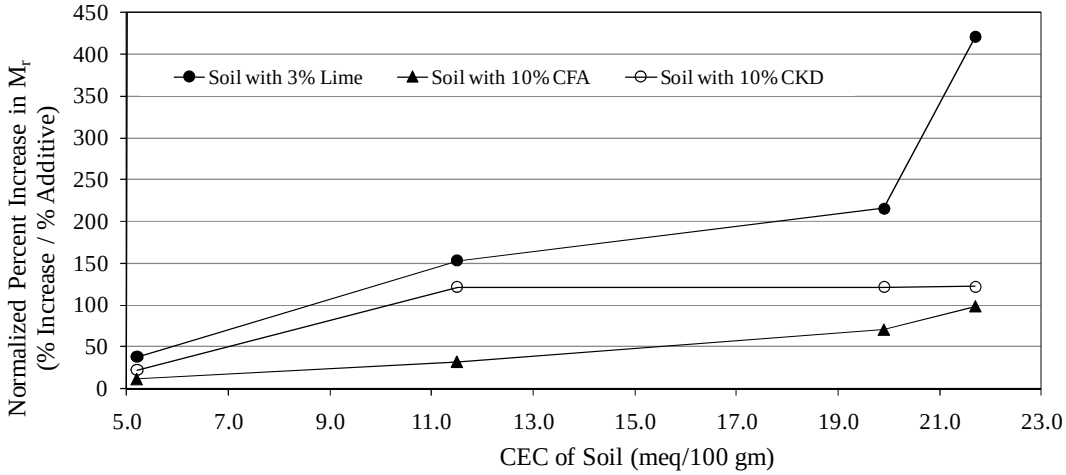

Figure 2.14 Variation of Normalized Percent Increase in M_r Values with Cation Exchange Capacity

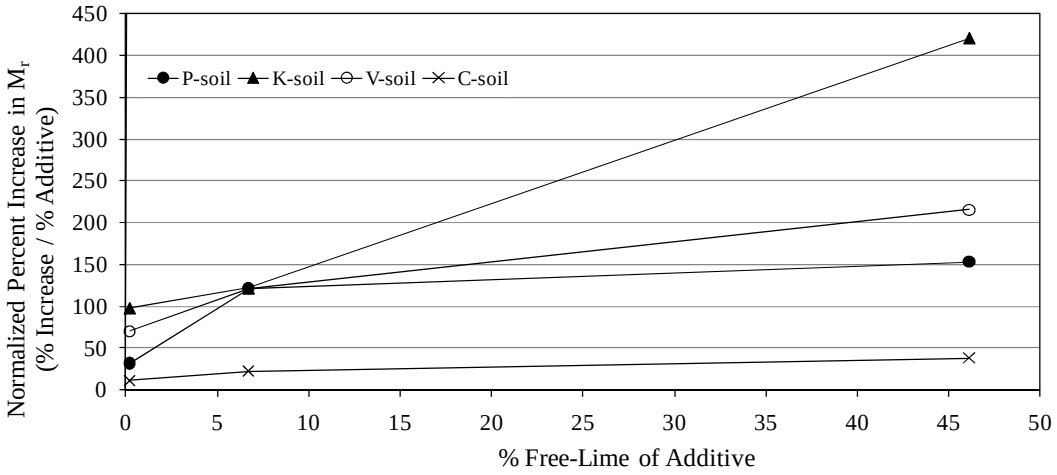

Figure 2.15 Variation of Normalized Percent Increase in M_r Values with Percent Free-Lime Content of Additive

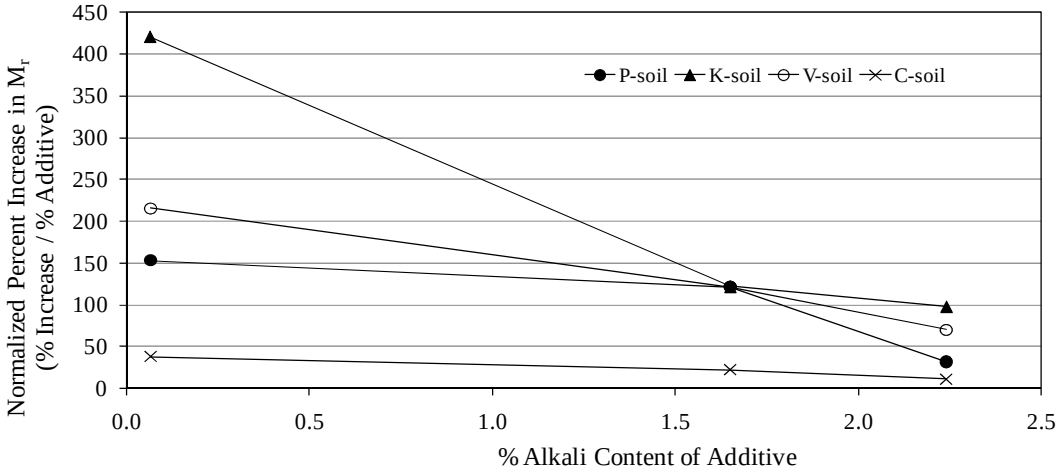

Figure 2.16 Variation of Normalized Percent Increase in M_r Values with Percent Alkali Content of Additive

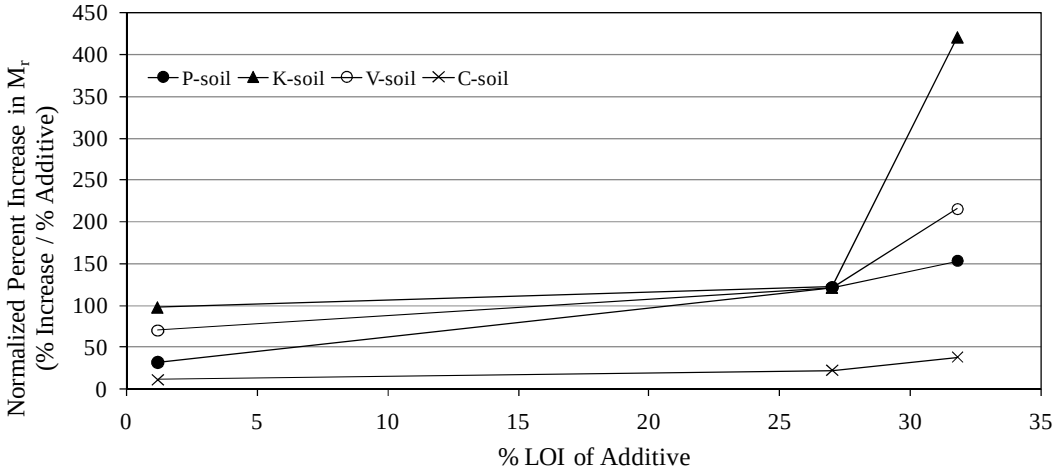

Figure 2.17 Variation of Normalized Percent Increase in M_r Values with Loss on Ignition Value of Additive

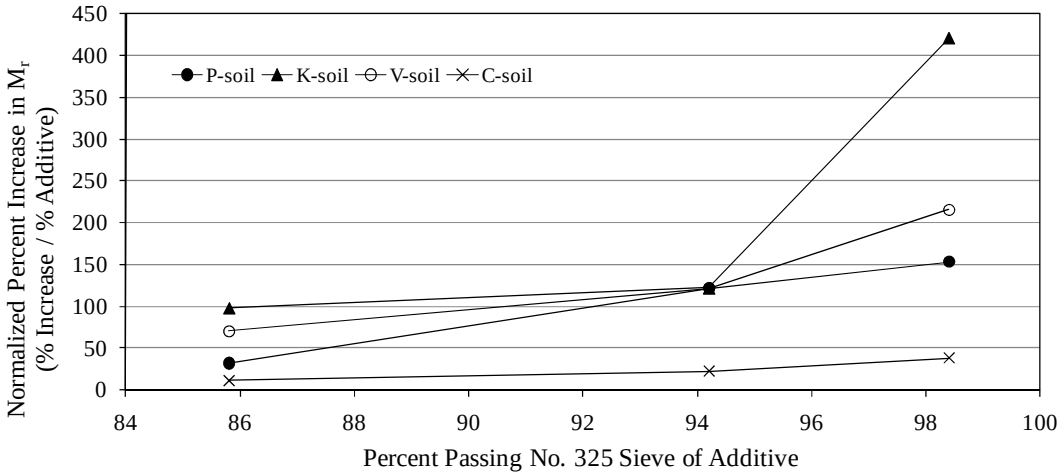

Figure 2.18 Variation of Normalized Percent Increase in M_r Values with Percent Passing No. 325 Sieve of Additive

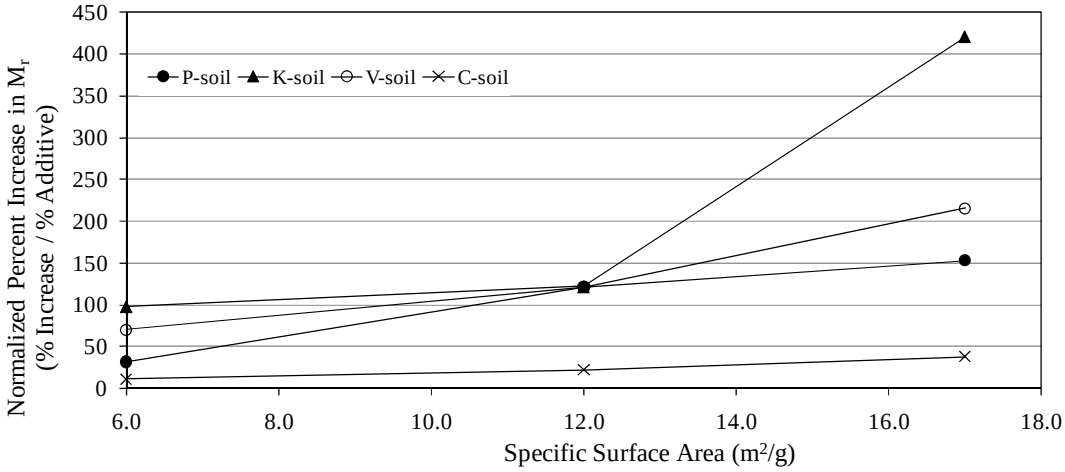

Figure 2.19 Variation of Normalized Percent Increase in M_r Values with Specific Surface Area of Additive

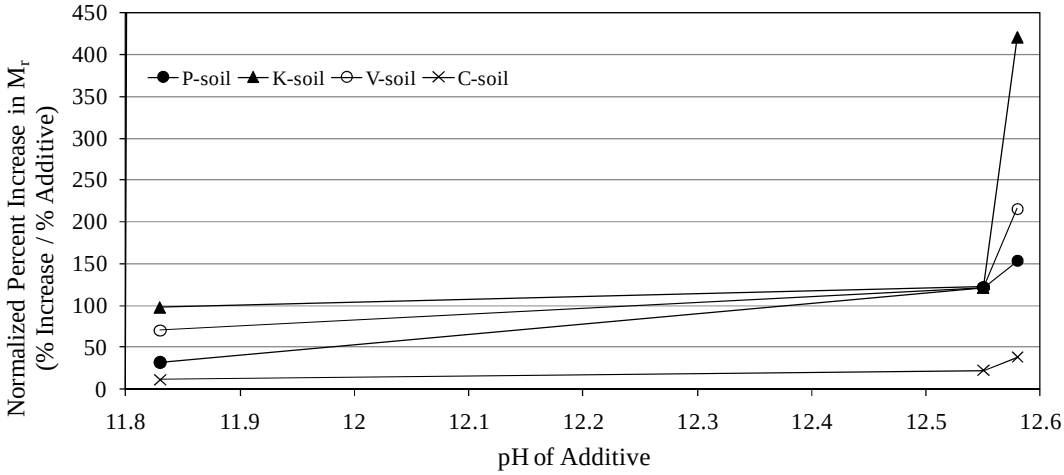

Figure 2.20 Variation of Normalized Percent Increase in M_r Values with pH of Additive

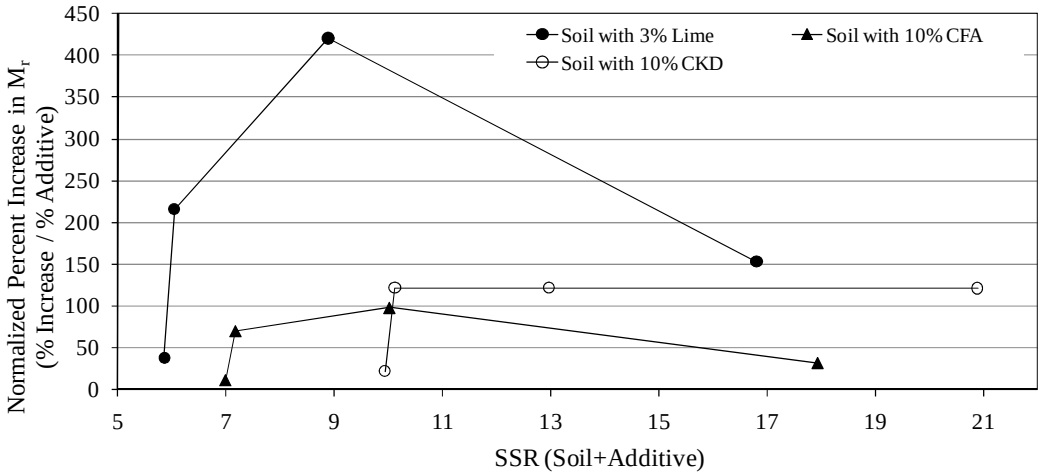

Figure 2.21 Variation of Normalized Percent Increase in M_r Values with Combined SSR Value of Soil-Additive Mixture

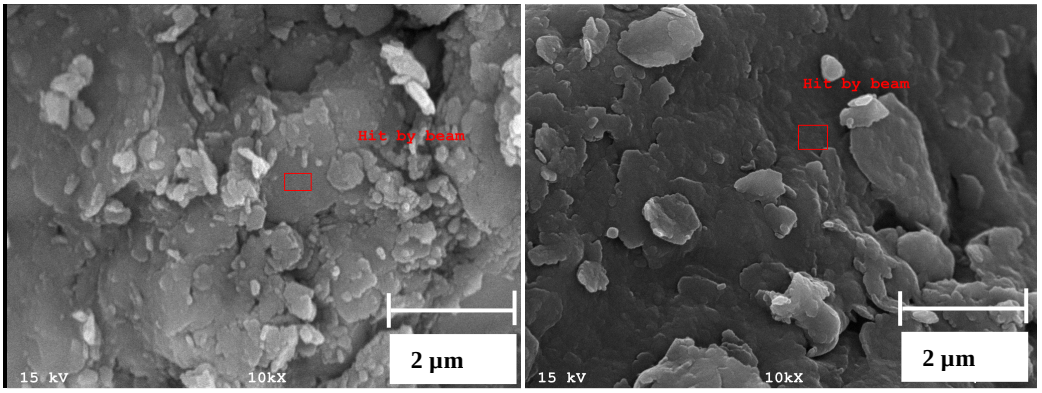

(a) (b)

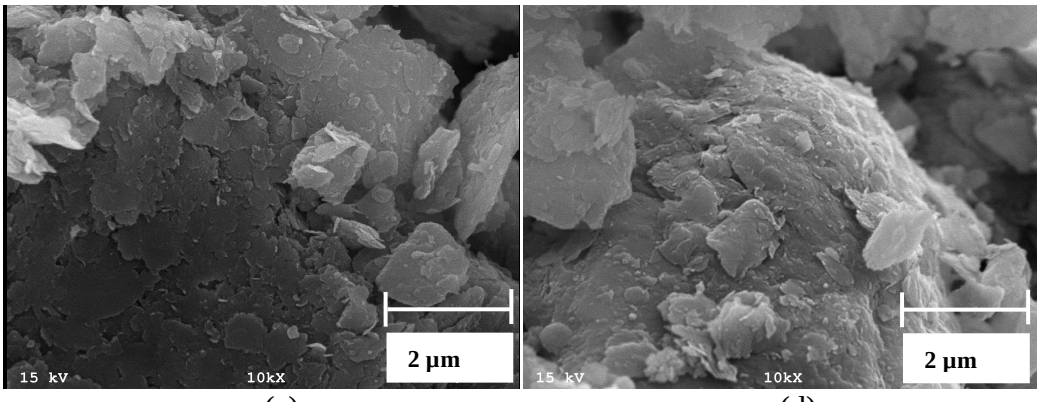

(c) (d)

Figure 2.22 SEM Micrographs of Raw (a) P-, (b) K-, (c) V-, and (d) C-Soil Specimens

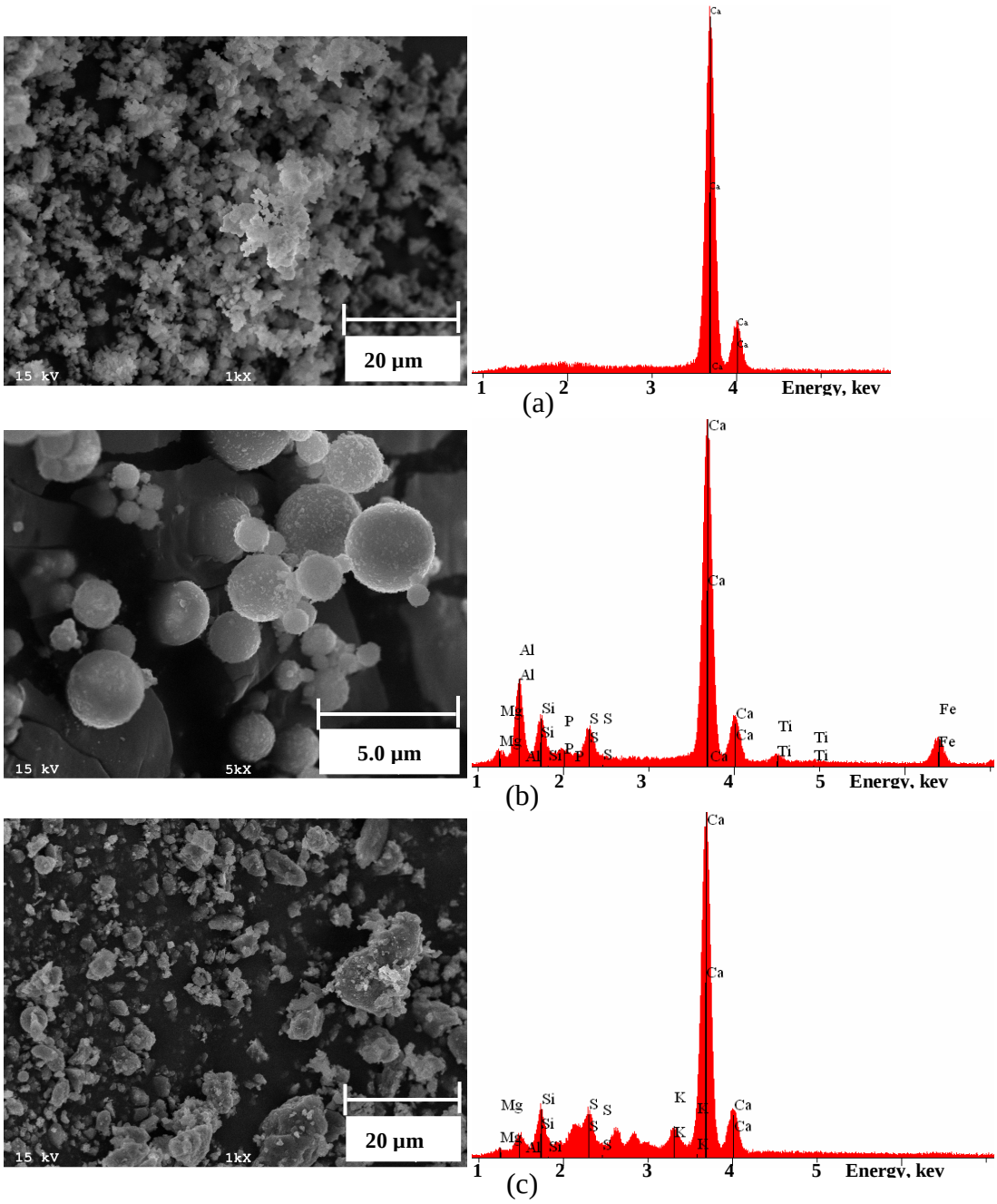

Figure 2.23 SEM/EDS of Raw (a) Lime, (b) CFA, and (c) CKD Powder

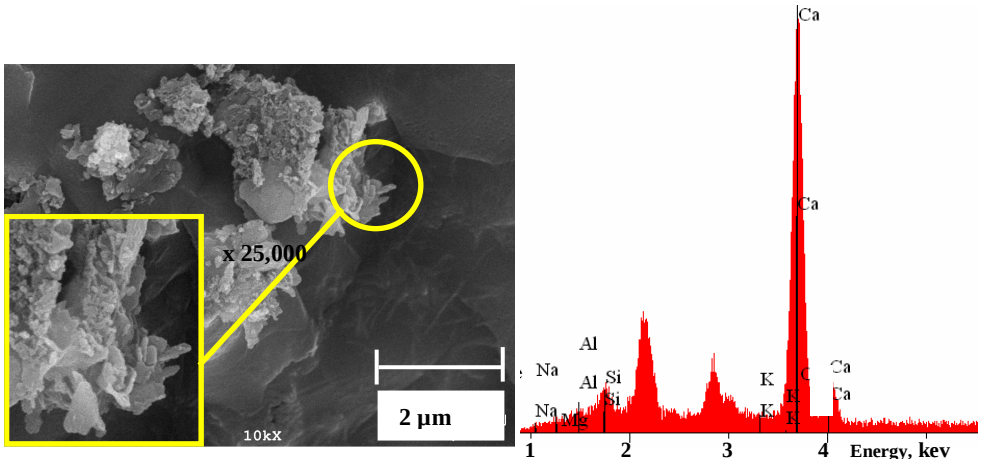

(a) Calcium-Silicate-Hydrate (C-S-H)

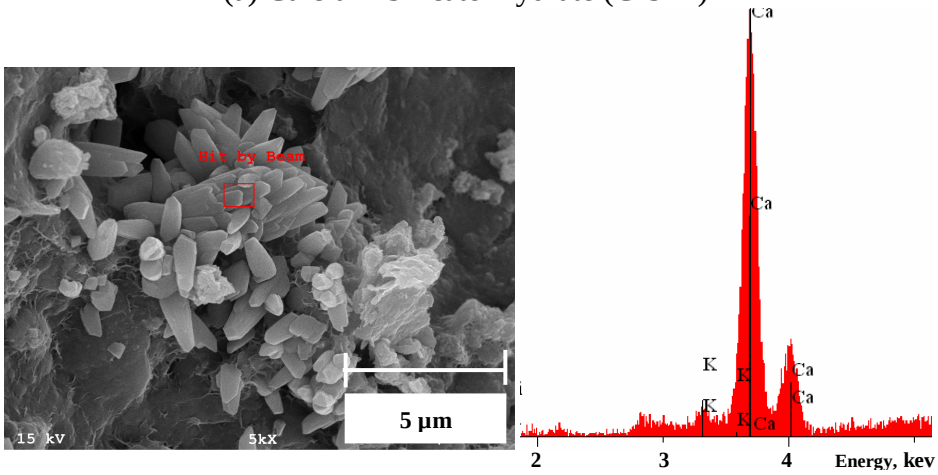

(b) Calcium Hydroxide (CH)

Figure 2.24 SEM Micrographs of 28-Day Cured 9% Lime-Stabilized C-Soil Specimen

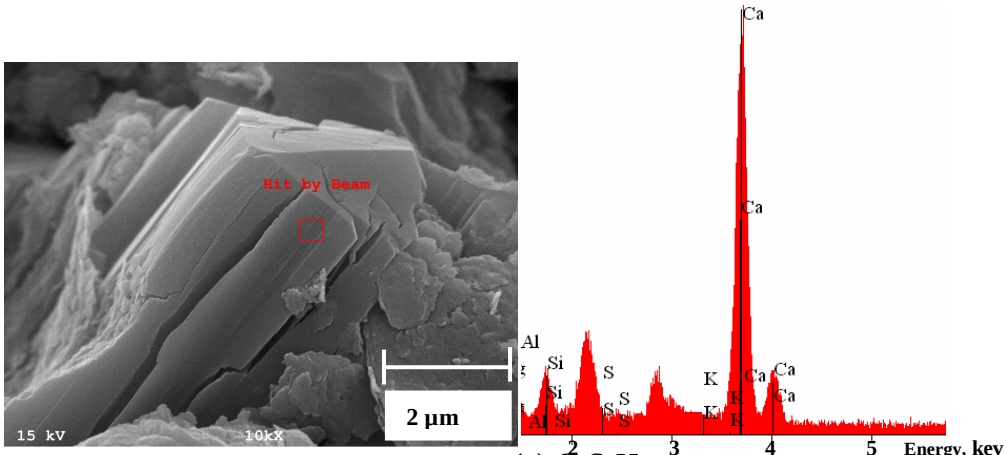

(a) C-S-H

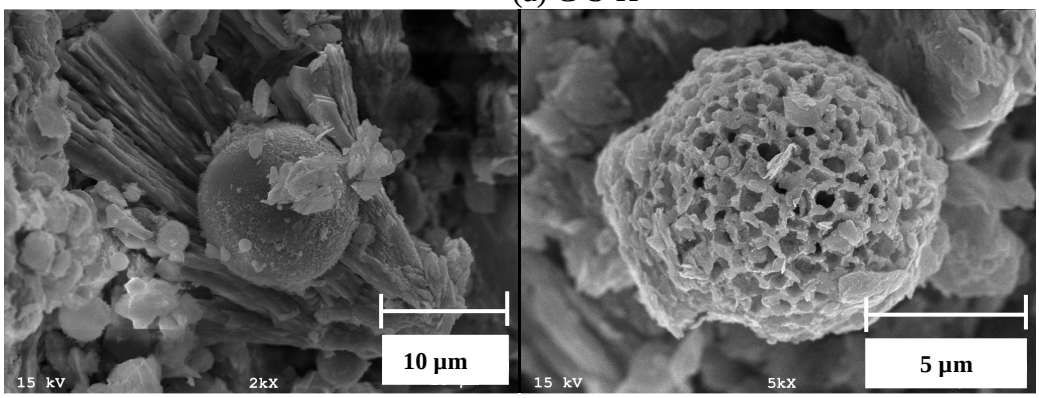

(b) Hydration Coatings

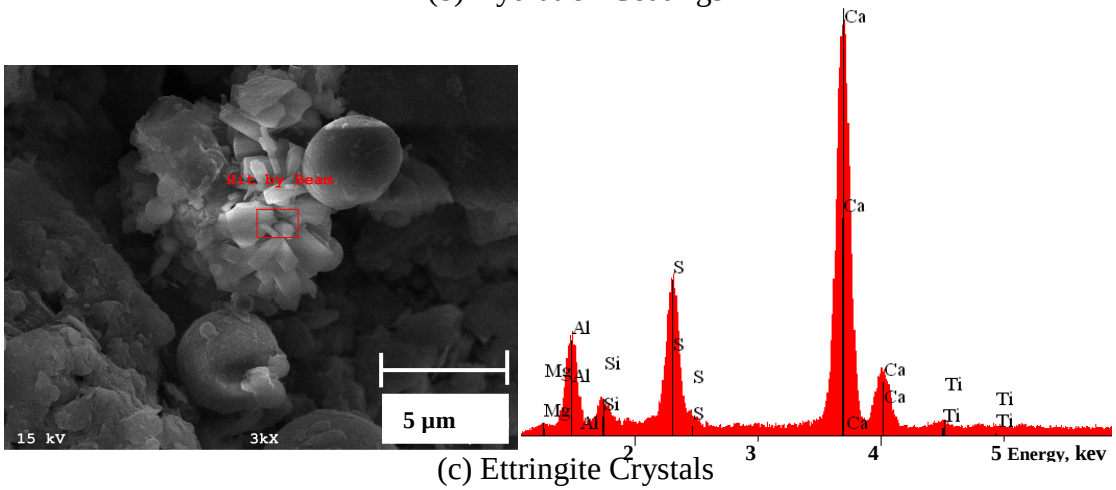

(c) Ettringite Crystals

Figure 2.25 SEM Micrographs of 28-Day Cured 15% CFA-Stabilized C-Soil Specimen

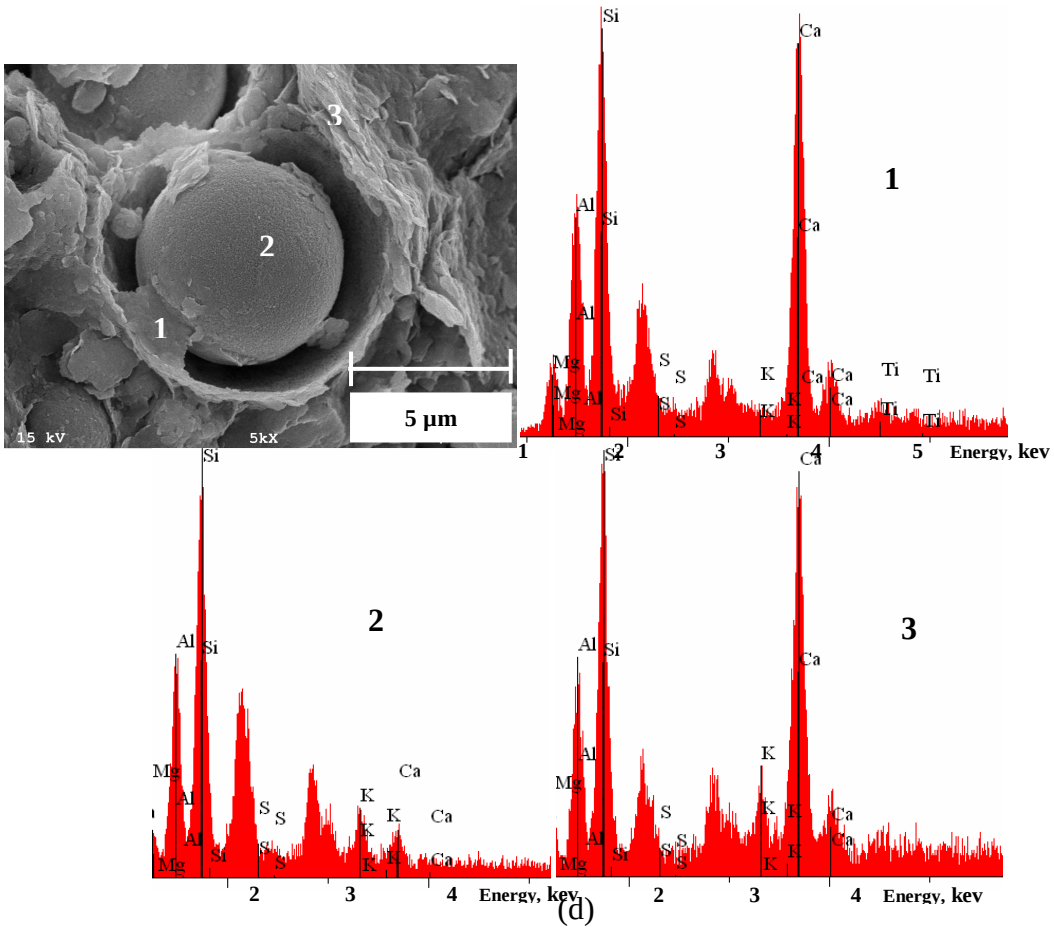

Figure 2.25 (Cont'd) SEM Micrographs of 28-Day Cured 15% CFA-Stabilized C-Soil Specimen

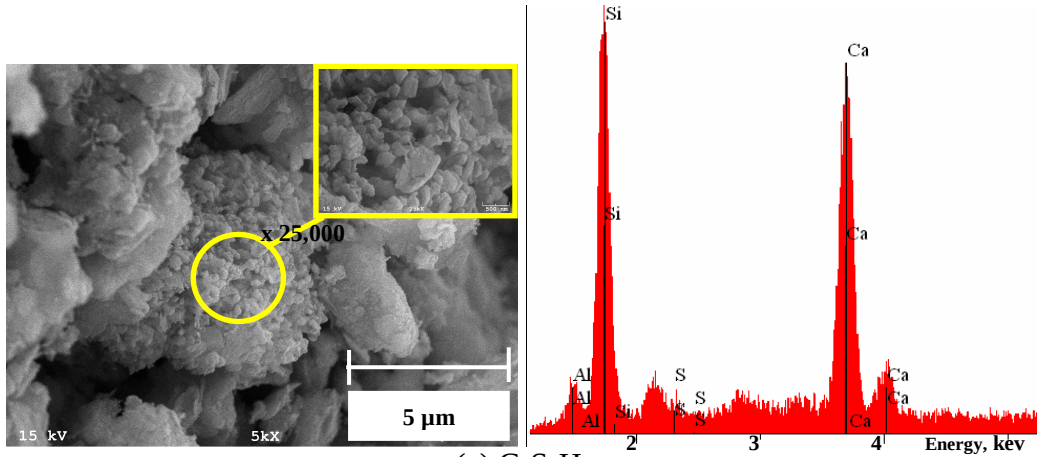

(a) C-S-H

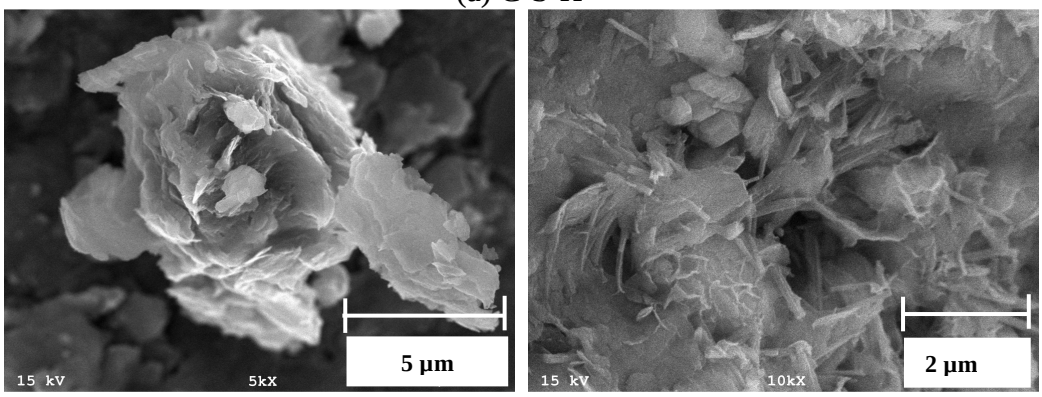

(b) Hydration Coatings

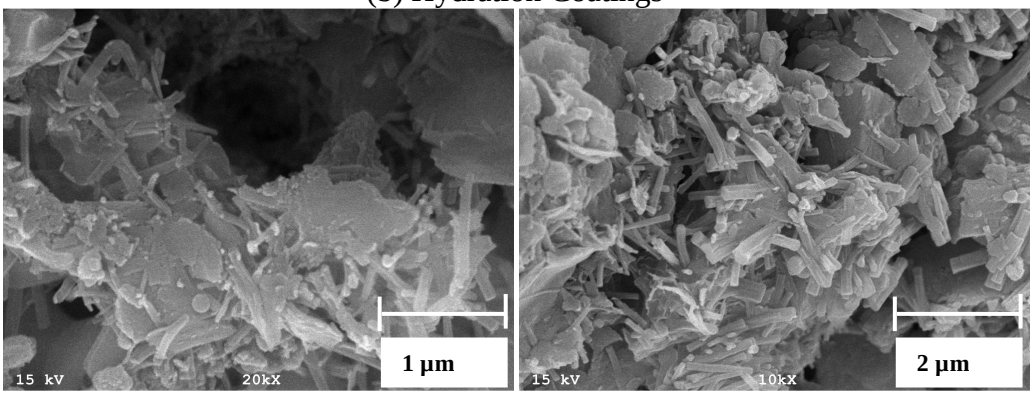

(c) Ettringite Crystals

Figure 2.26 SEM Micrographs of 28-Day Cured 15% CKD-Stabilized C-Soil Specimen

CHAPTER 3

INFLUENCES OF VARIOUS CEMENTITIOUS ADDITIVES ON THE DURABILITY OF STABILIZED SUBGRADE SOILS

3.1 Introduction

Durability (or long-term performance) of pavement materials induced by changes in climatic conditions namely, freeze-thaw and wet-dry, have been recognized by pavement engineers as a major factor in poor pavement performance. In cold regions, freeze-thaw (F-T) action is considered to be one of the most destructive actions that can induce significant damage to a pavement structure. Freezing of moisture present in the pore spaces of soil structure result in the formation of ice lenses. During times of temperate weather, the ice lenses thaw, and the structural capacity of the roadway may be dramatically reduced (Guthrie and Hermansson, 2003). The repeated action of F-T deteriorates the integrity of the pavement structure indicating possible changes in the engineering properties of pavement material such as resilient modulus and unconfined compressive strength. The importance of considering durability in mixture design has also been highlighted by AASHTO (2004), Transportation Research Circular E-C086: Evaluation of Chemical Stabilizers (Petry and Sobhan, 2005) and recent NCHRP Web-Only Document: Recommended Practice for Stabilization of Subgrade Soils and Base Materials (Little and Nair, 2009). To this end, durability (or long-term performance) of stabilized soil specimens was evaluated by conducting F-T cycling, vacuum saturation and tube suction tests. Also, specimens were capillary-soaked for 60 days and tested for M_r, as an additional indicator for evaluating long-term performance.

3.2 Overview of Previous Studies

A review of previous studies reveals no widely accepted laboratory procedure to evaluate the durability of cementitiously stabilized subgrade soils. Hence, a summary of different experimental procedures available in literature for evaluating durability of stabilized soil specimens is provided in this section.

3.2.1 Freeze-Thaw and Wet-Dry Cycling

Soil specimens subjected to freeze-thaw (F-T) or wet-dry (W-D) cycles provide an indication of how those specimens will maintain engineering parameters in the field exposed to diverse environmental conditions. Among "conventional" laboratory procedures, the ASTM D 559 and ASTM D 560 test methods are the only existing standardized procedures for evaluating effect of W-D and F-T cycles on cement-stabilized soil specimens, respectively. These methods consist of mixing soil and additive at optimum moisture content and compacting with standard effort in a 100 mm (4 in) diameter Proctor mold. After compaction, specimens are cured for 7 days in a humidity room and then subjected to a series of F-T or W-D cycles. After completion of each cycle, specimen is brushed on all sides with a wire brush and effect of F-T or W-D cycles is measured in terms of percent weight loss. As a result of the variability associated with the brushing process, many agencies and researchers omit the brushing portion of the test and replace it with unconfined compressive strength (UCS) testing after completion of all 12 cycles (Shihata and Baghdadi, 2001).

Petry and Wohlgemuth (1988) subjected highly plastic soils stabilized with lime and Portland cement (PI 64 to 77) to 12 W-D cycles, as specified in ASTM D 559, after 7 days of curing in a humidity room. However, the wire brushing called for in the

specification was not performed. The results indicated that the lime-stabilized specimens retained their integrity better than the Portland cement specimens, at each gradation level. The theory of "water proofing" was used to explain the differences in performance between cement and lime.

In a combined laboratory and field study from Oklahoma, Miller and Zaman (2000) investigated durability of CKD-stabilized soil by performing UCS on samples subjected to F-T and W-D cycles separately. Tests were conducted on 7-day cured three combinations of soil and additives, namely, CKD with sand, CKD with shale, and quicklime with shale. One W-D cycle consisted of immersing samples in water for 5 hours, followed by oven drying for 24 hours at 71^{o}C (160^{o}F). Samples that survived were subjected to UCS after 0, 1, 3, 7, and 12 W-D cycles. The UCS tests were conducted after the drying cycle so that moisture conditions would be uniform for each sample tested. The same procedure was used to prepare and cure samples during F-T testing. One F-T cycle consisted of placing samples in a freezer at -23^{o}C (-9^{o}F) for 24 hour and then pacing in a moisture chamber under controlled humidity of 95% and temperature of about 23^{o}C (73^{o}F). UCS tests were conducted after 0, 1, 3, 7, and 12 cycles. Specimens were tested at the end of thawing period. CKD-stabilized shale specimens showed increase in UCS values for the first three W-D cycles, beyond which sample did not survive immersion in water. On the other hand, specimens stabilized with quicklime survived only one W-D cycle. Sand specimens stabilized with CKD showed an increase in UCS values over the full 12 cycles of W-D. Contrary to W-D cycles, all the specimens survived 12 F-T cycles.

In a comparative study by Parsons and Milburn (2003), durability of soils treated with different additives, namely, lime, CFA, Portland cement and enzymatic stabilizer was evaluated. After compaction of the soil-additive mix, the samples were cured for 7 days in a humidity room and then subjected to a series of F-T and W-D cycles. The cement-treated soils had the least weight loss in F-T testing, while CFA-treated soils had lower weight losses in F-T testing than lime-treated soils. Relative performance in the W-D cycles was mixed; lime generally performed better on fine-grained materials and Portland cement on coarse-grained soils, although Portland cement performed relatively well with the CH clays. Additionally, CFA performed well only on the SM soil, where it survived the full 12 cycles.

In another study by Parsons and Kneebone (2004), eight different soils with classifications of CH, CL, ML, SM and SP were tested for F-T and W-D durability to evaluate the relative performance of CKD as a stabilizing agent. Results were compared with previous findings for the same soils stabilized with lime, cement, and fly ash. It was reported that the CKD treated soil samples' performance in W-D testing was similar to that for lime, fly ash and cement treated soils. However, CKD-stabilized samples were not as durable in F-T testing as lime, fly ash and cement treated soil samples.

Arora and Aydilek (2005) conducted F-T tests on silty sand (SM) stabilized with 40% class F fly ash in combination with cement or lime. It was found that the strength of specimens stabilized with class F fly ash and cement increased with increasing number of F-T cycles. The increase in strength was more enhanced for mixtures that contained 7% cement than for mixtures with 4 and 5% cement. Also, lime-stabilized specimens

survived during F-T cycles but their strengths decreased with increasing number of F-T cycles.

3.2.2 Vacuum Saturation

The vacuum saturation method was proposed by Dempsey and Thompson (1973) as a rapid and economical method for predicting the durability of stabilized materials. Currently, vacuum saturation test is outlined in ASTM C 593 as durability test for Class C fly ash, lime-fly ash, and lime-stabilized soils. This method consists of mixing soil and additive at optimum moisture content and compacting with standard effort in a 100 mm (4 in) diameter Proctor mold After compaction, specimens are cured for 7 days and placed in a vacuum chamber that is subsequently evacuated to a pressure of 610 mm Hg. (24 in. Hg., 11.8 psi). After 30 minutes, the chamber is flooded with de-ionized water, and the vacuum is removed. The specimens are allowed to soak for 1 hour and are then tested for UCS. Only few studies (e.g., McManis and Arman, 1989; Guthrie et al., 2008; Parker, 2008) are available in the literature.

McManis and Arman (1989) evaluated the durability of two CFA-stabilized sands, namely, A-3 and A-2-4 in accordance with the ASTM C 593 specifications. Specimens were conditioned in a vacuum saturation chamber and tested for UCS with the exception that they were cured in a humidity room at $22.7^{o}\pm1^{o}C$ ($73^{o}\pm3^{o}F$) rather than at $38^{o}C$ ($100^{o}F$), as specified in the ASTM procedure. A comparison of the differences in strength between specimens subjected to this procedure and those not subjected to this procedure provided a relative measure of durability of the sand mixtures. The strength loss in the A-3 specimens was inconsistent, but the A-2-4 specimens demonstrated a consistent loss in strength.

In a recent study, Parker (2008) conducted vacuum saturation test on silty sand and lean clay stabilized with different additives, namely, class C fly ash, lime-fly ash, lime or Type I/II Portland cement. It was found that the silty sand specimens stabilized with lime-fly ash had significantly higher UCS after vacuum saturation than specimens stabilized with CFA, lime or cement. Also, clay specimens stabilized with CFA or lime-fly ash had significantly higher UCS values than specimens stabilized with cement or lime. This study also proposed strong correlation between residual UCS values after F-T cycling and vacuum saturation.

3.2.3 Tube Suction Test

The Tube Suction Test (TST) was developed by the Finnish National Road Administration and the Texas Transportation Institute to evaluate the moisture susceptibility or the amount of "free" water present within a soil system (Syed et al., 1999; Guthrie et al., 2001). The TST involves measurement of surface dielectric values (DV) of the test specimens. During the test, the increase of moisture in the specimen is monitored with a dielectric probe, which measures the dielectric properties at the surface of the specimen. The DV is a measure of the unbound or "free" moisture within the specimen. High surface dielectric readings indicate suction of water by capillary forces and can be an indicator of a non-durable material that will not perform well under saturated or freeze-thaw cycling conditions (Scullion and Saarenketo, 1997). Guthrie and Scullion (2003) suggested that aggregate base specimens having final dielectric readings less than 10 are characterized as satisfactory with respect to moisture and/or frost susceptibility, while specimens with final readings above 16 are considered unsatisfactory. Aggregate base specimens with final dielectric values between 10 and 16

are expected to exhibit marginal long-term durability. To the author's knowledge, there are no recommended lower and upper DV values for stabilized soil specimens. Hence, in the present study DV values will be used to evaluate comparative moisture susceptibility of stabilized soil specimens.

In recent years, TST results have been correlated with bearing capacity, frost heave, and several other parameters (PCA, 1992; Saarenketo and Scullion, 1996; Scullion and Saarenketo, 1997; Little, 2000; Syed et al., 2000; Guthrie and Scullion, 2000; Saarenketo et al., 2001; Guthrie and Scullion, 2003; Saeed et al., 2003; Syed et al., 2003; Barbu et al., 2004; Zhang and Tao, 2008). Little (2000) evaluated moisture susceptibility of low, moderate, and high plasticity soils using TST. Moisture susceptibility was determined indirectly by measuring the DV of stabilized specimens using a Percometer^{TM}. Tests were performed on three versions of each soil: untreated, lime-treated with unsealed curing, and lime-treated with controlled curing (seal-cured). It was found that for low-plasticity soils, lime acted as a fine filler and increased the water content after capillary soaking. No significant difference was seen on the DV over that of the untreated soil. For moderate plasticity and high plasticity soils, lime treatment, with seal-curing, resulted in slightly lower moisture contents and substantial and statistically significant reductions in DVs.

Barbu et al. (2004) studied only the moisture susceptibility of 28 day cured silty sand specimens stabilized with 3.5% of cement. Different conditions for conducting TST were evaluated, such as specimen size, the effect of compaction energy and size of clods. The two different cylindrical specimen sizes used were 305 mm (12 in) by 152 mm (6 in) diameter and 180 mm (7 in) by 101.6 mm (4 in) diameter. DV readings were taken for

500 hours using Percometer™. It was concluded that the difference in final result due to different dimensions of the specimen, compaction energy or clod size is not significant. Zhang and Tao (2006) conducted wetting-drying test, along with the TST and 7-day UCS to determine the efficiency of cement stabilization on low plastic soils, which is frequently encountered in Louisiana. This study confirmed the equivalence among wetting-drying, TST, and 7-day UCS tests as an alternative to traditional durability tests.

In a recent study, Parker (2008) evaluated the moisture susceptibility of 7-day cured stabilized silty sand and lean clay specimens. Five additives, namely, class C fly ash, lime-fly ash, lime, and type I/II Portland cement were used in this study. DV values measured in the tube suction test were lowest for specimens treated with lime-fly ash and cement with respect to the sand and for specimens treated with class C fly ash and cement with respect to the clay. The lime-fly ash and cement successfully reduced the DV values of sand specimens to a marginal rating, while no stabilizer reduced the moisture susceptibility of the clay to a satisfactory level.

In another recent study, Zhang and Tao (2008) conducted TST for evaluating durability of cement-stabilized low plasticity soils. A series of specimens were molded at six different cement contents (2.5, 4.5, 6.5, 8.5, 10.5 and 12.5%) and four different molding moisture contents (15.4, 18.5, 21.5, and 24.5%). It was found that the final stable DV values of stabilized specimens were all above the value of 30. The maximum DVs generally decreased with increase in cement content. With increase in the molding moisture content, it was less effective for cement to reduce the maximum DV. Also, it was reported that at the low cement dosages, specimens molded on the dry side of compaction curve can suck in free water faster than those compacted on the wet side until

enough amount of cement is used. Further, the test results indicated that the water-cement ratio of cement-stabilized soil had the dominant influence on the maximum DV.

It is also worth mentioning here that there is no standardized procedure for conducting TST on stabilized materials. A summary of TST procedure used by different researchers is presented in Table 3.1. Hence, one of the objectives of this study is to develop TST procedure for stabilized soils, as will be discussed later.

3.2.4 Other Methods

Several researchers (see e.g., Kenai et al., 2006; Zhang and Tao, 2008; Osinubi et al., 2010) and agencies (see Table 3.2) use 7-day UCS values as an indicator of the durability for the soil stabilization mix design. For example, Zhang and Tao (2008) established equivalency of 7-day UCS and W-D durability. In a recent study, Osinubi et al. (2010) evaluated durability of soil-lime-slag mixtures by determining strength of moisture conditioned specimens. The resistance to loss in strength was determined as a ratio of the UCS of specimens wax-cured for 7 days, de-waxed top and bottom and later moisture conditioned in water for another 7 days to the UCS of specimens wax-cured for 14 days. It was found that the resistance to loss in strength decreased with higher slag content. For 8% lime-stabilized specimen, a peak value of 80% with highest durability was observed. However, soil-lime-slag mixtures containing 6 – 8% lime showed resistance to loss in strength values in the range between 50 – 70%.

Some researchers (e.g., Prusinski and Bhattacharja, 1999; Parsons and Milburn, 2003; Parsons and Kneebone, 2004) used leaching test for evaluating durability of stabilized soil specimens. The leaching durability test involves leaching de-ionized water through a Proctor specimen of soil for 28 days. Leachate samples are collected for

determining flow rate, calcium concentration, and pH at different intervals of 1, 3, 7, 14, 21, and 28 days. Only limited information is available on leaching of CFA- or CKD-stabilized soil specimens. However, extensive leaching investigations were performed on lime-stabilized specimens by McCallister and Petry (1990; 1991; 1992). According to McCallister and Petry (1990; 1991; 1992), lime-addition levels in soils are defined at two levels: lime modification optimum (LMO) as determined by pH test (ASTM D 6276) and lime stabilization optimum (LSO) as determined by the lime addition percentage which provides the maximum UCS. For the soils tested by McCallister and Petry (1990; 1991; 1992), the lime levels for LMO and LSO were 3 – 4% and 7 – 8%, respectively.

3.3 Materials

The three soils: (1) Port series soil (P-soil), (2) Kingfisher series soil (K-soil), and (3) Carnasaw series soil (C-soil), were used to evaluate the durability. Their properties are presented in Section 2.3.1, Chapter 2. Also, hydrated lime, class C fly ash (CFA) and cement kiln dust (CKD) were used. Their properties are presented in Section 2.3.2, and summarized in Table 2.4. As mentioned in the previous chapter, the differences between the chemical composition and physical properties among the selected additives are clearly evident in Table 2.4 and are expected to lead to different durability of stabilized specimens.

3.4 Laboratory Procedure

3.4.1 Conventional Freeze-Thaw Test

The freeze-thaw (F-T) test was performed in accordance with procedure outlined in ASTM D 560. Specimens were prepared by mixing raw soil mixed with specific

amount of additive. The amount of additive (6% for lime and 10% for CFA and CKD) was added based on the dry weight of the soil. The specimens were molded with a Harvard Miniature device (diameter = 33 mm i.e., 1.3 in and height = 71 mm i.e., 2.8 in). The Harvard Miniature procedure was calibrated in accordance with the ASTM D 4609 test method using each soil and additive mixture so that at the standard Proctor optimum moisture content (OMC) and the Harvard Miniature procedure produced a specimen having the standard Proctor maximum dry density (MDD). All specimens were compacted at the OMC and MDD of the soil-additive mixture, as presented in Tables 2.6, 2.7 and 2.9. After compaction, specimens were cured for 7 days at a temperature of 23.0 ± 1.7^{o}C (73.4 ± 3.1^{o}F) and a relative humidity of approximately 96%, as recommended by ASTM D 1632 test method. A total of two replicates were prepared for each combination and then subjected to 0, 1, 4, 8 and 12 F-T cycles after 7 days of curing. Each F-T cycle consists of freezing for 24 hours at a temperature not warmer than -23.3^{o}C (-10^{o}F) and thawing for 23 hours at 21.1^{o}C (70^{o}F) and 100% relative humidity (Figure 3.1). Free potable water was made available to the porous plates under the specimens to permit the specimens to absorb water by capillary action during the thawing period. After the completion of appropriate F-T cycle, unconfined compressive strength (UCS) tests were conducted by loading specimens in a displacement control mode at a strain rate of 1% per min.

3.4.2 Vacuum Saturation Test

The vacuum saturation test was performed in accordance with ASTM C 593 test method with slight modifications. This method consists of mixing soil and additive namely, 6% lime or 10% CFA or 10% CKD, and compacting with standard effort in a

Proctor mold (diameter = 100 mm i.e., 4 in and height = 115 mm i.e., 4.5 in). After compaction, specimens were cured in a humidity room at 23.0 ± 1.7^{o}C (73.4 ± 3.1^{o}F) rather than at 37.8^{o}C (100^{o}F), as specified in the ASTM procedure. Following curing, specimens were placed in a vacuum chamber that is subjected to a vacuum pressure of 81.3 kPa (11.8 psi; 24 in Hg). After 30 minutes, vacuum was removed and the chamber was flooded with water and the specimens were allowed to soak for 1 hour. After the saturation period the water was drained, and the specimens were immediately tested for UCS by loading specimens in a displacement control mode at a strain rate of 1% per min. A comparison of the differences in UCS values between specimens subjected to this procedure (UCS after vacuum saturation) and those not subjected to this procedure (UCS before vacuum saturation) provided a relative measure of durability of the stabilized specimens. Figure 3.2 shows photographic view of setup used for vacuum saturation test. The vacuum chamber consists of a 25 mm (1 in) thick Plexiglas lid. As shown in Figure 3.2, specimens were placed in an upright position on a perforated steel plate so that water could enter the soil from all surfaces.

3.4.3 Tube Suction Test

Since there is no standard protocol for conducting tube suction tests, durability of specimens was evaluated by preparing specimens by using following three different methods:

1. *Method-1*

   Compaction: Standard Proctor compaction (five layers/lifts) at the OMC and a target dry density of 95-100% of MDD

   Cylindrical specimen size: diameter = 101.6 mm (4 in), height = 203.2 mm (8 in)

2. *Method-2*

   Compaction: Superpave gyratory compactor (single layer/lift) at the OMC and a target dry density of 95-100% of MDD

   Cylindrical specimen size: diameter = 101.6 mm (4 in), height = 203.2 mm (4 in)

3. *Method-3*

   Compaction: Superpave gyratory compactor (single layer/lift) at the OMC and a target dry density of 95-100% of MDD

   Cylindrical specimen size: diameter = 152.4 mm (6 in), height = 152.4 mm (6 in)

Method-2 and Method-3 are similar to the method of compaction used by Harris et al. (2006). According to Harris et al. (2006), specimens should be molded in one lift because molding specimens in multiple lifts with a drop hammer generates permeability barriers. The permeability barriers do not allow the water to rise up through the sample beyond the bottom lift (Harris et al., 2006). In the present study, the specimen size compacted using Superpave gyratory compactor was restricted to 152.4 mm (6 in) (Method-3) due to the constraint of molding in one lift.

After compaction, specimens were cured for 7 days in a controlled environment of temperature of 23.0 ± 1.7^{o}C (73.4 ± 3.1^{o}F) and a relative humidity of approximately 96%. Then, specimens were dried in an oven at 40 ± 5^{o}C (104 ± 9^{o}F) for two days. After oven drying, the specimens were allowed to cool down at room temperature for 30 minutes, and then applied with a thin layer of grease around the lateral surface and placed on a porous stone in an open dish containing approximately 10 mm (0.4 in) of de-ionized (DI) water. Since the quality of the porous stones has an important influence on the final DV (Barbu and Scullion, 2005), clean porous stones were used. Further, the top surface

of specimen was covered with a plastic sheet and plate for avoiding loss of moisture due to evaporation. During wetting of specimens in DI water, the increase in dielectric value (DV) with time due to capillary rise of water was measured. Four measurements were taken along the circumference of the specimen in separate quadrants and the fifth reading was taken at the center of specimen and an average of all five readings was calculated. Measurements were taken daily for 10 days using a dielectric probe (or Percometer^{TM}) and the final 10th day reading was reported. A photographic view of the TST setup is shown in Figure 3.3. To ensure adequate contact of probe on the top of surface of the specimen, a surcharge of 2.2 kg (4.86 lb) was applied (Figure 3.3). After 10 days of TST, specimens prepared by using Method-1 and -2 were cut into five and three equal layers, respectively, and oven dried for moisture content.

3.4.4 Resilient Modulus Test on Capillary-Soaked Specimens

The new Mechanistic-Empirical Pavement Design Guide (MEPDG) (AASHTO, 2004) recommends the evaluation of resilient modulus (M_r) for critical performance prediction of stabilized subgrade layer. During the service life, however, subgrade undergoes moisture variations and consequently large strength and stiffness fluctuations as well. It is critical that the changes taking place in the modulus of proposed subgrade soil at the expected field condition be investigated beforehand (AASHTO, 2004). One of the modes of moisture variation includes capillary soaking, which involves sucking of water into the pavement matrix from a free water surface located at its base. In practice, the external water sources may come from rain, clogged up drains, or perched and shallow water tables. Hence, in this study, stabilized specimens already tested for M_r, as discussed in Section 2.6, were further subjected to capillary soaking under controlled

temperature (23.0 ± 1.7^{o}C i.e., 73.4 ± 3.1^{o}F) and relative humidity (>96%) in an ice chest. After 60 days of capillary soaking, specimens were again tested for M_r, as additional indicator of durability. Specifically, M_r test was conducted on two replicates of capillary soaked specimens of P-, K-, and C-soil stabilized with three additives namely, 6% lime, 10% CFA and 10% CKD. Further, details of the M_r tests are given in Section 2.6.

3.5 Presentation and Discussion of Results

3.5.1 Effect of Freeze-Thaw Cycles

The individual results of the UCS tests after 0, 1, 4, 8 and 12 F-T cycles are graphically illustrated in Figures 3.4, 3.5 and 3.6 for P-, K- and C-soil, respectively. All the specimens tested in this study, in general, showed decrease in the UCS values with increase in the number of F-T cycles. For example, the UCS value of raw, 6% lime-, 10% CFA-, and 10% CKD-stabilized K-soil specimen after 12 F-T cycle is approximately 97%, 89%, 93%, and 90% lower than a comparable specimen with a zero F-T cycle. A similar qualitative trend was observed for the P- and C-soil specimens, where the UCS values exhibited a decrease as the number of F-T cycles increased up to 12. The decrease in UCS values can be explained by a combined effect of pore structure and the increase of moisture content (Figure 3.7 for K-soil specimens) during the thawing portion of the cycle. Increase in moisture content during the thawing phase results in ice lenses within the void space of the specimens in the freezing phase; formation of ice lenses distorts the structure of raw and stabilized specimens (Khoury, 2005). On the other hand, higher density of stabilized soil specimen indicates fine pore structure. The capillary force exerted on a pore wall depends on the pore size: the smaller the pore, the higher the suction force. As water enters and exits the pores, it can generate considerable pressure

and degrade the surrounding material (Prusinski and Bhattacharja, 1999). Although lime-stabilized specimen had higher moisture content than corresponding CFA-stabilized specimens (Figure 3.7), it also had lower density indicating open pore structure which reduces F-T damage effects (16.8 kN/m^3 for K-soil-lime versus 17.4 kN/m^3 for K-soil-CFA mixtures). It is also clear from Figures 3.4 through 3.6 that decrease in UCS from F-T cycle 0 to 1 is higher than decrease in UCS between other F-T cycles. For example, UCS values of 6% lime-stabilized K-soil specimens decreased by approximately 40% between F-T cycles 0 – 1 and 34% between F-T cycles 1 – 4, respectively. It is speculated that freezing and thawing opened up the pores, reducing the damaging effects of later F-T cycles.

The effect of F-T action on UCS values varies from one soil-additive mixture to another, as shown in Figures 3.4 through 3.6. Table 3.3 shows the average percentage decrease in UCS values of raw and stabilized P-, K- and C-soil specimens due to F-T action. It is evident that for P-soil specimens, a silty clay with sand, the percentage decrease in UCS values of 10% CKD-stabilized specimens is lower than the corresponding 6% lime-stabilized specimens, followed by 10% CFA-stabilized specimens. For example, the UCS values of CKD-stabilized specimens subjected to 4 F-T cycles is approximately 65% lower than the corresponding UCS values of stabilized specimens with no such cycles. The corresponding percentage decrease is 75% and 82% for lime- and CFA-stabilized specimens, respectively. Although the percentage decrease in UCS values for lime-stabilized specimens subjected to 1 F-T cycle is higher than corresponding CKD-stabilized specimens, the UCS values for CKD-stabilized specimens were higher than the corresponding UCS values of the lime-stabilized specimens.

Specifically, the UCS values of CKD-stabilized specimens is 605 kPa (87.8 psi) which is approximately 91% higher than the corresponding UCS values of lime-stabilized specimens after 1 F-T cycle (Figure 3.4). Figure 3.8 shows a photographic view of the raw, 6% lime-, 10% CFA-, and 10% CKD-stabilized specimens of P-soil with no visual degradation evident. Consequently, CKD-stabilization provided better resistance than lime- and CFA-stabilization towards F-T durability of P-soil specimens.

Contrary to the behavior of stabilized P-soil specimens, F-T tests on both K-soil (lean clay) and C-soil (fat clay) stabilized specimens projected 6% lime-stabilized specimens showing highest UCS values followed by 10% CKD and 10% CFA. For example, the average UCS value of 6% lime-stabilized C-soil specimens subjected to 1 F-T cycles is 159 kPa (23 psi), as compared to 65 kPa (9 psi), and 21 kPa (3 psi) for 10% CKD- and 10% CFA-stabilized specimens, respectively. Further, the percentage decrease in UCS values from Table 3.3 supports the fact that 6% lime stabilized specimens are more durable against F-T cycles as compared to specimens stabilized with 10% CKD and 10% CFA. It is believed that presence of highest calcium content in lime among all additives used in this study (Table 2.4) will produce higher amount of cementitious products (e.g., calcium silicate hydrate, calcium aluminate hydrate) after combining with pozzolana (silicious and aluminacious material). Since K- and C-soil have very high clay content indicating higher amount of pozzolana as compared to P-soil (Table 2.2), more cementitious compounds are expected in K- and C-soil. Figures 3.9 and 3.10 show photographic view of raw and stabilized K- and C-soil specimens, respectively. It is clear from Figures 3.9 and 3.10 that raw and stabilized C-soil specimens show more degradation than corresponding K-soil specimens. Thus, one can conclude that durability

of C- and K-soil specimens against F-T cycles is higher with lime as compared to CFA and CKD.

3.5.2 Vacuum Saturation Test

A summary of UCS results conducted on P-, K- and C-soil specimens subjected to vacuum saturation procedure (UCS after vacuum saturation) and those not subjected to vacuum saturation procedure (UCS before vacuum saturation) is presented in Figure 3.11. The raw soil specimens deteriorated during the soaking stage and could not be tested for UCS. All of the stabilized specimens lost strength compared to the control specimens tested after 7 days. During vacuum saturation testing, the UCS of the P-soil specimens stabilized with lime, CFA and CKD decreased by an average of 44, 53 and 55%, respectively. Although lime-stabilized specimens showed lowest percentage decrease, the average UCS value of CKD-stabilized specimen was highest (258 kPa, i.e., 37 psi) after vacuum saturation test among all the additives used in this study. Similar to the trends of UCS values after F-T cycles, 6% lime-stabilized specimens of K- and C-soil specimens showed lowest percentage decrease in UCS values after vacuum saturation. For example, K-soil specimens stabilized with 6% lime, 10% CFA and 10% CKD showed a percentage decrease in UCS values of approximately 51%, 66% and 71%, respectively. Also, it is evident from Figure 3.11 that for K- and C-soil specimens, the UCS values after vacuum saturation of 6% lime-stabilized specimens is higher than the corresponding 10% CKD-stabilized specimens, followed by 10% CFA-stabilized specimens. Since UCS values of stabilized P-, K- and C-soil specimens after vacuum saturation showed similar trends to UCS values after F-T cycling, similar reasons as mentioned in the preceding Section 3.5.1 can be used to justify the observed trends.

3.5.3 Tube Suction Test

A summary of the final 10th day dielectric constant values (DVs) for the raw and stabilized P-, K- and C-soil specimens is summarized in Figures 3.12, 3.13 and 3.14, respectively.

3.5.3.1 Effect of Method of Specimen Preparation

It is clear from Figures 3.12 through 3.14 that the specimens prepared by using Method-1 showed a lower DV as compared to corresponding specimens prepared by using Method-2 and -3 which provided similar DVs. For example, raw K-soil specimens provided a DV of 18.1, 40.2 and 39.9 when specimens were prepared in accordance with Method-1, -2 and -3, respectively. This difference in DV between specimens prepared by using Method-1 and -2 or -3 could be attributed to the variation of the moisture content values along the height of specimens, as shown in Figures 3.15, 3.16 and 3.17, respectively, for P-, K- and C-soil specimens. Specimens prepared by using Method-1 showed that the moisture content of bottom layer is very high as compared to the moisture content of the top layer. This difference in moisture content between bottom and top layer varies between 1.3 – 3.9%, 1.3 – 6.9%, and 1.0 – 6.7% for P-, K- and C-soil specimens, respectively. On the other hand, all the P-, K- and C-soil specimens prepared by using Method-2 showed a difference in moisture content of less than 0.5% between bottom and top layer. Since the measured signal using Percometer™ depends only on the dielectric properties of top 20 – 30 mm (0.8 – 1.2 in) of material (Saarenketo, 2006; Adek, 2007), it is expected that the specimen having uniform moisture content will provide the representative behavior. Also, it is important to note that the specimens compacted in single layer (Method-2 and -3) are more representative of the field

conditions where stabilized subgrade layer is compacted in one lift. Figures 3.18 (a) and (b) show photographic view of 10% CKD-stabilized C-soil specimens prepared by using Method-1 and -2, respectively. It is evident from Figures 3.18 (a) and (b) that the specimen prepared by using Method-1 is dry at top while specimen prepared by using Method-2 is uniformly wet resulting in lower (28.9) and higher (41.1) DVs, respectively, as shown in Figure 3.14.

3.5.3.2 Effect of Additive and Soil Type

Since Method-2 and -3 provided similar and representative DVs of stabilized soil specimens, DVs obtained by using Method-2 were used for further evaluation of effect of additive and soil type on durability. The raw P-, K-, and C-soil specimens showed an average DV of approximately 35.3, 40.2 and 39.2, respectively (Figures 3.12 – 3.14). Stabilization with 10% CFA is more effective in reducing the DV of P-soil specimens followed by 6% lime. For example, DV reduced by 18% and 17% by treating P-soil with 10% CFA and 6% lime, respectively. Similar to the qualitative trend noticed in preceding sections, K- and C-soil specimens showed more effectiveness with 6% lime by decreasing the DVs of corresponding raw soil specimens by 20% and 15%, respectively. These results are consistent with the observations made by Little (2000) and Barbu and McManis (2005). The percentage decrease in DV due to 10% CFA was found to be approximately 7% and 4% for K- and C-soil specimens, respectively, consistent with the observations reported by Guthrie et al. (2008) and Parker (2008). It is an indication that lime and CFA stabilization has more or less same degree of effectiveness in reducing the DV for K- and C-soils.

On the other hand, the DVs of 10% CKD-stabilized P-, K- and C-soil specimens exhibited an increase, an opposite trend as compared to lime- and CFA-stabilized specimens. For example, P-, K- and C-soil specimens prepared with 10% CKD showed an average increase of approximately 5%, 4% and 5% as compared to raw specimens. Hence, CKD was found to show no significant improvement in DVs for the P-, K- and C-series. Similar behavior of increase in DV with addition of 2% CKD in limestone base material was reported by Si and Herrera (2007). This behavior of increase in DV of CKD-stabilized specimens may be attributed to the presence of extra CKD in the specimen which is not reacting with the host material; hence it absorbs water increasing the moisture content (Figures 3.15 – 3.17) and dielectric constant.

3.5.4 Resilient Modulus Test on Capillary-Soaked Specimens

The M_r test results of P-, K- and C-soil specimens tested after 60 days of capillary soaking are presented in Tables 3.4, 3.5 and 3.6, respectively. All M_r values listed in Tables 3.4 through 3.7 are mean of results from testing conducted on two specimens. In general, it is clear that all P-, K- and C-soil capillary-soaked specimens showed decrease in M_r values with respect to corresponding specimens tested before soaking, as mentioned in Section 2.7. For comparison, M_r values at a particular stress level (σ_3 = 41 kPa, i.e., 6.0 psi, σ_d = 25 kPa, i.e., 3.6 psi) are graphically shown in Figure 3.19. After capillary soaking, 6% lime-stabilization of K- and C-soil showed the best performance by providing highest M_r values (Figure 3.19). As compared to capillary-soaked raw K-soil specimens, 6% lime produced 759% higher M_r values. On the other hand, C-soil specimens stabilized with 6% lime produced M_r values enhanced by 356%, as compared to raw C-soil specimens. Stabilization with 10% CFA produced a moderate effect after

capillary soaking. For example, 10% CFA enhanced M_r values by an approximate percentage of 422% and 67% respectively, for K- and C-soil specimens. With P-soil, the degree of effectiveness after capillary soaking was found more for 10% CFA-stabilized (approximately 1,237% increase) specimens than corresponding 6% lime-stabilized (approximately 538% increase) specimens.

On the contrary to before capillary soaking behavior, CKD-stabilized specimens showed the worst performance after 60-day capillary soaking. For example, specimens stabilized with 10% CKD showed an increase in M_r values only by 245%, lowest among all stabilized P-soil specimens. Similarly, addition of 10% CKD in K-soil specimens showed an increase of approximately 349% in M_r values, compared to raw soil specimens. Capillary-soaked C-soil specimens stabilized with 10% CKD showed no improvement in M_r values.

Further, to discuss the comparative long-term effectiveness of lime, CFA, and CKD, a chart of ratio of M_r values before and after capillary soaking versus type of additive was plotted (as shown in Figure 3.20). It is clear from Figure 3.20 that P-soil specimens stabilized with 10% CFA showed maximum resistance towards moisture damage with reduction in M_r values by an average factor of 1.7. On the other hand, 6% lime-stabilization proved more effective with K- and C-soils. For example, M_r value of K- and C-soil specimens stabilized with 6% lime decreased by a factor of 15.3 and 4.8, respectively. K- and C-soil specimens stabilized with 10% CFA showed moderate behavior with reduction in M_r values by a factor of 18.7 and 7.1 for K- and C-soil, respectively. Stabilization of specimens with CKD yielded least resistance to moisture damage among all the three additives used in this study. For example, M_r values of P-, K-

and C-soil specimens stabilized with 10% CKD decreased by a factor of 20.0, 26.6 and 30.7, respectively.

3.6 Discussion

Based on aforementioned UCS results, P-soil specimens, a silty clay with sand, showed better performance with 10% CKD against F-T cycles. On the other hand, K-(lean clay) and C-soil (fat clay) specimens showed higher degree of improvement against F-T cycles with 6% lime. Similar qualitative trend of P-, K- and C-soil specimens were observed for the retained UCS values after vacuum saturation test. It is also important to note that C-soil specimens stabilized with lime, CFA and CKD showed lowest retained UCS values as compared to corresponding specimens of P- and K-soil. This can be attributed to the acidic nature of C-soil (pH = 4.17) which will decrease the rate of cementitious reactions. Further, analyses of the test results indicated that the UCS values after 12 F-T cycle were lower than the corresponding values associated with UCS values retained after vacuum saturation. This observation suggests that the 12 F-T cycles are more severe than the vacuum saturation test for these particular fine-grained soils. Figure 3.21 shows a plot of UCS after F-T cycles (1 and 12) versus UCS after vacuum saturation. The R^2 value associated with this correlation is comparatively high at 0.9401 and 0.7361 after F-T cycle 1 and 12, respectively. Thus, a strong correlation exists between UCS values retained after vacuum saturation and F-T cycles.

The final DVs of all the raw and stabilized specimens were above the value of 16. Referring to the maximum DV criterion proposed by Guthrie and Scullion (2003), which was mainly for coarse soils or aggregates, the soil tested in this study were moisture susceptible with its maximum DV above 16. However, based on increase of 7-day UCS

by 345 kPa (50 psi) over raw specimens criterion, recommended by several highway agencies (Table 3.2) for selection of additive content, 10% CKD-stabilized P-soil and all stabilized K-soil specimens should be durable. Thus, the maximum DV criterion seems more conservative since no specimen satisfied the maximum DV criterion; consistent with the observations reported by Zhang and Tao (2006; 2008). Also, no correlation was observed between the final DV after TST and durability evaluated by using retained UCS values after F-T or vacuum saturation test. For example, P-soil specimens stabilized with 10% CKD showed best performance against F-T cycles among all the additives used in this study. On the other hand, TST projected 10% CKD-stabilized specimens showing the worst performance with a very high DV of approximately 37.2. Figure 3.22 shows that the final DV is affected by the moisture content of specimens. However, it is worth noticing that the final DV is dependent on material type and is influenced by properties such as clay content, saturation history, degree of bonding of water molecules around soil particle, optimum moisture content, and plastic limit (Saarenketo, 2006).

The qualitative trend of M_r values of stabilized soil specimens tested after 60 days of capillary soaking were similar to the behavior of corresponding specimens tested for DV by using Method-2. For example, M_r tests on capillary-soaked specimens showed that P-soil specimens stabilized with 10% CFA have maximum resistance towards moisture damage consistent with the lowest DV (28.8) of 10% CFA-stabilized specimens. Figure 3.23 shows a plot of M_r after 60 days of capillary soaking versus final 10^{th} day DV. The R^2 value of 0.6786 associated with this correlation suggests similar qualitative trend of results obtained using the two testing procedures.

3.7 Conclusions

The following conclusion can be drawn from the aforementioned results of this study:

1. All the specimens tested in this study showed decrease in the UCS values with increase in the number of F-T cycles. Such a decrease could be explained by the increase in moisture absorbed by specimen during the thawing portion of the cycle and pore structure of the stabilized specimen.
2. For the percentages of additives used in this study, results showed that lime provides higher resistance against F-T cycles for lean clay (K-soil) and fat clay (C-soil). On the other hand, CKD-stabilization is more effective with silty clay (P-soil) against damage caused by F-T cycles. A similar qualitative trend of behavior was observed for retained UCS after vacuum saturation test.
3. The test results indicated that the 12 F-T cycles are more severe than the vacuum saturation test for the particular soils used in this study. Also, a strong correlation exists between UCS values retained after vacuum saturation and F-T cycles.
4. The final dielectric constant values measured by conducting Tube Suction Test are influenced by the method of specimen preparation. However, final DV is not affected by the specimen size, as evident from similar results obtained by using Method-2 and -3.
5. Stabilization with 10% CFA is more effective in reducing the DV of silty clay specimens followed by 6% lime. However, 6% lime proved more effective in reducing DV of lean clay and fat clay specimens. On the contrary, 10% CKD was found to show no significant improvement in DVs for the soils used in this study. Also, a strong correlation was found between the final DV and moisture content of

specimens suggesting that DV is affected by the amount of moisture present in the specimens.

6. The maximum DV criterion for selecting durable aggregate base material seems more conservative for raw and stabilized soil specimens.
7. No correlation was observed between the final DV after TST and durability evaluated by using retained UCS values after F-T or vacuum saturation test.
8. After capillary soaking, 6% lime-stabilization of lean clay and fat clay showed the best performance by providing highest M_r values. With silty clay, the degree of effectiveness after capillary soaking was found more for 10% CFA-stabilized specimens than corresponding 6% lime-stabilized specimens. Contrary to before capillary soaking behavior, CKD-stabilized specimens showed the worst performance after 60-day capillary soaking. Thus, the qualitative trend of M_r values after capillary soaking were similar to the behavior of corresponding specimens tested for DV.
9. For all the soils used in this study, raw and stabilized C-soil (fat clay) specimens showed worst performance in F-T UCS, vacuum saturation and M_r after capillary soaking tests. This can be attributed to the acidic nature of C-soil (pH = 4.17) which will decrease the rate of cementitious reactions.

Table 3.1 Summary of Literature Review of Tube Suction Test on Stabilized Materials

Reference	Type of Soil /Aggregate (Additive)	Curing period	Specimen Size	Drying Period	Duration of reading	Experimental Details
Little (2000)	Silty soil (L)	7 days	152.4 mm x 152.4 mm (6.0 in) x 6.0 in)	4 days (40^{o} C)	311 hours (13 days)	Specimen was placed in a tray with a porous plate at the bottom of the specimen (No mold was used)
Syed et al. (2000)	Aggregates (CLS)	NA	152.4 mm x 203.2 mm (6.0 in x 8.0 in)	--	240 hours (10 days)	Specimen was compacted in cylindrical plastic molds. These molds were having 1.0mm diameter holes around the circumference(at height of 6 mm from the bottom) of the mold at a horizontal spacing of 12.5 mm
Guthrie and Scullion (2003)	Hanson Aggregates	NA	152.4 mm x 203.2 mm (6.0 in x 8.0 in)	2 days (60±5^{o} C)	240 hours (10 days)	Specimen was compacted in cylindrical plastic molds. These molds were having 1.5mm diameter holes around the circumference(at height of 6 mm from the bottom) of the mold at a horizontal spacing of 12.5 mm
Saeed et al. (2003)	NA	NA	152.4 mm x 203.2 mm (6.0 in x 8.0 in)	3 days (38^{o} C)	--	Specimens were compacted in cylindrical plastic molds. These molds were having 1/16 in diameter holes (¼ in above the outside bottom of the mold)around the circumference of the mold at a horizontal spacing of 0.5 in. This equates to 38 or 39 holes around the cylinder base. In addition it also consisted of one 1/16 in diameter hole in each quadrant of the circular bottom of the mold, with each hole about 2 in from the center
Syed et al. (2003)	Aggregates (C)	0 day	101.6 mm x 116.8 mm (4.0 in x 4.6 in)	3-4 days (40^{o} C)	240 hours (10 days)	Specimen was placed in a tray with a porous plate at the bottom of the specimen (No mold was used)
Barbu et al. (2004)	Silty sand (C)	28 days	152.4 mm x 304.8 mm, 101.6 mm x 177.8 mm (6.0 in x 12.0 in, 4.0 in x 7.0 in)	2 days (50^{o} C)	500 hours (21 days)	The bottom of the tube was cut and replaced with aluminum foil pierced with a 1.mm nail, to form 3 concentric circles and with a distance between holes of approximately 4 cm
Zhang and Tao (2008)	Lean clay (C)	1 day	101.6 mm x 177.8 mm (4.0 in x 7.0 in)	14 days (40^{o} C)	240 hours (10 days)	Specimens were placed in plastic tube with holes at their bottoms, and then plastic tubes were placed in a large plastic container with a porous stone underneath and 20 mm water above the bottom= of the samples

L-Lime; C-Cement; CLS-Concentrated liquid stabilizer; NA-Not Applicable

Table 3.2 Summary of Recommended Procedures by Different Agencies for Evaluating Durability of Stabilized Soils

Agency	Specification/ Reference	Type of additive	Procedure	Requirements
American Society for Testing and Materials (ASTM)	ASTM D 4609 (2001)	Chemicals	Unconfined compressive strength on raw, cured specimens and 2-day moisture conditioned samples	$UCS_t > 50$ psi + UCS_r
Department of Air Force and Army	AFJMAN (1994)	Lime, PC	Cured specimens (28-day for lime-stabilized, 7-day cement-stabilized at 73°F) are subjected to 12 cycles of W-D or F-T in accordance with ASTM D 559 or 560, respectively and tested for UCS	$UCS_t \geq 250$ psi (for flexible pavement), $UCS_t \geq 200$ psi (for rigid pavement)
Illinois DOT (ILDOT)	PTA-D7/ IDOT (2005)	Lime, PC	Unconfined compressive strength on raw and treated specimens	$UCS_{t,L} > 50$ psi + UCS_r $UCS_{t,L} \geq 100$ psi $UCS_{t,PC} \geq 500$ psi
Indiana DOT (INDOT)	INDOT (2008)	Lime, PC	Unconfined compressive strength on cured specimens (2-days at 120°F)	$UCS_{t,L} > 50$ psi + UCS_r $UCS_{t,c} \geq 100$ psi + UCS_r
Ohio DOT (OHDOT)	Supplement 1120/ OHDOT (2007)	Lime, PC	Cured specimens (7-day at 104°F) followed by moisture conditioning of specimens through capillary soaking for 1-day before UCS test	$UCS_{t,L} > 50$ psi + UCS_r $UCS_{t,L} \geq 100$ psi $UCS_{t,PC} > 50$ psi + UCS_r $UCS_{t,PC} \geq 150$ psi
Oklahoma DOT (ODOT)	OHD L-50/ ODOT (2006)	PC, CFA, CKD	Cured specimens (one for 7-day, another for 5-day followed by 2-day of moisture conditioning through immersion in water) at 73°F before UCS test	Without moisture conditioning: $UCS_{t,PC,CFA,CKD} > 50$ psi + UCS_r $UCS_{t,PC,CFA,CKD} < 150$ psi Moisture conditioned: $UCS_{t,PC,CFA,CKD} > 50$ psi + UCS_r
Texas DOT (TXDOT)	Tex 121-E/ TXDOT (2002)	Lime	Cured specimens (7-day at room temperature) and air dried at 140°F to loose 1/3 – ½ of molding moisture content	$UCS_{t,L} > 50$ psi + UCS_r
Texas DOT (TXDOT)	Tex 135-E/ TXDOT (2002)	PC	Cured specimens (7-day at 140°F) are subjected to 12 cycles of F-T in accordance with ASTM D 560, and weight loss is determined	---

DOT: Department of Transportation; UCS: unconfined compressive strength; t: treated soil; r: raw soil
W-D: wet-dry; F-T: freeze-thaw; L: Lime; PC: Portland cement; CFA: class C fly ash; CKD: cement kiln dust

Table 3.3 Percentage Decrease in UCS Values of Raw and Stabilized P-, K- and C-soil Specimens Due to F-T Cycles

Additive	Number of F-T Cycles			
Type	1	4	8	12
		P-soil		
None	96	96	97	97
6% Lime	33	75	82	85
10% CFA	57	82	87	87
10% CKD	48	65	78	83
		K-soil		
None	95	95	96	97
6% Lime	40	79	86	89
10% CFA	69	91	92	93
10% CKD	66	83	88	90
		C-soil		
None	95	95	96	100
6% Lime	62	91	95	98
10% CFA	97	98	98	99
10% CKD	88	94	98	99

Table 3.4 A Summary of Resilient Modulus Values of Stabilized P-soil Specimens (After 60-Day Capillary Soaking)

σ_3	σ_d	M_r (MPa)											
(kPa)	(kPa)	Raw	SD	CV	6% Lime	SD	CV	10% CFA	SD	CV	10% CKD	SD	CV
41	12	33	6	18	181	28	15	391	38	10	98	19	19
41	25	29	5	17	186	31	17	388	41	11	100	18	18
41	37	25	4	16	209	22	11	344	37	11	117	17	15
41	50	24	4	17	227	28	12	261	42	16	126	21	17
41	62	24	5	21	236	13	6	218	39	18	131	18	14
28	12	32	5	16	169	21	12	258	41	16	87	11	13
28	25	26	6	23	189	11	6	241	38	16	101	16	16
28	37	23	4	17	204	10	5	232	37	16	107	19	18
28	50	23	3	13	215	19	9	232	41	18	112	21	19
28	62	22	4	18	224	17	8	225	38	17	116	16	14
14	12	24	2	8	156	18	12	271	39	14	83	14	17
14	25	18	3	16	173	22	13	273	43	16	83	17	21
14	37	17	1	6	183	17	9	277	29	10	86	13	15
14	50	18	1	5	193	22	11	269	34	13	92	11	12
14	62	18	2	11	203	29	14	249	31	12	96	9	9

1 psi = 6.89 kPa; 1 ksi = 6.89 MPa; SD: standard deviation; CV: coefficient of variation (%)

σ_d : deviator stress; σ_3 : confining pressure; M_r : resilient modulus (using internal LVDTs)

* Deformations are out of the measuring range of LVDTs

Table 3.5 A Summary of Resilient Modulus Values of Stabilized K-soil Specimens (After 60-Day Capillary Soaking)

σ_3	σ_d	M_r (MPa)											
(kPa)	(kPa)	Raw	SD	CV	6% Lime	SD	CV	10% CFA	SD	CV	10% CKD	SD	CV
41	12	11	4	40	72	17	24	47	11	23	41	8	19
41	25	9	3	36	79	16	20	48	9	19	41	9	22
41	37	[a]	[a]	[a]	79	12	15	46	10	22	39	6	15
41	50	-	-	-	83	13	15	45	6	13	38	6	16
41	62	-	-	-	87	14	16	45	8	18	38	8	20
28	12	-	-	-	56	11	19	43	9	21	39	10	25
28	25	-	-	-	58	14	24	37	9	23	35	6	16
28	37	-	-	-	64	13	20	37	10	27	35	8	23
28	50	-	-	-	71	10	13	39	11	28	37	5	15
28	62	-	-	-	78	11	14	41	10	24	39	9	23
14	12	-	-	-	48	9	20	36	7	19	39	7	18
14	25	-	-	-	50	9	18	31	6	19	32	5	15
14	37	-	-	-	56	12	21	31	8	25	31	4	13
14	50	-	-	-	64	10	16	33	6	18	32	4	12
14	62	-	-	-	72	14	20	36	4	11	34	5	15

1 psi = 6.89 kPa; 1 ksi = 6.89 MPa; SD: standard deviation; CV: coefficient of variation (%)

σ_d : deviator stress; σ_3 : confining pressure; M_r : resilient modulus (using internal LVDTs)

* Deformations are out of the measuring range of LVDTs

Table 3.6 A Summary of Resilient Modulus Values of Stabilized C-soil Specimens (After 60-Day Capillary Soaking)

σ_3	σ_d	M_r (MPa)											
(kPa)	(kPa)	Raw	SD	CV	6% Lime	SD	CV	10% CFA	SD	CV	10% CKD	SD	CV
41	12	30	4	14	104	21	20	40	9	23	15	3	20
41	25	23	3	14	105	18	17	38	4	11	14	4	29
41	37	18	2	14	101	20	20	36	7	20	12	3	23
41	50	16	2	12	100	17	17	34	11	32	[a]	[a]	[a]
41	62	[a]	[a]	[a]	101	21	21	33	7	21	-	-	-
28	12	-	-	-	87	15	18	34	4	11	-	-	-
28	25	-	-	-	79	12	15	27	3	11	-	-	-
28	37	-	-	-	79	11	14	26	4	15	-	-	-
28	50	-	-	-	83	12	15	27	2	7	-	-	-
28	62	-	-	-	87	13	15	28	2	8	-	-	-
14	12	-	-	-	67	11	16	25	2	8	-	-	-
14	25	-	-	-	62	10	16	21	3	14	-	-	-
14	37	-	-	-	64	9	14	21	2	10	-	-	-
14	50	-	-	-	68	11	15	22	2	9	-	-	-
14	62	-	-	-	74	8	11	23	3	13	-	-	-

1 psi = 6.89 kPa; 1 ksi = 6.89 MPa; SD: standard deviation; CV: coefficient of variation (%)

σ_d : deviator stress; σ_3 : confining pressure; M_r : resilient modulus (using internal LVDTs)

* Deformations are out of the measuring range of LVDTs

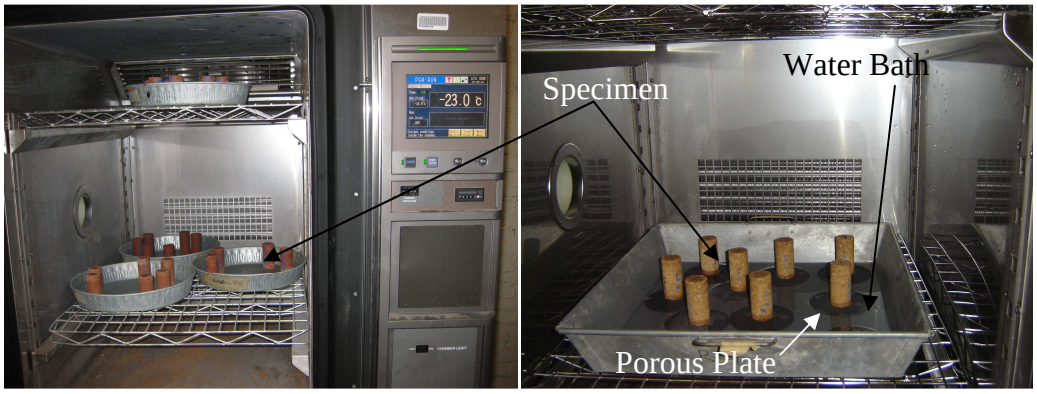

(a) (b)

Figure 3.1 Setup for (a) Freezing (b) Thawing Test

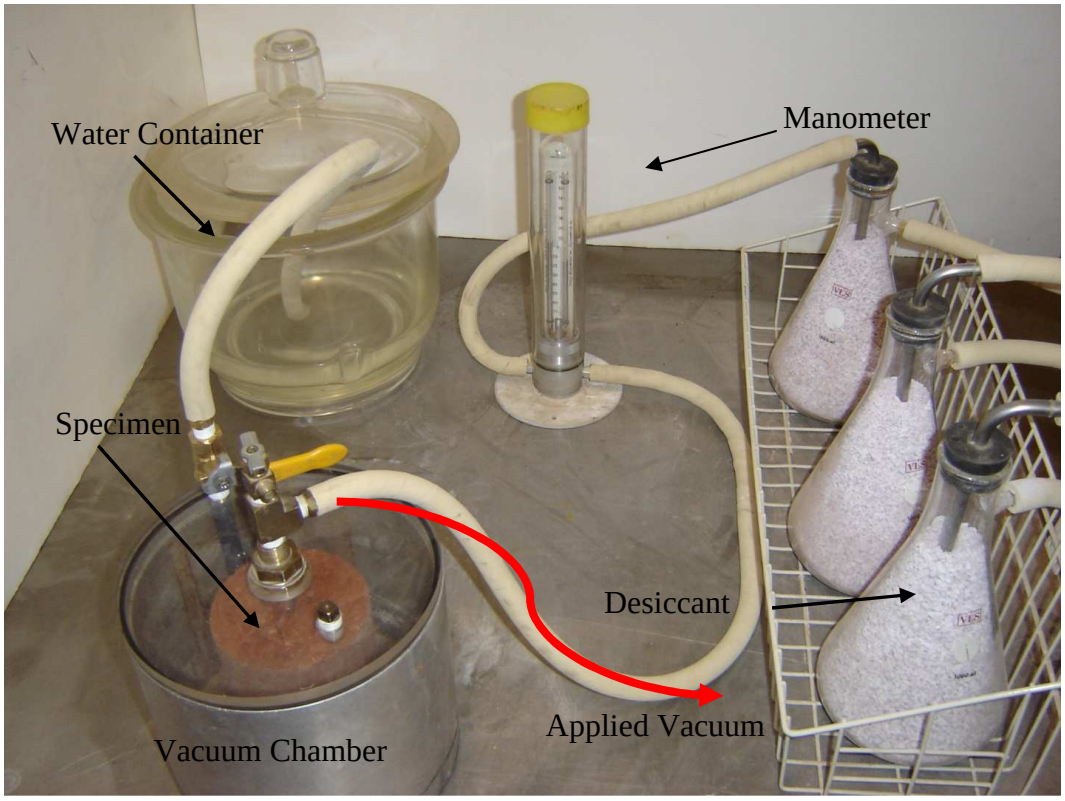

Figure 3.2 Setup for Vacuum Saturation Test

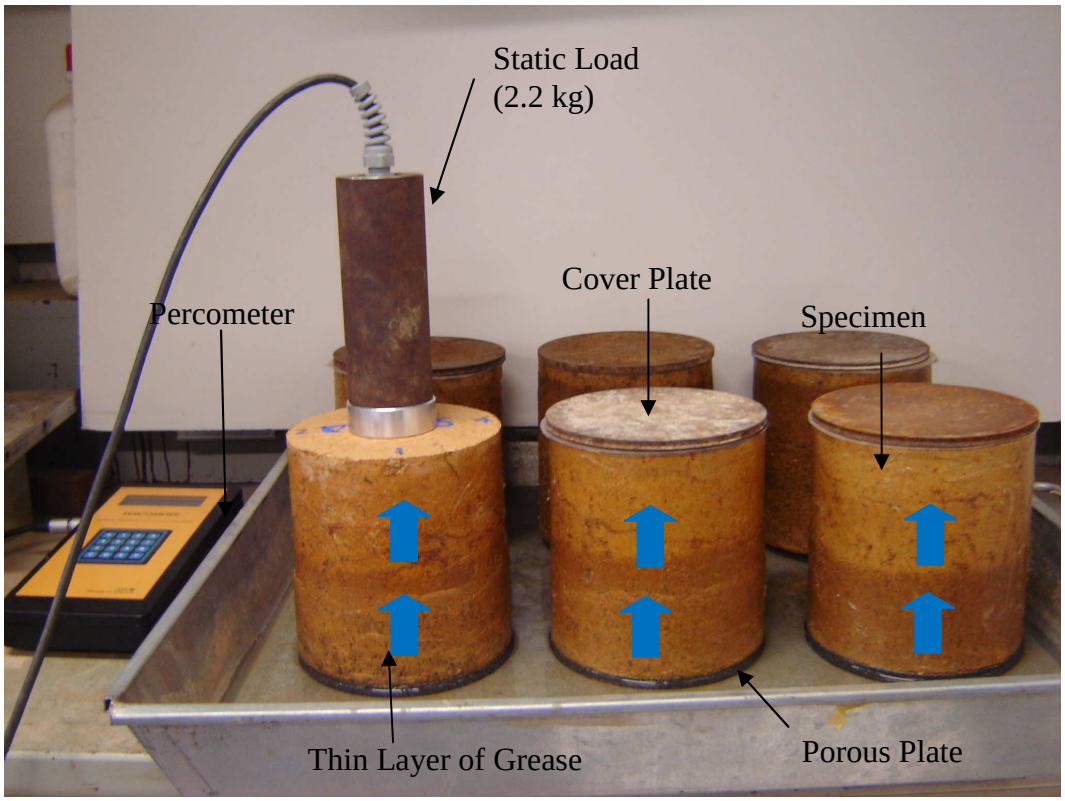

Figure 3.3 Setup for Tube Suction Test

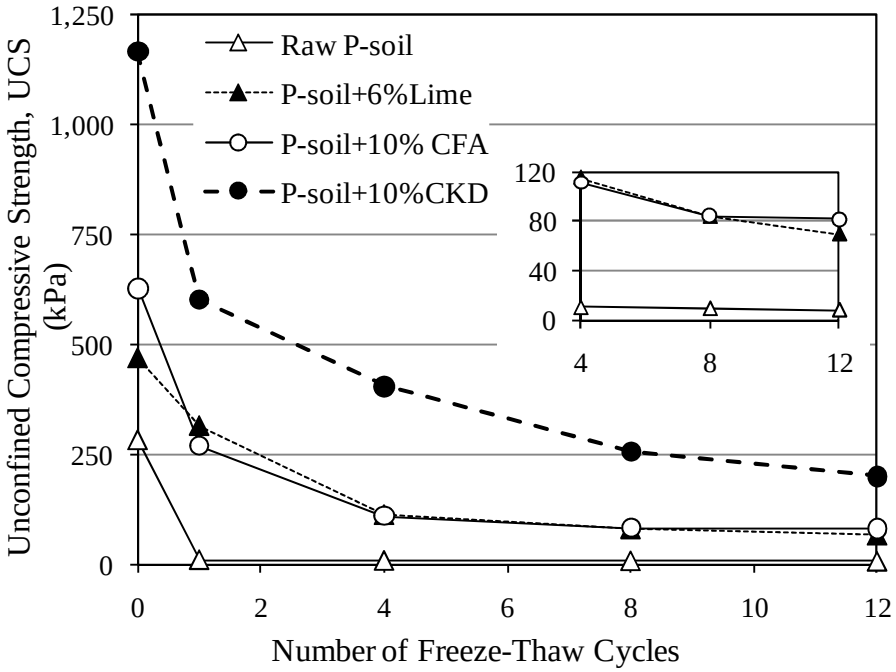

Figure 3.4 UCS of Raw and Stabilized P-Soil Specimens at the End of 0, 1, 4, 8 and 12 Freeze-Thaw Cycles

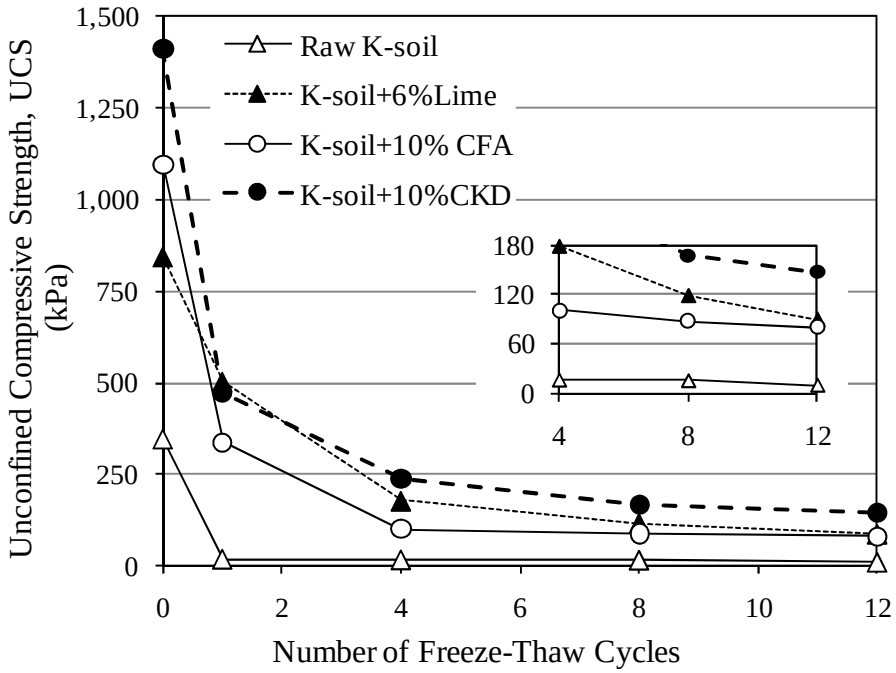

Figure 3.5 UCS of Raw and Stabilized K-Soil Specimens at the End of 0, 1, 4, 8 and 12 Freeze-Thaw Cycles

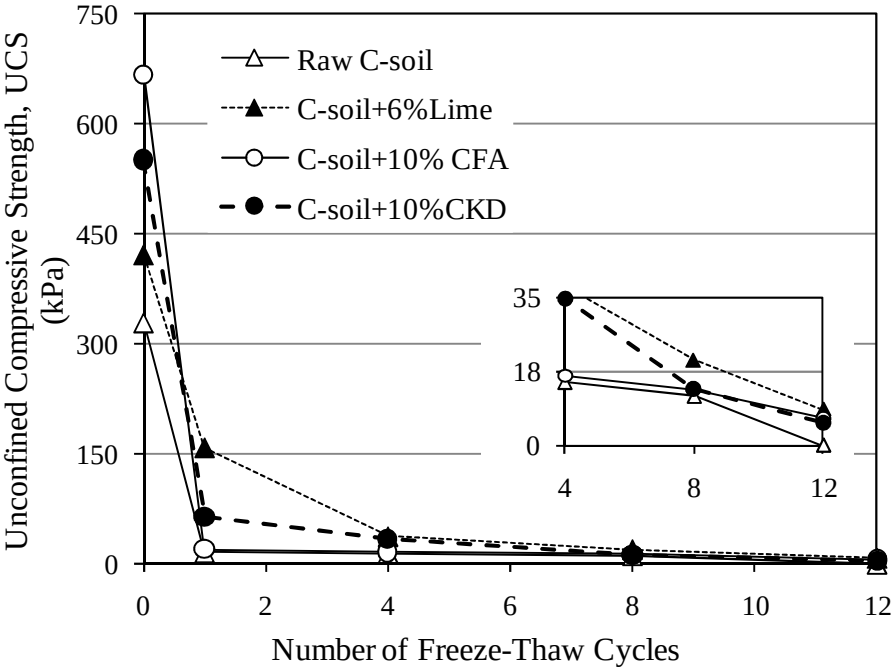

Figure 3.6 UCS of Raw and Stabilized C-Soil Specimens at the End of 0, 1, 4, 8 and 12 Freeze-Thaw Cycles

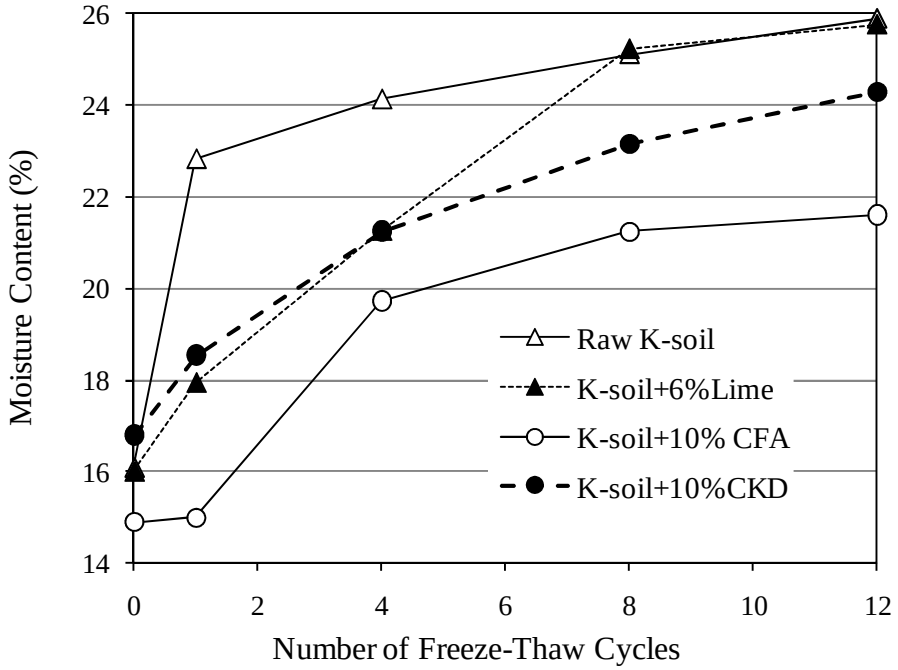

Figure 3.7 Moisture Content of Raw and Stabilized K-Soil Specimens at the End of 0, 1, 4, 8 and 12 Freeze-Thaw Cycles

(a) Raw (b) 6% Lime (c) 10% CFA (d) 10% CKD

Figure 3.8 P-soil Specimens at the End of 12 Freeze-Thaw Cycles

(a) Raw (b) 6% Lime (c) 10% CFA (d) 10% CKD

Figure 3.9 K-soil Specimens at the End of 12 Freeze-Thaw Cycles

(a) Raw (b) 6% Lime (c) 10% CFA (d) 10% CKD

Figure 3.10 C-soil Specimens at the End of 12 Freeze-Thaw Cycles

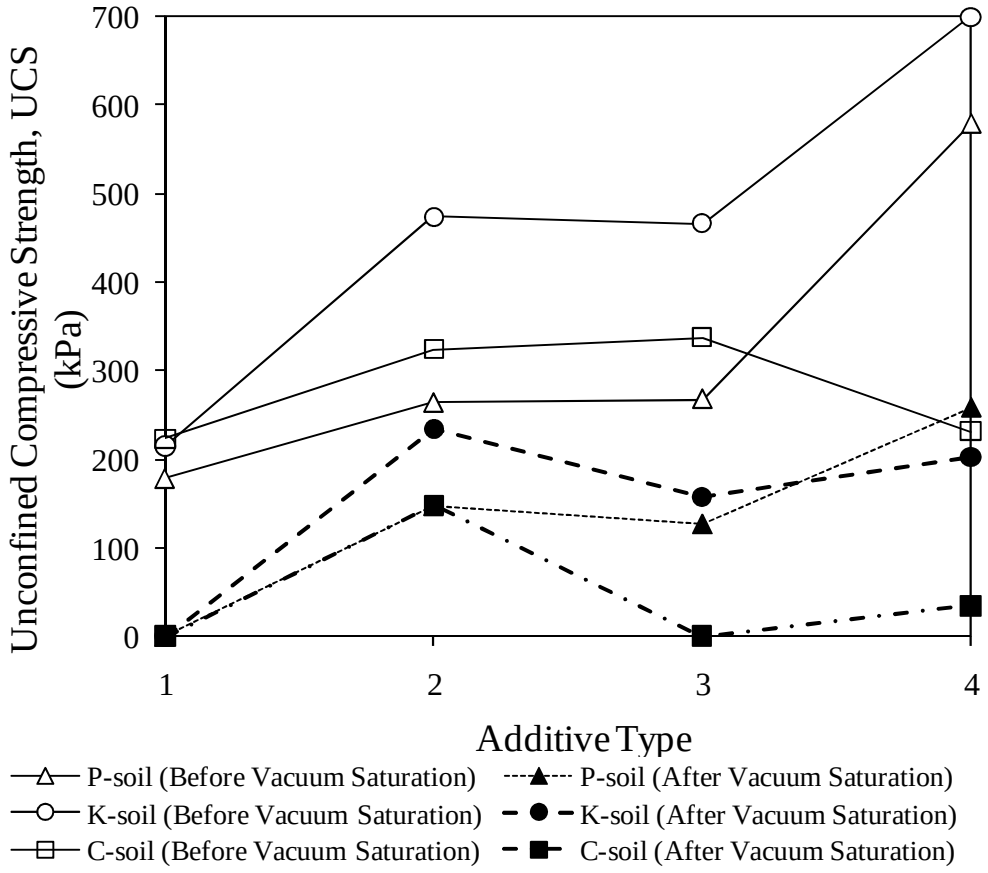

Figure 3.11 UCS of Raw and Stabilized Soil Specimens Before and After Vacuum Saturation Test

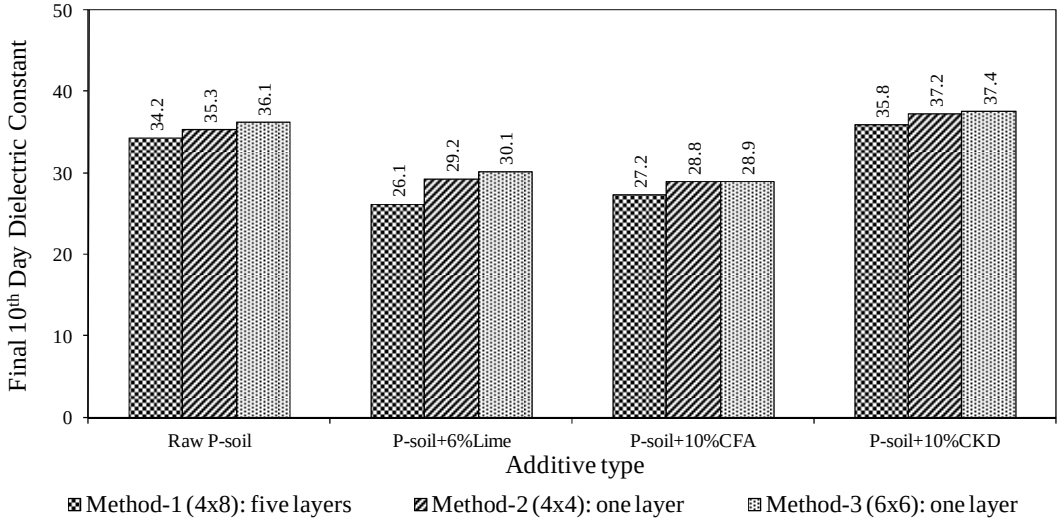

Figure 3.12 Final 10th Day Dielectric Values of Raw and Stabilized P-Soil Specimens

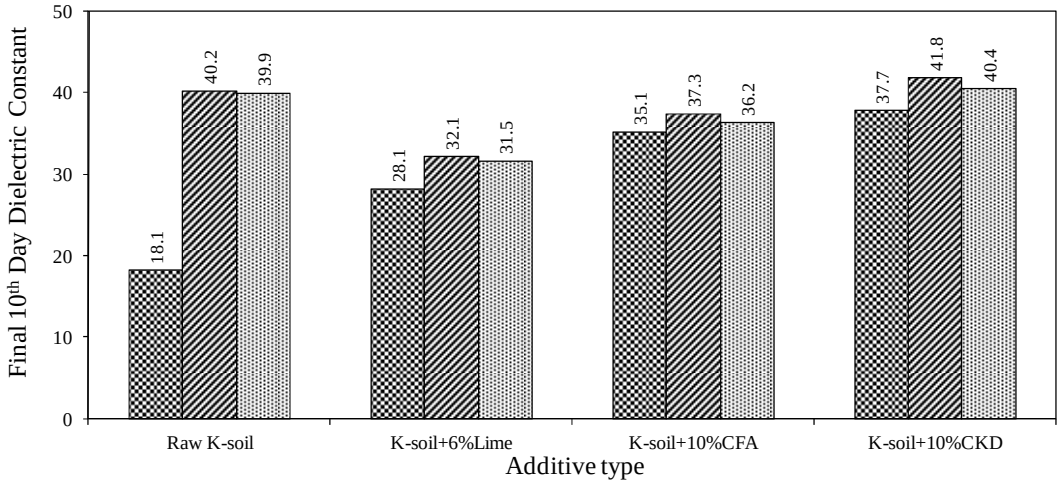

Figure 3.13 Final 10th Day Dielectric Values of Raw and Stabilized K-Soil Specimens

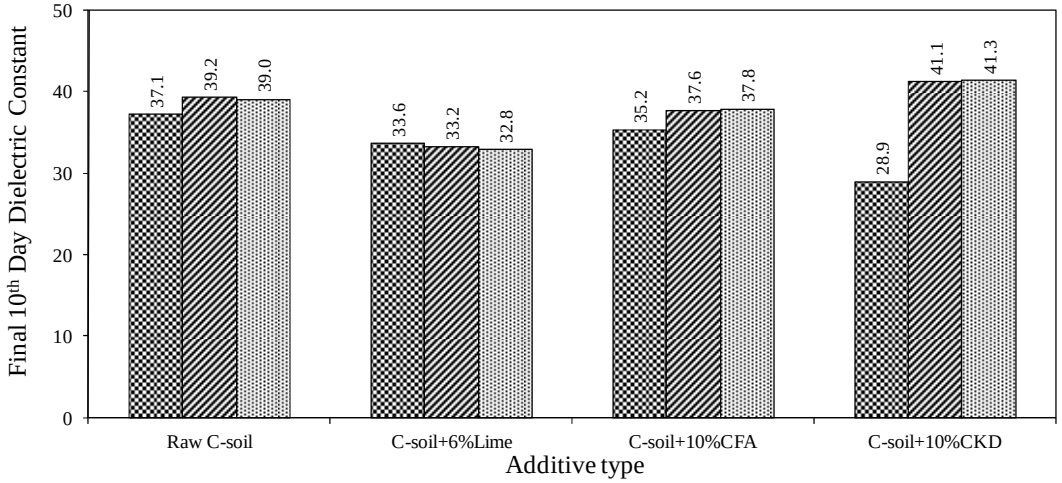

Figure 3.14 Final 10th Day Dielectric Values of Raw and Stabilized C-Soil Specimens

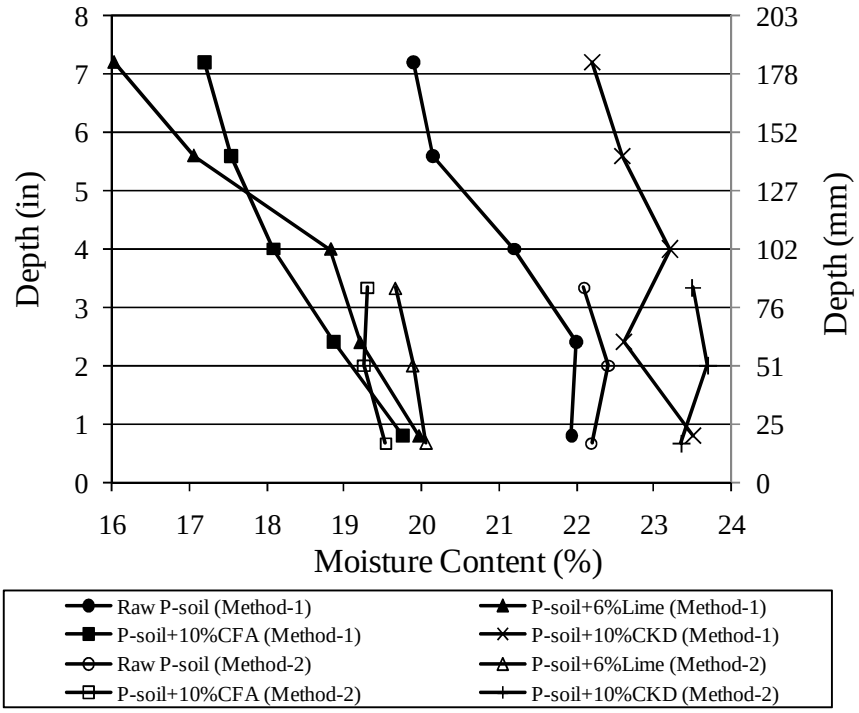

Figure 3.15 Variation of Moisture Content Along the Height of Stabilized P-Soil Specimens

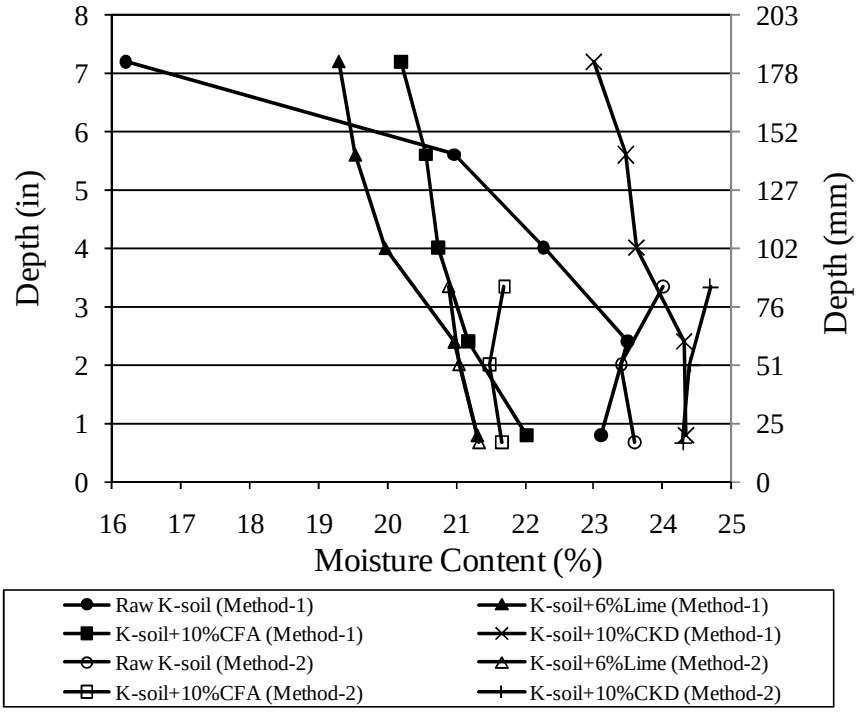

Figure 3.16 Variation of Moisture Content Along the Height of Stabilized K-Soil Specimens

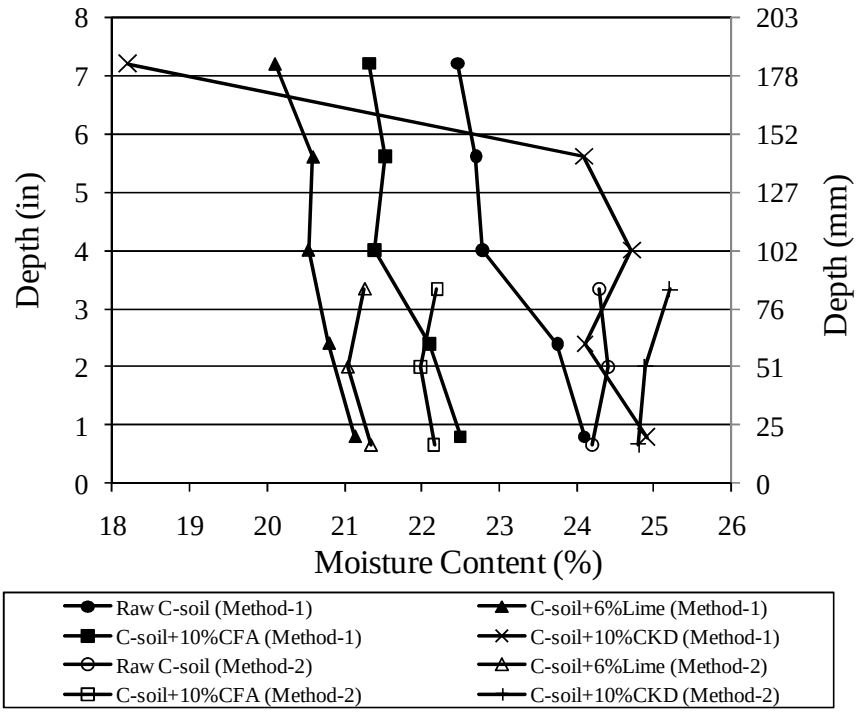

Figure 3.17 Variation of Moisture Content Along the Height of Stabilized C-Soil Specimens

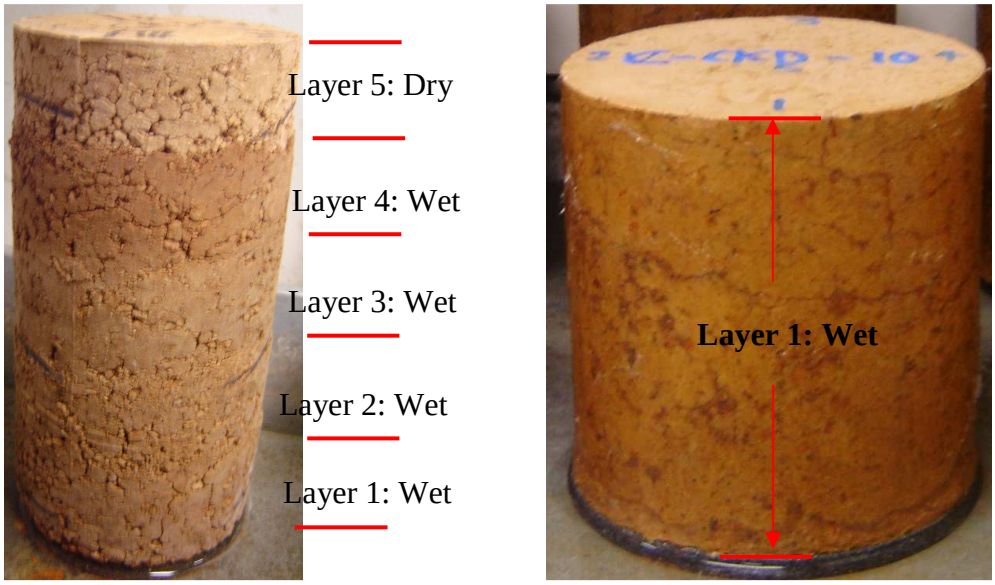

(a) Method-1 (b) Method-2

Figure 3.18 Photographic View of C-soil Specimens Stabilized with 10% CKD Under Tube Suction Test (After 10 Days)

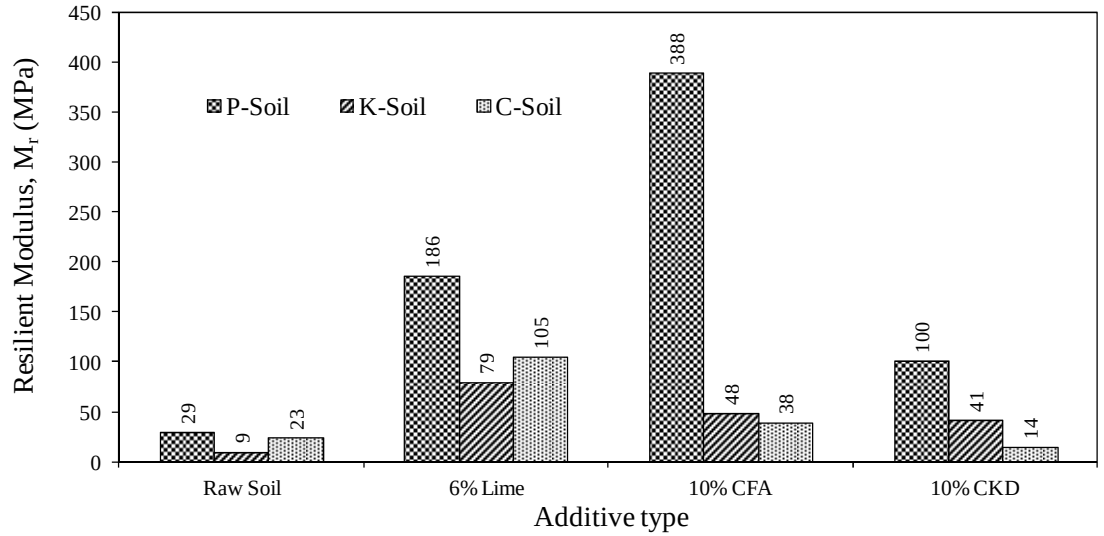

Figure 3.19 M_r Values (σ_3 = 41 kPa, σ_d = 25 kPa) Versus Type of Additive for P-, K- and C-Soil Specimens After 60-Day Capillary Soaking

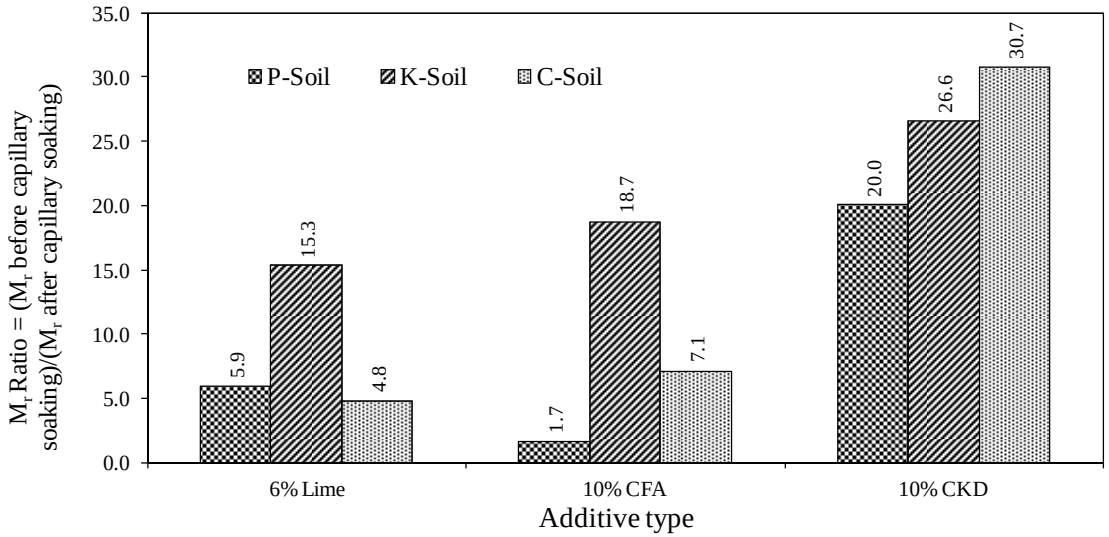

Figure 3.20 M_r Ratio (M_r Before Capillary Soaking/M_r After Capillary Soaking) Versus Type of Additive (σ_3 = 41 kPa, σ_d = 25 kPa)

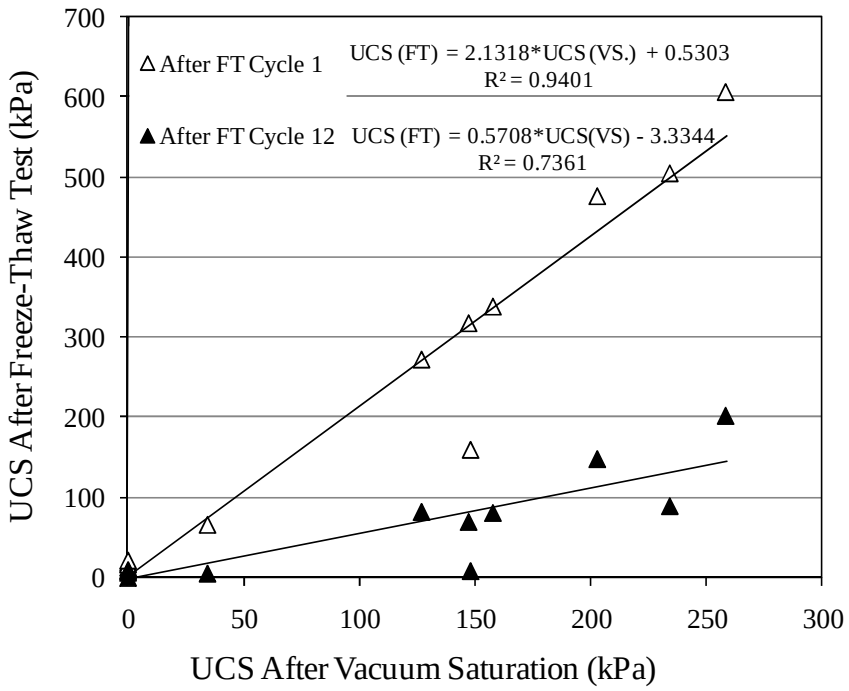

Figure 3.21 Correlation between UCS After the Freeze-Thaw (FT) Test and UCS After the Vacuum Saturation (VS) Test

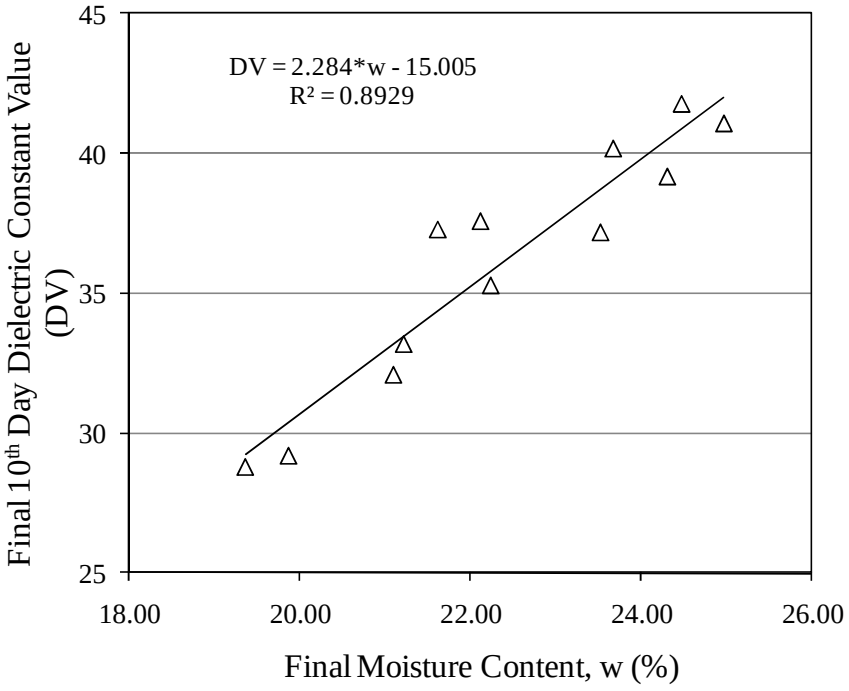

Figure 3.22 Correlation between Final Dielectric Constant Value and Moisture Content (Method-2)

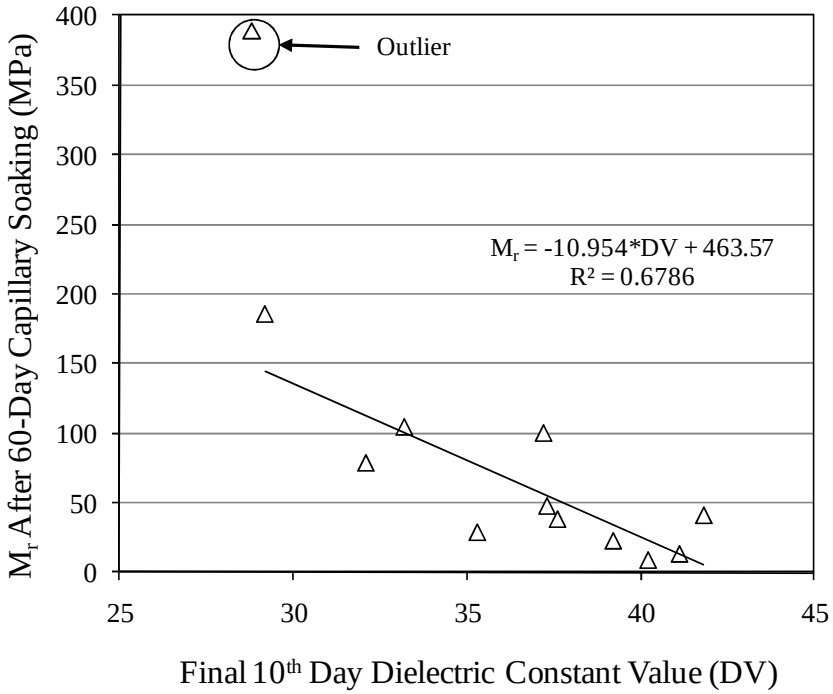

Figure 3.23 Correlation between M_r After 60-Day Capillary Soaking and Final 10^{th} Day Dielectric Constant Values

CHAPTER 4

INFLUENCES OF VARIOUS CEMENTITIOUS ADDITIVES ON PERFORMANCE OF SULFATE BEARING SOIL

4.1 Introduction

Sulfate bearing natural soils are ubiquitous in southern, western, and southwestern states of the United States (Hunter, 1988; Mitchell and Dermatas, 1990; Petry and Little, 1992; Kota et al., 1996; Rollings et al., 1999; Puppala et al., 2001). These states mainly include Texas, Nevada, Louisiana, Kansas, Colorado, and Oklahoma where calcium-based additives such as lime, ordinary Portland cement, and fly ash, are traditionally used to stabilize natural subgrade soils rich with sulfate (Kota et al., 1996; Rollings et al., 1999). Primary "sulfate-induced heaving" problems arise when natural sulfate rich soils are stabilized with calcium-based additives (Puppala et al., 2004), also known as "sulfate attack." Calcium ions of the additive are known to react with free alumina and soluble sulfates in soils to form ettringite, $Ca_6[Al(OH)_6]_2.(SO_4)_3.26H_2O$, causing expansion of up to 250 percent when completely formed (Hunter, 1988; Berger et al., 2001). Ettringite, a weak sulfate mineral, undergoes significant heaving when subjected to hydration. This heave is known to severely affect the performance of pavements, and other geotechnical engineering structures built on sulfate rich soils stabilized with calcium-based additive (Hunter, 1988; Mitchell and Dermatas, 1990; Petry and Little, 1992; Rajendran and Lytton, 1997; Rollings et al., 1999; Puppala et al., 2004).

Consequently, a research program was undertaken with the objective of exploring potential additives with different amount of calcium that are locally produced and economically available, namely, lime, class C fly ash (CFA), and cement kiln dust (CKD) for stabilizing natural sulfate rich lean clay from northwestern Oklahoma. The research

presented in this chapter is unique in several ways: short-term and long-term strength-stiffness parameters of stabilized sulfate rich lean clay are evaluated for pavement application and volume change behavior of stabilized lean clay is addressed. Short-term performance evaluation included determination of resilient modulus (M_r), modulus of elasticity (M_E), and unconfined compressive strength (UCS), after 28 days of curing, consistent with the MEPDG, as presented in Chapter 2. Long-term performance was evaluated in terms of three-dimensional (3-D) swell during 120 days of capillary soaking of selected specimens. At the end of capillary soaking, specimens were further tested for M_r, modulus of elasticity, and unconfined compressive strength, as additional indicators to long-term pavement performance. Furthermore, pH values, Atterberg limits, and percent passing No. 200 sieve were also determined after 28 days of curing. Mineralogical studies such as scanning electron microscopy, energy dispersive spectroscopy, and X-ray diffraction were used to verify research findings observed from the macro test results. The evaluation results presented here could potentially lead to the selection of type and amount of locally available additive for stabilization of sulfate rich lean clay in pavement construction projects.

4.2 Background

Sherwood (1958) was the one of the early investigators who noticed the problem concerning sulfate attack on stabilized soil. Sherwood (1962) conducted an experiment to determine the effect of the presence of sulfate ions in soils on the durability of cement- and lime-stabilized soils. The method of investigation consisted of observing the behavior of specimens of stabilized soil when totally immersed in water. The laboratory study showed disintegration of lime-and cement-stabilized clay specimens within few days,

whereas cement-stabilized sand mixtures containing the same proportions of sulfates were unaffected even after being immersed for one year. On the basis of results, it was proposed that sulfate attack on cement-stabilized soils is principally due to the reaction involving clay minerals and that the relatively slow combination of the sulfates with the cement is of secondary importance.

Cordon (1962) conducted similar laboratory test concerning sulfate attack resistance of soil cement. Type I, Type II and Type V Portland cements and a coarse-grained soil and a fine-grained soil were used for specimen preparation, which would be immersed in sulfate solution. A photographic record, taken at different time intervals, was used as a method of demonstrating progress of the sulfate attack. Major conclusions included: (1) soil-cement is subject to sulfate attack much in the same manner as cement concrete, but deterioration in soil-cement is much more rapid than in cement concrete; (2) soil cement specimens prepared with Type V and Type II cements were more resistant to the sulfate attack than soil cement specimens fabricated with Type I cement; and (3) soil cement specimens made with fine-grained soils deteriorated more rapidly.

Mitchell (1986), in a Terzaghi lecture, reintroduced the profession to calamities associated with sulfate-induced heave in lime stabilized clay soils. An investigation was carried out concerning a section of a major arterial street with lime treated expansive soil base in Las Vegas, Nevada. The completed construction appeared to be of good quality and the initial performance was excellent but after two years pavement failed in the form of surface heaving and cracking. The investigation of the failed pavement indicated that structural design of the pavement section was adequate and the failure was not traffic-induced. Further tests provided the following information: the soil contained significant

amounts of soluble sodium sulfate (up to 1.5 percent by weight); samples taken from intact and un-failed zones swelled if exposed to water; clay minerals were present in the soil; a significant amount of ettringite was indicated by X-ray diffraction in both the failed and un-failed zones. This landmark paper was followed by a comprehensive study by Hunter (1988), which provided a geochemical analysis of the phenomenon of sulfate-induced heave in clay soils stabilized with calcium-based additives. Both papers focused on a case study of failure at Stewart Avenue in Las Vegas, Nevada.

The phenomenon of sulfate-induced heave received much attention during the 1990s and continues to pose problems for those stabilizing soils where soluble sulfates are present, especially in the western United States. Better understanding of this phenomenon was provided by Mitchell and Dermatas (1990), Little and Petry (1992), Petry (1995), Rollings et al. (1999), and Little et al. (2010). Petry and Little (1992) reviewed the background on sulfate-induced heave in lime- and cement-stabilized clay soils and some examples of projects affected by this phenomenon. In another study by Petry and Little (2002), future research needs for establishing more effective ways to stabilize sulfate-bearing clays have been identified.

The problem of stabilizing sulfate bearing soils with lime as well as plausible stabilization schemes were recently reviewed by Harris et al. (2004). Among the stabilization schemes identified were mellowing for 1 to 3 days, higher molding moisture contents (2% above optimum), and single application of lime instead of double application. However, conclusions were made on the basis of only three-dimensional swelling tests and no attempt was made to study the performance using other tests such as resilient modulus, unconfined compressive strength and modulus of elasticity, as

recommended by the MEPDG. Moreover, 1 to 3 days of mellowing could be problematic for design applications.

Further, Puppala et al. (2004) addressed the effectiveness of sulfate resistant cement additives Types I/II and V, for providing better treatment of four different sulfate rich soils. Experimental design included evaluation of compaction relationships, Atterberg limits, linear shrinkage and free swell strain potentials, unconfined compressive strength, and low strain shear moduli properties. Overall test results showed that both cement types provided effective stabilization of sulfate rich soils of varying sulfate levels. Also, this study addressed some of the design inputs for the MEPDG. However, it was carried out by using sulfate resistant additives which are not readily available in the Oklahoma area and are expensive (Nevels and Laguros, 2005). Also, sulfate resistant cement additives may provide protection against the Type I sulfate attacked, but they will be completely ineffective against the Type II sulfate attack (Wang, 2002), as will be discussed later. This makes it necessary to investigate locally available additives.

In a recent study, Hilbrich and Scullion (2010) successfully stabilized soils containing high sulfate concentration (30,000 to 50,000 ppm) using traditional additives and non-traditional construction methods. A total of four combinations of traditional additives, namely, 6% lime, 4% lime with 4% class F fly ash, 4% lime with 6% class F fly ash, and 4% lime with 8% class F fly ash were considered. The subgrade was pre-treated with 3% lime slurry at OMC+2% and kept wet and reworked approximately 3 to 5 times for a period of 7 days. After 7 days, remaining percent of stabilizer was added followed by another mellowing period and compaction. Good performance in the field indicated that stabilization with extended mellowing is feasible, even with very high

sulfate bearing subgrade soils. However, several days of mellowing could be problematic for design applications.

4.3 Factors Affecting Sulfate Attack

Similar to cement concrete, the pH, moisture availability, lime dosage, temperature, sulfate levels, reactive alumina, and clay mineralogy may all affect sulfate attack of stabilized soils (Hunter, 1988; Roy et al., 2003; Puppala et al., 2005; Little et al., 2010). These factors should therefore be determined when stabilized soils are susceptible to sulfate attack. The thermal and chemical stability of ettringite, under varying conditions of pH value, has been evaluated by a number of investigators, for example Gabrisova et al. (1991). It was reported that in a calcium alumino-sulfate system at room temperature, ettringite is no longer stable when pH is 10, and decomposes to form gypsum and hydrogarnet (C_3AH_6).

The ettringite formation process was given by Harris (2004) as:

(i) Ionization of lime: $Ca(OH)_2 \rightarrow Ca^{2+}+2OH^-$

(ii) Dissolution of clay mineral: $Al_4Si_4O_{10}(OH)_8+4OH^-+10H_2O \rightarrow Al(OH)_4^- +4H_4SiO_4$

(iii) Dissolution of gypsum: $CaSO_4.2H_2O \rightarrow Ca^{2+}+SO_4^{2-}+2H_2O$

(iv) Formation of ettringite: $6Ca^{2+}+2Al(OH)_4^-+4OH^-+3SO_4^{2-}+26H_2O \rightarrow Ca_6[Al(OH)_6]_2.(SO_4)_3.26H_2O$

Thus, when calcium-based additive is added in sufficient quantities to clay, the pH is raised. Once the pH exceeds 10.5, dissolution of the clay surface occurs, and Si and Al ions are released. If sulfates, either in solid or groundwater form, are present in sufficient quantity, they may initiate a reaction between the calcium and the silica and

alumina released from clay minerals to form significant quantities of ettringite or monosulfate hydrates. Mehta and Klein (1966) determined that the formation of monosulfate hydrates is favored in high alumina environments, but the formation of ettringite is favored in low alumina environments. Also, there appears to be two ettringite formation mechanisms, namely, Type I and Type II (Wang, 2002). The Type I mechanism refers to the conventional sulfate attack, analogous to attack on conventional Portland cement concrete, where the Portland cement hydration products provide the calcium and alumina to react with sulfates to form ettringite. On the other hand, the Type II mechanism is clay-based sulfate attack where the Portland cement hydration products provide calcium and the clay minerals in the soil provide alumina to react with sulfates, when it is present, to form ettringite (Wang, 2002).

Based on several investigations of sulfate attack on lime-stabilized soils in Texas, Petry (1995) suggested that soils containing sulfate contents of 2,000 ppm have the potential to cause swelling, and levels of 10,000 ppm have the potential to cause serious damage due to lime addition. According to current understanding, “low to moderate” and high sulfate soils are those with sulfate less than 2,000 ppm and more than 2000 ppm, respectively (Kota et al., 1996; Mitchell and Dermatas, 1990; Puppala et al., 2002; Rao and Shivananda, 2005; Little et al., 2010).

Time frame to form ettringite in stabilized soils is not well established. Several case studies reported that the time frame for sulfate heaving varied from a few days to several weeks (Kota et al., 1996). The time generally depends on the solubility of sulfates, amount of reactive alumina liberated from soil particles and the amount of calcium present in the additive, which helps in the formation of ettringite (Puppala et al.,

2004). Recently, Little et al. (2010) suggested that the time required to form ettringite in stabilized soils depends upon: amount of water used, the relative activities of ions in the aqueous solution, uniform pH regime, mineralogy, and the ability to solubilize sufficient reactants into an aqueous phase.

In the laboratory controlled environments, the effects of these variables and conditions are somewhat minimized since heave studies were conducted on stabilized soil specimens subjected to capillary soaking in high humidity environment (>96%) and controlled temperature of 23.0 ± 1.7^{o}C (73.4 ± 3.1^{o}F). In such ideal conditions, ettringite mineral was formed in treated clays in less than 24 hours after stabilization and maximum heaving was noted within seven days after curing (Inthrasombat, 2003). Hence, the present capillary soaking time frame of 120 days (4 months) is considered more than sufficient for sulfate heave assessment in this study. Moreover, pH values were monitored before and after 28 days of curing (before capillary soaking). A soil having sulfate content of greater than 10,000 ppm was selected to ascertain the formation of ettringite.

4.4 Materials and Test Procedure

The lean clay used in this study belongs to the "Vernon series" in northwestern Oklahoma. Selection of this particular clay was based on the soluble sulfate content measured in this soil. Sulfate was present in the form of gypsum ($CaSO_4.2H_2O$) outcrops, as shown in Figure 4.1 (a). Figure 4.1 (b) demonstrates the presence of small gypsum crystals in Vernon series soil, also called as V-soil in this study. Soluble sulfate content in the lean clay was measured using the Oklahoma Department of Transportation procedure for determining soluble sulfate content: OHD L-49 (ODOT, 2006). This soil

has a sulfate content of 15,400 ppm (>10,000 ppm). Physical properties of this soil were determined from the Atterberg limit test, hydrometer tests, and standard Proctor compaction tests. The chemical analyses include pH, and cationic exchange capacity (Chapman, 1965) test. These results are presented in Table 2.2. As per the ASTM D 4318 test method, the selected lean clay has an average liquid limit of approximately 37% and a plasticity index (PI) of approximately 11. The chemical properties of the clay determined using X-ray Fluorescence analyses are given in Table 2.3.

As noted previously, three different additives, namely, hydrated lime, CFA and CKD were used in this study. The chemical and physical properties of the additives are presented in Table 2.4. Hydrated lime is high calcium-based additive with 46.1% of available free lime. On the other hand, CFA and CKD are low (free lime content = 0.2%) and moderate (free lime content = 6.7%) calcium-based additives, respectively (Wang, 2002). It is worth mentioning that properties of CKD can vary significantly from plant to plant depending on the raw materials and type of collection process used (Miller and Zaman, 2000). Similarly, fly ash properties may be unique to the same source while it may differ from ashes obtained from other sources (ACAA, 1999). These differences in physical and chemical properties of additives can lead to different performance of stabilized soil specimens.

4.4.1 Specimen Preparation

A total of 40 specimens were prepared in this study. The procedure consists of adding a specific amount of additive to the raw clay. The amount of additive (3%, 6%, or 9% for lime and 5%, 10%, or 15% for CFA and CKD) is expressed as a percentage of the dry weight of the soil. The additive and clay were mixed to achieve a uniform mix. After

the blending process, a desired amount of water was added based on the optimum moisture content (OMC). Then, the mixture was compacted in a mold having a diameter of 101.6 mm (4.0 in) and a height of 203.2 mm (8.0 in) to reach a dry density of between 95%-100% of the maximum dry density (MDD). A summary of OMCs and MDDs of raw and soil-additive mixes is presented in Table 2.8; OMCs and MDDs were determined in accordance with the ASTM D 698 test method. As evident from Table 2.8, laboratory experiments showed an increase in OMC and a decrease in MDD with the amount of lime. This is consistent with the results reported by Nagaraj (1964), Haston and Wohlegemuth (1985), Ali (1992), and Little (1995). For CFA stabilization, MDD decreased for 5 percent and then increased for 10 and 15 percent fly ash. On the other hand, a decrease in OMC was observed with increase in CFA content. A similar observation was made by McManis and Arman (1989), and Misra (1998), McManis and Arman (1989) reported that the reduction in OMC can be attributed to the spherical shape of the fly ash particles in the soil voids, which lubricated the mix and aided in the densification efforts. On the contrary, for soil-CKD mixtures the moisture-density results were more complex. Laboratory experiments showed that MDD decreased with 5 percent CKD, and then increased with the increase in the percentage of additive. On the other hand, OMC increased with 5 percent CKD and then decreased with the increase in the amount of CKD, as evident from Table 3. This behavior is consistent with the observations made by other researchers (see e.g., Baghdadi and Rahman, 1990; Baghdadi et al., 1995; Parsons et al., 2004).

After compaction, specimens were cured at a temperature of 23.0 ± 1.7^{o}C (73.4 ± 3.1^{o}F) and a relative humidity of approximately 96% for 28 days; 28-day curing period is

recommended by the new MEPDG (AASHTO, 2004). A total of four replicates were prepared for each additive content, of which two specimens were tested for M_r and then followed by the three-dimensional (3-D) swell test by subjecting specimens to capillary soaking under controlled temperature (23.0 ± 1.7^oC i.e., 73.4 ± 3.1^oF) and humidity (>96%) in an ice chest. After 120 days of capillary soaking, specimens were again tested for M_r and then followed by M_E and UCS tests. The other two specimens were tested for M_r and then followed by M_E and UCS tests, without capillary soaking. After the UCS test, broken specimens were air dried for approximately 2 days, and then pulverized and passed through a No. 40 sieve. The finer material was reconstituted with moisture for 1 day, and then tested for liquid limit and plastic limit in accordance with ASTM D 4318. Moreover, pH values were monitored before and after 28 days of curing (before capillary soaking), in accordance with the test method recommended by ASTM D 6276. Since M_r, M_E and UCS tests are already discussed in Section 2.6, only three-dimensional swell tests and mineralogical studies will be discussed in the chapter.

4.4.2 Three-Dimensional Swell Test

The oedometer swell testing method is most widely used to evaluate the swelling behavior of soils. This is mainly because of the simplicity of its operation and the availability of conventional oedometer in most soil mechanics laboratories (Al-Shamrani and Al-Mhaidib, 2000). However, a large discrepancy is observed between swell predicted using parameters obtained from oedometer tests and that actually realized in the field. Comparison of field and laboratory data obtained from oedometer tests revealed that the laboratory results from 1-D swell tests overestimate the in situ heave by a factor of about 3 (see e.g., Johnson and Snethen, 1979; Erol, 1992). Hence, to investigate the

swelling potential of specimens, three-dimensional (3-D) swell test were conducted in accordance with a procedure described by Harris et al. (2004). The 3-D swell values were measured by determining the height to the nearest 0.025 mm (0.001 in) in 3 places that are 120^{o} apart. The diameter was measured to the nearest 0.025 mm (0.001 in) near the top, in the middle, and near the base of each sample. The three height and diameter measurements were averaged and the 3-D volume change was calculated.

4.4.3 Mineralogical Studies

The Scanning Electron Microscopy (SEM) technique was employed to qualitatively identify the micro-structural developments in the matrix of the stabilized soil. After the UCS test on capillary-soaked 9% lime- and 15% CKD-stabilized specimens, the broken mix was air-dried for approximately four days. Three representative tiny pieces were mounted on stubs (1 cm wide discs that have a pin-mount on the base of the disc) and coated with a thin layer (≈ 5 nm) of Iridium by sputter coating technique to provide surface conductivity. A JEOL JSM 880 scanning electron microscope operating at 15 kV was used to visually observe the coated specimens. The JEOL JSM 880 was fitted with an energy-dispersive X-ray spectrometer (EDS). The EDS was used to analyze chemical compositions of the specimen. In this technique, electrons are bombarded in the area of desired elemental composition; the elements present will emit characteristic X-rays, which are then recorded on a detector. EDS was performed on selected specimens where needle-shaped crystals of ettringite were identified. The micrographs were taken using EDS2000 software.

To confirm the SEM results, X-ray diffraction (XRD) tests were performed on raw soil and capillary-soaked 9% lime- and 15% CKD-stabilized specimens. Four-day air

dried mix was pulverized with a mortar and pestle, sieved through a U.S. standard No. 325 sieve (45 μm) and the powder finer than 45 μm was collected and placed on a specimen holder prior to testing. This holder was then mounted on a Rigaku D/Max X-ray diffractometer for analysis. This diffractometer is equipped with bragg-brentano parafocusing geometry, a diffracted beam monochromator, and a conventional copper target X-ray tube set to 40 kV and 30 mA. The measurements were performed from 5^o to 70^o (2θ range), with 0.03^o step size and 1 seconds count at each step. Data obtained by the diffractometer were analyzed with Jade 3.1, an X-ray powder diffraction analytical software, developed by Materials Data, Inc. (Jade, 1999). Generated diffractograms (using the peaks versus 2θ and d-spacing) were used to determine the presence of ettringite.

4.5 Laboratory Test Results

4.5.1 pH Testing

Since the pH level of soil indicates strong pozzolanic reaction and stability of ettringite, pH values were also determined after 28 days of curing, before capillary soaking. The results of pH tests for mixtures of clay and different amounts of additives are presented in Figure 4.2. The comparison of pH values of specimens stabilized for zero and 28 days revealed that specimens prepared with higher lime content and cured for 28 days exhibited lower reduction in pH, as compared to specimens prepared with lower lime content. For example, specimens prepared with 9% lime and cured for 28 days exhibited no significant reduction (1.9%) in pH values compared to 3% (11.3%) and 6% (6.3%), as shown in Figure 4.2. It is believed that the excess of lime caused the presence of high amounts of un-reacted lime and thus reduced the strength values, as noted

subsequently. In addition, all percentage of CFA- and CKD-stabilized specimens showed significant decrease in 28-day pH value, as revealed in Figure 4.2. A decrease in pH value indicates consumption of calcium oxide (CaO) in cementitious reactions and thus an increase in strength values. In addition, it is also clear that pH is greater than 10 for 28-day cured clay specimens stabilized with 3%, 6% and 9% lime, and 10% and 15% CKD. This pH value provides a good stable environment for the development of ettringite (Gabrisova et al., 1991; Little et al., 2005).

4.5.2 Effect of Additives on M_r After Capillary Soaking

The M_r test results of V-soil stabilized with different percentages of lime, CFA and CKD after capillary soaking are presented in Tables 4.1, 4.2 and 4.3, respectively. A convenient way to observe the effect of different percentages of additives is to compare M_r values obtained before and after capillary soaking at a particular stress level (Drumm et al., 1997). The mean M_r at a deviatoric stress of 25 kPa (3.6 psi) and a confining pressure of 42 kPa (6.0 psi) have been compared for this purpose (Figure 4.3). Further, to study the comparative effectiveness of lime, CFA, and CKD on V-soil, a chart of percent improvement in M_r values versus percentage of additive was plotted (Figure 4.4).

4.5.2.1 Effect of Lime Content

It is clear that the M_r values decreased after 120 days of capillary soaking due to damage caused by moisture. For example, 3%, 6% and 9% lime showed a decrease of approximately 91%, 89% and 88%, respectively (Figure 4.3). This decrease is maximum for 3% beyond which a reduction in percentage decrease was observed. Although 3% lime showed maximum percentage decrease, 6% lime provided highest M_r values ranging

between 52 – 93 MPa (2.0 – 3.7 ksi), as shown in Table 4.1. Also, comparison with the M_r values of raw soil specimens after capillary soaking shows that 6% lime produced highest percentage increase in M_r values of approximately 99% (Figure 4.4).

4.5.2.2 Effect of CFA Content

From Table 4.2 and Figure 4.3, one can see that the average M_r value decreased by approximately 89%, 87% and 42% after capillary soaking for specimens stabilized with 5%, 10% and 15% CFA, respectively. However, the percentage decrease in M_r value was lower for specimens stabilized with higher amount of CFA. It is also clear from Figure 4.3 that specimens with a lower percentage of CFA (i.e. 5%) showed an increase in M_r values by 55% as compared M_r values of the raw specimen after capillary soaking. Higher percentages of CFA resulted in an increase in the improvement of M_r values, as shown in Figure 4.4. For example, 10% and 15% CFA-stabilized specimens magnified the M_r values by 186% and 1,552% with respect to the raw specimens tested after capillary soaking.

4.5.2.3 Effect of CKD Content

Table 4.3 illustrates the M_r values of CKD-stabilized specimens after capillary soaking. It is evident from Table 4.3 that after capillary soaking, specimens showed a decrease in M_r values. For example, 5%, 10% and 15% CKD-stabilized specimens showed a decrease in M_r values by approximately 69%, 90% and 95%, respectively. With respect to M_r values of raw specimens after capillary soaking, CKD-stabilized specimens showed maximum effectiveness with 10% CKD (Figure 4.4). For example, at a deviatoric stress of 25 kPa (3.6 psi) and a confining pressure of 42 kPa (6.0 psi),

specimens stabilized with 5%, 10% and 15% CKD showed an increase of approximately 201%, 258% and 122%, respectively.

It is also evident from Tables 4.1 through 4.3 that the M_r values at other stress levels follow similar trends of behavior, as discussed in the above paragraphs. It is clear in general for 120-day capillary-soaked specimens that the highest improvement for CKD-stabilized specimens is observed at application rates of less than 10% (Figure 4.4). At application rates between 10% and 15%, CFA-stabilized specimens showed the highest improvement in the M_r values. Overall, the 15% CKD-stabilized specimen showed highest improvement (1,473%) before capillary soaking (as discussed in Section 2.7), while 15% CFA-stabilized specimen showed the highest improvement (1,561%) after 120-day of capillary soaking. This difference in M_r values before and after capillary soaking can be attributed to difference in chemical properties of the additives, as illustrated in Table 2.4, which will result in different swell behavior of stabilized specimens. This issue will be illustrated in subsequent sections.

4.5.3 Effect of Additives on M_E and UCS After Capillary Soaking

The variation of modulus of elasticity (M_E) and UCS values with the additive content is shown graphically in Figures 4.5 and 4.6, respectively. Also, results of both specimens before and after capillary soaking are included in the same graph for comparative purpose. It is evident that there is significant increase in M_E and UCS with increasing additive content in the treated soils. However, capillary-soaked specimens showed decrease in M_E and UCS values than the corresponding specimens tested before capillary soaking. For example, the M_E values of lime-, CFA- and CKD-stabilized specimens subjected to capillary soaking is approximately 88 – 89%, 31 – 92%, and 82 –

95% lower, respectively, than the corresponding M_E values of stabilized specimens before capillary soaking. Similarly, UCS values of capillary-soaked specimens showed a decrease ranging between 86 – 88%, 40 – 90%, and 77 – 88% for lime-, CFA- and CKD-stabilized specimens, respectively, corresponding to specimens tested before capillary soaking.

Further, to study the comparative effectiveness of lime, CFA and CKD after capillary soaking, graphs of percent improvement in M_E and UCS values versus percentage of additive were plotted in Figures 4.7 and 4.8, respectively. For lime-stabilized specimens, 3% lime showed maximum enhancements of approximately 110% and 157% for M_E and UCS values, respectively. Specimens stabilized with 15% CFA projected highest improvements (1,635% for M_E and 1,222% for UCS) among all the percentages of different additives used in this study. CKD showed improvements in M_E and UCS values ranging between 82 – 271% and 87 – 465%, respectively, with 10% providing maximum enhancements in M_E and UCS values. This behavior is contrary to the behavior observed before capillary soaking where 15% CKD provided maximum enhancements before capillary soaking. It is believed that excessive CKD (>10%) increases the moisture susceptibility and swelling of specimens resulting in decreased M_E and UCS values.

4.5.4 Effect of Additives on Atterberg Limits

A summary of the Atterberg limits and percent passing No. 200 (< 75 μm) sieve determined after 28 days of curing for different percentages of additives is presented in Table 4.4. Results show that lime produced highest plasticity index (PI) reductions by substantially increasing plastic limit and a small increase in liquid limit. For example, 3%

lime increased plastic limit and liquid limit by approximately 69% and 32%, respectively. Reduction in PI values for lime-stabilized soils can be attributed to ion-exchange and associated flocculation reactions between lime and soil which made soil non-plastic by agglomerating it into a more friable and aggregated structure (Prusinski and Bhattacharja, 1999; IRC, 2000; Little, 2000).

The addition of CFA to V-soil produced only a small increase (8%) in liquid limit values. The maximum liquid limit occurred at a CFA content of 5%. Additional CFA beyond 5% resulted in decrease in liquid limit for 10% and increase for 15%. Plastic limit showed monotonic increase with increase in the percentage of CFA used in this study. For example, 15% CFA increased plastic limit value by approximately 27%. The combined effect of change in liquid and plastic limit decreased PI values. For example, 15% CKD decreased PI values by approximately 45%.

Adding CKD to the V-soil also produced changes in the plasticity. However, effectiveness of CKD in reducing the plasticity of V-soil is low as compared to lime and CFA. It is also clear from Table 4.4 that increase in CKD content produced similar order of magnification in liquid limit and plastic limit values which resulted in small changes in PI values. For example, 5% CKD increased liquid and plastic limit by approximately 3% and 4%, respectively. One of the explanations could be the large contents of sulfates and alkalis present in the CKD used in this study (Table 2.4). The presence of these compounds can lead to the formation of gypsum, ettringite, and possibly syngenite crystals during the hydration process (Peethamparan et al., 2008). These reaction products may induce stiffening and increased absorption of water, resulting in less effectiveness in the reduction of PI values. Similar observations of effect of CKD on PI

were reported by other researchers (Miller and Azad, 2000; Parsons et al., 2004; Peethamparan et al., 2008; Snethen et al., 2008).

Further, percent passing No. 200 sieve results clearly shows that lime is the most effective additive in decreasing the fine content than CFA, followed by CKD. For example, 9% lime, 15% CFA and 15% CKD decreased the percent passing No. 200 sieve by approximately 61.4%, 15.2% and 6.6%, respectively.

4.5.5 Effect of Additives on Three-Dimensional Swell

Figure 4.9 shows three-dimensional swell progressing with time for raw V-soil and stabilized specimens. Final three-dimensional swell values after 120 days are presented in Table 4.4. Negative swells from day 0 to day 4 are a result of drying of the specimens before the start of the swell test. These results demonstrate an unmistakable trend of increasing swell with the increasing percent of lime and CKD. As discussed in the background section, sulfate-induced heave is attributed to the increase in volume. After 120 days, the 9% lime-stabilized specimen showed the highest magnitude of swell, equal to 22.3%, compared to the value of 0.8% measured on the raw soil. Swelling was also seen with V-soil stabilized using 10% and 15% CKD. On the contrary, CFA stabilization helped by reducing the swelling. For example, 15% CFA-stabilized specimens reduced the swelling by a factor of 138%. It is clear from Figure 4.9 that sulfate-induced heave is pronounced only in lime- and CKD-stabilized specimens. This can be attributed to comparatively high pH values (> 10) after 28 days of curing (beginning of 3-D swell test) and high concentration of calcium ions in lime (95.9% of calcium hydroxide) and CKD (47.0% of calcium oxide), as compared to CFA (pH < 10 and 24.4% of calcium oxide). At higher pH values (> 10) ettringite is more stable, as

discussed in the background section. Similar behavior of reduced sulfate-induced heaving with low calcium-based stabilizers was reported by other researchers (e.g., Kota et al., 1996; Wild 1996, 1998; Wang, 2002). For example, Wild (1996, 1998) demonstrated that partial substitution of lime with granulated blast furnace slag substantially reduce the damaging expansion and have positive effect on strength development.

4.5.6 Assessment of Sulfate-Induced Heave

Figure 4.10 shows SEM/EDS test results conducted on representative tiny pieces of 9% lime- and 15% CKD-stabilized specimens, after 120 days of capillary soaking. The SEM micrograph (magnification = 10,000 times) clearly shows needle-like ettringite crystals. The length of ettringite crystal is less than 2 µm for both 9% lime- and 15% CKD-stabilized specimens. This observation is consistent with the findings reported by other researchers (e.g., Mitchell and Dermatas, 1992; Roy et al., 2003; Intharasombat, 2003; Moon et al., 2007; Little et al., 2010). Furthermore, EDS was used on specific needle-shaped crystal for analyzing elemental composition. EDS for the selective identified crystals showed the presence of sulfur (S) along with other elements such as calcium (Ca), aluminum (Al) and oxygen (O), which is an indication of the presence of ettringite. No areas were found showing normal ettringite spectra without traces of silica (Si).

To confirm the ettringite formation, XRD tests were also conducted on 9% lime- and 15% CKD-stabilized specimens. For comparison raw V-soil was also tested, as shown in Figures 4.11 (a-c). Figure 4.11 (a) indicates that no ettringite peaks were noticed in raw V-soil. The ettringite peaks were observed for 9% lime- and 15% CKD-stabilized V-soil specimens. This substantiates that formation of ettringite resulted in

heaving as noted in Figure 4.9. Furthermore, the ettringite traces detected in 9% lime-stabilized soil were of higher intensity level as compared to 15% CKD-stabilized specimen. As a result, 9% lime-stabilized soil undergoes higher sulfate induced heaving. Based on SEM, EDS and XRD studies, it can be concluded that the ettringite was formed in lime- and CKD-stabilized specimen which yielded swelling and a decrease in strength-stiffness of the mix, after 120 days of capillary soaking.

4.6 Conclusions

This study was undertaken to evaluate natural sulfate bearing lean clay (V-soil) from northwestern Oklahoma for the effect of type and amount of additive on the short- and long-term performance by evaluating material properties as recommended by the new Mechanistic-Empirical Pavement Design Guide (MEPDG). Lean clay (CL) specimens stabilized with lime (high calcium additive), CFA (low calcium additive), and CKD (moderate calcium additive)were molded, cured for 28 days, and then subjected to different stress sequences to study the M_r. The same specimens were then tested for modulus of elasticity (M_E) and UCS or 3-D swell. Specimens tested for 3-D swell were further tested for M_r, M_E, and UCS, after 120 days of capillary soaking. Based on the study presented in this chapter the following conclusions can be derived:

1. All three additives helped by improving M_r, UCS and M_E values after 28 days of curing. However, after 120 days of capillary soaking, raw and all stabilized specimens showed reduction in M_r, UCS, and M_E values. Overall, the 15% CKD-stabilized specimen showed the highest improvement after 28 days of curing, while the 15% CFA-stabilized specimen showed the highest M_r, UCS, and M_E values after 120 days of capillary soaking.

2. For the different percentages of additive used in this study, the range of M_r values after capillary soaking were 47 – 93 MPa (1.9 – 3.7 ksi) for lime–stabilized specimens, 37 – 755 MPa (1.5 – 29.7 ksi) for CFA-stabilized specimens and 53 – 180 MPa (2.1 – 7.1 ksi) for CKD-stabilized sulfate bearing lean clay specimens.
3. For CFA-stabilization, the amount of improvement after capillary soaking increases with increase in the additive content; however, a reduction in M_r, M_E and UCS values was observed beyond a certain percentage of lime or CKD content (between 3 – 6% for lime, between 10 – 15% for CKD).
4. The M_E and UCS values of lime-, CFA- and CKD-stabilized specimens showed decrease ranging between approximately 86 – 89%, 31 – 92%, and 77 – 95% due to 120 days of capillary soaking.
5. Atterberg limit results showed that lime produced the best results in decreasing the plasticity index of clay followed by CFA and CKD. Results showed that lime produced highest plasticity index (PI) reductions by substantially increasing plastic limit and a small increase in liquid limit. However, CFA produced only a small increase in liquid limit values and monotonic increase in plastic limit with increase in CFA content. Increase in CKD content produced similar order of magnification in liquid limit and plastic limit values which resulted in small changes in PI
6. Three-dimensional swelling test showed an increase in volume for lime- (22.3% for 9% lime) and CKD-stabilized (6.4% for 15% CKD) specimens, while a reduction in volume for the specimens stabilized with low calcium based stabilizer (i.e., CFA), as compared to raw sulfate bearing clay specimens. This increase in volume is attributed to sulfate-induced heaving and presence of calcium in additive which results in the

formation of expansive mineral ettringite. Further, the presence of ettringite was verified using SEM/EDS tests in conjunction with XRD analyses.

7. Development of ettringite depends on several factors such as pH (or calcium content), moisture availability, lime dosage, temperature, sulfate levels, reactive alumina and clay mineralogy. In this study, pH value greater than 10.0 and availability of moisture were verified as two dominant factors required for the formation of ettringite.

Table 4.1 A Summary of Resilient Modulus Values of Lime-Stabilized V-soil Specimens (After 120-Day Capillary Soaking)

σ_3	σ_d	M_r (MPa)											
(kPa)	(kPa)	Raw	SD	CV	3% Lime	SD	CV	6% Lime	SD	CV	9% Lime	SD	CV
41	12	48	1	1	84	9	10	93	9	10	87	1	1
41	25	44	1	2	82	6	7	88	9	10	82	11	13
41	37	38	0	0	75	8	11	80	6	8	74	10	13
41	50	32	0	1	72	8	11	76	4	5	71	8	11
41	62	29	1	4	70	6	9	75	4	5	69	4	6
28	12	33	1	3	63	6	9	76	8	11	71	13	18
28	25	28	1	4	60	8	13	70	8	11	65	12	18
28	37	26	1	4	59	7	13	68	3	4	63	10	16
28	50	26	1	5	61	8	13	68	2	3	63	6	10
28	62	26	1	5	61	6	10	66	3	4	61	4	7
14	12	25	1	5	48	8	17	57	4	7	53	8	15
14	25	21	2	8	45	5	11	52	3	5	48	10	21
14	37	21	1	7	46	6	13	52	1	2	47	9	19
14	50	21	2	8	48	7	14	53	3	6	49	7	13
14	62	22	1	6	49	7	14	52	8	15	47	5	10

1 psi = 6.89 kPa; 1 ksi = 6.89 MPa; SD: standard deviation; CV: coefficient of variation (%)

σ_d : deviator stress; σ_3 : confining pressure; M_r : resilient modulus (using internal LVDTs)

* Deformations are out of the measuring range of LVDTs

Table 4.2 A Summary of Resilient Modulus Values of CFA-Stabilized V-soil Specimens (After 120-Day Capillary Soaking)

σ_3	σ_d	M_r (MPa)											
(kPa)	(kPa)	Raw	SD	CV	5% CFA	SD	CV	10% CFA	SD	CV	*15% CFA*[#]	SD	CV
41	12	48	1	1	73	6	8	125	8	7	*755*	46	6
41	25	44	1	2	69	4	6	127	3	2	*731*	16	2
41	37	38	0	0	63	5	7	122	2	1	*696*	13	2
41	50	32	0	1	60	3	5	119	1	1	*685*	16	2
41	62	29	1	4	60	4	6	119	9	7	*684*	17	2
28	12	33	1	3	61	5	8	99	8	9	*677*	32	5
28	25	28	1	4	52	4	8	93	3	3	*646*	18	3
28	37	26	1	4	50	4	8	93	2	2	*629*	12	2
28	50	26	1	5	50	4	7	97	1	1	*632*	11	2
28	62	26	1	5	49	4	7	101	2	1	*638*	11	2
14	12	25	1	5	40	4	10	71	9	13	*638*	17	3
14	25	21	2	8	35	5	15	68	4	6	*593*	15	3
14	37	21	1	7	35	3	9	70	3	4	*580*	31	5
14	50	21	2	8	36	3	8	76	2	2	*588*	25	4
14	62	22	1	6	37	3	8	80	1	1	*590*	16	3

1 psi = 6.89 kPa; 1 ksi = 6.89 MPa; SD: standard deviation; CV: coefficient of variation (%)

σ_d : deviator stress; σ_3 : confining pressure; M_r : resilient modulus (using internal LVDTs)

* Deformations are out of the measuring range of LVDTs

[#]Additive content providing maximum enhancements

Table 4.3 A Summary of Resilient Modulus Values of CKD-Stabilized V-soil Specimens (After 120-Day Capillary Soaking)

σ_3	σ_d	M_r (MPa)											
(kPa)	(kPa)	Raw	SD	CV	5% CKD	SD	CV	10% CKD	SD	CV	15% CKD	SD	CV
41	12	48	1	1	145	9	6	180	8	5	104	12	11
41	25	44	1	2	133	7	5	158	4	2	98	5	5
41	37	38	0	0	118	7	6	138	6	4	88	3	3
41	50	32	0	1	109	5	5	128	6	5	83	3	4
41	62	29	1	4	104	3	3	123	5	4	80	6	7
28	12	33	1	3	108	10	9	127	5	4	73	8	11
28	25	28	1	4	94	6	6	108	4	4	66	7	11
28	37	26	1	4	89	5	6	104	6	6	65	4	6
28	50	26	1	5	89	5	6	104	7	7	67	4	5
28	62	26	1	5	88	4	5	105	6	6	68	8	12
14	12	25	1	5	79	9	11	89	4	4	52	7	13
14	25	21	2	8	68	9	13	78	8	11	47	8	16
14	37	21	1	7	66	7	11	76	8	10	47	6	13
14	50	21	2	8	68	6	9	79	8	10	50	5	10
14	62	22	1	6	69	5	8	81	8	10	53	4	8

1 psi = 6.89 kPa; 1 ksi = 6.89 MPa; SD: standard deviation; CV: coefficient of variation (%)

σ_d : deviator stress; σ_3 : confining pressure; M_r : resilient modulus (using internal LVDTs)

* Deformations are out of the measuring range of LVDTs

Table 4.4 A Summary of Stabilized V-Soil Specimens 28-Day Atterberg Limits and Final 3-D Swell Volume

Percentage of additive	% passing No. 200 sieve (28-day)	Atterberg limits (28-day curing)			3-D Swell Volume (%) (120-day)
		LL (%)	PL (%)	PI (%)	
Raw V-Soil					
0	100.0	37	26	11	0.8
Lime					
3	69.0	49	44	5	13.4
6	48.2	51	NP	NP	21.3
9	38.6	48	NP	NP	22.3
CFA					
5	99.4	40	30	10	0.7
10	90.6	37	30	7	0.2
15	84.8	39	33	6	-0.3
CKD					
5	99.8	38	27	11	0.6
10	96.2	40	30	10	1.5
15	93.4	43	34	9	6.4

LL: Liquid Limit; PL: Plastic Limit; PI: Plasticity Index; NP: Non-plastic

(a) (b)

Figure 4.1 (a) Outcrops Containing Gypsum in Western Oklahoma (*Source: Adams, 2008*), and (b) Gypsum Crystals in Vernon Series Soil

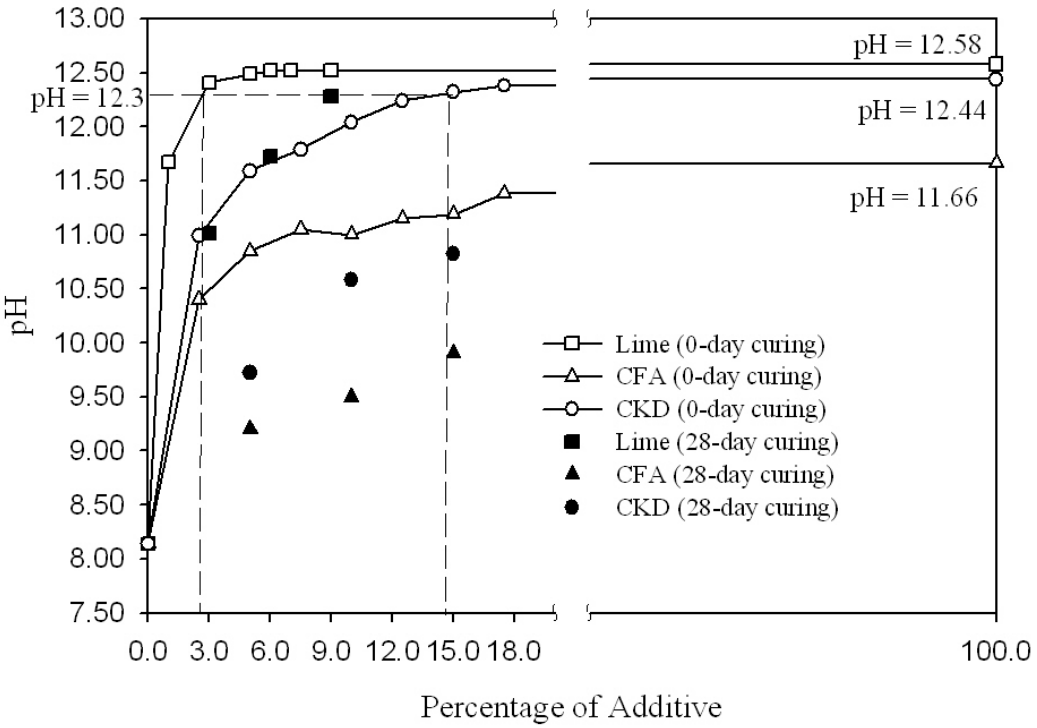

Figure 4.2 Variation of pH with Type and Amount of Additive

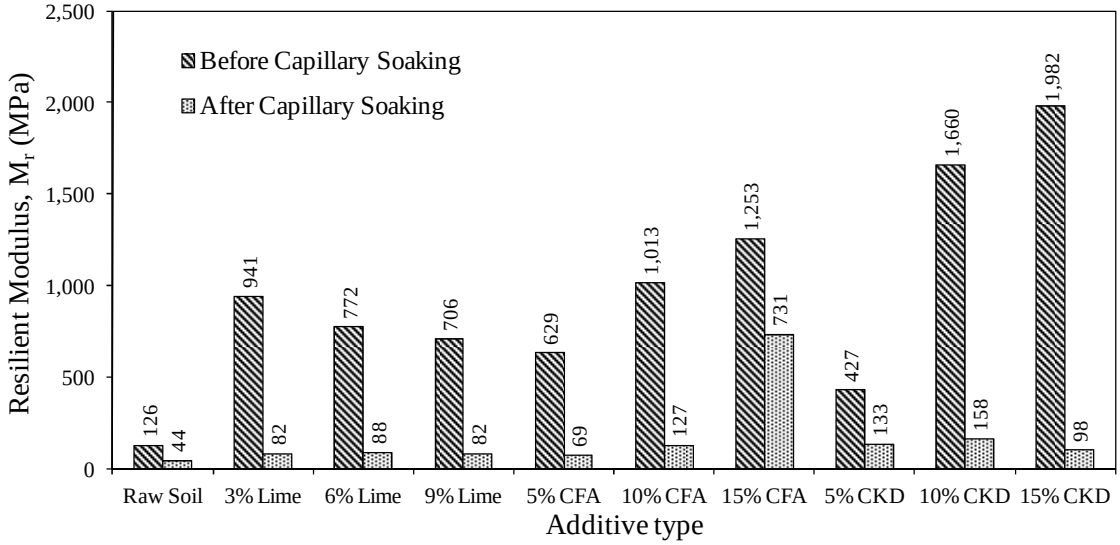

Figure 4.3 Variation of M_r (σ_d = 25 kPa, σ_3 = 42 kPa) After Capillary Soaking with Type and Amount of Additive

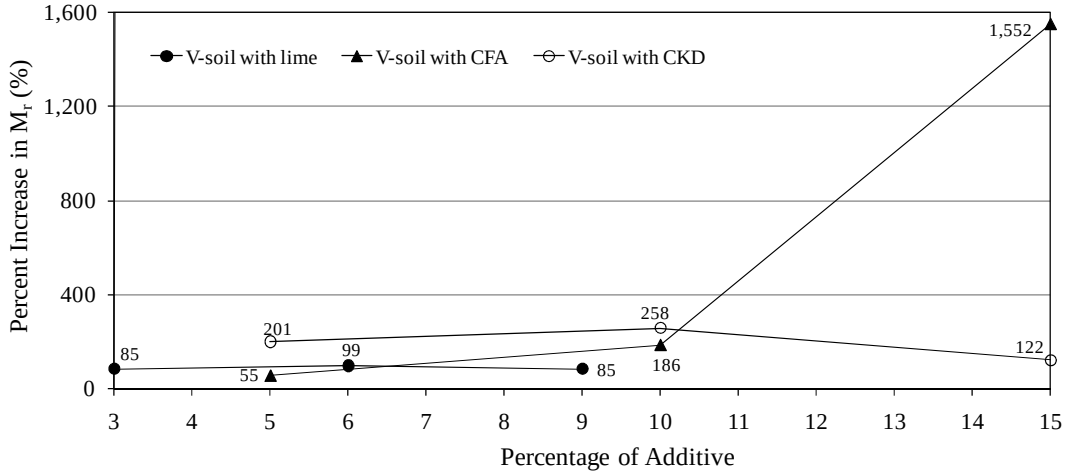

Figure 4.4 Increase in M_r (σ_d = 25 kPa, σ_3 = 42 kPa) With Respect to M_r Values of Raw Soil Specimens After Capillary Soaking

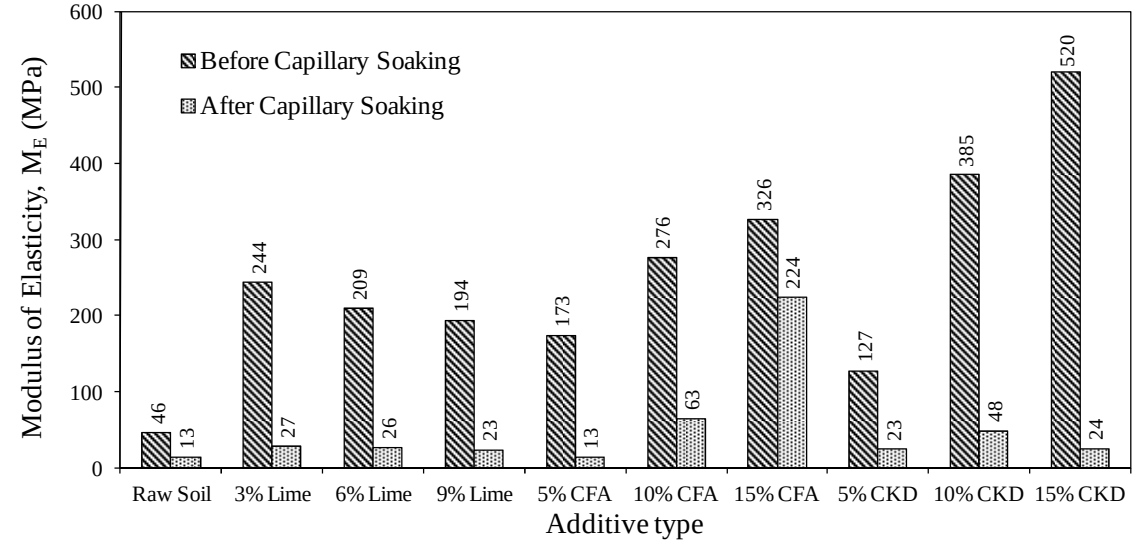

Figure 4.5 Variation of Modulus of Elasticity After Capillary Soaking with Type and Amount of Additive

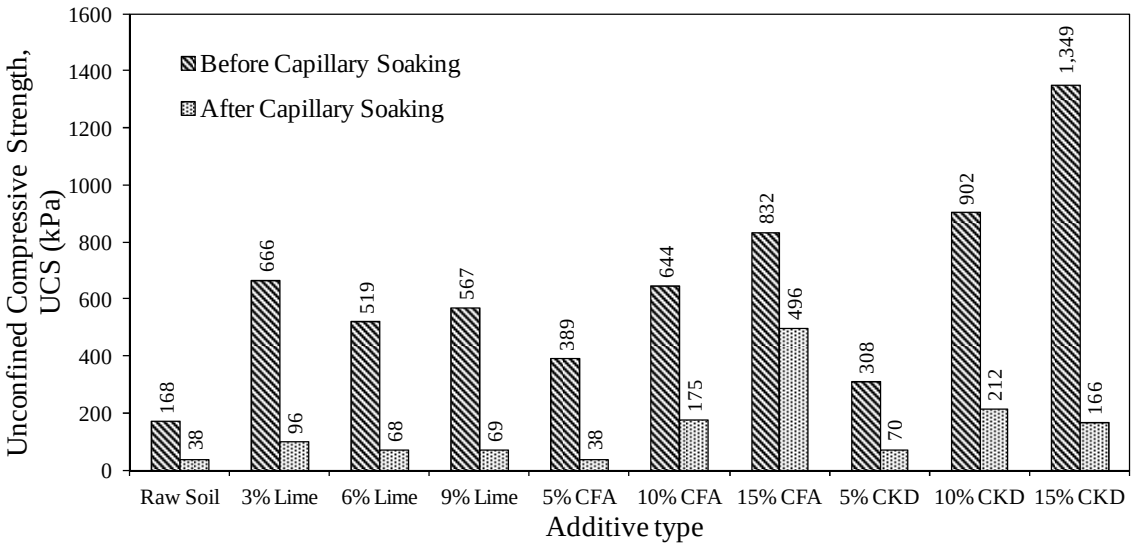

Figure 4.6 Variation of Unconfined Compressive Strength After Capillary Soaking with Type and Amount of Additive

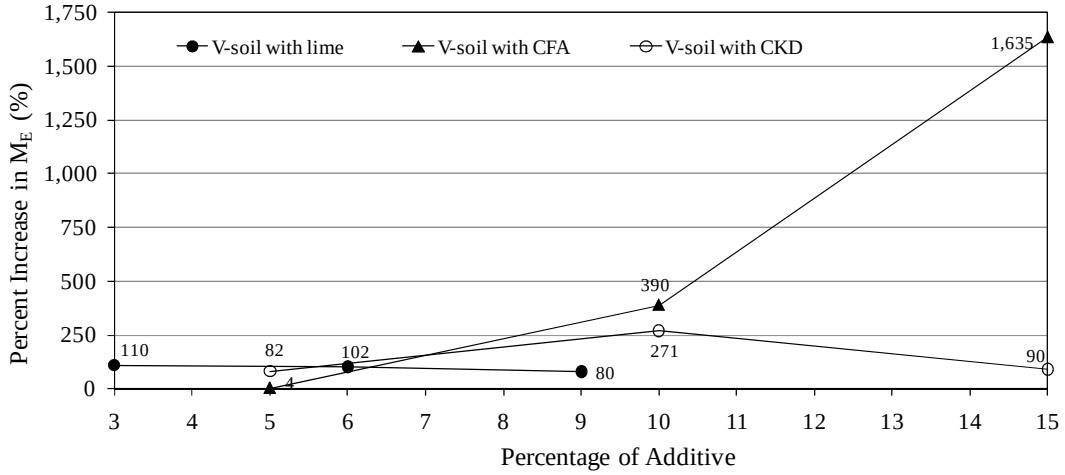

Figure 4.7 Increase in M_E Values With Respect to Corresponding Values of Raw Soil Specimens After Capillary Soaking

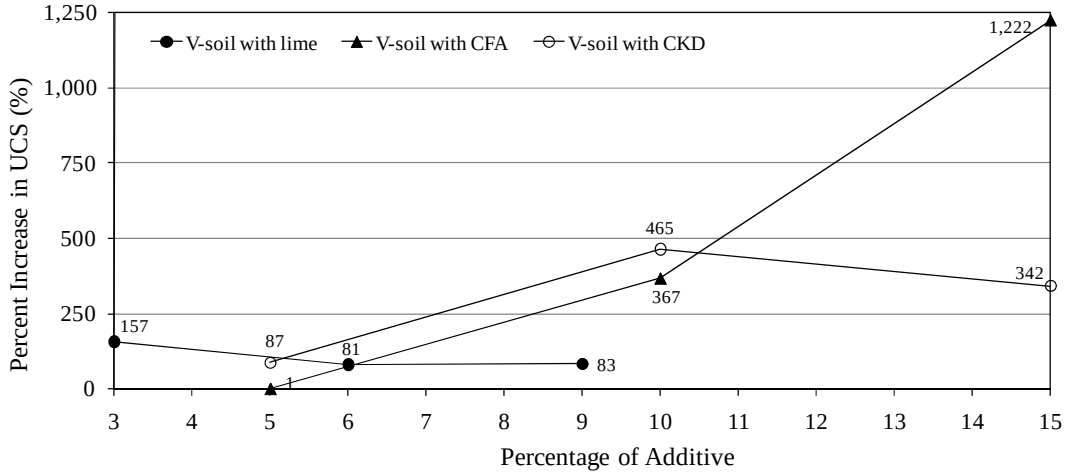

Figure 4.8 Increase in UCS Values With Respect to Corresponding Values of Raw Soil Specimens After Capillary Soaking

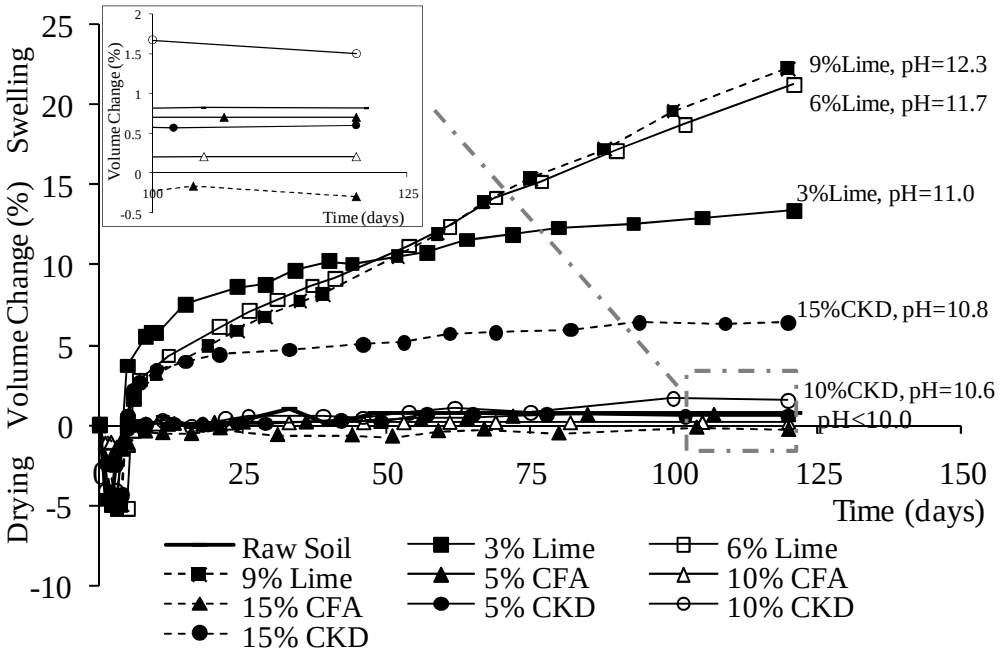

Figure 4.9 Three-Dimensional Swell Test Results

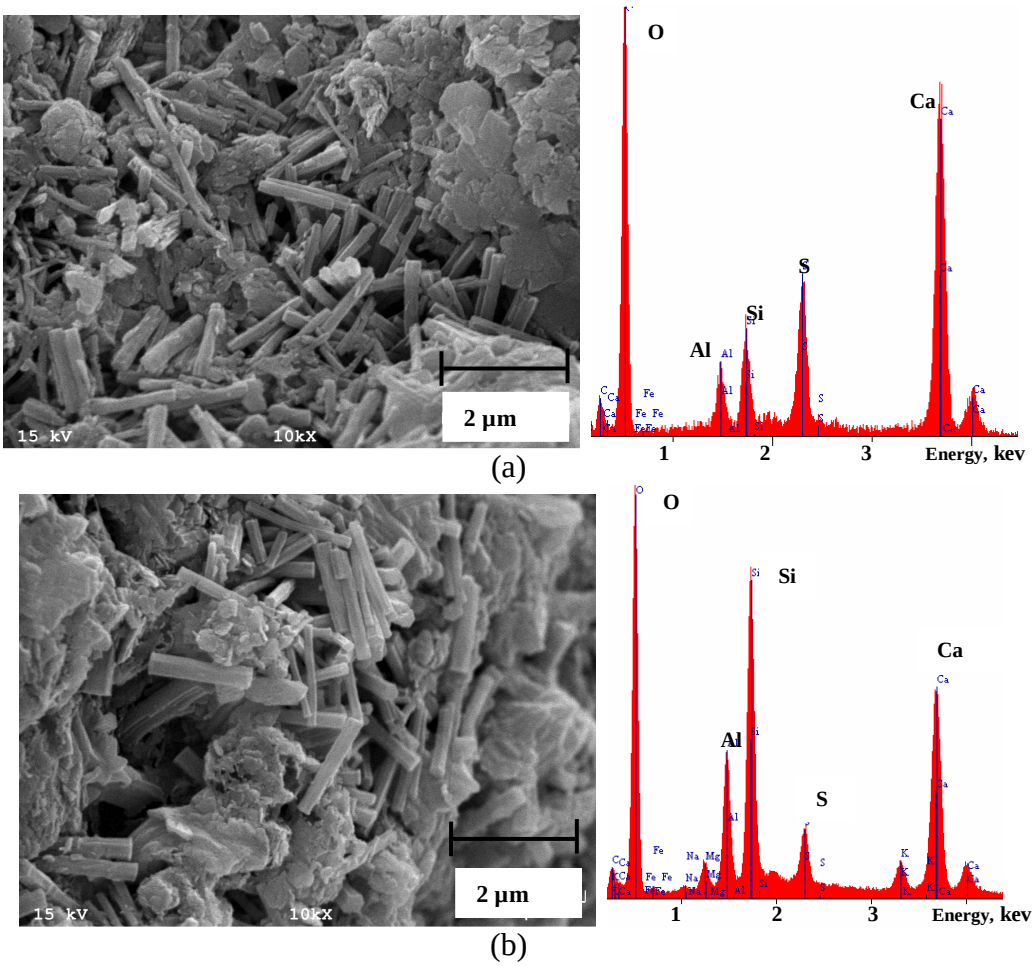

Figure 4.10 SEM/EDS of Ettringite Deposited in the (a) 9% Lime- and (b) 15% CKD-Stabilized Specimens (After 120 Days of Capillary Soaking)

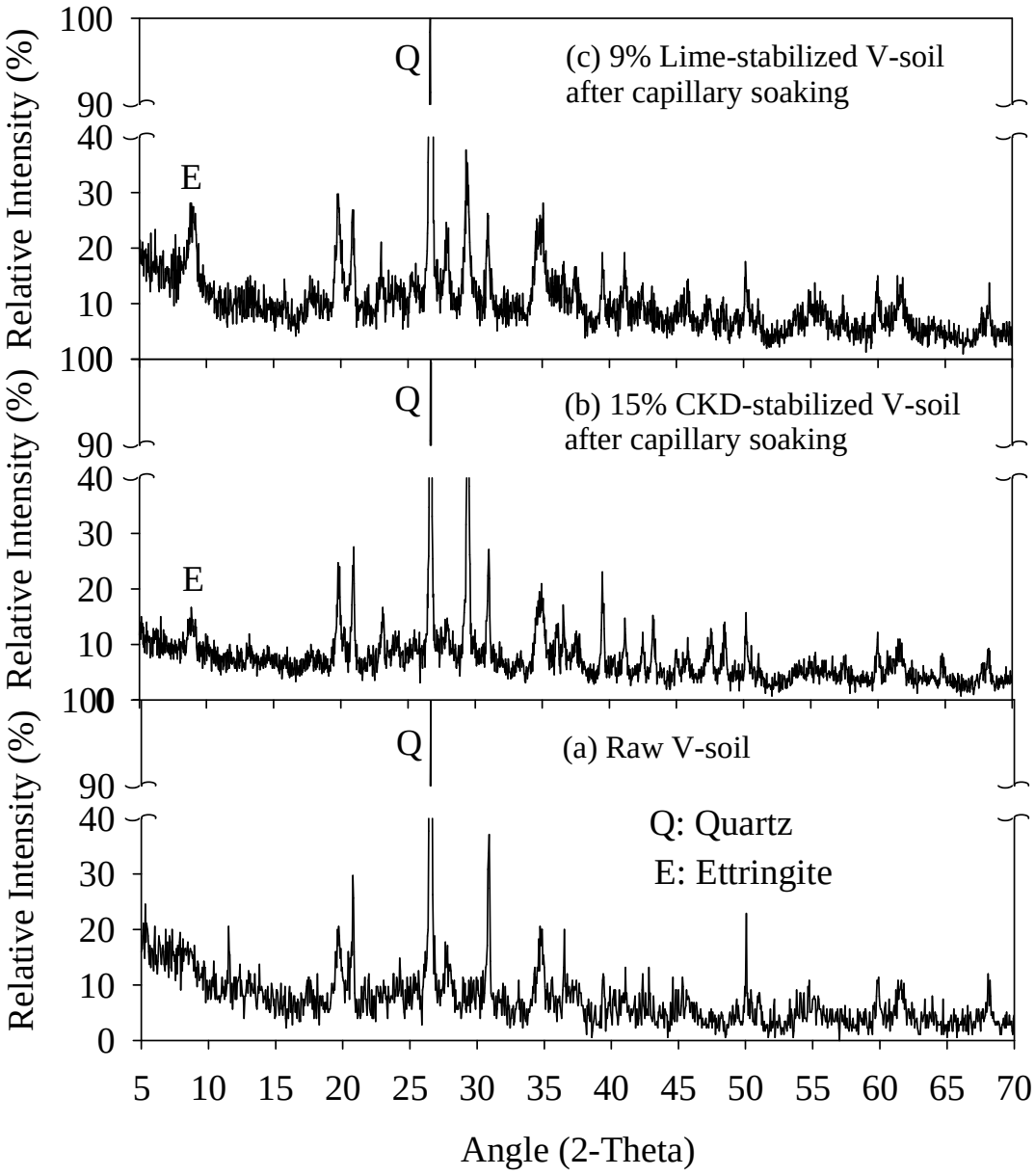

Figure 4.11 X-Ray Diffraction Results

CHAPTER 5

STATISTICAL AND ARTIFICIAL NEURAL NETWORK MODELING

5.1 Introduction

Empirical design methods for flexible pavement structures are primarily based on the equations that were developed largely from the AASHO Road Tests conducted in 1950's. These methods fail to reflect the dynamic nature of traffic loads. Therefore, the mechanistic design methods referred to as the "AASHTO Guide for Design of Pavement Structure" (AASHTO, 1986) recommended the use of resilient modulus (M_r), a dynamic-strength parameter, to characterize flexible pavement materials. The M_r accounts for the cyclic nature of vehicular traffic loading, and is defined as the ratio of deviatoric stress to recoverable strain.

Several laboratory and field procedures are either currently being used or evaluated for determining a design M_r value of subgrade soil. Direct laboratory methods used for evaluating M_r during the past two decades include resonant column, torsional shear, gyratory, and repeated load triaxial testing (AASHTO, 1986, Kim and Stokoe, 1992, George 1992, Kim et al., 1997). Among these, the M_r from repeated load triaxial test (RLTT) is used most frequently because of the repeatability of test results and its representation of field stress in a controlled laboratory environment. RLTT is conducted in the laboratory on remolded or undisturbed samples according to different AASHTO test methods of which AASHTO T307 is used frequently (AASHTO, 2004). The AASHTO T307 test method can be a time consuming and expensive test method, particularly for small projects.

In the new 2002 AASHTO guide, which is currently in the evaluation stage, a hierarchical approach is used to determine different design inputs including M_r (AASHTO, 2004). It requires evaluation of pertinent engineering properties of subgrade soils in laboratory or field to pursue a Level 1 (most accurate) design. For a Level 2 (intermediate) design, however, the design inputs are user selected, possibly from an agency database or from a limited testing program or could be estimated through correlations (AASHTO, 2004). A Level 3 design, which is the least accurate and generally not recommended, uses only the default values. For Level 2 designs, a regression model for M_r can be very useful as it provides the designer with significant flexibility in obtaining the design inputs for a project.

Consequently, the primary objective of the study presented herein is to develop correlations or models for M_r of some common subgrade soils in Oklahoma stabilized with locally available cementitious additives for Level 2 pavement design applications. Two different modeling options, namely regression models and artificial neural networks (ANN) are employed. The strengths and the weaknesses of the developed models were examined using additional M_r test results that were not used in the development of these models. Further, possible correlations of M_r with compacted specimen characteristics and soil/additive properties are investigated. The models and correlations developed in this study are expected to be useful in the Level 2 designs of pavements in Oklahoma.

5.2 Review of Previous Studies

5.2.1 Statistical Models

Several studies have previously been undertaken to develop empirical correlations for estimating M_r values in terms of other soil properties (see e.g., Lee et al., 1997;

Mohammad et al., 1999; Ooi et al., 2004; Rahim and George, 2004; Elias and Titi, 2006; Hossain, 2009; Mohammad et al., 2009). However, only a few models and correlations are available for cementitiously stabilized soils in the literature (Table 4.1); these correlations are either limited to one type of additive (e.g., Achampong, 1996; Arora and Aydilek, 2005, Ling et al., 2008) or applicable only for a particular stress level (e.g., Achampong et al., 1997; AASHTO, 2004; Hillbrich and Scullion, 2006; Mooney and Toohey, 2010). No studies to the author's knowledge, have addressed the statistical modeling of stabilized soils specimens correlating soil/additive properties with M_r values at different stress levels.

One of the commonly used models to represent M_r is the power model (see e.g. Dunlap, 1963; Seed et al., 1967; Thompson and Robnett, 1976; Moossazadeh and Witczak, 1981; May and Witczak, 1981; Uzan, 1985; Farrar and Turner, 1991; Yau and Quintus, 2002; NCHRP 2003; Hopkins at el., 2004; Rahim and George, 2004; Khazanovich et al., 2006). A number of researchers have utilized other index properties to estimate M_r (see e.g., Gomes and Gillet, 1996; Paute and Hornych, 1996; Rada and Witczak,1981; Raad et al., 1992; Zaman et al. 1994; Dai and Zollars, 2002). For example, Drumm et al. (1990) developed two regression models for M_r of fine-grained soils as a function of deviator stress and soil-index properties, namely, percentage passing No. 200 sieve (P_{200}), plasticity index (PI), dry density (γ_d), and unconfined compressive strength (UCS). A relatively small (twenty-two) number of these samples were used in developing these models. Also, this study was limited to raw soil and no additive was used.

In a similar study, Lee et al. (1997) investigated the M_r of raw cohesive soils, mainly clayey subgrade soils, with RLTT. Specimens were compacted using standard and modified Proctor methods at near optimum moisture content (OMC) in a mold with a diameter of 38 mm (1.5 in) and a height of 100 mm (4.0 in). It was seen that the custom-compaction results were in close agreement with the maximum dry density (MDD) and the optimum moisture content (OMC) from the standard and modified Proctor tests. Regression analyses were conducted to obtain a relationship between M_r and the stress in unconfined compressive strength test causing 1% strain ($S_{U1.0\%}$) in laboratory compacted specimens. The relationship between M_r and $S_{U1.0\%}$ for a given soil was found to be unique regardless of moisture content and compaction effort. The results showed that the M_r and $S_{U1.0\%}$ vary with the moisture content in a similar manner. Furthermore, four different compactive efforts were used in that study, but a single relationship between M_r and $S_{U1.0\%}$ was obtained, as presented in following equation:

$$M_r = 695.4\ (S_{U1.0\%}) - 5.93\ (S_{U1.0\%})^2 \qquad (5.1)$$

where, M_r = resilient modulus at maximum axial stress of 41.4 kPa (6.0 psi) and confining pressure of 20.7 kPa (3.0 psi), and $S_{U1.0\%}$ = stress causing 1% (strain kPa) in conventional UCS test.

Moreover, the relationship was similar for different cohesive soils, indicating that it may be applicable for different types of clayey soils. The limited data suggested that the same correlation might be used to estimate the M_r for both laboratory and field compacted conditions.

Achampong et al. (1997) tested the M_r values for soils stabilized with Portland cement or lime by using a RLTT with variable deviator stress, moisture content, additive

content, curing period and soil type. It was found that the M_r values of stabilized specimens are dependent on deviator stress and the curing time. However, this study was conducted on synthetic soils and limited to only two additives namely, lime and Portland cement.

In a field study, Yau and Von Quintus (2002) proposed the following correlation using the M_r data obtained from the Long Term Pavement Performance (LTPP) test sections:

$$M_r = k_1 P_a (\theta/P_a)^{k2}[(\tau_{oct}/P_a)+1]^{k3} \quad (5.2)$$

where, τ_{oct} is the octahedral shear stress, and k_1, k_2, and k_3, are the regression constants. Yau and Quintus (2002) expressed these regression constants as a function of moisture content, dry density, optimum dry density, liquid limit, percent silt, percent clay, and percent passing different sieve sizes. The soils were classified into three different groups (coarse grained sandy soils, fine grained silty soils, and fine grained clayey soils), and the regression constants were developed for each soil type.

The new AASHTO 2002 MEPDG (AASHTO, 2004) and Mallela et al. (2004) indicated that the design M_r for lime-stabilized subgrade can be approximated from the UCS results using following equation:

$$M_r = 0.124\ UCS + 9.98 \quad (5.3)$$

where, M_r is resilient modulus in ksi and *UCS* is unconfined compressive strength in psi. Mallela et al., (2004) cites Thompson (1966) as the source of aforementioned equation and indicates that the design M_r and UCS values should be based on testing of specimens cured at room temperature for 28 days and strength tested in accordance with ASTM D 5102 test method. Also, Eqn. 5.3 was developed by Thompson (1966) from

unconsolidated undrained compression testing of cylindrical specimens having a diameter of 50 mm (2 in) and a height of 100 mm (4 in). However, there is a lack of proper information by AASHTO 2002 MEPDG as no particular stress level is suggested for Eqn. 5.3. Also, in a recent study Mooney and Toohey (2010) concluded that Eqn. 5.3 is conservative in its prediction of M_r from UCS of lime-stabilized specimens.

In Minnesota, Khazanovich et al. (2006) used M_r results for 23 samples from several locations and evaluated the regression constants for use in the mechanistic-empirical-based pavement designs. However, because the mineralogical and textural characteristics of soils in Oklahoma are different than those in Minnesota, those results may not be directly used for pavements in Oklahoma for a Level 2 design.

Malla and Joshi (2008) used long-term pavement performance (LTPP) information for 259 test specimens for developing model consisting bulk stress (θ) and τ_{oct} relating to soil properties, namely, moisture content (w), OMC, γ_d, MDD, liquid limit (LL), and PI. Predictions models were developed by conducting multiple linear regression analysis using computer software SAS.

Another study performed by Ling et al. (2008) recommended models for predicting M_r values of lime- and lime-cement-stabilized soils with curing time, degree of saturation, and wet-dry cycles. The proposed M_r prediction models were verified and calibrated by means of a laboratory experimental program and on-site testing. It was found that the predicted values were close to the laboratory results and the former were consistently higher. In most cases the prediction error of lime-cement-stabilized soil is less than 10% while the difference between predicted M_r of lime-stabilized and tested

values could be as much as 30% depending on the saturation levels. The prediction models developed in their study, however, were limited to only one particular stress level.

In a recent study, Hossain (2009) evaluated three different models namely, Model 1, 2 and 3. Model 1 is used by the Virginia Department of Transportation for predicting design M_r value:

$$M_r = k_1(\sigma_3)^{k_2}(\sigma_d)^{k_5} \quad (5.4)$$

where, σ_3 is confining stress, σ_d is deviator stress and k_1, k_2, k_5 are regression coefficients. Model 2 was developed by Von Quintus and Killingsworth (1997) for pavement design and is recommended by AASHTO 1993 design guide:

$$M_r = k_1 P_a (\theta/P_a)^{k_2} (\sigma_d/P_a)^{k_3} \quad (5.5)$$

where, θ is bulk stress and k_1, k_2, k_3 are regression coefficients. Model 3 is recommended by the new AASHTO 2002 MEPDG and is given by Eqn. 5.2. Further, correlations were developed for estimating M_r values from CBR and stress at 1% strain from triaxial shear test. As in any many previous studies, this study was limited to raw soils.

5.2.2 Artificial Neural Network Models

ANN has become an important modeling technique due to its success in many engineering applications including geotechnical engineering problems (see e.g., TRB, 1999; Najjar et al., 2000; Shahin et al., 2004; Zaman et al., 2010). One of the common artificial neural networks in use currently is the feed-forward network. As evident from its name, a feed-forward network only allows the data flow in the forward direction (Zurada, 1992; Fausett, 1994; Ripley, 1996; Hill and Lewicki, 2006). Based on the architecture, a number of feed-forward networks are available such as multi-layer perceptrons, radial basis function, probabilistic neural networks, generalized regression

neural networks, and linear networks (TRB, 1999; Shahin et al., 2004; StatSoft Inc, 2006; Sharma and Das 2008; Far et al., 2009).

ANN contains a number of simple, highly interconnected processing elements, known as "nodes" or "units." In a typical processing element, each input connection has a weighting value. With the weighting value, input data and bias value, a net input is described into the processing element. Then, a transfer function provides an output from the net input. Finally, a single output is produced and transmitted to other processing elements (Skapura, 1996; Najjar et al., 2000; Shahin et al., 2001).

The weights between the processing elements are adjusted during the "training or learning" phase. In the training process, a number of epochs are performed in the network. After each epoch, the weights are adjusted and a sum of mean squared error between target and output values is calculated. The training process stops when the sum of mean squared error is minimized or falls within an acceptable range (Shahin et al., 2001; Shahin et al., 2004).

Different algorithms can be used to train a network. In general, the training algorithms can be divided into two types: supervised and unsupervised. The supervised algorithms adjust the weights and the thresholds using the input and target output values, while the unsupervised algorithms only use the input values. The supervised training algorithms include back propagation, conjugate gradient descent, Levenberg-Marquardt, Pseudo-inverse, etc. (Mehrotra et al., 1996; Shahin et al., 2004; StatSoft Inc., 2006).

A number of researchers have utilized ANN technique in pavement applications. For example, Meier et al. (1996) augmented a computer program, WESDEF, with ANN models to back-calculate pavement layer moduli. The ANN models were trained to

compute the layer M_r from falling weight deflectometer (FWD) data from flexible pavements (Meier et al., 1996).

In another pavement application study, Sharma and Das (2008) used ANN models to back-calculate layer moduli with better accuracy compared with other software, namely, EVERCALC and ExPaS. In a recent study, Far et al. (2009) utilized ANN for estimating the dynamic modulus of asphalt concrete. The results showed that the predicted and measured dynamic modulus values are in close agreement using ANN models.

In another study by Far et al. (2010), ANN models for estimating dynamic moduli of LTPP sections were developed. A large national data set that covers a substantial range of potential input conditions was utilized to train and verify the ANNs. First, the ANN predictive models were trained and ranked using a common independent data set that was not used for calibrating any of the ANN models. A decision tree was developed from these rankings to prioritize the models for any available inputs. Next, the models were used to estimate the dynamic moduli for the LTPP database materials and ultimately to characterize the master curve and shift factor function. It was found that ANN models predict reliable dynamic moduli of LTPP sections over a wide range of temperature and frequencies.

5.3 Characteristics of Soils and Database

In this study, a total of four clay subgrade soil series namely, Port series (P-soil), Vernon series (V-soil), Carnasaw series (C-soil) and Kingfisher series (K-soil) are used. Of these, three soils (P-, V- and C-soil) were used in the development/evaluation of models and are collectively referred to as the "development/evaluation dataset." The

remaining one soil (K-soil) was used for the validation of the models. Data for stabilized K-soil is collectively referred to as the "validation dataset." P-soil, V-soil, C-soil and K-soil are CL-ML, CL, CH and CL clays, respectively, in accordance with the Unified Soil Classification System (USCS). As noted previously, three different additives, namely, hydrated lime, CFA and CKD were used in this study. The physical and chemical properties of soils and additives are presented in Tables 2.3 and 2.4, respectively.

A M_r database developed using laboratory test results on 160 specimens prepared by using four soils stabilized with three additives namely, lime (3%, 6% and 9%), CFA (5%, 10% and 15%) and CKD (5%, 10% and 15%) was used. The specimen preparation and laboratory testing procedure are already discussed in Sections 2.5 and 2.6, respectively. An outlier approach was used by employing *t*-statistic to discard the test results if a sample result deviates significantly from the average of M_r results obtained from four replicates. The critical value (*t*-critical) for student's *t*-test is taken at a significance level (α) of 0.05. If the calculated *t*-statistic value is greater or equal to this value (*t*-critical), then one chance in twenty the value is from the same population.

5.4 Statistical Models

5.4.1 Selection of Models

Several constitutive models are available in the transportation literature for M_r calculation/prediction. The input required in MEPDG Level 1 design consists of the regression coefficients (k-values) determined from laboratory test results. The following four stress dependent models are considered in this study:

1. Model 1, a log-log model recommended by the 1993 AASHTO Design Guide for unbound materials (1993).

$$M_r = k_1 p_a \left(\frac{\theta}{P_a}\right)^{k_2} \left(\frac{\sigma_d}{P_a}\right)^{k_3} \quad (5.6)$$

where, p_a = atmospheric pressure (101.283 kPa), θ = bulk stress (sum of three principal stresses), σ_d = cyclic deviatoric stress acting on the material, k_1, k_2 and k_3 are the model constants.

2. Model 2, a log-log model recommended by NCHRP 1-28 (1997) for stabilized specimens.

$$M_r = k_1 p_a \left(\frac{\sigma_3}{P_a}\right)^{k_2} \left(\frac{\sigma_d}{P_a}\right)^{k_3} \quad (5.7)$$

where, σ_3 = confining stress acting on the material.

3. Model 3, a model similar to semi-log k_1, k_2, k_3 (σ_3, σ_d) model reported by Andrei et al. (2004).

$$M_r = k_1 P_a k_2^{\left(\frac{\sigma_3}{P_a}\right)} k_3^{\left(\frac{\sigma_d}{P_a}\right)} \quad (5.8)$$

One of the advantages of using the aforementioned semi-log model is that it is valid for either $\sigma_3 = 0$ or $\sigma_d = 0$.

4. Model 4, a log-log model recommended by the new AASHTO 2002 MEPDG for unbound materials (AASHTO 2004).

$$M_r = k_1 p_a \left(\frac{\theta}{P_a}\right)^{k_2} \left(\frac{\tau_{oct}}{P_a} + 1\right)^{k_3} \quad (5.9)$$

where, τ_{oct} = octahedral shear stress acting on the material

$$= 1/3[(\sigma_1 - \sigma_2)^2 + (\sigma_1 - \sigma_3)^2 + (\sigma_2 - \sigma_3)^2]^{1/3}$$

Tables 5.2, 5.3 and 5.4 present the aforementioned average model constants (k_1, k_2 and k_3) for P-, V- and C-soil, respectively. These values could easily be used for pavement design using both the 1993 AASHTO Design Guide and MEPDG Level 2 design/analysis provided the state of stress is known from layered elastic analysis or some other means. In this study, the design M_r values were calculated at a deviatoric stress of 41.34 kPa (6.0 psi) and a confining pressure of 13.78 kPa (2.0 psi), as recommended by Jones and Witczak (1977) and Ping et al. (2001).

5.4.2 Evaluation of Models

Four models were evaluated using the following criteria: (1) S_e/S_y ratio represents the ratio of the standard deviation of the errors to the standard deviation of the sample. A lower value of this ratio is a measure of the improvement in prediction achieved by using the model instead of the mean. (2) R^2, the square of the correlation coefficient (or coefficient of regression), is probably the most widely used indicator for identifying the accuracy of prediction. The new MEPDG recommends a R^2 value greater than 0.90 (AASHTO, 2004). (3) Visual examination of the predicted versus measured M_r is used to identify local bias (i.e. incorrect model form) (Andrei et al., 2004).

Figures 5.1 (a) and (b) show the frequency diagrams of R^2 and S_e/S_y values of the samples used in this study. Compared to other models, AASHTO 2002 MEPDG model (Model 4) for unbound material has the worst overall goodness of fit statistics with only seven samples having R^2 values greater than 0.9 and 19 samples having $S_e/S_y < 0.2$. Hence, Model 4 was rejected for further development of correlations and validation. Both Models 1 and 2, resulted in 62 samples with a R^2 value greater than 0.9. Additionally, Models 1 and 2 gave 33 and 36 samples with a S_e/S_y value of less than 0.2. Therefore,

Models 1 and 2 were selected for further development of correlations and validation. Although Model 3 gave less number of samples (only 55) with $R^2 > 0.9$, it showed the highest number of samples with $S_e/S_y < 0.2$. Hence, Model 3 was also selected for further development of correlations and validation.

5.4.3 Correlations

The model constants were correlated with commonly used compacted specimen characteristics and basic soil/additive properties. Specifically, the correlations developed herein consider the following compacted specimen characteristics – unconfined compressive strength, dry density, moisture content, percent of additive, silica sesquoxide ratio (SSR); soil properties – percent passing No. 200 sieve, plasticity index, clay content, pH, specific surface area, cationic exchange capacity; and additive properties – silica content, alumina content, iron oxide content, SSR, calcium oxide content, magnesium oxide content, alkali content, free-lime, specific surface area, loss on ignition, percent passing No. 325 sieve, pH. The stepwise method of multiple linear regression ($\alpha = 0.05$) option in SAS 9.1 was used for correlating model constants with the aforementioned properties. The F test for the multiple regressions was conducted using SAS 9.1 to validate significance of the relationship between M_r and independent variables included in the model constants. The associated probability is designated as Pr > F or p-value. A small p-value implies that the model is significant in explaining the variation in the dependent variables. For example, the relative effects of mechanical properties of mixture and chemical/physical properties of soil and additive for Model 3 are summarized in Table 5.5. The analyses of variance (ANOVA) results show that the M_r (in MPa) values

were significantly influenced by the compacted specimen characteristics, soil/additive properties and stress levels at α = 0.05. The following correlations were established:

Model 1

$$\log k_1 = 17.2068 + 1.6903\log\left(\frac{UCS}{P_a}\right) + 3.3183\log MC + 12.4465\log\left(\frac{DUW}{\gamma_w}\right) - 4.8520\log P_{200}$$

$$+ 0.3224\log PI - 0.2526\log Al_2O_3 - 12.7414\log pH_s \quad (5.10)$$

$$k_2 = 0.0905\log\left(\frac{UCS}{P_a}\right) + 0.0641\log MC + 2.4389\log\left(\frac{DUW}{\gamma_w}\right) - 0.0224\log(P_{200})$$
$$+ 0.0089\log(CC) - 0.0029\log(SSA_s) - 0.0534\log(ACA) - 0.2633\log(pH_a) \quad (5.11)$$

$$k_3 = 0.2331\log\left(\frac{UCS}{P_a}\right) + 0.1159\log MC + 4.7928\log\left(\frac{DUW}{\gamma_w}\right) - 0.0242\log(P_{200})$$

$$+ 0.0080\log(CC) + 0.0152\log(PA) + 0.0118\log(CaO) - 0.7610\log(pH_a) \quad (5.12)$$

(R^2 = 0.9249; F value = 633; Pr < 0.0001)

Model 2

$$\log k_1 = -0.8970 + 1.6698\log\left(\frac{UCS}{P_a}\right) + 3.1629\log MC + 9.3711\log\left(\frac{DUW}{\gamma_w}\right) + 0.6549\log PI$$

$$-1.4771\log(SSA_s) - 0.4329\log(Fe_2O_3) - 1.1828\log(CaO) \quad (5.13)$$

$$k_2 = 0.1322\log\left(\frac{UCS}{P_a}\right) + 0.0482\log(MC) + 0.0141\log(CC) - 0.0138\log(SSA_s)$$
$$- 0.0099\log(CEC) - 0.0059\log(PA) + 0.0144\log(Al_2O_3) - 0.0061\log(SSR_m) \quad (5.14)$$

$$k_3 = 0.1732\log\left(\frac{UCS}{P_a}\right) + 0.1245\log MC + 6.1274\log\left(\frac{DUW}{\gamma_w}\right) - 0.0233\log SSA_s - 0.011\log CEC$$
$$+ 0.0212\log PA - 0.2311\log(CaO) + 1.4412\log P_{325} - 10.7460\log pH_s - 0.1559\log SSR_m$$
(5.15)

(R^2 = 0.9262; F value = 609; Pr < 0.0001)

Model 3

$$\log k_1 = 1.6417 + 1.3171 \log\left(\frac{UCS}{P_a}\right) - 0.2554 \log MC - 0.5917 \log pH_s + 0.1585 \log CEC$$

$$- 0.1220 \log PA - 0.1066 \log SiO_2 + 0.2942 \log SSR_m \quad (5.16)$$

$$\log k_2 = -0.3369 \log\left(\frac{UCS}{P_a}\right) - 0.1957 \log MgO - 0.1593 \log LOI + 0.2671 \log SSR_m \quad (5.17)$$

$$\log k_3 = 0.4326 \log\left(\frac{UCS}{P_a}\right) - 1.0421 \log\left(\frac{DUW}{\gamma_w}\right) + 0.2791 \log CC \quad (5.18)$$

(R^2 = 0.9078; F value = 1022; Pr < 0.0001)

where,

UCS	=	28-day unconfined compressive strength (kPa),
P_a	=	atmospheric pressure (101.283 kPa),
MC	=	molding moisture content (%),
DUW	=	molding dry unit weight (kN/m^3),
γ_w	=	density of water (9.81 kN/m^3)
PA	=	additive content in specimen (%),
P_{200}	=	passing No. 200 sieve for soil (%),
PI	=	plasticity index,
CC	=	clay content in soil (%),
pH_s	=	pH of pure soil,
SSA_s	=	specific surface area of soil (m^2/g),
SiO_2	=	silica content of additive (%),
Al_2O_3	=	alumina content of additive (%),
SSR_a	=	SSR of additive,

CaO = calcium oxide content of additive (%),

MgO = magnesium oxide content of additive (%),

ACA = alkali content of additive (%),

FL = free-lime content of additive (%),

LOI = loss on ignition of additive (%),

P_{325} = passing No. 325 sieve for additive (%),

pH_a = pH of pure additive,

SSR_m = SSR of soil-additive mixture.

A comparison between the measured M_r results and predicted values for Models 1, 2 and 3 by using aforementioned correlations are shown in Figures 5.2, 5.3 and 5.4, respectively. It is evident that the predicted values are closer to the equality line when the M_r values are less than 1,600 MPa. This observation may be due to the distribution of dataset. Only 133 M_r values out of 1181 M_r values (approximately 11%) are in the upper range of 1,600 MPa. The remaining 89% of the M_r values for this study are in the lower range of the evaluation dataset. Overall, all the three models showed similar performance based on the R^2 (> 0.90) and F values (600 – 1000). Therefore, all the three models were selected for further validation.

5.4.4 Validation of Models

The evaluated models were validated using M_r values of a lean clay (K-soil) stabilized with lime (3%, 6%, 9%), CFA (5%, 10%, 15%) and CKD (5%, 10%, 15%). This provides different views on the prediction quality and the importance of datasets on statistical analysis. As noted previously, R^2, S_e/S_y value and visual examination are

utilized as the basis of comparing the three models in regard to the goodness of fit and significance of the model.

The M_r values of 31 stabilized K-soil specimens were predicted using the correlations developed with stabilized P-, V- and C-soil specimens dataset. Then, the predicted M_r values were compared to the measured M_r values, as shown in Figure 5.5. As evident from Figure 5.5, Model 3 showed superior performance with the highest R^2 value of 0.9791 and the lowest average S_e/S_y value of 0.4817. Although Models 1 and 2 predicted M_r values with high R^2 value (~ 0.9), but both models gave an average S_e/S_y value greater than 1. Also, it is evident from Figure 5.5 that the scatters for Model 3 are closer to the equality line as compared to scatters of Models 1 and 2. It is an indication that Model 3 is capable of predicting the M_r values of stabilized subgrade clays reasonable well, as compared to other models.

5.4.5 Correlations Developed Using Selected Parameters

As noted earlier, a total of 23 input parameters were used for developing correlations. However, some of the inputs parameters (e.g., specific surface area, cationic exchange capacity) require test setup(s) which are not readily available in the geotechnical engineering laboratories. Hence, it was decided to use selected parameters that are readily available from the additive supplier and/or evaluated commonly in the geotechnical laboratory. Specifically, the correlations developed herein consider the following compacted specimen characteristics – unconfined compressive strength, dry density, moisture content, percent of additive; soil properties – percent passing No. 200 sieve, plasticity index, clay content, pH; additive properties – free lime content, loss on ignition, percent passing No. 325 sieve, pH. Since Model 3 showed best acceptable

performance, the stepwise method (as discussed in Section 5.4.3) was used for developing Model 3 correlations. The following correlations were established:

$$\log k_1 = 33.8689 + 1.3106 \log\left(\frac{UCS}{P_a}\right) - 0.4539 \log MC - 0.2246 \log pH_s$$

$$- 0.1073 \log PA + 0.4926 \log FL \tag{5.19}$$

$$\log k_2 = -16.3817 \log P_{325} - 0.3620 \log\left(\frac{UCS}{P_a}\right) + 1.2722 \log\left(\frac{DUW}{\gamma_w}\right)$$

$$- 0.1552 \log CC \tag{5.20}$$

$$\log k_3 = 0.3969 \log\left(\frac{UCS}{P_a}\right) - 2.6845 \log\left(\frac{DUW}{\gamma_w}\right) + 0.2384 \log PI$$

$$+ 0.2778 \log pH_s - 0.0530 \log FL \tag{5.21}$$

A comparison between the measured and predicted M_r values for Model 3 correlations developed using all 23 parameters (Eqns. 5.16 – 5.18) and selected 12 parameters (Eqns. 5.19 – 5.21) is shown in Figure 5.6. It is evident from Figure 5.6 that both models show very similar prediction with high R^2 value (> 0.90). As an example, Model 3, developed using selected 12 parameters, predicted design M_r values of 6% lime-stabilized K-soil specimens approximately 0.2% higher than corresponding M_r values predicted using Model 3 developed using all 23 parameters. The corresponding percentage difference in predicted design M_r value is approximately 0.8% and 1.2% higher for 10% CFA- and 10% CKD-stabilized K-soil specimens, respectively.

5.5 Artificial Neural Network Models

5.5.1 Development and Evaluation of Models

In the present study, two feed-forward-type ANN models, namely, Radial Basis Function Network (RBFN) and Multi-Layer Perceptrons Network (MLPN), were developed using the M_r dataset of P-, V- and C-soils. Previous studies show that RBFN and MLPN are two best ANN models for predicting M_r values of subgrade soils (Zaman et al., 2010). A commercial software, STATISTICA 8, was used to develop these models. In the present application, the input layer consists of 25 nodes (or neurons), one node for each of the independent variables, namely UCS/P_a, MC, DUW/γ_w, P_{200}, PI, CC, pH_s, SSA_s, CEC_s, PA, SiO_2, Al_2O_3, Fe_2O_3, SSR_a, CaO, MgO, ACA, FL, LOI, P_{325}, pH_a, SSA_a, SSR_m, σ_3/P_a, and σ_d/P_a. The output layer consists of one node, representing M_r/P_a. For each ANN model developed, a trial and error approach was used to find the number of nodes in the hidden layer(s), in search of the optimum model. After the architecture was set, the development dataset was fed into the model for training. To examine the strengths and weaknesses of the developed models, they were evaluated by comparing the predicted M_r values with the experimental values (or measured values) with respect to the R^2 values. Thus, a higher R^2 value was considered a better fit of the evaluation dataset. Previously, several researchers have used R^2 as an indicator of model performance (Tarefder et al., 2005; Rankine and Sivakugan, 2005; Solanki et al., 2008).

5.5.1.1 Radial Basis Function Network (RBFN)

The radial basis function network (RBFN) divides the modeling space using hyperspheres. The centers and radii are used to characterize these hyperspheres. The

RBFN units respond non-linearly to the distance of points from the center represented by a radial unit. The response surface of a single radial unit is the Gaussian (bell-shaped) function, peaked at the center, and descending outwards (Haykin, 1994; Bishop, 1995; Hill and Lewicki, 2006). Therefore, the RBFN has three layers, namely input, hidden, and output layers. The hidden layer consists of radial units. It models the Gaussian response surface. The two most common methods for assigning the center of the radial units are sub-sampling and K-Means algorithm (Bishop, 1995; Hill and Lewicki., 2006).

The RBFN model has one hidden layer. A trial and error approach was used to determine the optimum number of node in the hidden layer. Following this approach, the optimum number of node in the hidden layer producing the least root mean square error (RMSE) was found to be 18, as shown in Figure 5.7. The R^2 value of the RBFN model is 0.6207, which is lowest among all the statistical and ANN models used in this study. Figure 5.8 shows an overall comparison between measured and predicted M_r values for this model. Significant scatter is observed for the entire data range, justifying a low R^2 value. Based on these results, it is clear that RBFN is incapable of predicting the development dataset. However, the R^2 value for fewer specimens is close to 1. For example, predicted M_r values show a good correlation (R^2 = 0.9012) with experimental M_r values for 3% lime-stabilized P-soil and 5% CKD-stabilized V-soil specimens, as shown in Figure 5.9. The correlation becomes weaker as more soil and additives types are included in the dataset.

5.5.1.2 Multi-Layer Perceptrons Network (MLPN)

The MLPN is one of the popular network architecture in use today (Rumelhart and McClelland, 1986; Bishop, 1995; Narayan, 2002; Zaman et al., 2010). The MLPN

consists of an input layer, a number of hidden layers, and an output layer. In each of the hidden layers, the number of nodes (also called neuron) can be varied. Due to the number of layers and the number of nodes in each layer, the MLPN can adjust the architecture of the network based on the complexity of a problem. In STATISTICA 8.0, the MLPN has up to three hidden layers available. Each of the nodes in the network performs a biased weighted sum of their inputs and passes this activation level through a transfer function to produce its output. The weights and biases in the network are adjusted using a training algorithm. The training algorithms available in STATISTICA 8 are back propagation, gradient descent, conjugate gradient, and quasi-Newton (Hill and Lewicki, 2006).

In MLPN, the weighted sum of input components are calculated as (Yilmaz and Yuksek, 2007; Canakci and Pala, 2007):

$$S_j = \sum_{i=0}^{n} W_{ij} x_i + Q_i \tag{5.22}$$

where i is number of inputs, j is number of neurons in hidden layers, S_j is the weighted sum of the j^{th} neuron for the input received from the preceding layer with n neurons (or inputs for MLPN with one hidden layer), W_{ij} is the weight between the j^{th} neuron and the i^{th} neuron in the preceding layer, x_i is the output of the i^{th} neuron in the preceding layer (or inputs for MLPN with one hidden layer), and Q_i is the constant bias term. Once the weighted sum S_j is computed, the output of the j^{th} neuron y_j is calculated with an activation function, sigmoid in this case, as follows:

$$y_i = f\left(S_j\right) = \frac{1}{1+\exp\left(-\eta S_j\right)} \tag{5.23}$$

where η is a constant used to control the slope of the semi-linear region. The sigmoid nonlinearity activates in every layer except the input layer (Yeh, 1998; Canakci and Pala, 2007).

In the present study, the MLPN model was developed with one hidden layer. The number of nodes in hidden layers was selected nine based on minimum RMSE by using a trial and error approach, as shown in Figure 5.10. The architecture of the developed MLPN model is illustrated in Figure 5.11. The neurons of input layer receive information from outside environment and transmit to the neurons of the hidden layer without performing any calculation. The hidden layer then processes the incoming information and extracts useful features to construct the mapping from the inputs space and interconnects each other through weights. The neuron of last layer called the output layer produce the network prediction to the outside world in the form of M_r values.

The training algorithm used in the study is conjugate gradient algorithm, activation function is sigmoid function, and number of epochs is 5,000 producing an error of less than 10^{-6} per 100 cycles. As a result of the training, the network produced 9 x 25 weights (W) and 9 bias values (Q_i) connecting input and hidden layer, 9 x 1 weights (W^2) and 1 bias value (Q) connecting hidden layer and output layer. Table 5.6 presents a list of the final weights and bias values. With these weights and bias values, the network is able to simulate M_r values with the trained data and to predict M_r values with the untrained data by using following equations:

$$\frac{Mr}{Pa} = \frac{30.54}{1+\exp\left(\frac{1.4071}{1+e^{-F_1}}+\frac{0.6943}{1+e^{-F_2}}+\frac{0.7252}{1+e^{-F_3}}+\frac{1.3595}{1+e^{-F_4}}+\frac{0.4442}{1+e^{-F_5}}-\frac{0.3108}{1+e^{-F_6}}-\frac{0.2729}{1+e^{-F_7}}-\frac{0.7253}{1+e^{-F_8}}+\frac{0.6157}{1+e^{-F_9}}\right)} \quad (5.24)$$

where,

$$F_1 = W_{1-1}\left(\frac{UCS}{P_a}\right) + W_{2-1}(MC) + W_{3-1}\left(\frac{DUW}{\gamma_w}\right) + W_{4-1}(P_{200}) + W_{5-1}(PI) + W_{6-1}(CC)$$

$$+ W_{7-1}(pH_s) + W_{8-1}(SSA_s) + W_{9-1}(CEC) + W_{10-1}(PA) + W_{11-1}(SiO_2) + W_{12-1}(Al_2O_3)$$

$$+ W_{13-1}(Fe_2O_3) + W_{14-1}(SSR_a) + W_{15-1}(CaO) + W_{16-1}(MgO) + W_{17-1}(ACA) + W_{18-1}(FL)$$

$$+ W_{19-1}(LOI) + W_{20-1}(P_{325}) + W_{21-1}(pH_a) + W_{22-1}(SSA_a) + W_{23-1}(SSR_m) + W_{24-1}\left(\frac{\sigma_3}{P_a}\right)$$

$$+ W_{25-1}\left(\frac{\sigma_d}{P_a}\right) + Q_1 \qquad (5.25)$$

Functions F_2, F_3,…, F_9 can be obtained by employing weights W_{i-2}, W_{i-3}, …, W_{i-9} (i = 1 – 25), respectively in Eqn. 5.25. By employing the aforementioned approach, the R^2 values of the MLPN model was found to be 0.9872, indicating that the MLPN model is expected to better correlate the M_r values than the RBFN (0.6207) model. Figure 5.12 shows a comparison between the experimental and predicted values of M_r values for the MLPN model. It is clear that the level of scatter in data points reduced significantly for this model. Also, it is evident that the predicted values are closer to the equality line.

5.5.2 Validation of Models

As noted earlier, a different dataset of M_r values of stabilized V-soil specimens was used for validation. This provides different views on the prediction quality and the importance of datasets on regression analysis (Montgomery et al., 2006; Myers et al., 2001; Solanki et al., 2008). Additionally, a comparison was made between the differences in the R^2 values of the development/evaluation dataset and the validation dataset.

The RBFN model predicted the M_r values of the validation dataset with a low R^2 value of 0.3172. Figure 5.13 shows a comparison of the prediction quality of the RBFN

model for the validation dataset. It is observed that the data points start to deviate to a "banded" distribution ranging between approximately 700 – 1000 MPa, as shown in Figure 5.13. The effect is presented as a narrow band across indicating a poor prediction. Also, S_e/S_y value of greater than 1 indicates low quality of M_r prediction achieved by using the RBFN model. On the other hand, the R^2 of the validation dataset for the MLPN model was found to be 0.9582 (Figure 5.13). The corresponding S_e/S_y value for the MLPN model was found to be less than 1 (0.5985). It is also evident from Figure 5.13 that the scatters for MLPN model are closer to equality line as compared to scatter of the RBFN model. Overall, the MLPN model appears to be the best model for the present (development/evaluation and validation) datasets.

5.6 Sensitivity Analysis

A sensitivity study was conducted on the best performing statistical (Model 3) and ANN (MLPN) model to evaluate the effect of each independent variable. In pursuing this sensitivity analysis, only one independent variable was changed at a time. First, the average and standard deviation of each independent variable were determined from the combined evaluation/development and validation datasets. The corresponding results of the mean and standard deviation of each independent variable for Model 3 and MLPN models are shown in Tables 5.7 and 5.8, respectively. Then, M_r value was calculated by inputting the average values of each independent variable into the corresponding models and this calculated value was called the "primary M_r value." A series of M_r values were then calculated by changing (within plus and minus of one-half standard deviation) one independent variable at a time, while the rest of the independent variables were kept at their mean values. The series of the M_r values thus obtained were compared with the

primary M_r value. Also, it is worth noticing that one-half standard deviation was used instead of one standard deviation because it was found that one standard deviation may change the independent value to an extent beyond the range of the original independent parameters used in this study.

5.6.1 Sensitivity Analysis For Stress-Based Statistical Model 3

The results (as percent difference) of the sensitivity analysis of the stress-based statistical Model 3 are presented in Table 5.7. It is seen that unconfined compressive strength, pH of soil, cationic exchange capacity, silica content of additive, and SSR of soil-additive mixture were more sensitive variables in the statistical Model 3. These five independent variables contributed to more than 2% differences in the comparison of M_r values. The unconfined compressive strength had the highest (approximately 24%) sensitivity followed by the pH of soil, SSR of soil-additive mixture, silica content of additive, and CEC of soil. The confining and deviatoric stress contributed to less than 2% of difference for the dataset considered herein which is consistent with the observation reported in Section 2.7.4. The dry unit weight and deviatoric stress had the least sensitivity of less than 0.5%.

5.6.2 Sensitivity Analysis For Neural Network MLPN Model

The results of the sensitivity analysis of MLPN model are presented in Table 5.8. Only unconfined compressive strength followed by moisture content showed significant sensitivity in the MLPN model. These two independent variables had more than 5% differences in the comparison of M_r values. Free-lime content followed by passing No. 325 sieve of additive, passing No. 200 sieve of additive, SSA of additive, percent of

additive, PI of soil, calcium oxide content of additive, Fe_2O_3 content, loss on ignition, deviatoric stress, SSR of soil-additive mixture had only modest influence (2 – 5 percent) on M_r. This behavior is consistent with the observations reported in Section 2.9; M_r values are better correlated with free-lime content, loss on ignition, percent passing No. 325 sieve, SSA of additive, and SSR of soil-additive mixture. Dry unit weight, clay content, pH of soil, CEC, and confining stress had less than 1% difference in the comparison of M_r values. The rank of each independent variable considered here based on the sensitivity result is presented in Table 5.8. Dry unit weight and confining stress showed the least significance in the sensitivity analysis. The reason for the low effect of dry unit weight may be that the influence of dry unit weight is over shadowed by other material parameters. Low sensitivity of confining stress is consistent with the observations reported in Section 2.7.4.

The overall sensitivity study showed that the sensitivity of independent variables was dependent on the type of models. The sensitivity ranking of independent variables was different for each model (Tables 5.7 and 5.8). However, unconfined compressive strength consistently remained one of the most sensitive independent variables in both statistical Model 3 and MLPN models. The confining stress, on the other hand, was always the least sensitive independent variable for the soils and additives considered in this study. Also, SSR of soil-additive mixture showed intermediate influence on the M_r values predicted by using both statistical Model 3 and MLPN model. These observations are consistent with the observations reported in Section 2.9.

5.7 Concluding Remarks

In this study, a total of four stress-based statistical models and two feed-forward-type ANN models, were evaluated to correlate resilient modulus with specimen characteristics and soil/additive properties. A M_r database developed using laboratory test results on 160 specimens prepared by using four soils stabilized with three additives namely, lime (3%, 6% and 9%), CFA (5%, 10% and 15%) and CKD (5%, 10% and 15%) was used. Of these, three soils namely, P- (silty clay), V- (lean clay) and C- (fat clay) soil were used in development/evaluation, and the remaining one soil (K-soil, lean clay) was used in the validation of the selected models. The following points highlight the assessments and evaluations of these models:

1. One semi-log (σ_3, σ_d) and three log-log (θ, σ_d; σ_3, σ_d; θ, τ_{oct}) stress-based statistical models were evaluated. The log-log model recommended by AASHTO 2002 Design Guide (θ, τ_{oct}) for unbound materials showed the least acceptable performance.
2. The model constants of the three selected statistical models were calibrated through multiple linear regressions by using common compacted specimen characteristics and soil/additive properties. The developed correlations were the most accurate in producing R^2 values ranging from 0.90 to 0.93.
3. All three stress-based statistical models were validated by using additional M_r data of stabilized K-soil specimens. Overall, a semi-log (σ_3, σ_d) model was found to show best acceptable performance with the highest R^2 value (0.98) and lowest average S_e/S_y value of 0.48.
4. From the correlations of best performing statistical model (Model 3), it appears that the model constants for 28-day M_r were mainly governed by compacted specimen

characteristics – UCS, molding moisture content, molding dry unit weight, percentage of additive, silica sesquoxide ratio of soil-additive mixture; soil properties – clay content, pH, cationic exchange capacity; and additive properties – silica content, calcium oxide, magnesium oxide content, loss on ignition.

5. Model 3 developed using selected parameters showed that the model constants are governed by compacted specimen characteristics – UCS, molding moisture content, molding dry unit weight, percentage of additive; soil properties – clay content, plasticity index, pH; and additive properties – free lime content, percent passing No. 325 sieve.
6. For the RBFN model, with one hidden layer, the R^2 value for the development/evaluation dataset showed worst performance (0.62) among all the statistical and ANN models used in this study. Also, it was found that the R^2 value for fewer specimens is close to 1 but the correlation becomes weaker and appears in a "banded" distribution as more soil and additives types are included in the dataset. Further, study showed that RBFN model predicts M_r values of validation dataset with lowest reliability ($R^2 = 0.32$, $S_e/S_y = 1.26$).
7. The R^2 value of the MLPN model with one hidden layer was found to be 0.99 for evaluation/development dataset. Based on R^2 value and visual examination, this model appeared to be the best model. Further, validation of MLPN model using a different dataset showed S_e/S_y value of 0.60 and R^2 value of 0.96 indicating high quality of M_r prediction achieved by using the MLPN model.

8. Overall, the MLPN model was found to be the best model for the present development/evaluation and validation datasets. This model as well as the other models could be refined using an enriched database.
9. The sensitivity ranking of independent variables was different for each model. However, unconfined compressive strength consistently remained one of the most sensitive independent variables in both statistical Model 3 and MLPN models. The confining stress, on the other hand, was always the least sensitive independent variable for the soils and additives considered in this study. Also, SSR of soil-additive mixture showed intermediate influence on the M_r values predicted by using both statistical Model 3 and MLPN model.

Table 5.1 A Summary of Relevant Laboratory Studies on Soils Stabilized with Different Additives

Reference	Type of soil[a]	Type of additive	Parameters/Tests[b] (Statistical Analysis for M_r: Yes/No)
Chang (1995)	Lateritic soil	FA, Lime	UCS, M_r (No)
Achampong (1996)	CL, CH	PC, Lime	UCS, M_r (**Yes**)
Misra (1998)	Clays	FA	UCS (No)
Little (2000)	Fine grained soils	Lime	UCS, M_r, Swell (No)
Miller and Azad (2000)	CH, CL, ML	CKD	UCS (No)
Qubain et al. (2000)	CL	Lime	UCS, M_r (No)
Kim and Siddiki (2004)	A-4, A-6, A-7-6	Lime, LKD	UCS, CBR, volume stability, M_r (**Yes**)
Rahim and George (2004)	A-2-4, A-3, A-6	None	M_r (**Yes**)
Arora and Aydilek (2005)	SM	FA	UCS, CBR, M_r (**Yes**)
Hillbrich and Scullion (2006)	A-3	PC	M_r, Seismic Modulus (**Yes**)
Osinubi and Nwaiwu (2006)	CL	Lime	UCS (No)
Peethamparan et al. (2008)	Kaolinite clay	CKD, Lime	UCS, Modulus (No)
Ling et al. (2008)	Silty clay	Lime, PC	M_r (**Yes**)
Hossain (2009)	A-1, A-2, A-4, A-5, A-6, A-7	None	M_r (**Yes**)
Mohammad et al. (2009)	A-4, A-6, A-7-5, A-7-6	None	M_r (**Yes**)
Mooney and Toohey (2010)	A-6, A-7-6	Lime	UCS, M_r (**Yes**)

[a]Soils according to USCS and AASHTO classification; [b]Compaction and Atterberg limit tests are not included in the list; M_r: Resilient Modulus test; CBR: California Bearing Ratio; FA: Fly Ash; PC: Portland Cement; CKD: Cement Kiln Dust; LKD: Lime Kiln Dust

Table 5.2 Average Model Constants for P-soil Stabilized with Lime, CFA and CKD

Percentage of additive	*Model 1* : $M_r = k_1 p_a \times (\theta/p_a)^{k_2} \times (\sigma_d/p_a)^{k_3}$				*Model 2* : $M_r = k_1 p_a \times (\sigma_3/p_a)^{k_2} \times (\sigma_d/p_a)^{k_3}$			
	k_1	k_2	k_3	M_r*	k_1	k_2	k_3	M_r*
Raw soil	803	0.342	-0.341	103	1,266	0.223	-0.248	103
3% Lime	3,946	0.095	-0.482	604	4,595	0.074	-0.456	604
6% Lime	4,384	0.073	-0.545	713	5,087	0.037	-0.522	764
9% Lime	4,177	0.274	-0.541	650	5,754	0.143	-0.470	668
5% CFA	1,297	0.403	-0.323	162	2,285	0.276	-0.209	161
10% CFA	4,145	0.195	-0.175	472	5,415	0.134	-0.122	468
15% CFA	7,960	0.025	-0.635	1,417	8,185	0.013	-0.625	1,415
5% CKD	2,924	0.110	-0.371	404	3,396	0.073	-0.340	403
10% CKD	14,547	0.004	-0.296	1,920	14,805	0.005	-0.295	1,935
15% CKD	22,399	-0.046	-0.100	2,505	21,163	-0.024	-0.117	2,500
Percentage of additive	*Model 3* : $M_r = k_1 p_a \times (k_2)^{\sigma_3/p_a} \times (k_3)^{\sigma_d/p_a}$				*Model 4* : $M_r = k_1 p_a \times (\theta/p_a)^{k_2} \times (\tau_{oct}/p_{a+1})^{k_3}$			
Raw soil	1,296	2.563	0.439	107	1,425	0.040	-1.580	118
3% Lime	10,801	1.410	0.246	646	8,593	-0.217	-2.352	685
6% Lime	11,881	1.699	0.303	794	9,454	-0.317	-2.030	799
9% Lime	9,551	2.013	0.397	730	8,462	0.007	-1.932	678
5% CFA	1,797	3.339	0.528	165	2,251	0.275	-1.748	175
10% CFA	5,176	1.770	0.652	476	5,402	0.098	-0.364	513
15% CFA	23,751	1.057	0.277	1,436	17,650	-0.362	-2.424	1,436
5% CKD	6,328	1.367	0.373	447	5,256	-0.142	-1.476	458
10% CKD	27,751	0.943	0.441	1,997	22,667	-0.211	-1.549	1,988
15% CKD	29,077	0.889	0.719	2,534	26,139	-0.110	-0.548	2,534

*M_r values calculated at p_a = 101.28 kPa, σ_3 = 13.78 kPa, σ_d = 41.34 kPa, θ = 82.68 kPa, τ_{oct} = 12.99 kPa

Table 5.3 Average Model Constants for V-soil Stabilized with Lime, CFA and CKD

Percentage of additive	*Model 1* : $M_r = k_1 p_a \times (\theta/p_a)^{k_2} \times (\sigma_d/p_a)^{k_3}$				*Model 2* : $M_r = k_1 p_a \times (\sigma_3/p_a)^{k_2} \times (\sigma_d/p_a)^{k_3}$			
	k_1	k_2	k_3	M_r* (MPa)	k_1	k_2	k_3	M_r* (MPa)
Raw soil	575	0.285	-0.408	79	856	0.198	-0.328	78
3% Lime	8,419	0.010	0.030	828	8,546	0.011	0.032	822
6% Lime	6,430	0.030	-0.074	692	6,698	0.020	-0.066	692
9% Lime	6,098	0.043	-0.085	660	6,460	0.028	-0.071	660
5% CFA	4,695	0.082	-0.145	533	5,252	0.055	-0.119	531
10% CFA	8,763	0.016	-0.092	960	8,964	0.016	-0.089	954
15% CFA	11,116	0.060	-0.010	1,123	12,032	0.038	0.008	1,122
5% CKD	4,827	0.117	-0.182	562	5,342	0.079	-0.149	529
10% CKD	14,013	-0.015	-0.136	1,609	13,773	-0.013	-0.141	1,624
15% CKD	18,950	0.028	0.016	1,881	19,370	0.015	0.024	1,865
Percentage of additive	*Model 3* : $M_r = k_1 p_a \times (k_2)^{\sigma_3/p_a} \times (k_3)^{\sigma_d/p_a}$				*Model 4* : $M_r = k_1 p_a \times (\theta/p_a)^{k_2} \times (\tau_{oct}/p_{a+1})^{k_3}$			
Raw soil	1,122	2.310	0.337	82	1,102	0.012	-1.852	89
3% Lime	7,792	1.077	1.111	832	8,147	0.038	-0.069	812
6% Lime	7,416	1.098	0.807	697	7,198	-0.018	-0.274	708
9% Lime	7,130	1.132	0.799	670	6,961	-0.011	-0.399	673
5% CFA	5,884	1.270	0.718	538	5,728	-0.017	-0.322	560
10% CFA	10,729	0.583	0.318	632	10,188	-0.050	-0.320	1,003
15% CFA	10,804	1.177	1.012	1,124	11,267	0.053	-0.014	1,127
5% CKD	6,034	1.431	0.624	529	5,936	-0.011	-0.840	545
10% CKD	19,512	0.970	0.703	1,704	16,979	-0.098	-0.423	1,667
15% CKD	17,549	1.090	1.166	1,915	17,092	-0.094	0.653	1,909

*M_r values calculated at p_a = 101.28 kPa, σ_3 = 13.78 kPa, σ_d = 41.34 kPa, θ = 82.68 kPa, τ_{oct} = 12.99 kPa

Table 5.4 Average Model Constants for C-soil Stabilized with Lime, CFA and CKD

Percentage of additive	*Model 1* : $M_r = k_1 p_a \times (\theta/p_a)^{k_2} \times (\sigma_d/p_a)^{k_3}$				*Model 2* : $M_r = k_1 p_a \times (\sigma_3/p_a)^{k_2} \times (\sigma_d/p_a)^{k_3}$			
	k_1	k_2	k_3	M_r* (MPa)	k_1	k_2	k_3	M_r* (MPa)
Raw soil	1,214	0.026	-0.315	162	1,275	0.026	-0.306	161
3% Lime	3,432	0.060	-0.173	401	3,736	0.042	-0.155	400
6% Lime	5,879	0.044	-0.154	678	6,257	0.029	-0.139	677
9% Lime	4,332	0.086	-0.204	518	4,863	0.058	-0.180	516
5% CFA	2,057	0.163	-0.249	252	2,583	0.115	-0.203	250
10% CFA	2,591	0.175	-0.221	309	3,286	0.121	-0.170	304
15% CFA	3,420	0.231	-0.179	388	4,735	0.159	-0.113	386
5% CKD	1,235	0.171	-0.294	157	1,566	0.119	-0.248	156
10% CKD	2,958	0.076	-0.143	335	3,295	0.053	-0.121	335
15% CKD	7,732	-0.030	-0.111	871	7,447	-0.021	-0.115	872
Percentage of additive	*Model 3* : $M_r = k_1 p_a \times (k_2)^{\sigma_3/p_a} \times (k_3)^{\sigma_d/p_a}$				*Model 4* : $M_r = k_1 p_a \times (\theta/p_a)^{k_2} \times (\tau_{oct}/p_{a+1})^{k_3}$			
Raw soil	2,477	1.118	0.354	167	2,050	-0.186	-1.679	176
3% Lime	4,830	1.197	0.603	408	4,531	-0.055	-0.829	420
6% Lime	7,884	1.123	0.663	686	7,424	-0.060	-0.750	695
9% Lime	6,413	1.279	0.544	524	5,920	-0.080	-0.637	564
5% CFA	3,121	1.622	0.514	257	3,086	-0.002	-1.287	268
10% CFA	3,615	1.219	0.305	232	3,705	0.019	-1.234	322
15% CFA	4,111	1.973	0.693	393	4,591	0.121	-0.951	404
5% CKD	2,089	1.648	0.437	162	2,034	-0.041	-1.646	170
10% CKD	3,811	1.261	0.673	339	3,725	-0.019	-0.712	348
15% CKD	10,126	0.936	0.718	888	9,261	-0.099	-0.597	890

*M_r values calculated at p_a = 101.28 kPa, σ_3 = 13.78 kPa, σ_d = 41.34 kPa, θ = 82.68 kPa, τ_{oct} = 12.99 kPa

Table 5.5 Analyses of Variance on Test Results of Lime-, CFA- and CKD-Stabilized P-, V- and C-Soil Specimens Using Statistical Model 3

Independent Variable	Parameter Estimate	Standard Error	Type II Sum of Squares	F-value	Pr>F	[a]Significant
Intercept	1.64172	0.09938	2.11074	272.91	<.0001	Yes
$Log(UCS/P_a)$[b]	1.31709	0.03879	8.91834	1153.12	<.0001	Yes
$Log(MC)$[b]	-0.25544	0.05975	0.14135	18.28	<.0001	Yes
$Log(pH_s)$[c]	-0.59169	0.15015	0.1201	15.53	<.0001	Yes
$Log(CEC_s)$[c]	0.15846	0.06837	0.04154	5.37	0.0206	Yes
$Log(PA)$[b]	-0.12202	0.01743	0.37903	49.01	<.0001	Yes
$Log(SiO_2)$[d]	-0.10662	0.00984	0.90738	117.32	<.0001	Yes
$Log(SSR_m)$[b]	0.29422	0.04942	0.27408	35.44	<.0001	Yes
(σ_3/P_a) x $Log(UCS/P_a)$[b]	-0.33687	0.08824	0.11271	14.57	0.0001	Yes
(σ_3/P_a) x $Log(MgO)$[d]	-0.19567	0.13117	0.01721	2.23	0.0136	Yes
(σ_3/P_a) x $Log(LOI)$[d]	-0.15934	0.06462	0.04703	6.08	0.0138	Yes
(σ_3/P_a) x $Log(SSR_m)$[b]	0.26706	0.09875	0.05657	7.31	0.0069	Yes
(σ_d/P_a) x $Log(UCS/P_a)$[b]	0.43256	0.06043	0.3963	51.24	<.0001	Yes
(σ_d/P_a) x $Log(DUW/\gamma_w)$[b]	-1.04209	0.3414	0.07206	9.32	0.0023	Yes
(σ_d/P_a) x $Log(CC)$[c]	0.27905	0.04761	0.26567	34.35	<.0001	Yes
(σ_d/P_a) x $Log(CaO)$[d]	-0.18864	0.05323	0.09714	12.56	0.0004	Yes

[a]Significant at probability level (alpha) = 0.05; [b]molded specimen properties; [c]soil properties; [d]additive properties; σ_d: deviatoric stress; σ_3: confining stress; P_a: atmospheric pressure (101.283 kPa); UCS: 28-day unconfined compressive strength; MC: molding moisture content; DUW: molding dry unit weight (kN/m^3); γ_w: unit weight of water (9.81 kN/m^3); PA: additive content (%); pH_s: pH of pure soil; CC: clay content in soil (%); SiO_2: silica content of additive (%); MgO: magnesium oxide content of additive (%); LOI: loss on ignition; SSR: silica sesquoxide ratio of mix

Table 5.6 Weight and Bias Values for MLPN 25-9-1

Weights (ij)	Number of hidden layer neurons (j)								
	1	2	3	4	5	6	7	8	9
Between Input and Hidden Layer									
W_{1j} (UCS/P_a)	0.7849	-0.2768	-0.4757	-0.7488	-0.3004	-0.6057	-0.2175	-0.6374	-0.5808
W_{2j} (MC)	-0.2339	-0.3610	-0.4485	-0.3660	0.1410	0.0192	-0.3717	-0.2784	-0.0769
W_{3j} (DUW/γ_w)	0.1414	0.0763	0.1269	0.0510	0.3162	-0.4473	-1.9853	-1.0919	0.9099
W_{4j} (P_{200})	-0.1455	0.2050	-0.6296	-0.3227	-0.0140	0.2394	-0.0842	-0.6616	-0.0189
W_{5j} (PI)	-0.1268	-0.0302	0.4097	-0.0823	-0.0651	0.1827	-0.2170	0.0563	-0.0482
W_{6j} (CC)	0.0414	-0.0964	0.0139	-0.0245	-0.1234	0.5100	-0.2283	0.1011	0.3436
W_{7j} (pH_s)	0.6026	0.6030	-0.1112	0.4181	0.0286	0.5532	0.2384	0.2701	0.2605
W_{8j} (SSA_s)	0.0932	-0.0469	0.2761	0.2811	-0.0070	0.0062	-0.0125	-0.0087	-0.0044
W_{9j} (CEC)	-0.1407	0.5116	1.4874	0.7090	0.1179	0.2400	-0.1110	0.4663	0.3095
W_{10j} (PA)	0.3427	-0.4081	0.5317	0.5927	-0.1045	-0.1115	-0.0787	-0.0072	-0.0460
W_{11j} (SiO_2)	-0.0769	-0.0565	-0.0937	-0.0767	-0.0852	-0.0178	-0.0697	0.0973	0.0112
W_{12j} (Al_2O_3)	0.2679	0.0830	0.2180	0.3672	-0.1492	0.1319	0.0133	-0.1156	-0.2717
W_{13j} (Fe_2O_3)	0.0508	0.8503	-0.1267	-0.1323	-0.1328	0.0454	-0.2398	-0.1594	-0.1061
W_{14j} (SSR_a)	-0.3170	-0.2456	-0.2431	-0.2376	-0.2884	-0.0872	0.0412	0.6130	-0.0230
W_{15j} (CaO)	-0.0830	-0.0955	-0.2227	0.0881	-0.0618	0.1889	-0.3144	0.0350	0.4890
W_{16j} (MgO)	-0.0860	0.0378	-0.0123	-0.4499	0.1731	0.0169	-0.2102	0.3254	0.0249
W_{17j} (ACC)	0.1233	0.0478	0.1394	0.1016	0.0063	-0.1280	0.2603	0.4927	-1.0806
W_{18j} (FL)	0.6707	-1.5454	-0.7059	0.0926	0.8779	0.0639	0.4461	0.1220	0.2625
W_{19j} (LOI)	0.2201	-0.7126	0.0994	0.2387	-0.2065	0.3945	-0.1745	-0.0968	-0.1482
W_{20j} (P_{325})	0.0653	-0.5064	-0.0065	0.2077	-2.7049	-0.6988	0.1553	0.2068	-0.3732
W_{21j} (pH_a)	-0.1558	-0.0510	0.2445	-0.0054	0.6924	0.0392	-0.1549	-0.0408	0.9005
W_{22j} (SSA_a)	-0.1839	-0.0622	0.4394	-0.5280	0.1013	-0.0296	0.0777	-0.1034	0.0928
W_{23j} (SSR_m)	0.0014	0.2497	0.0841	-0.3350	-0.3646	-0.1201	-0.1905	-0.2597	-0.3332
W_{24j} (σ_3/P_a)	0.2257	-0.6296	-0.3056	0.1483	0.1646	0.1695	0.0118	0.1503	0.1561
W_{25j} (σ_d/P_a)	0.1277	0.1610	0.1236	0.1076	0.0899	0.1620	0.0953	0.0014	-0.5593
Bias Q_j	-0.3421	-0.0373	0.2645	-0.1617	-0.3442	0.0294	0.0885	-0.0228	0.2484
Between Hidden and Output Layer									
W^2_j (M_r/P_a)	1.4071	0.6943	0.7252	1.3595	0.4442	-0.3108	-0.2729	-0.7253	0.6157
Bias Q	0.6435								

Table 5.7 Sensitivity Study for the Statistical Model 3

Independent Variables	Average[a]	Standard Deviation	Percent Different[b] +	Rank[b] +	Percent Different[c] –	Rank[c] –
Primary M_r (MPa)	690.4	---	---	---	---	---
UCS (kPa)	810.5	543.3	17.85	1	-23.76	1
MC (%)	77.3	43.3	-1.31	8	1.45	8
DUW (kN/m^3)	19.3	4.0	-0.48	13	0.49	13
CC (%)	17.6	9.1	0.91	9	-1.10	10
pH_s	37.5	13.6	-4.04	2	4.65	2
CEC (meq/100g)	98.3	25.6	1.78	5	-2.27	5
PA (%)	14.4	6.9	-1.36	7	1.74	6
SiO_2 (%)	8.4	4.0	-1.99	4	3.12	4
CaO (%)	3.6	1.8	-0.66	12	0.80	12
MgO (%)	46.2	18.0	-0.88	10	1.29	9
LOI (%)	17.1	20.1	-0.66	11	0.94	11
SSR_m	11.6	4.5	3.70	3	-4.59	3
σ_3 (kPa)	10.6	4.5	0.18	14	-0.18	14
σ_d (kPa)	27.6	11.2	-1.64	6	1.64	7

[a]reference value; [b]independent variable plus one-half standard deviation (Note: some plus one standard deviation values are out of variables range); [c]independent variable minus one-half standard deviation

Table 5.8 Sensitivity Study for the Neural Network MLP 25-9-1 Model

Independent Variables	Average[a]	Standard Deviation	Percent Different[b] +	Rank[b] +	Percent Different[c] –	Rank[c] –
Primary M_r (MPa)	889.8	---	---	---	---	---
UCS (kPa)	810.5	543.3	32.72	1	-36.14	1
MC (%)	77.3	43.3	6.34	2	-5.86	2
DUW (kN/m^3)	19.3	4.0	1.30	14	0.13	25
P_{200} (%)	16.5	0.8	-3.04	5	3.65	5
PI	92.8	4.7	3.94	3	-2.96	8
CC (%)	17.6	9.1	0.08	24	-0.59	22
pH_s	37.5	13.6	1.59	9	-0.84	21
SSA_s (m^2/g)	7.3	2.0	-2.67	7	1.03	18
CEC (meq/100g)	98.3	25.6	-1.37	13	0.96	20
PA (%)	14.4	6.9	-3.35	4	3.01	7
SiO_2 (%)	8.4	4.0	0.85	20	-0.99	19
Al_2O_3 (%)	17.8	15.3	-0.24	23	-1.07	17
Fe_2O_3 (%)	7.1	7.4	-1.40	12	-2.47	10
SSR_a	2.7	2.3	-2.59	8	0.28	23
CaO (%)	3.6	1.8	1.26	15	-2.81	9
MgO (%)	46.2	18.0	-0.79	22	-1.89	14
ACA (%)	2.5	1.9	-0.95	17	-1.54	16
FL (%)	1.4	0.9	-0.92	18	-4.23	3
LOI (%)	17.1	20.1	0.97	16	-2.27	11
P_{325} (%)	19.7	13.5	1.47	11	-3.66	4
pH_a	92.7	5.2	2.73	6	-1.81	15
SSA_a	12.3	0.3	0.80	21	-3.36	6
SSR_m	11.6	4.5	0.85	19	-2.12	13
σ_3 (kPa)	10.6	4.5	-0.02	25	0.16	24
σ_d (kPa)	27.6	11.2	-1.55	10	2.12	12

[a]reference value; [b]independent variable plus one-half standard deviation (Note: some plus one standard deviation values are out of variables range); [c]independent variable minus one-half standard deviation

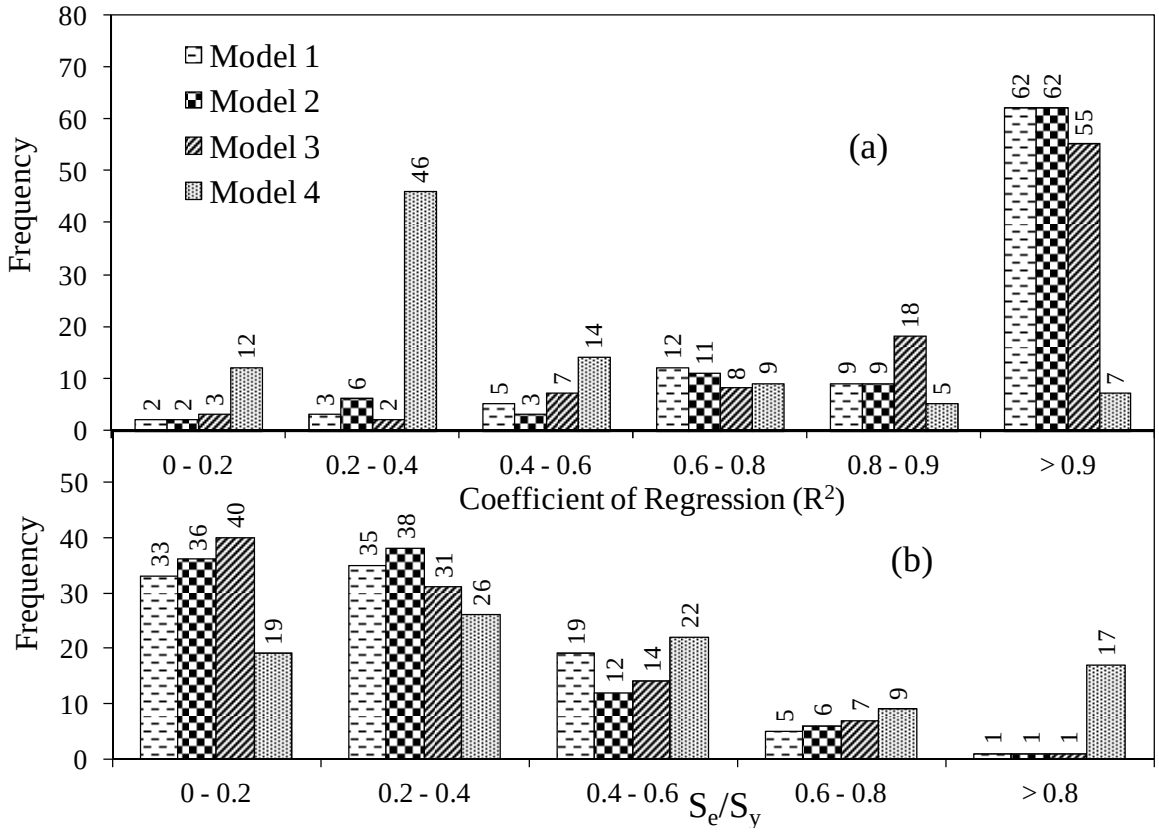

Figure 5.1 Frequency diagram for (a) Coefficient of Regression (R^2), and (b) S_e/S_y

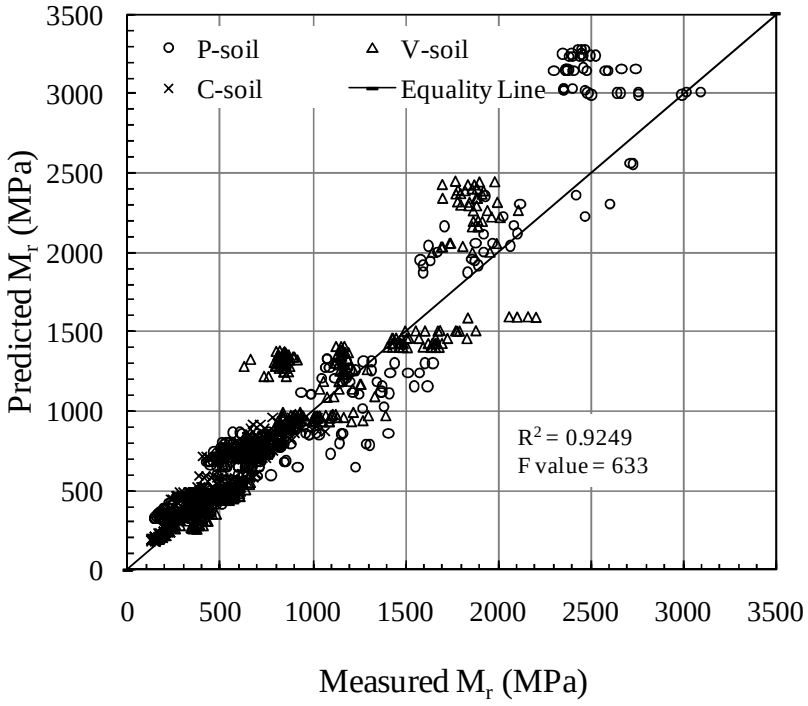

Figure 5.2 Predicted M_r Versus Measured M_r for P-, V- and C-soil using Statistical Model 1

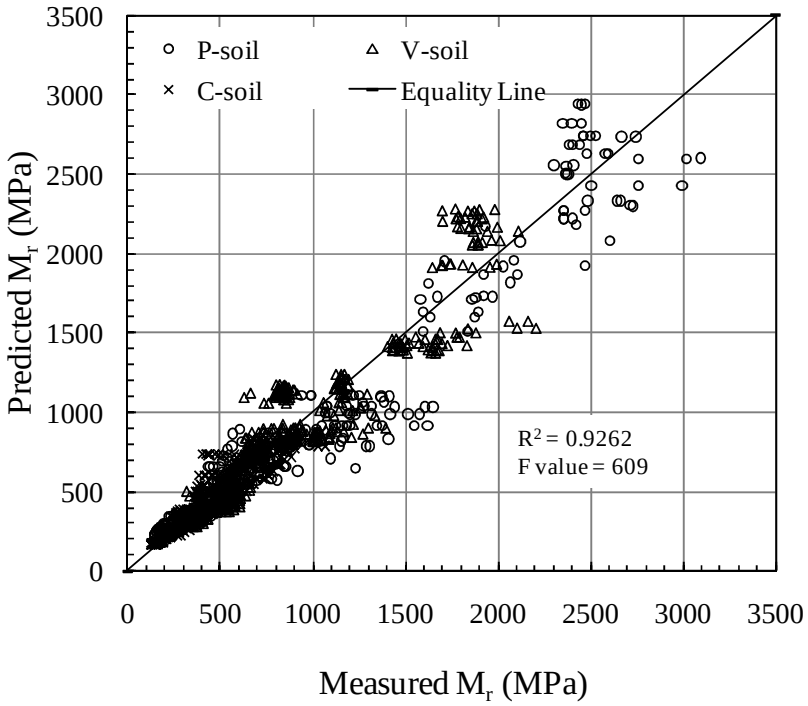

Figure 5.3 Predicted M_r Versus Measured M_r for P-, V- and C-soil using Statistical Model 2

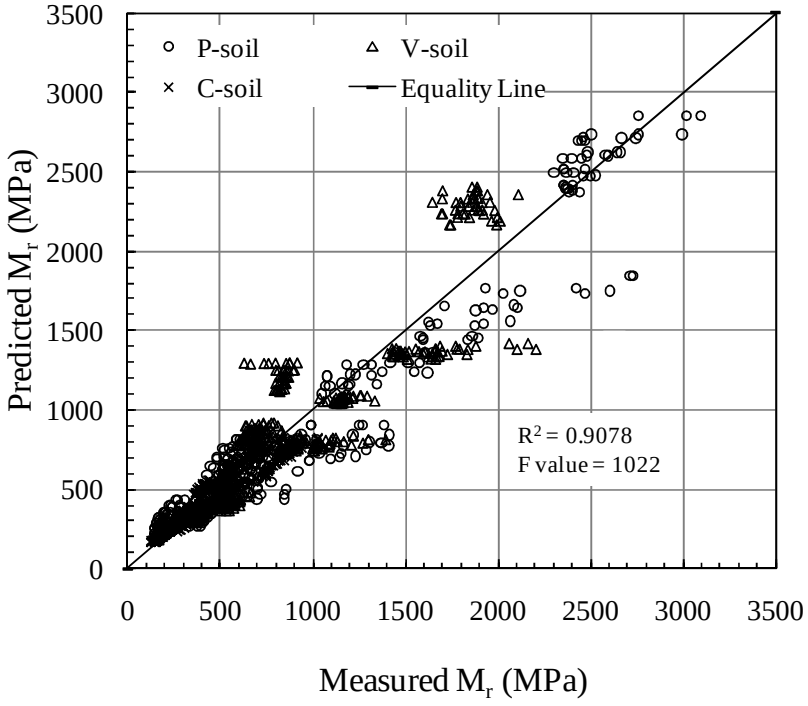

Figure 5.4 Predicted M_r Versus Measured M_r for P-, V- and C-soil using Model 3

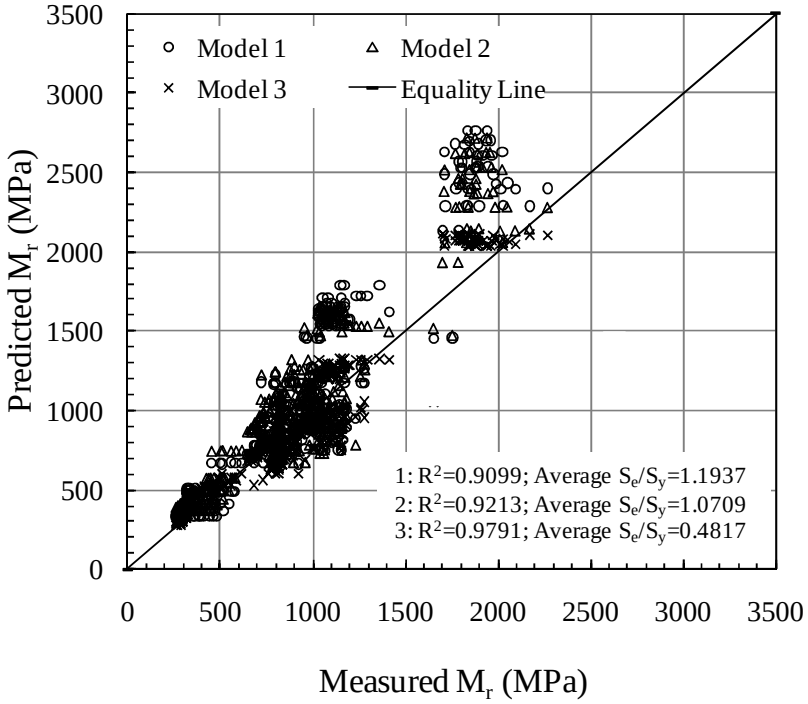

Figure 5.5 Predicted M_r Versus Measured M_r for K-soil using Statistical Models 1, 2 and 3

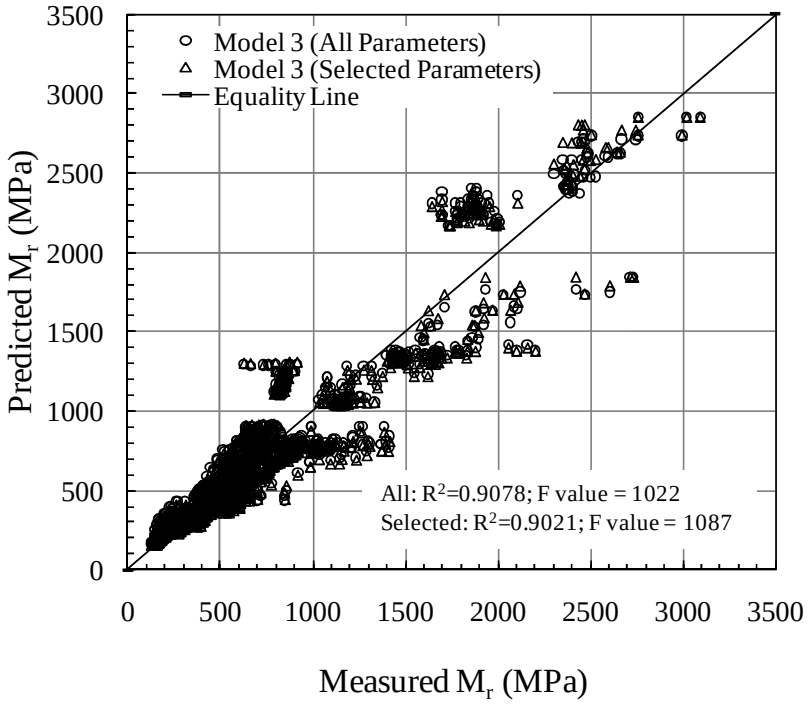

Figure 5.6 Predicted M_r Versus Measured M_r for P-, V- and C-soil using Statistical Model 3 Developed using All and Selected Parameters

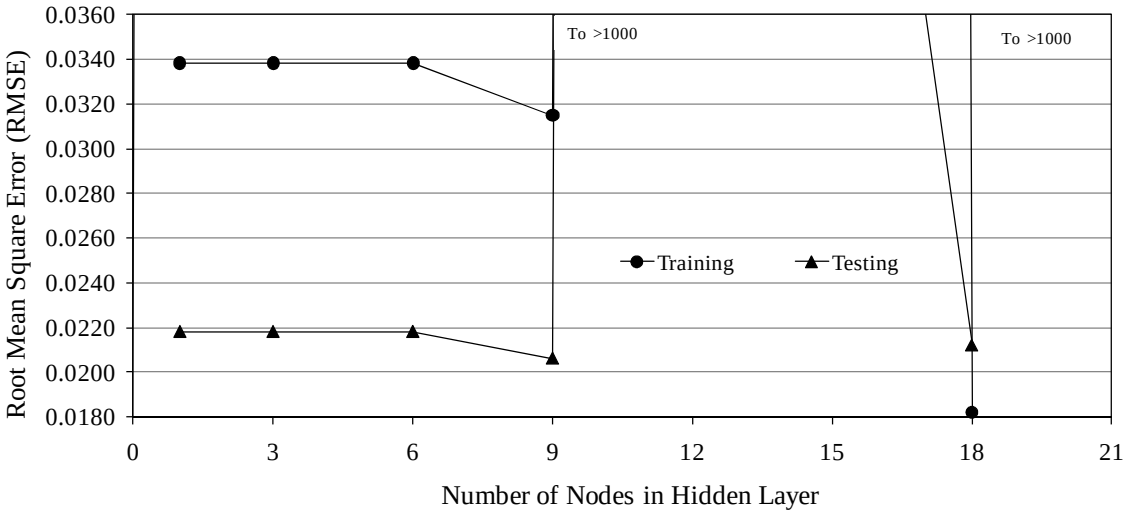

Figure 5.7 Selection of Number of Nodes in Hidden Layer (RBFN) for Training and Testing Sets

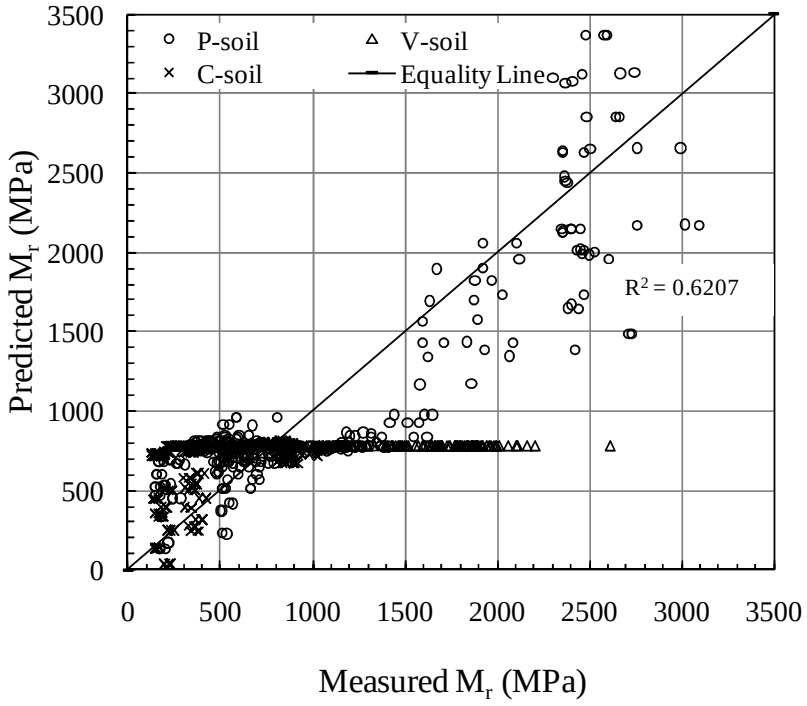

Figure 5.8 Predicted M_r Versus Measured M_r for P-, V- and C-soil using RBFN 25-18-1 Neural Network Model

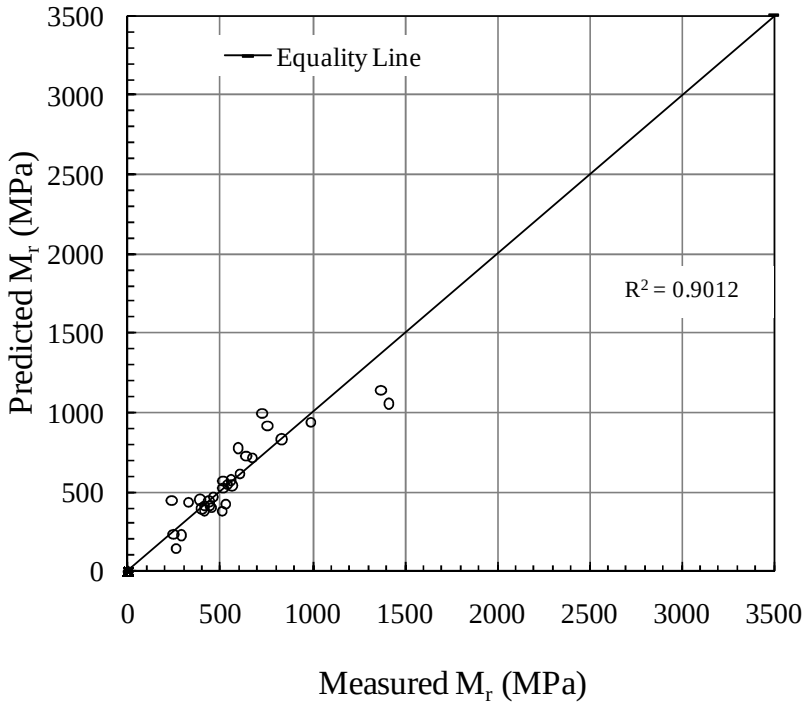

Figure 5.9 Predicted M_r Versus Measured M_r for Two M_r Tests: 3% lime-stabilized P-soil and 5% CKD-stabilized V-soil using RBFN 25-10-1 Neural Network Model

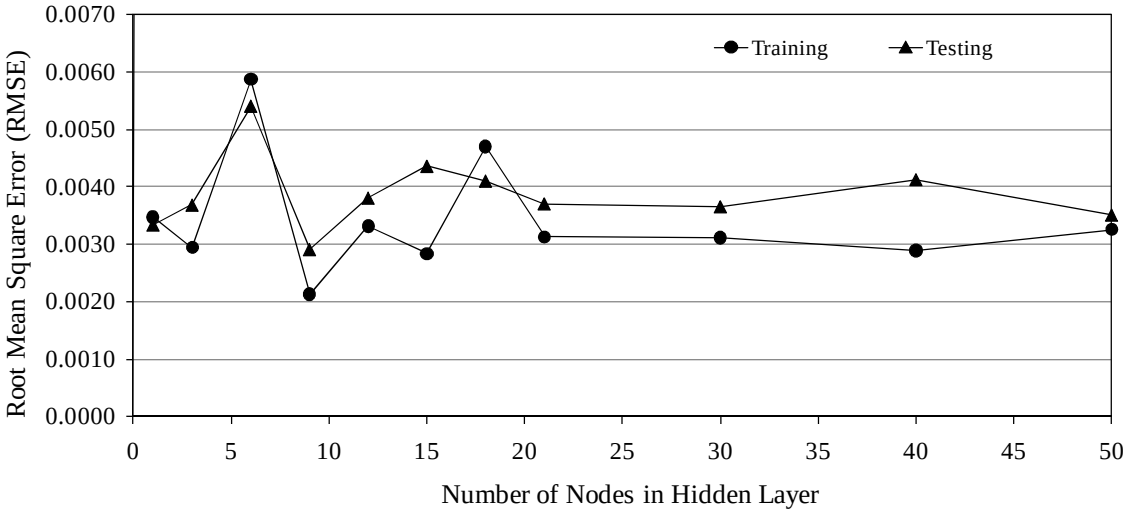

Figure 5.10 Selection of Number of Nodes in Hidden Layer (MLPN) for Training and Testing Sets

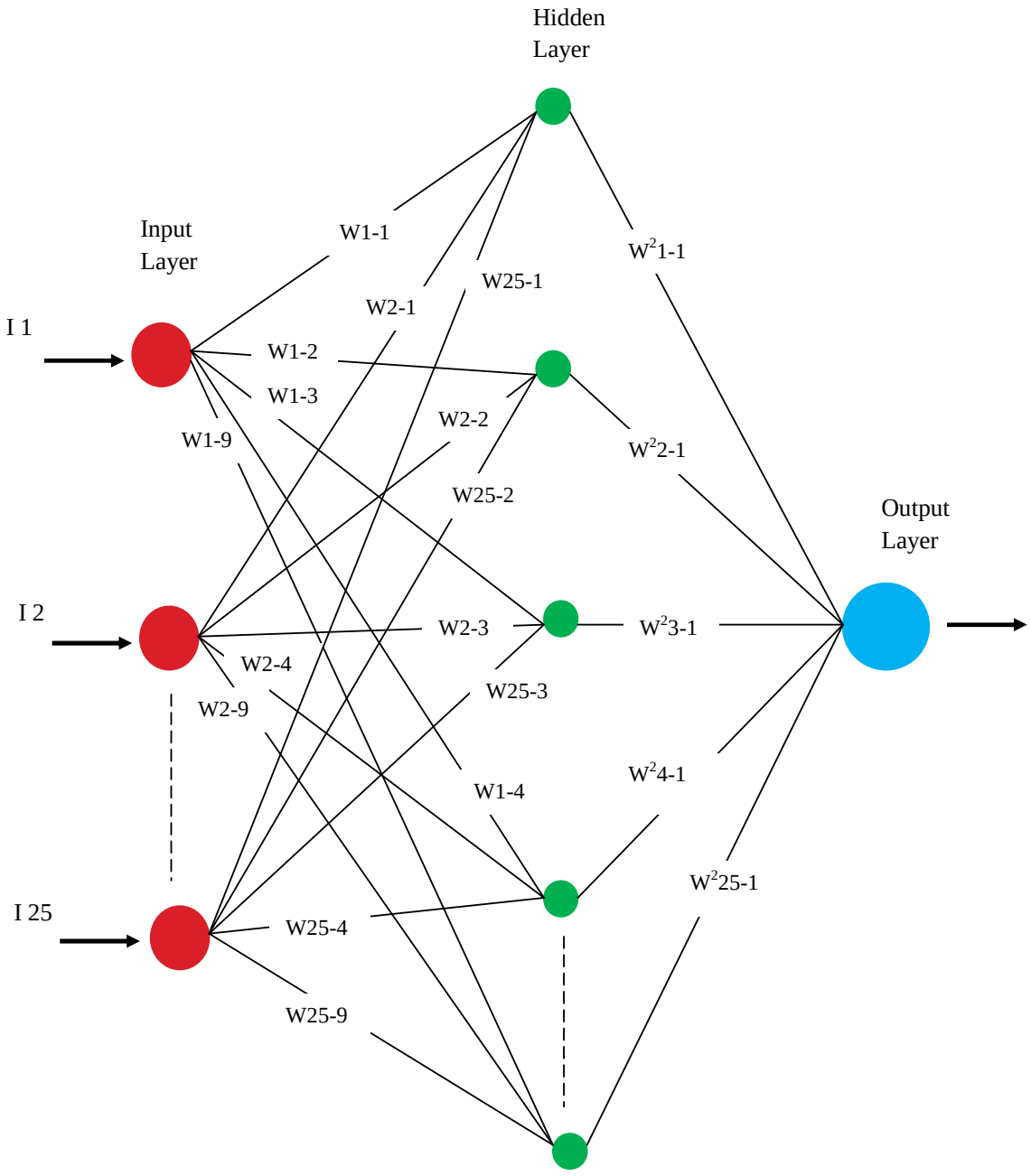

Figure 5.11 Neural Network Architecture of MLPN 25-9-1

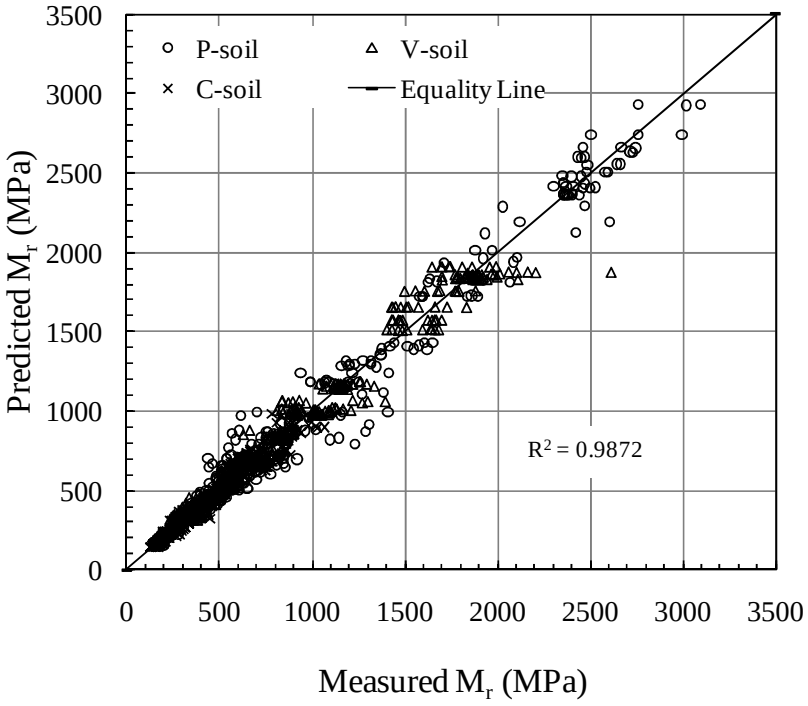

Figure 5.12 Predicted M_r Versus Measured M_r for P-, V- and C-soil using MLPN 25-9-1 Neural Network Model

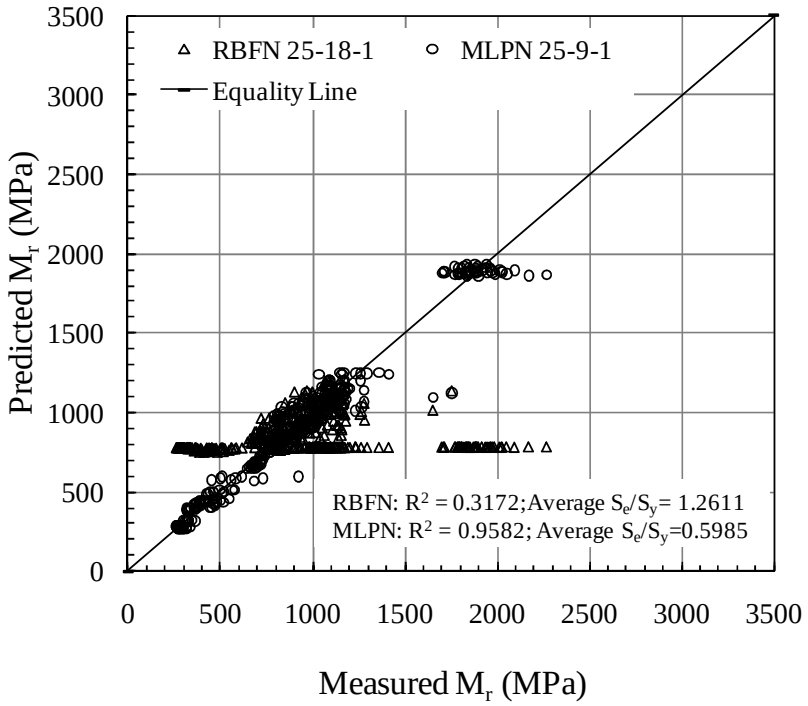

Figure 5.13 Predicted M_r Versus Measured M_r for K-soil Using RBFN 25-18-1 and MLPN 25-9-1 Neural Network Models

CHAPTER 6

BEHAVIOR OF CEMENTITIOUSLY STABILIZED SUBGRADE SOILS UNDER TENSION AND FLEXURE

6.1 Introduction

In the absence of any stress relief layer such as aggregate base, the location of critical tensile stress completely changes the potential performance of the flexible pavement, from the mechanistic standpoint (e.g., AASHTO, 2004; Adaska and Luhr, 2004; Lav et al., 2006; Molenaar and Pu, 2008; Agostinacchio et al., 2008). This phenomenon is demonstrated through parametric study of different pavement sections, as illustrated in Table 6.1. The pavement configuration is shown in Figure 6.1 which is commonly used by Oklahoma Department of Transportation (ODOT) in low water table regions and defined as *semi-rigid* type flexible pavement by the new MEPDG, as will be discussed later in Section 7.2. The section consists of three layers: (1) The top layer is 178 mm (7 in) thick asphalt concrete (AC); type "S-4" asphalt concrete with M_r value of approximately 3,445 MPa containing PG 64-22 binder is used. (2) The layer below is a 203 mm (8 in) thick cementitiously stabilized subgrade layer; V-soil stabilized with 6% lime or 10% CFA or 10% CKD is used for making the case realistic and design M_r values are reproduced from Table 5.3. (3) The bottom layer is the natural subgrade soil (V-soil). The linear analysis of the aforementioned section is conducted using a multi-layer elastic theory-based computer program, KENLAYER (Huang, 2004), for different cases. Case 1 is the only case without any stabilized layer. This is achieved by using design M_r value of raw V-soil for both stabilized and natural subgrade layers. In Case 2, analysis was conducted after reducing the thickness of AC layer by 50%, whereas for Case 3 thickness of stabilized layer was reduced by 50%. Case 4 consists of AC layer with a M_r value of

1,723 MPa which is approximately 50% of the M_r value of 10% CKD-stabilized V-soil. Cases 5 (6% lime-stabilized layer), 6 (10% CFA-stabilized layer) and 7 (10% CKD-stabilized layer) were evaluated to demonstrate the effect of stabilized subgrade layer moduli on critical stresses. Following discussion can be drawn from the critical responses calculated by using KENLAYER and presented in Table 6.1:

1. Case 1 indicates that the critical tensile stresses are present only at the bottom of AC layer. However, a comparison of Cases 5, 6, and 7 with Case 1 reveals increase in tensile stresses with increase in the M_r value of stabilized subgrade layer. For example, an increase in M_r value by 1,978% (10% CKD) induced tensile stresses of approximately 372 kPa (54 psi) at the bottom of stabilized subgrade layer. Also, decrease in tensile stresses at the bottom of AC layer by 85% is evident from Table 6.1.
2. A comparison of Case 3 with Case 7 indicates that decrease in stabilized subgrade layer thickness by 50% causes approximately 59% increase in tensile stresses at the bottom of stabilized subgrade layer. However, the tensile stresses at the bottom of AC layer also increases by approximately 108%.
3. A comparison of Cases 2 and 4 with Case 7 shows disappearance of tensile stresses at the bottom of AC layer (positive stresses). On the other hand, an increase in tensile stress at the bottom of stabilized subgrade by a factor of 63% and 16% was observed for Case 2 and 4 with respect to Case 7, respectively.
4. It is also interesting to note that the maximum tensile stress of 605 kPa (88 psi) is generated at the bottom of stabilized subgrade layer for Case 2. This tensile stress

value is higher than the indirect tensile strength and modulus of rupture values of 6% lime-, 10% CFA- and 10% CKD-stabilized V-soil specimens, as presented later.

From above discussion, it is clear that the presence of thin AC layers in combination with stabilized subgrade layer having high M_r values generates critical tensile stresses at the bottom of stabilized subgrade layer. As the pavement is subjected to repeating loading, stabilized subgrade layer experiences fatigue-induced cracking which may accelerate to surface in the form of reflective cracking (Adaska and Luhr, 2004; Lav et al., 2006; Molenaar and Pu, 2008; Agostinacchio et al., 2008; Saxena et al., 2010; Prozzi and Aguiar-Moya, 2010).

Consequently, the primary objective of the study presented herein is to evaluate engineering properties, namely, flexural strength (or modulus of rupture), flexural stiffness (M_{rf}) and fatigue life of selected soils stabilized with different cementitious additives namely, 6% lime, 10% CFA and 10% CKD. However, due to difficulties associated with preparing and handling of a beam specimen, indirect tensile strength and resilient modulus in indirect tension (M_{rt}) on cylindrical specimens are also evaluated, as a possible alternative to the flexural beam test.

It is important to note that the potential of reflection of stabilized subgrade cracks through asphalt surface could be minimized by reducing crack size through the use of "pre-cracking" (Scullion, 2002; Guthrie et al., 2002; Adaska and Luhr, 2004), and relief of stress concentrations through the use of aggregate bases and geosynthetic layers (Adaska and Luhr, 2004; Luo and Prozzi, 2008) in the pavement structure. Also, the actual stresses and strains measured in the field will be different than the responses calculated using KENLAYER (Solanki et al., 2009c). This difference between the

measured and calculated responses could be attributed to the major assumptions of the layered elastic theory used by KENLAYER. The major assumptions of the layered elastic theory are the following (Huang, 2004; Loulizi et al., 2006): (1) each layer is assumed homogeneous, isotropic, and linear elastic; (2) all materials are weightless (no inertia effect is considered); (3) all layers are assumed to be infinite in lateral extent and layer interfaces are assumed to be completely bonded; (4) all layers have a finite thickness except for the subgrade, which is assumed to be infinite; (5) pavement systems are loaded statically over a uniform circular area; and (6) the compatibility of strains and stresses is assumed to be satisfied at all layer interfaces.

6.2 Previous Studies

As noted in Section 6.1, cementitiously stabilized subgrade layer is subjected to tensile stresses and strains under applied traffic loads. Therefore, tensile properties are typically required for design purposes. The direct tension test is generally believed to provide a more accurate measure of tensile characteristics. However, the primary disadvantage with the direct tension test is that no standard test has been adopted by ASTM or AASHTO to provide a direct measurement of the tensile strength of cementitiously stabilized materials because the means of holding the specimens create secondary stresses that influence the test results. Thus, the test results are difficult to reproduce (Arellano and Thompson, 1998). The splitting tension and the flexural test are the two primary types of indirect tension modes utilized to characterize tensile behavior. The following section details the findings from previous studies conducted for characterizing cementitiously stabilized materials in indirect tensile or fatigue modes.

6.2.1 Indirect Tensile Characteristics

Only a few studies are available in the literature which evaluated indirect tensile characteristics of cementitiously stabilized materials (Table 6.2). These studies are either limited to one type of additive (e.g., Mohammad et al., 2000; Khattak and Alrashidi, 2006) or applicable for stabilized aggregate base courses (e.g., White and Gnanendran, 2005; Gnanendran and Piratheepan, 2008).

In his earlier study, Raad (1976) demonstrated that the tensile strengths from the indirect tensile strength test and the direct tension test are about equal. The validity of analysis was subsequently demonstrated through comparisons of direct tension and indirect tensile strength tests. In another study, Raad (1988) explained the difference of modulus in tension and compression (i.e., bimodular properties) and the practical significance of bimodular behavior in response prediction and fracture of stabilized layers. It was found that the tensile modulus for a given applied stress is lower than the compressive modulus. Also, tensile modulus was found much greater (2.6 to 11.6 times) than the flexural modulus obtained from central beam deflections. The bimodular ratio (modulus in compression/modulus in tension) was found to be stress dependent and increased in general for stress ratio (applied stress/ultimate strength) greater than 80%.

In a laboratory study, Mohammad et al. (2000) evaluated indirect tensile characteristics of soil-cement mixtures used in the construction of soil base courses for test lanes at the Louisiana Pavement Testing Facilities. The soil used in the mixtures was silty clay (A-4) with a plasticity index of 22. The indirect tensile characterization test matrix included indirect tensile strength and indirect tensile resilient modulus tests on cylindrical specimens having 102 mm diameter (4 in) and 64 mm (2.5 in) height. It was

found that increase in compaction effort and curing period significantly increased the indirect tensile strength. Also, decrease in cement content significantly reduced the indirect tensile strength and M_{rt}.

Sobhan and Mashnad (2003a) evaluated indirect tensile strength of recycled aggregates stabilized with Portland cement, fly ash and high density polyethylene (HDPL) fibers. Twenty-one different mixture designs were utilized to test cylindrical specimens in indirect tension. The mixture proportions included 4 – 8% cement, 4 – 8% fly ash, 0.25 – 1.25% waste HDPE strips, and 84 – 92% recycled aggregate. It was found that inclusion of 0.5% of plastic strips to this mixture significantly improved the post peak load-bearing capacity or toughness of the specimens in indirect tension mode. The toughness was determined by calculating the total areas under the load deformation curves.

In a study from Australia, White and Gnanendran (2005) evaluated effect of compaction methods and density on the indirect tensile strength and M_{rt}. Two host materials, namely, reclaimed material from the base of an existing road pavement, and new quarried crushed rock stabilized with slag-lime were investigated. Specimens were compacted by using standard Proctor as well as gyratory compaction methods. It was found that the influence of compaction method on indirect tensile strength and M_{rt} is not significant.

In a recent study, Gnanendran and Piratheepan (2008) characterized lightly stabilized granular material by indirect tensile testing. The material selected for this research was a freshly quarried granular base material (sandy gravel with some fines) which was stabilized with slag-lime. The cylindrical specimens were prepared by using

gyratory compaction method and cured in a humidity room. After 28 days, specimens were tested for indirect tensile strength and M_{rt}. It was found that the addition of slag-lime is effective in enhancing the indirect tensile strength. For example, the strength value increased by approximately 50% when the slag-lime content was increased from 3 to 4%. The M_{rt} was found to increase approximately linearly with the amount of slag-lime, density and indirect tensile strength.

6.2.2 Flexure Characteristics

The flexural characteristics of cementitiously stabilized materials have been studied in terms of radius of curvature, flexural stiffness, modulus of rupture, and fatigue life. One of the earliest studies of the flexural characteristics of lime- and cement-stabilized soil was conducted by Laguros (1965). The Winkler model was used to provide the approximation for stabilized beams resting on natural subgrade. This model required evaluation of modulus of rupture of stabilized beams. In this study, however, no laboratory tests were performed for evaluating the fatigue life and flexural strength of stabilized soil specimens.

In another early study, Larsen and Nussbaum (1967) attempted to duplicate pavement loading conditions by testing cement-stabilized soil beams supported on a simulated subgrade composed of neoprene pads. Varying the number of pads simulated variations in subgrade support. A total of one fine-grained and two coarse-grained soils were used for preparing beams. The following fatigue model based on radius of curvature of the loaded beam as the basic response was used to characterize the observed behavior:

$$R_c/R_i = a\, N_f^{-b} \qquad (6.1)$$

where, R_c = critical radius of curvature, the radius of curvature that would cause failure due to a single load application, R_i = the initial radius of curvature of the test beam under the fatigue loading, N_f = number of load applications to failure, and a, b = fatigue factors determined from the tests. It is important to note that the failure was defined as the development of a visible crack. Also, no affect of subgrade strength on flexural characteristics demonstrated need of more fundamental models based on stress or strain levels.

Raad (1985) conducted flexural tests on cement-stabilized silty clay specimens. Cylindrical specimens (diameter = 101.6 mm, i.e., 4 in; height = 76.2 mm, i.e., 3 in) and beam specimens 533 mm x 152 mm x 152 mm (21 in x 6 in x 6 in) were prepared using a drop hammer compactor. All the specimens were tested after curing for 42 days in a humidity room. However, this study was limited to only one soil and one additive. No attempt was made to evaluate the flexural characteristics of soils stabilized with additives commonly used in Oklahoma, namely, lime, CFA and CKD.

Bhattacharya and Pandey (1986) stabilized laterite soil with lime to evaluate the flexural strengths and fatigue life. Tests were carried out on four types of stabilized laterite soil beams compacted at three dry density ranges – light, medium, and heavy. The beams were subjected to rate of loading of 1.83 Hz (110 cycles/min) with a cycle length of 0.54 sec and the distribution of loading to unloading time adjusted to 1:1. It was reported that the fatigue resistance of lime-laterite soils is increased to a considerable extent at the higher dry density. Heavily compacted materials can be subjected to almost twice the flexural stresses as compared with the lightly compacted beams for the same number of repetitions of failure.

In another study by Laguros and Keshawarz (1987), the effectiveness of shale stabilization with cement (14%), quicklime (4.5%), fly ash (25%) and a mixture of 8% cement + 3% quicklime + 18% fly ash was evaluated under flexural loads. Beam specimens 406 mm x 101 mm x 76 mm (16 in x 4 in x 3 in) were molded, cured and tested under the third point beam loading configuration. An increase in modulus of rupture and modulus of elasticity in flexure due to stabilization was reported.

In the laboratory, two types of controlled loading are generally applied for flexural characterization: constant stress (load) and constant strain (deformation). In constant stress testing, the applied stress during the fatigue testing remains constant. As the repetitive load causes damage in the test specimen, the stiffness of the specimen is decreased while tensile strain is increased (El-Basyouny and Witczak, 2005). In the constant strain test, however, the strain remains constant with the number of repetitions. Because of specimen damage due to repetitive loading, the stress is reduced leading decreased stiffness. The constant stress type of loading is generally considered applicable to thick asphalt pavements (> 200 mm, i.e., 8 in). On the other hand, the constant strain type of loading is considered more applicable to thin asphalt pavement layers (El-Basyouny and Witczak, 2005).

In the literature, both stress- and strain-based model are available for cementitiously stabilized layers. A summary of such stress- and strain-based models is provided in Table 6.3. Thompson (1986, 1994) used a stress-based model which was later adopted by Illinois Department of Transportation for pavement designs. The relationship which shows the stress ratio (applied stress/ultimate strength) as a function of the number of loading cycles to failure is represented by the following equation:

$$log(N_f) = (0.9722 - S)/0.0825 \quad (6.2)$$

where, S = stress ratio (applied flexural stress/modulus of rupture).

Sobhan and Mashnad (2003a) evaluated the improvement in flexural strength and fatigue life due to the addition of HDPE fibers to recycled aggregates and Portland cement, with or without fly ash. Beam specimens 762 mm x 152 mm x 152 mm (30 in x 6 in x 6 in) were prepared by compacting the mix in detachable steel molds in three equal layers. The compacted beams were cured for 28 days and tested in a third-point loading configuration for modulus of rupture and fatigue life. It was reported that aggregates stabilized with cement and fly ash could develop adequate strength to serve as a high quality base course material. Additionally, the following relationship between the stress ratio and number of loading cycles to failure (or fatigue life) was reported:

$$S = - 0.038\ ln(N_f) + 1.047 \quad (6.3)$$

Mallela et al. (2004) and AASHTO (2004) also identified 28-day flexural strength as one of the important pavement performance parameters for stabilized materials. According to AASHTO (2004), the stabilized layer must resist flexural and tensile stresses to prevent the occurrence of fatigue cracks. Thus, its fatigue strength needs to be considered. In such instances, the number of allowable load applications is calculated in accordance with the following equation, also known as '*transfer function*':

$$log(N_f) = (k_1\beta_1 - S)/ k_2\beta_2 \quad (6.4)$$

or, $$log(N_f) = (a_1 - S)/ a_2 \quad (6.5)$$

where, k_1, k_2 = global calibration factors, β_1, β_2 = local calibration factors, and a_1, a_2 = constants.

Lav et al. (2006) also recognized fatigue cracking as the primary mode of failure of stabilized materials in which cracks initiate due to the repeated tensile stresses. Mixtures of class F fly ash with different percentages of cement (2%, 4%, 8%, and 10%) were used as stabilized base material. Utilizing accelerated full scale road test data for the fatigue performance of mixtures and performing a mechanistic-empirical design procedure, required layer thickness for different lives were obtained for different amount of cement content. It was reported that cement content is the most important parameter controlling the design life (fatigue performance) of stabilized layers. Also, fatigue performance of stabilized fly ash was established using the following relationship:

$$N_f = (a/\mu\varepsilon)^b \quad (6.6)$$

where, $\mu\varepsilon$ = maximum value of the initial tensile strain (microstrain), and a, b = regression coefficients.

In another study by Sobhan and Das (2007), flexural characteristics were evaluated by testing stabilized beam specimens under a constant stress mode. A total of three different mixes containing different percentages of recycled aggregates, cement and fly ash were used. Eight prismatic beam specimens with dimensions of 762 mm x 152 mm x 152 mm (30 in x 6 in x 6 in) were prepared for the flexural fatigue tests. It was found that the fatigue endurance limit of stabilized recycled aggregate is comparable to concrete and other traditional stabilized materials. Also, a best-fit curve through the data for stabilized beams tested for fatigue life gave following relationship:

$$S = -0.038 \ln(N_f) + 1.08 \quad (6.7)$$

In a study from Europe, Molenaar and Pu (2008) developed a field fatigue relationship for sand cement treated bases which are often used in the Netherlands. The

relationship was obtained by an extensive analysis of the Strategic Highway Research Program-Netherlands (SHRP-NL) data base which contained performance data of a number of pavements with a cement treated base. The following equation for the prediction of the fatigue life of cement treated base course materials was proposed:

$$log(N) = 8.5 - 0.034\varepsilon \quad (6.8)$$

where, N = allowable number of 100 kN equivalent single axles, and ε = tensile strain at the bottom of the cement treated base due to a 50 kN falling weight load (µm/m). Also, an endurance limit for cement treated bases was developed. In case of good load transfer across transverse cracks is guaranteed, a strain value of 50 µm/m can be taken as such a limit. In case the load transfer across cracks must be assumed to be poor, this limit is 41 µm/m.

It is also important to note that the flexural test better simulates the mode of stress to which a pavement layer is subjected by wheel loading (Arellano and Thompson, 1998). However, because elastic behavior does not occur up to failure, the tensile strength (i.e., modulus of rupture) obtained by the flexural test is higher than the values obtained from direct tension tests (Williams, 1986; Arellano and Thompson, 1998).

6.3 Soils and Additives

The two soils: (1) Port series soil (P-soil) and (2) Vernon series soil (V-soil), were used to evaluate the indirect tensile and fatigue characteristics. Their properties are presented in Section 2.3.1, Chapter 2. P-soil is classified as silty clay with sand (CL-ML) while V-soil is classified as lean clay (CL) in accordance with USCS. Also, 6% hydrated lime, 10% class C fly ash (CFA) and 10% cement kiln dust (CKD) were used as

cementitious additives. Their properties are presented in Section 2.3.2, and summarized in Table 2.4.

6.4 Testing Plan and Details

As noted earlier, the performance tests conducted in this study included tensile strength and resilient modulus in indirect tension for indirect tensile characteristics. On the other hand, flexural strength (or modulus of rupture) and fatigue life tests were performed for evaluating characteristics of stabilized soil specimens in flexure. All the aforementioned tests except fatigue tests were conducted on two replicate specimens for each of the eight soil-additive mixtures (raw P-soil, P-soil + 6% lime, P-soil + 10% CFA, P-soil + 10% CKD, raw V-soil, V-soil + 6% lime, V-soil + 10% CFA, V-soil + 10% CKD) evaluated in this study. Fatigue tests were conducted only on P- and V-soil beams stabilized with 6% lime and 10% CKD.

6.4.1 Specimen Preparation

The specimens were prepared in a rather unique manner for this study. For indirect tensile strength and M_{rt}, cylindrical specimens having diameter of 101.6 mm (4 in) and 63.5 mm (2.5 in) were compacted using the Superpave gyratory compactor in a single lift. The weight of soil-additive-water mixture used for compaction was selected to achieve near OMC and MDD, as discussed in Section 2.5 (Tables 2.6 and 2.8). After compaction, specimens were extruded and covered with latex membranes for avoiding any moisture loss. Compacted specimens were cured for 28 days in a controlled environment as discussed in Section 2.5. A total of 32 cylindrical specimens were

prepared, of which 16 were tested for indirect tensile strength, and the remaining 16 for M_{rt}.

A new laboratory procedure was employed in molding the beam specimens (length = 381 mm i.e., 15 in; width = 63.5 mm i.e., 2.5 in; height = 50.8 mm i.e., 2 in) for determining flexural characteristics. The procedure consisted of the following steps: (1) adding specified amount of additive (6% for lime, 10% for CFA and CKD of dry weight of soil) and mixing thoroughly with the raw soil; (2) adding half of the required water based on OMC (Tables 2.6 and 2.8) to the soil-additive mixture and mixing thoroughly; (3) adding the remaining water and mixing thoroughly until a uniform mixture was achieved. The resulting mixture was weighed for required amount to achieve near MDD and additional mixture was discarded. A split compaction mold assembly was designed and fabricated for compaction (see Figure 6.2a). The mold assembly consists of four parts namely, Part A, Part B, Part C and Part D, as shown in Figures 6.2 (a) and (b). Part A (406.4 mm x 152.4 mm x 3.6 mm, i.e., 16 in x 6 in x 1/7 in) is the bottom rectangular plate and is used to lift the beam once it is extracted from the mold. Parts B (406.4 mm x 88.9 mm x 158.75 mm, i.e., 16 in x 3.5 in x 6.25 in) and C (152.4 mm x 63.5 mm x 25.4 mm, i.e., 6 in x 2.5 in x 1 in) are hollow and solid plates, respectively, used for supporting the specimen. Part D (381 mm x 63.5 mm x 107.95 mm, i.e., 15 in x 2.5 in x 4.25 in) is a hollow plate which is pressed inside the mold for preparing the specimen. All the four parts were covered with plastic wrap on the facing exposed to the specimen and placed inside the main mold assembly of Linear Kneading Compactor, as shown in Figure 6.3. It is important to note that according to ASTM C 192 for concrete, the minimum cross-sectional dimension of a rectangular section shall be at least three times

the nominal maximum size of the coarse aggregate in the concrete for minimizing size effect. For the soils used in the study, the nominal maximum size of coarsest particle is less than 4.75 mm (0.18 in). Hence, the minimum cross-sectional dimension of 63.5 mm (2.5 in) of beam specimen is justified.

Each beam specimen was compacted in a single lift. Soil-additive-water mixture was poured and compacted in the mold by applying a pressure ranging between 3,445 – 4,823 kPa (500 – 700 psi) using the hydraulic cylindrical arm until the compacted height of beam was 50.8 mm (2 in), as shown in Figure 6.3. The average time for preparing a beam specimen varied between 45 and 60 minutes. Following the compaction process, each specimen was wrapped carefully with a plastic wrap and placed in a controlled environment of temperature 23.0 ± 1.7^{o}C (73.4 ± 3.1^{o}F) and a relative humidity of approximately 96% for 28 days. A total of 24 beams were prepared, of which 16 were tested for modulus of rupture, and the remaining 8 for fatigue life. In fact, the actual test matrix included a number of exploratory fatigue tests in addition to the 8 tests. For example, some of the beams were tested at lower (< 300) or higher (> 600) microstrain level. But those results were not reported in this study because beams either failed within few cycles (< 5) or didn't fail at all in 2 million cycles. No fatigue life test was conducted on raw and 10% CFA-stabilized P- and V-soil beam specimens.

6.4.2 Indirect Resilient Modulus and Tensile Strength Tests

The test procedure for M_{rt} consisted of applying six stress sequences, as listed in Table 6.4. Each test sequence consisted of a haversine-shaped load pulse having a duration of 0.1 second and a rest period of 0.9 second. A Material Testing System (MTS) electro-hydraulic test system was used to load the specimen. The load-deformation

response was recorded for the last 5 cycles of each stress sequence by using a computer controlled FlexTest SE Test Controller, as discussed in Section 2.6.1 (see Figure 2.3). A 22.2 kN (5,000 lbs) load cell was used for applying load on the specimens, as shown in Figure 6.4. The vertical and horizontal deformations were measured by two LVDTs having a stroke length of 2.54 mm (0.1 in), attached in the diametrically perpendicular direction of one face of the specimen, as shown in Figure 6.4. A closer look of specimens with LVDTs is shown in Figure 6.5. As evident from Figure 6.5, specially prepared brass rods with pin on one end were prepared. To keep the rods stable on the specimen's wet surface, instant Krazy glue was applied on the end with pin and inserted inside the specimen. A gauge length of approximately 71 mm (2.8 in) was used to mount the LVDTs on one face of the specimen, as shown in Figure 6.5.

A set of four specimens were prepared for each soil-additive mixture. Two specimens were tested for indirect tensile strength without any LVDTs by loading them at a deformation rate of 50.8 mm/min (2 in/min) in accordance with ASTM D 6931 test method. The other two specimens were tested for M_{rt} by applying different stress levels. The applied stress level for M_{rt} test was chosen according to the indirect tensile strength of the specimen of each set. A load corresponding to 0.20 stress ratio (applied stress/tensile strength) was used for the conditioning sequence. For the remaining five sequences, a starting load at the first sequence corresponding to 0.30 stress ratio was used and a 0.10 stress ratio increment in each subsequent sequence was applied. In order to make full contact between specimen and loading strip, 10% of the peak applied load was used as the seating load in each loading cycle. The M_{rt} for each sequence was calculated

from the average recoverable deformation and average load from last five cycles by using the following expression (Tarefder, 2003; Navratnarajah, 2006):

$$M_{rt} = \frac{2P}{\pi D t.\Delta H_T \left(D^2 + {D_g}^2\right)} \left\{ (3+\nu) D^2 D_g + (1-\nu) \left[{D_g}^3 - 2D\left(D^2 + {D_g}^2\right) \tan^{-1}\left(\frac{D_g}{D}\right) \right] \right\} \quad (6.9)$$

where, t = thickness of the specimen, P = repeated load, ΔH_T = total recoverable horizontal deformation, D = diameter of specimen, υ = Poisson's ratio, and D_g = distance between LVDTs measuring horizontal deformations. The value of Poisson's ratio was used as 0.2 consistent with the range of 0.1 – 0.3 reported by the new MEPDG (AASHTO, 2004).

6.4.3 Flexural Strength and Fatigue Life Tests

As noted in Section 6.2.2, there is no widely accepted laboratory test procedure to determine the flexural strength and fatigue life of cementitiously stabilized beam specimens. In the present study, beams were tested for flexural strength and fatigue life under four-point loading inside a beam fatigue apparatus in accordance with AASHTO T 321 test method (Figure 6.6). The advantage of using four-point fatigue apparatus is that it produces a constant bending moment over the center third span between the H-frame contact points on the beam specimen (ASTM D 7460). This apparatus also allows free rotation and translation at all load and reaction points, as shown in Figure 6.6.

To evaluate the modulus of rupture, flexural strength was performed by subjecting specimens to vertical displacement control loading rate of 1.27 mm/min (0.05 in/min) in accordance with ASTM D 1635 test method. This loading rate produced a tensile stain of approximately 2300 microstrain at the bottom of beam specimens. Deformation values were recorded during the test using LVDTs having a maximum stroke length of 5.0 mm

(127 mm). The tip of the LVDT was supported on the aluminum target glued at the center of the neural axis of the beam, as shown in Figure 6.7 (a). The load values were obtained from a load cell having a capacity of 2.23 kN (500 lb). The modulus of rupture was calculated from failure load by using the following expression:

$$MOR = \frac{PL}{bh^2} \tag{6.10}$$

where, MOR = modulus of rupture, P = failure load, L = length of the beam between supports (35.56 mm, i.e., 14 in), b = average width of beam specimen, and h = average height of beam specimen.

The fatigue life tests consist of applying a repeated constant vertical strain to a beam specimen in flexural tension mode until failure or up to a specified number of load cycles. In this test, the input strain was sinusoidal shaped, applied at a frequency of 5 Hz in accordance with AASHTO T 321 test method for asphalt concrete specimens. The test was conducted at a strain level of approximately 500 microstrain (deflection of approximately 0.27 mm, i.e., 0.01 in) consistent with the AASHTO T 321 and ASTM D 7460 test method recommendations for conventional asphalt concrete. Although Table 6.1 showed a strain level ranging between 150 and 300 microstrain at the bottom of stabilized subgrade layer, a higher strain level was selected to reduce the test time while at the same time capturing sufficient data for analysis. Failure is assumed to occur when the stiffness reached half of its initial value, which is determined from the load at 50^{th} cycle. The fatigue life (N_f) is the total number of load repetitions that cause a 50 percent decrease in initial stiffness (AASHTO T 321). The test is terminated manually when the initial stiffness has diminished by 50 percent or when a preset number of load cycles

(2,000,000) is reached. The flexural stress, strain and stiffness of beams were determined by using the following expressions (AASHTO T 321):

$$\sigma_f = \frac{3aP}{bh^2} \tag{6.11}$$

$$\varepsilon_f = \frac{12\delta h}{\left(3L^2 - 4a^2\right)} \tag{6.12}$$

$$M_{rf} = \frac{\sigma_f}{\varepsilon_t} = \frac{aP\left(3L^2 - 4a^2\right)}{4b\delta h^3} \tag{6.13}$$

where, σ_f = tensile stress at the bottom of beam, ε_t = tensile strain at the bottom of beam, M_{rt} = flexural stiffness, P = applied peak load, a = spacing between inside clamps (119 mm, i.e., 4.69 in), b = average beam width, h = average beam height, δ = beam deflection in neutral axis, L = length of beam between outside clamps or supports (35.56 mm, i.e., 14 in). The duration of fatigue test ranged between 1 and 110 hours (approximately 4 days and 14 hours). Hence, each beam specimen was covered with a plastic wrap before placing inside the beam fatigue apparatus to avoid any moisture loss due to exposure of specimen to open environment for extended period of time (Figure 6.7b). Figure 6.7 (c) shows photographic view of a typical beam specimen after failure.

6.5 Presentation and Discussion of Results

6.5.1 Resilient Modulus in Indirect Tension

The variations of M_{rt} values with the stress ratio are presented in Tables 6.5 and 6.6 for specimens prepared by using P- and V-soil, respectively. It is clear that the M_{rt} values increased due to stabilization. This increase, however, depends on the type of additive and soil. For example, at a stress ratio of 0.36, 6 % lime, 10% CFA and 10%

CKD provided an increase of approximately 1,066%, 649% and 1726% with P-soil (CL-ML), respectively. On the other hand, an increase of approximately 1,071%, 1,322% and 1,451% was observed for V-soil (CL) specimens stabilized with 6% lime, 10% CFA and 10% CKD, respectively, at a stress ratio of 0.36. Overall, CKD provided the highest M_{rt} values ranging between 776 – 1,673 MPa (113 – 243 ksi) for P-soil and 641 – 915 MPa (93 – 133 ksi) for V-soil. In the case of CKD-stabilized specimens, the current test results are similar to those reported by Mohammad et al. (2000) and Khattak and Alrashidi (2006) for 28-day cured Portland cement-stabilized specimens. For example, Mohammad et al. (2000) reported M_{rt} values ranging between approximately 1,000 and 2,000 MPa (145 – 290 ksi) for 28-day cured Portland cement-stabilized specimens of CL-ML soil. The M_{rt} studies on lime- and CFA-stabilized specimens were not available or reported in the literature and, hence, no comparison related assessments were made.

The variation of M_{rt} with the stress ratio is graphically illustrated in Figure 6.8. As depicted in these figures, the M_{rt} value decreased with the stress ratio. This behavior is consistent for all the soil-additive mixtures tested in this study. For example, the M_{rt} value of P-soil specimen stabilized with 6% lime exhibited a decrease from approximately 908 MPa (132 ksi) to 443 MPa (64 ksi) as the stress ratio increased from 0.27 to 0.63. It is also clear from Figure 6.8 that the amount of decrease in M_{rt} with increase in stress ratio is dependent on soil and additive properties. For example, an increase of stress ratio from 0.27 to 0.63 reduced the M_{rt} value by approximately 51%, 52% and 54% for P-soil specimens stabilized with 6% lime, 10% CFA and 10% CKD, respectively. For a similar change in stress ratio, V-soil specimens stabilized with 6% lime, 10% CFA and 10% CKD exhibited a decrease in M_{rt} values by approximately 36%,

31% and 30%, respectively. Hence, it can be concluded that stabilized P-soil specimens were more sensitive towards change in stress level as compared to stabilized specimens prepared by using V-soil.

Further, resilient modulus values of specimens in compression and tension mode were plotted on same graphs for comparison. Figures 6.9 and 6.10 illustrate the variation of M_{rt} and M_r with deviatoric stress for P- and V-soil specimens, respectively. It should be noted that specimens discussed in Section 2.6.1 were subjected to additional five sequences (σ_3 = 0 kPa; σ_d = 12, 25, 37, 50, 62 kPa, i.e., 1.8, 3.6, 5.4, 7.2, 9 psi) after first 15 sequences. The M_r values calculated from the aforementioned additional data was used for comparison with M_{rt}. It is clear from Figures 6.9 and 6.10 that the magnitude of M_r is higher than the M_{rt} values at similar deviatoric stress levels. For example, at a σ_d of 50 kPa (7.2 psi), the M_{rt} values of 6% lime-, 10% CFA- and 10% CKD-stabilized P-soil specimens were approximately 38%, 30% and 2% lower, respectively, with respect to M_r values of corresponding specimens. For V-soil specimens (σ_d = 50 kPa, i.e. 7.2 psi), however, 6% lime, 10% CFA and 10% CKD exhibited M_{rt} values approximately 22%, 24% and 45% lower with respect to M_r values of corresponding specimens, respectively. The lower resilient modulus values in tension than it is in compression is consistent with the studies conducted by other researchers on cementitiously stabilized materials (see e.g., Raad, 1976; Das and Dass, 1995). For example, Das and Dass (1995) reported that the M_{rt} ranges in the order of 1.0 – 0.6 times of M_r for sand stabilized with Portland cement.

6.5.2 Indirect Tensile Strength and Modulus of Rupture

The maximum indirect tensile strength (σ_t) of the raw and stabilized specimens from monotonic loading in indirect tension was calculated according to the following elastic theory solution (ASTM D 6931):

$$\sigma_t = \frac{2P}{\pi D t} \tag{6.15}$$

Figure 6.11 illustrates the variation of indirect tensile strength of P- and V-soil specimens with different type of additives. It is evident that for both P- and V-soil specimens, 10% CKD provided highest increase in tensile strength values followed by 10% CFA and 6% lime. For example, the tensile strength values of P-soil specimens stabilized with 10% CKD is approximately 835% higher than the corresponding indirect tensile strength of raw P-soil specimens. The corresponding percentage increase is 288% and 406% for 6% lime- and 10% CFA-stabilized specimens, respectively.

A summary of the MOR values along with the standard deviation and coefficient of variation is presented in Table 6.7. It can be observed that the MOR improved with the addition of additives. The average MOR value of P-soil specimens increased by approximately 76%, 137% and 333% with the addition of 6% lime, 10% CFA and 10% CKD, respectively. Similarly, V-soil specimens stabilized with 6% lime. 10% CFA and 10% CKD showed an increase by approximately 166%, 181% and 203%, respectively. These observations are consistent with the earlier observations of UCS and σ_t where 10% CKD provided highest enhancements with both P- and V-soil specimens.

To compare the tensile and flexural behavior with compressive strength, variation of MOR and σ_t with UCS of corresponding specimens were plotted on the same graph (Figure 6.12). It is evident that for both P- and V-soil specimens, UCS was consistently

higher followed by MOR and σ_t values. For example, P-soil specimens stabilized with 6% lime provided a UCS, MOR and σ_t value of 392, 187 and 66 kPa (i.e., 57, 27 and 10 psi), respectively. These results are consistent with the observations made by Arellano and Thompson (1998) and Sobhan and Mashnad (2003b). The best-fit curve through all points can be represented by the following equations:

$$\sigma_t = 0.16\ UCS \qquad (R^2 = 0.93) \tag{6.16}$$

$$MOR = 0.41\ UCS \qquad (R^2 = 0.84) \tag{6.17}$$

The R^2 value associated with Eqns. 6.16 and 6.17 is comparatively high at 0.93 and 0.84, respectively. Thus, a strong correlation exists between UCS values and σ_t or MOR values. According to above correlations, indirect tensile strength can be estimated as approximately 16% of UCS. On the other hand, MOR is approximately 41% of UCS. Based on the literature, the σ_t is generally about 10 to 15 percent of the UCS and the MOR is about 20 to 25 percent of the compressive strength (Kennedy et al., 1971; Little, 1995; Sobhan and Mashnad, 2003a). In the current study, σ_t versus UCS correlation is similar to previous studies. However, correlation between MOR and UCS values over-predict the MOR values. This could be attributed to the fact that the previous MOR versus UCS correlations (Little, 1995) were developed by evaluating MOR values in a three-point loading mode. Based on theory of elasticity, three-point loading on a beam specimen (ASTM C 78) develops a bending stress 1.5 times higher than the bending stress developed in four-point loading mode (ASTM C 293; Hibbeler, 2008). Thus, higher MOR values for a four-point loading configuration are expected. Also, higher MOR values with respect to σ_t values of corresponding specimens can be explained by the fact that the flexure formula assumes that the stress varies linearly across the cross-

section of the beam. However, cementitiously stabilized beams have a nonlinear stress-strain curve. Additionally, a relatively small volume of the specimen near the bottom of the beam is stressed under flexure.

6.5.3 Flexural Stiffness and Fatigue Life

Testing data were analyzed using Eqns. 6.11 – 6.13 presented earlier to compute the stress, strain and flexural stiffness per cycle as the function of the number of load cycles. In this study, fatigue life was defined as the number of repeated cycles corresponding to a 50 percent reduction in initial stiffness, which was measured at the 50^{th} load cycle. Figure 6.13 illustrates flexural stiffness (M_{rf}) which was computed at various cycles from the raw data of stabilized P- and V-soil specimens. It can be seen that the M_{rf} decreases as the number of cycles increases. That is, at the same strain level, a greater stress is needed to reach the desired strain values at the beginning of fatigue test than at the end of the test.

The initial M_{rf} values and number of cycles to failure (N_f) of fatigue beams determined by initial tensile stress and strain, are presented in Table 6.8. It is clear that the M_{rf} values of stabilized specimens are strongly associated with type of additive, the beams stabilized with 10% CKD exhibited a greater initial stiffness value, but its stiffness reduces more rapidly than 6% lime-stabilized beams under repeated load. The average M_{rf} of P-soil specimens stabilized with 6% lime and 10% CKD were 563 MPa (81,713 psi) and 1,056 MPa (153,266 psi), respectively. The set#2 beam of 10% CKD-stabilized P-soil showed very low (47%) initial M_{rf} as compared to corresponding beam of set#1 because the beam in set#1 failed in less than 50 cycles. On the other hand, the average M_{rf} of 6% lime- and 10% CKD-stabilized V-soil specimens showed an initial average M_{rf}

value of 801 MPa (116,255 psi) and 990 MPa (143,687 psi), respectively. It is clear that 10% CKD provided higher initial M_{rf} values (88% for P-soil and 24% for V-soil) as compared to 6% lime.

Table 6.8 shows that the mean fatigue life of P-soil beams stabilized with 6% lime is greater than 2 million cycles. On the other hand, beams of P-soil stabilized with 6% lime failed at a relatively low N_f value (approximately 50). The 6% lime- and 10% CKD-stabilized beams of V-soil exhibited mean fatigue life of 1,430,000 and 965,000, respectively. The standard deviations of the fatigue test results for each soil-additive mixture are large since the variability of fatigue life is generally based upon the microstructure of beams (e.g., the soil-additive interface, moisture and void size distribution, distribution of cementitious products). Similar behavior has been reported by other researchers for the recycled asphalt concrete beam specimens (Xiao, 2006).

Attempts were made to develop the strain-based model (or transfer function) for predicting fatigue life of cementitiously stabilized beams using the limited fatigue data; Figure 6.14 was plotted between $\log(N_f)$ and strain ratio (tensile strain at bottom of beam/maximum tensile strain at bottom of beam from flexural strength test, $\varepsilon_t/\varepsilon_m$) in this regard. The best-fit curve through all points (except P-soil + 10% CKD due to high standard deviation) can be represented by the following equations:

$$log(N_f) = -0.68\ (\varepsilon_t/\varepsilon_m) + 6.55 \qquad (R^2 = 0.69) \qquad (6.18)$$

Although the R^2 value associated with Eqn. 6.18 is high ($R^2 = 0.69$), it is based only on four data points. Hence, to see the validity of above equation, N_f values were predicted from another recent strain-based model proposed by Prozzi and Aguiar-Moya (2010) for cementitiously stabilized materials (see Table 6.3). It is clear from Figure 6.14

that the experimental fatigue life and predicted N_f values from Eqn. 6.18 and model proposed by Prozzi and Aguiar-Moya (2010) are very similar (difference < 10%) for 6% lime- and 10% CKD-stabilized V-soil specimens. However, a considerable percent difference (> 50%) exists between experimental fatigue life and predicted N_f values from Prozzi and Aguiar-Moya (2010) for P-soil specimens stabilized with 10% CKD. This could be attributed to the fact that P-soil specimens stabilized with 10% CKD failed at a very low number of cycles (< 100) with very high coefficient of variation (60%). The models developed by Prozzi and Aguiar-Moya (2010) and others (Table 6.3) are typically based on fatigue life greater than 10,000. Hence, lower reliability of Prozzi and Aguiar-Moya (2010) fatigue model is expected.

6.6 Conclusions

This study was undertaken to evaluate two soils namely, P-soil (silty clay) and V-soil (lean clay) from Oklahoma for the effect of type of additive on the indirect tensile and fatigue characteristics for critical performance prediction. Cylindrical specimens stabilized with 6% lime, 10% CFA and 10% CKD were molded using a Superpave gyratory compactor, cured for 28 days and subjected to different stress sequences in indirect tension mode to study the M_{rt}. On the other hand, 6% lime-, 10% CFA- and 10% CKD-stabilized beam specimens were compacted using a Linear Kneading Compactor and subjected to repeated cycles of reloading-unloading after 28 days of curing for evaluating fatigue life and flexural stiffness. Also, stabilized cylindrical and beam specimens were tested for indirect tensile strength and modulus of rupture, respectively. Based on the study presented in this chapter the following conclusions can be derived:

1. All the three additives improved the M_{rt}, σ_t and MOR values of P- and V-soil specimens; however, degree of improvement varied with the type of additive and soil.
2. The resilient modulus in tension ranged between approximately 443 – 908 MPa (64 – 132 ksi), 315 – 656 MPa (46 – 95 ksi) and 776 – 1,673 MPa (113 – 243 ksi), respectively, for 6% lime-, 10% CFA-, and 10% CKD-stabilized silty clay specimens. On the other hand, stabilization of lean clay with 6% lime, 10% CFA and 10% CKD provided M_{rt} values ranging between approximately 444 – 691 MPa (64 – 100 ksi), 580 – 839 MPa (84 – 122 ksi) and 641 – 915 MPa (93 – 133 ksi), respectively. Overall, CKD provided highest M_{rt} values with both silty (P-soil) and lean clay (V-soil).
3. The test results suggest that the M_{rt} depends on the applied load. Based on the test results, the M_{rt} decreased with increase in stress ratio.
4. The magnitude of resilient modulus in tension is lower than it is in compression, consistent with the studies conducted by other researchers on cementitiously stabilized materials.
5. For both silty clay and lean clay specimens, 10% CKD provided highest increase in tensile strength values followed by 10% CFA and 6% lime.
6. The average MOR value of silty clay specimens increased by approximately 76%, 137% and 333% with the addition of 6% lime, 10% CFA and 10% CKD, respectively. Similarly, lean clay specimens stabilized with 6% lime. 10% CFA and 10% CKD showed an increase by approximately 166%, 181% and 203%, respectively.

7. The range of MOR values (187 – 255 kPa, i.e., 27 – 37 psi) of lime-stabilized soil specimens is similar to the MOR value of 172 kPa (25 psi) recommended by MEPDG for lime-stabilized specimens. The MOR value of CFA- and CKD-stabilized specimens are approximately 50% lower than the recommended MOR value of 689 kPa (100 psi) for soil-cement by the new MEPDG.
8. Correlations developed between indirect tensile strength, MOR and UCS suggest that σ_t can be estimated as approximately 16% of UCS. On the other hand, MOR is approximately 41% of UCS.
9. The beams stabilized with 10% CKD exhibited greater initial stiffness value, but its stiffness reduces more rapidly than 6% lime-stabilized beams under repeated load.
10. Beam specimens stabilized with 10% CKD provided higher initial M_{rf} values (88% for P-soil and 24% for V-soil) as compared to 6% lime.
11. The fatigue life tests conducted on beam specimens showed that the mean fatigue life of silty clay (P-soil) beams stabilized with 6% lime is greater than 2 million cycles. On the other hand, beams of silty clay stabilized with 6% lime failed at a relatively low N_f value (approximately 50). The 6% lime- and 10% CKD-stabilized beams of lean clay (V-soil) exhibited mean fatigue life of 1,430,000 and 965,000, respectively.
12. A strain-based model was proposed for predicting fatigue life of cementitiously stabilized soil and comparisons were made with the existing model in the literature. This model could be refined using an enriched database.
13. Although CKD-stabilized specimens showed best performance in enhancing the indirect tensile characteristics (M_{rt}, σ_t) and MOR, worst performance was observed in the fatigue life tests.

Table 6.1 Effect of Stabilized Subgrade Layer (V-Soil) on Pavement Response by Using Linear Analysis (KENLAYER)

Location	Response	Case 1: $M_{r,SSG}$ = $M_{r,SG}$ = 82 MPa	Case 2: h_{AC} = 89 mm.; $M_{r,SSG}$ = 1,704 MPa	Case 3: h_{SSG} = 102 mm; $M_{r,SSG}$ = 1,704 MPa	Case 4 $M_{r,AC}$ = 1,723 MPa; $M_{r,SSG}$ = 1,704 MPa	Case 5: $M_{r,SSG}$ = 697 MPa (6% lime)	Case 6: $M_{r,SSG}$ = 632 MPa (10% CFA)	Case 7: $M_{r,SSG}$ = 1,704 MPa (10% CKD)
Bottom of AC	σ_r (kPa)	-1834	50	-567	53	-800	-859	-272
	ε_t (µm/m)	-357	-63	-135	-75	-179	-189	-90
Top of SSG	σ_z (kPa)	111	710	275	467	273	262	377
	ε_c (µm/m)	1318	364	236	268	444	470	242
Bottom of SSG	σ_r (kPa)	3	-605	-592	-433	-202	-186	-372
	ε_t (µm/m)	-192	-260	-254	-186	-226	-232	-160
Top of SG	σ_z (kPa)	60	66	65	48	51	53	39
	ε_c (µm/m)	754	857	836	619	675	692	511

AC: Asphalt Concrete; SSG: Stabilized Subgrade Layer; SG: Natural Subgrade; σ_z: Vertical Stress; σ_r: Radial Stress; ε_t: Radial Strain; ε_c: Vertical Strain; h: Thickness of Layer; M_r: Design Resilient Modulus (σ_3 = 13.78 kPa, σ_d = 41.34 kPa; See Table 5.3, Model 3); Note: Negative sign indicate tensile stresses and strains

Table 6.2 A Summary of Relevant Resilient Modulus Studies in Indirect Tension for Cementitiously Stabilized Materials

Reference	Type of Additive	Resilient modulus (M_{rt})/Modulus of Elasticity in tension (M_{Et})	Horizontal tensile strain/Poisson's Ratio	Cylindrical Specimen Size	Load
ASTM D 4123	Not Applicable	$M_{rt} = \frac{P(\nu + 0.27)}{t.\Delta H_T} = \frac{3.59P}{t.\Delta V_T}$	$\nu = \frac{3.59\Delta H_T}{\Delta V_T} - 0.27$	100 mm diameter by 50 mm height	Haversine (0.33, 0.5 and 1.0 Hz)
Raad (1985)	Not Applicable	$M_{Et} = \frac{P(\nu + 0.2732)}{t.\Delta H_T}$	None	100 mm diameter by 75 mm height	NA
Mohammad et al. (2000)	Portland Cement	$M_{rt} = \frac{3.59P}{t.\Delta V_T}$	$\varepsilon_t = 0.5207 H_T$	100 mm diameter by 63 mm height	Haversine (2 Hz) (0.1s Loading, 0.5s Rest)
White and Gnanendran (2005)	Slag+Lime	M_{Et} from slope of stress versus strain curve from Indirect Tensile Strength test	None	Not Available	Static load
Navaratnarajah (2006)	Not Applicable	$M_{rt} = \frac{2P}{\pi D t.\Delta H_T \left(D^2 + {D_g}^2\right)} \left\{ \left[(3+\nu) D^2 D_g + (1-\nu) {D_g}^3 - 2D\left(D^2 + {D_g}^2\right) \right] \tan^{-1}\left(\frac{D_g}{D}\right) \right\}$	$\nu = 0.35$	100 mm diameter by 75 mm height	Haversine (1.0 Hz) (0.1s Loading, 0.9s Rest)
Khattak and Alrashidi (2006)	Portland Cement	$M_{rt} = \frac{P(\nu + 0.27)}{t.\Delta H_T}$	$\nu = \frac{3.59\Delta H_T}{\Delta V_T} - 0.27$	100 mm diameter by 63 mm height	Haversine (2.0 Hz) (0.1s Loading, 0.9s Rest)
Gnanendran and Piratheepan (2008)	Slag+Lime	$M_{rt} = \frac{P(\nu + 0.27)}{t.\Delta H_T}$	None	150 mm diameter	Sinusoidal (3 Hz)

t = thickness of the specimen; M_{rt} = resilient modulus in indirect tension; P = repeated load; ΔH_T = total recoverable horizontal deformation; ΔV_T = total recoverable vertical deformation; D = diameter of specimen; υ = Poisson's ratio; ε_t = horizontal tensile strain; D_g = distance between LVDTs measuring horizontal deformations

Table 6.3 A Summary of Relevant Fatigue Relationships for Cementitiously Stabilized Materials

Reference	Type of material	Specimen size	Experimental details (Parameter evaluated)	Fatigue Model
Verstraeten et al. (1982)	NA	NA	NA	$\varepsilon_t/\varepsilon_m = 1- 0.05\log(N_f)$
Raad (1985)	Silty clay with cement	21 in. x 6 in. x 6 in.	Strain gages at the top and bottom of specimen in middle-third portion. Displacement controlled third-point loading of 0.0120 in./min. (Flexural modulus)	NA
Bhattacharya and Pandey (1986)	Laterite soil with lime	---	Beams were subjected to third-point loading at a loading frequency of 1.83 Hz (110 cycles/min.) (Fatigue life); Rate of loading = 0.05 in./min (Flexural strength)	$S = 0.96 – 0.114 \log(N_f)$
Laguros and Keshawarz (1987)	Shale stabilized with cement, quicklime, fly ash	16 in. x 4 in. x 3 in.	Beams were tested under third-point loading (Flexural strength)	NA
ACAA (1991); Thompson (1994)	CSM	NA	NA	$\log(N_f) = (0.9722-S)/0.0825$
Lav et al. (2006)	Fly ash with cement	NA	Accelerated loading facility	$N_f = (a/\mu\varepsilon)^b$
Sobhan and Mashnad (2003)	Aggregates with cement + fly ash + HDPE strips	30 in. x 6 in. x 6 in.	Beams were tested in a third-point loading configuration under load control conditions using a sinusoidal load pulse with a constant amplitude at a frequency of 2 Hz (120 cycles/min.) (Fatigue life)	$S = -0.038 \ln(N_f) + 1.047$
AASHTO 2002 MEPDG (2004)	CSM	NA	NA	$\log(N_f) = (a_1-S)/a_2$
Molenaar and Pu (2008)	Cement treated base	NA	Used pavement database (SHRP-NL)	$\log(N) = 8.5 – 0.034\varepsilon_t$
Prozzi and Aguiar-Moya (2010)	Cement treated base	NA	Pavement data from South Africa	$\log(N_f) = 7.131 -0.8629 \varepsilon_t/\varepsilon_m$

NA: Not applicable; N_f: No. of cycles to failure; S: Stress ratio = applied stress/ultimate strength; με: maximum value of initial tensile strain; HDPE: High density polyethylene; ε: tensile strain at the bottom of cement treated base due to a 50 kN falling weight load; N: allowable no. of 100 kN ESAL; CSM: cementitiously stabilized material; a: material constants; ε_t: tensile strain at bottom of layer; ε_m: maximum allowable strain at bottom of beam from flexural strength tests

Table 6.4 Testing Sequence used for Resilient Modulus Test in Indirect Tension

Sequence Number	Maximum Tensile Stress	Cyclic Tensile Stress	Constant Tensile Stress	No. of Load Applications
Conditioning	$0.20\sigma_t$	$0.18\sigma_t$	$0.02\sigma_t$	500
1	$0.30\sigma_t$	$0.27\sigma_t$	$0.03\sigma_t$	100
2	$0.40\sigma_t$	$0.36\sigma_t$	$0.04\sigma_t$	100
3	$0.50\sigma_t$	$0.45\sigma_t$	$0.05\sigma_t$	100
4	$0.60\sigma_t$	$0.54\sigma_t$	$0.06\sigma_t$	100
5	$0.70\sigma_t$	$0.63\sigma_t$	$0.07\sigma_t$	100

σ_t: Average indirect tensile strength of 28-day cured stabilized specimen

Table 6.5 A Summary of Resilient Modulus Values in Indirect Tension of Stabilized P-soil Specimens

σ_d/σ_t	M_{rt} (MPa)											
	Raw	SD	CV	6% Lime	SD	CV	10% CFA	SD	CV	10% CKD	SD	CV
0.27	75	2	2	908	152	17	656	67	10	1,673	214	13
0.36	65	2	3	758	117	15	487	21	4	1,187	36	3
0.45	60	1	2	648	24	4	429	19	4	965	50	5
0.54	55	1	2	516	17	3	351	9	3	848	28	3
0.63	49	0	1	443	9	2	315	6	2	776	25	3

1 psi = 6.89 kPa; 1 ksi = 6.89 MPa; SD: standard deviation; CV: coefficient of variation (%)

σ_d : deviator stress; σ_t : tensile strength; M_{rt} : resilient modulus in indirect tension

Table 6.6 A Summary of Resilient Modulus Values in Indirect Tension of Stabilized V-soil Specimens

σ_d/σ_t	M_{rt} (MPa)											
	Raw	SD	CV	6% Lime	SD	CV	10% CFA	SD	CV	10% CKD	SD	CV
0.27	59	8	14	691	25	4	839	32	4	915	8	1
0.36	29	4	14	633	15	2	722	23	3	862	10	1
0.45	18	1	5	570	24	4	670	5	1	822	16	2
0.54	13	1	6	506	7	1	614	12	2	733	9	1
0.63	11	0	3	444	3	1	580	7	1	641	6	1

1 psi = 6.89 kPa; 1 ksi = 6.89 MPa; SD: standard deviation; CV: coefficient of variation (%)

σ_d : deviator stress; σ_t : tensile strength; M_{rt} : resilient modulus in indirect tension

Table 6.7 A Summary of Modulus of Rupture Values of Raw and Stabilized P- and V-Soil Specimens

Soil Type	Additive Type	Average MOR (kPa)	SD (kPa)	CV (%)
P-Soil	None	106	12	11
	6% Lime	187	26	14
	10% CFA	251	43	17
	10% CKD	459	87	19
V-Soil	None	96	12	13
	6% Lime	255	16	6
	10% CFA	270	41	15
	10% CKD	291	28	9

MOR: Modulus of Rupture or Flexural Strength; SD: Standard Deviation; CV: Coefficient of Variation

Table 6.8 Results of Fatigue Test on Stabilized P- and V-Soil Specimens

Soil Type	Additive Type	Set#1		Set#2		SD (N_f)	CV (N_f)
		M_{rf} (Cycle 50) (MPa)	Cycles to Failure (N_f)[a]	M_{rf} (Cycle 50) (MPa)	Cycles to Failure (N_f)[a]		
P-Soil	6% Lime	535	*	591	*	NA	NA
	10% CKD	731	< 50 (29)**	1,381	72	30	60
V-Soil	6% Lime	839	1,250,000	763	1,610,001	254,559	18
	10% CKD	952	1,100,001	1,028	830,000	190,920	20

[a]Cycle at which specimen stiffness is reduced to 50 percent of the initial stiffness; *Specimen didn't fail in 2 million cycles; **Stiffness dropped suddenly at 29th cycle; NA: not applicable; SD: standard deviation; CV: coefficient of variation (%)

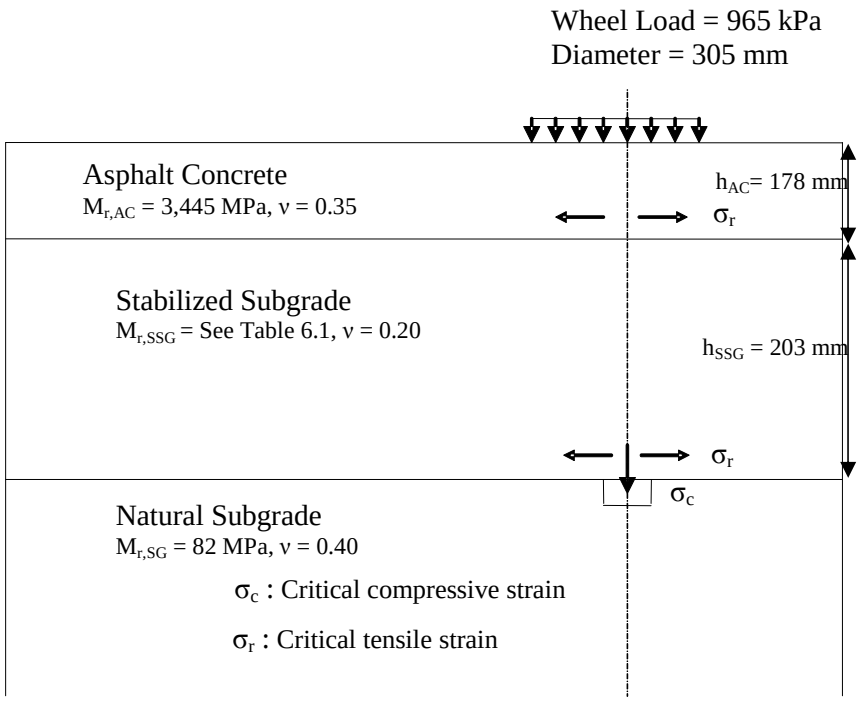

Figure 6.1 Pavement Configuration with Stabilized Subgrade Layer

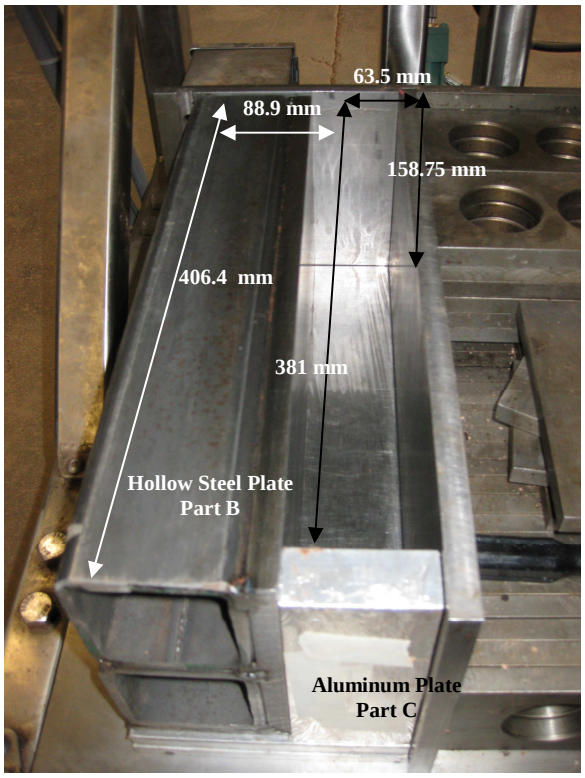

(a)

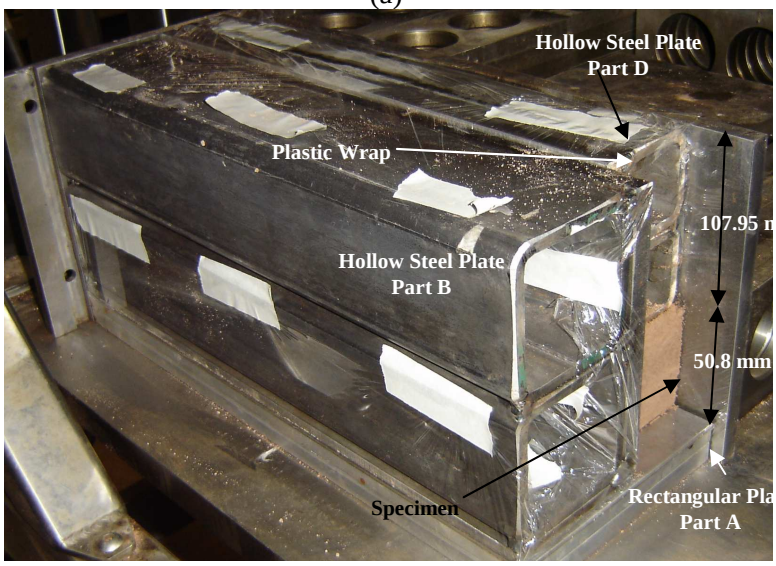

(b)

Figure 6.2 Photograph Showing the Fatigue Specimen Preparation Mold

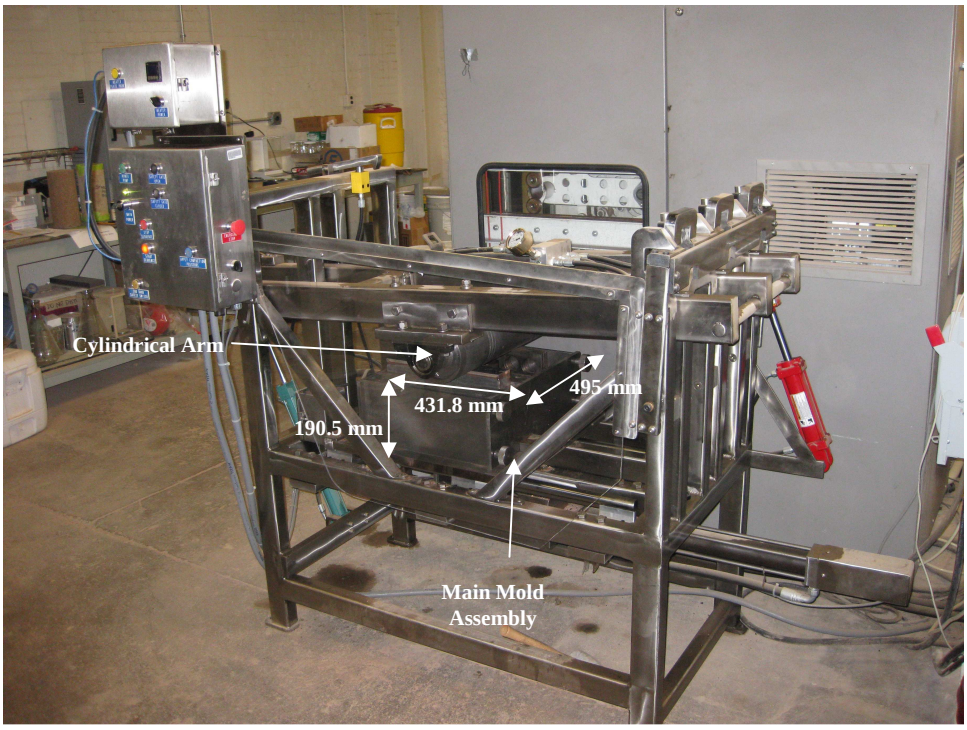

Figure 6.3 Compaction of Fatigue Specimen Using Linear Kneading Compactor

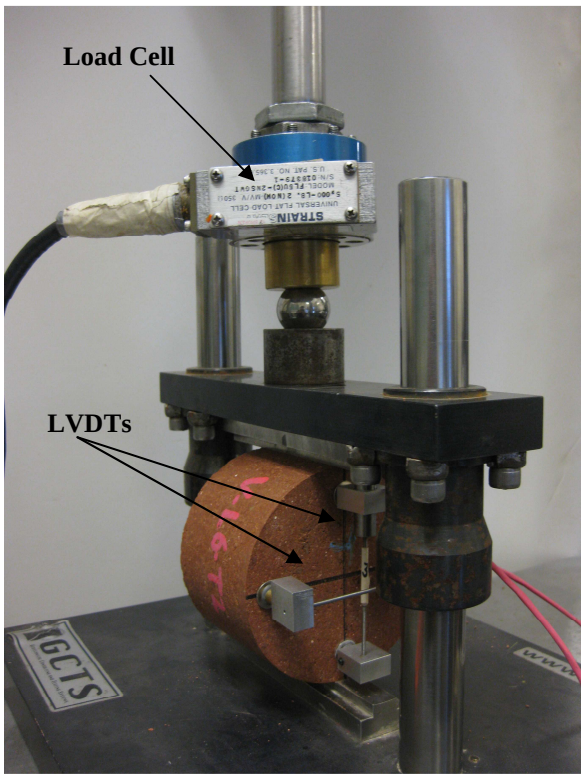

Figure 6.4 Setup for Resilient Modulus Test in Indirect Tension

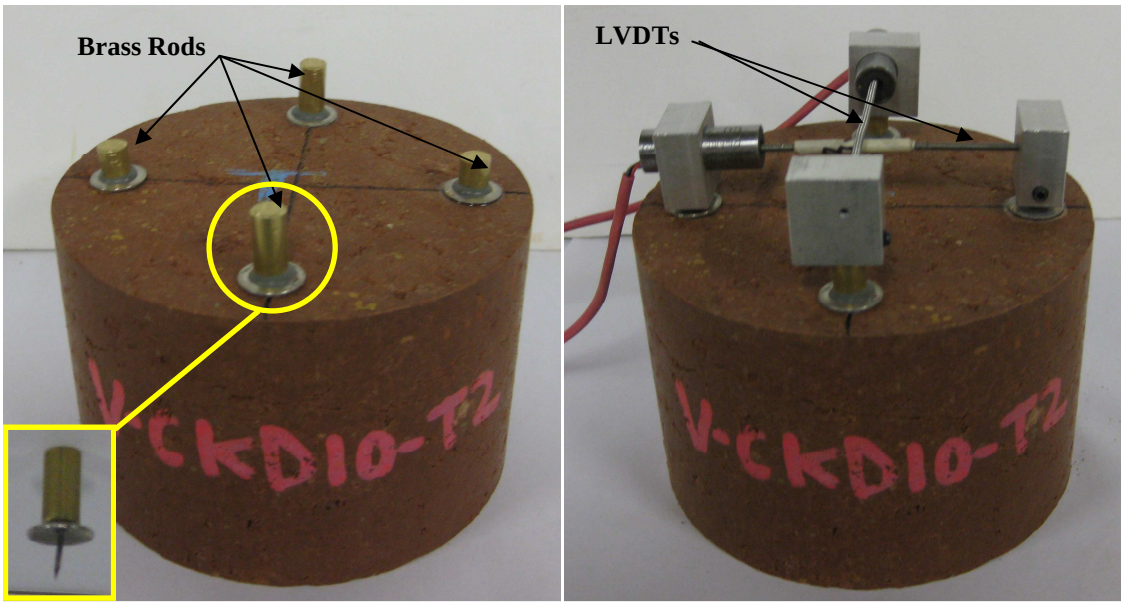

Figure 6.5 LVDTs Attached to Resilient Modulus in Indirect Tension Test Specimen

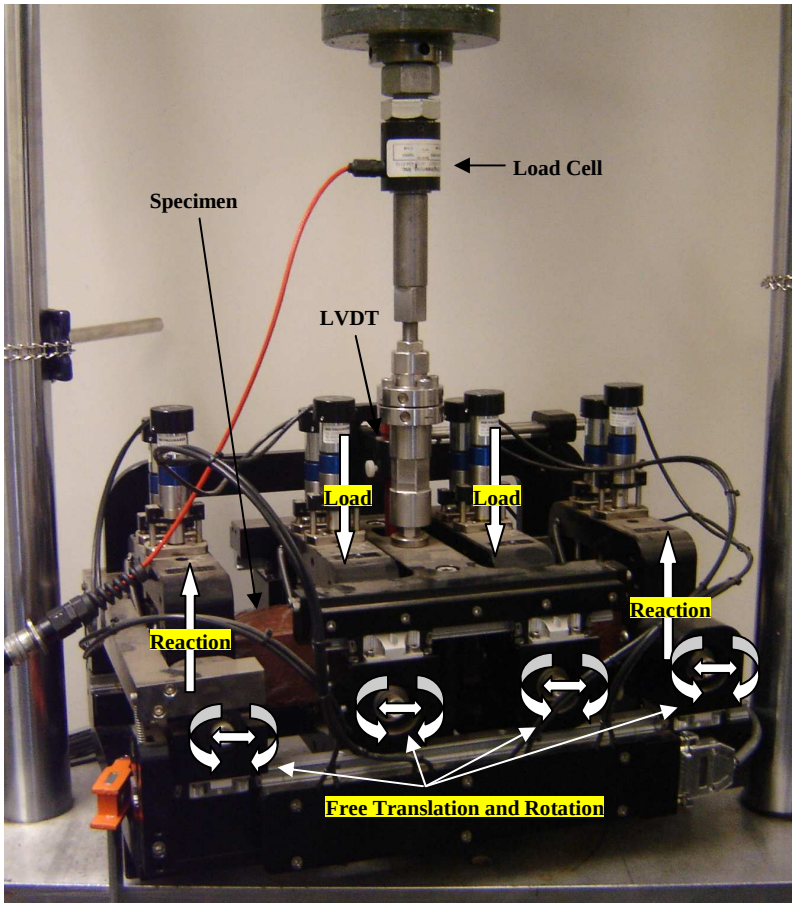

Figure 6.6 Setup for Four-Point Fatigue Test

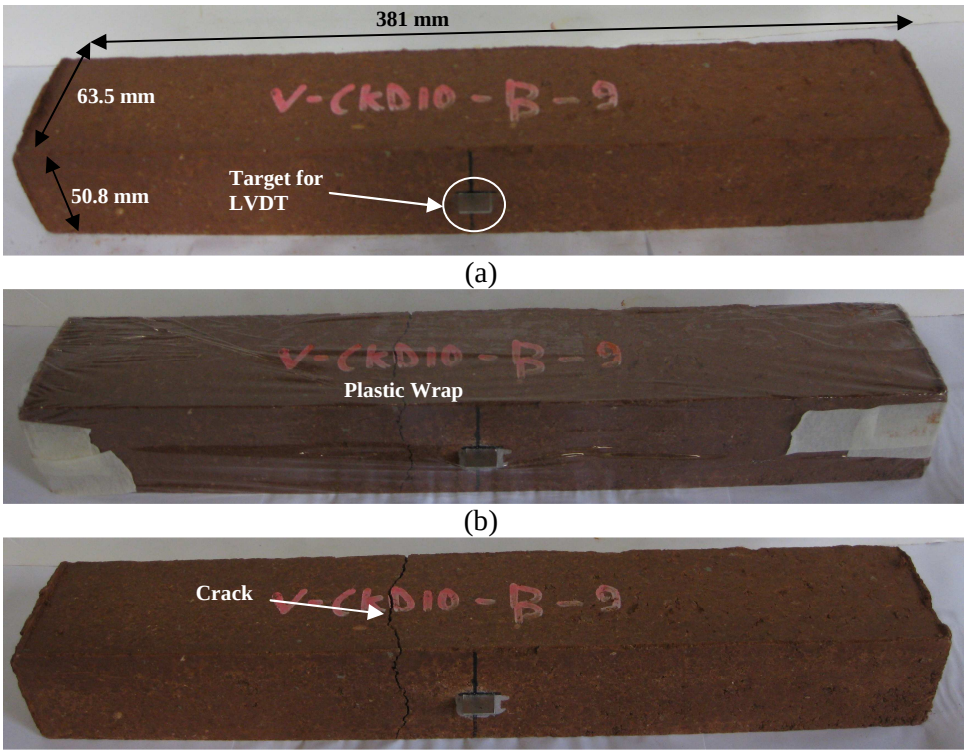

Figure 6.7 Fatigue Beams (a) Before Testing (b) Covered With Plastic Wrap To Prevent Moisture Loss During Testing (c) After Testing

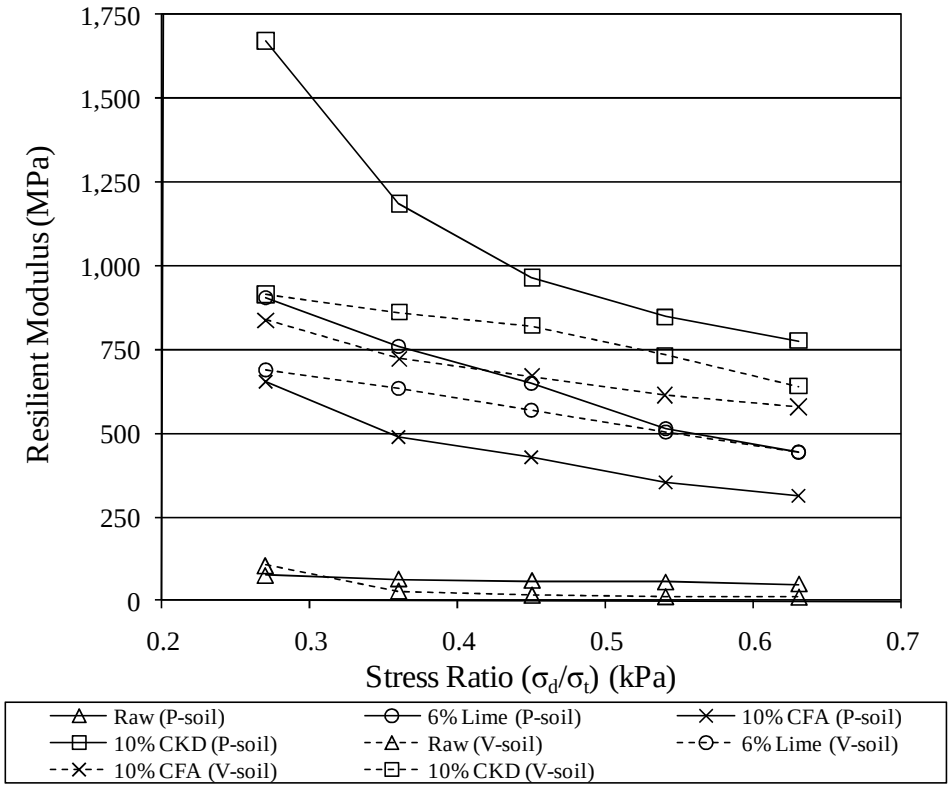

Figure 6.8 Variation of M_{rt} of P- and V-soil Specimens with Stress Ratio

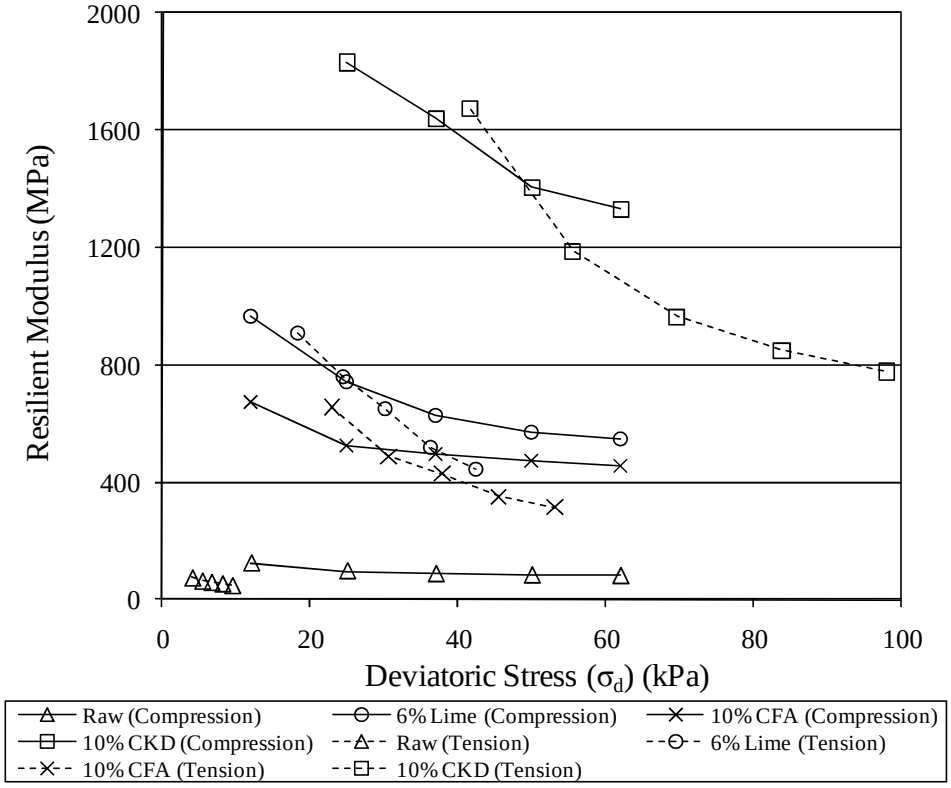

Figure 6.9 Comparison of Resilient Modulus Values of Raw and Stabilized P-Soil Specimens Tested in Compression and Indirect Tension Modes

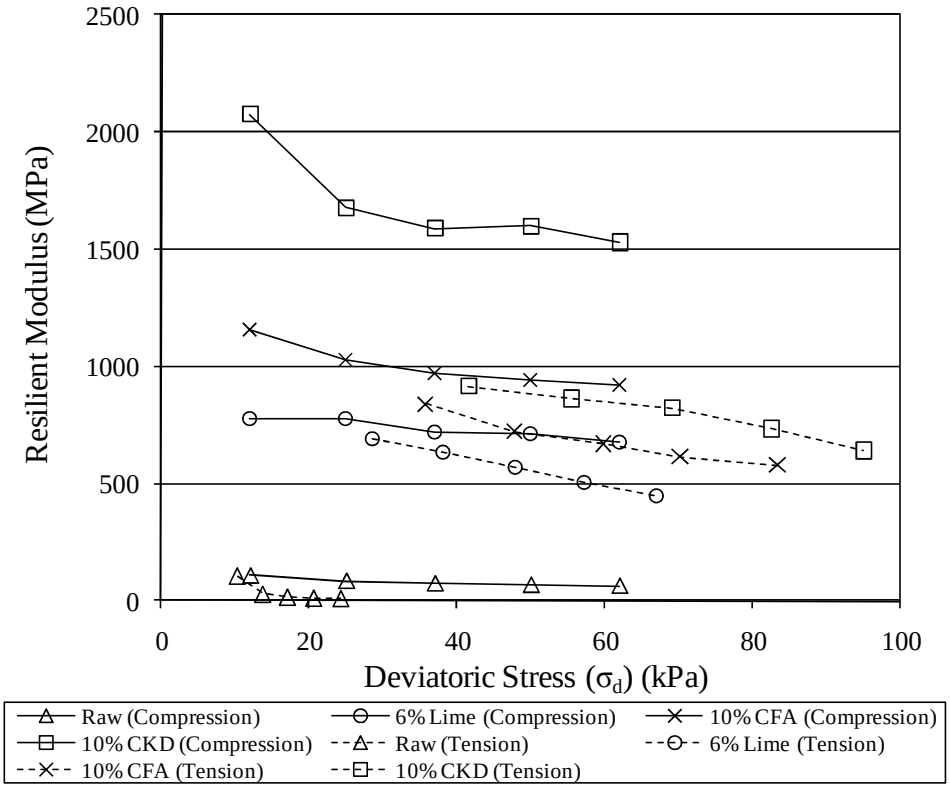

Figure 6.10 Comparison of Resilient Modulus Values of Raw and Stabilized V-Soil Specimens Tested in Compression and Indirect Tension Modes

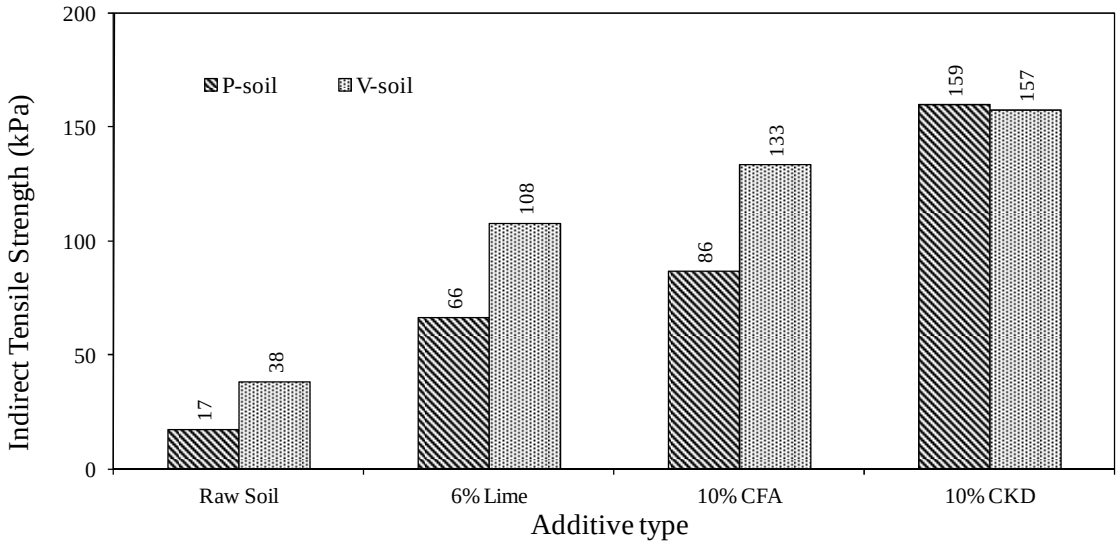

Figure 6.11 Indirect Tensile Strength Values of Raw and Stabilized V- and P-Soil Specimens

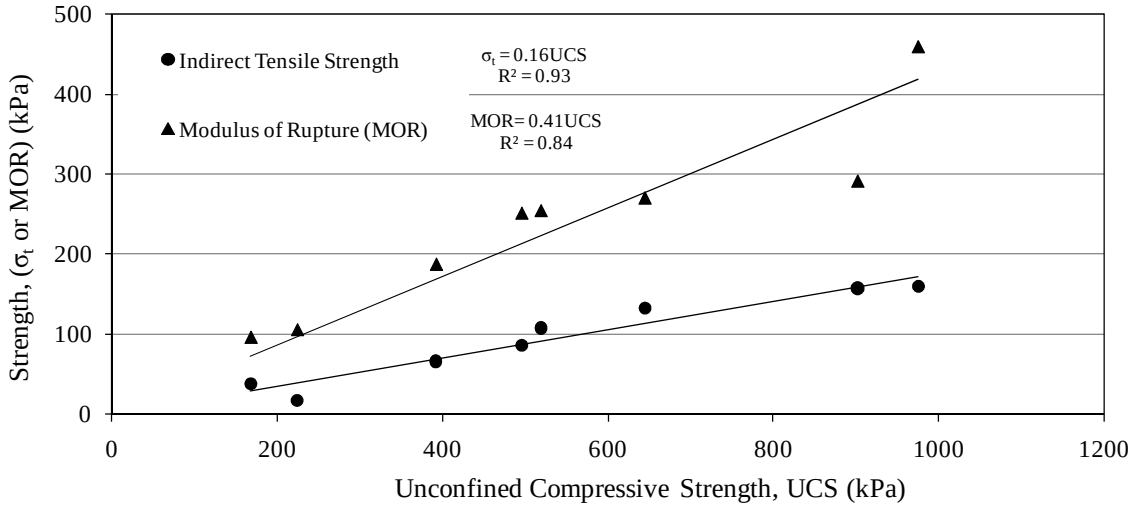

Figure 6.12 Correlation Between Indirect Tensile Strength, Modulus of Rupture and Unconfined Compressive Strength

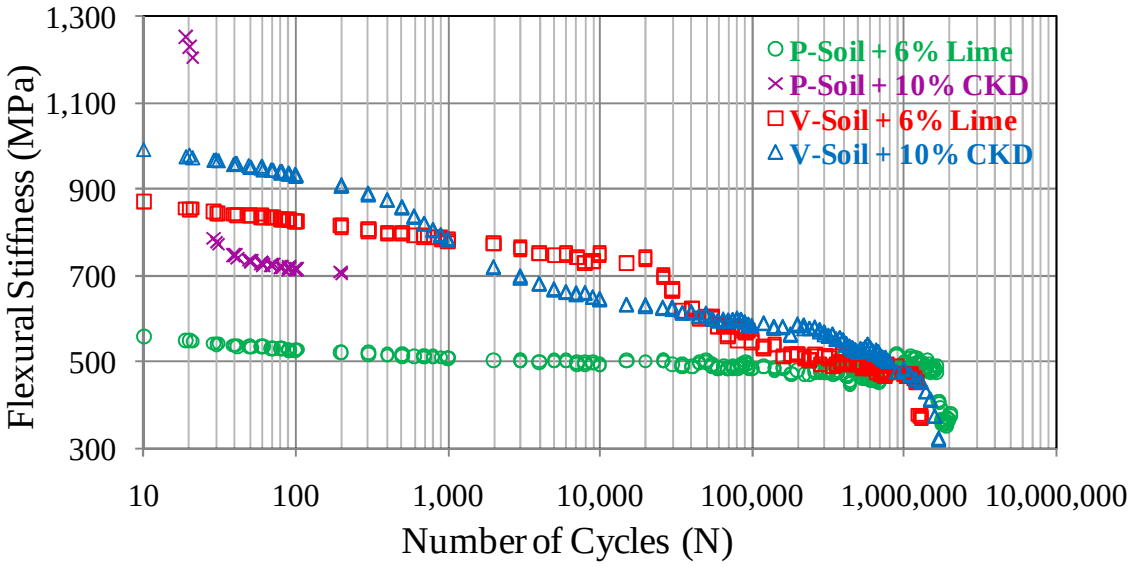

Figure 6.13 Flexural Stiffness Versus Number of Fatigue Cycles for Stabilized P- and V-Soil Specimens

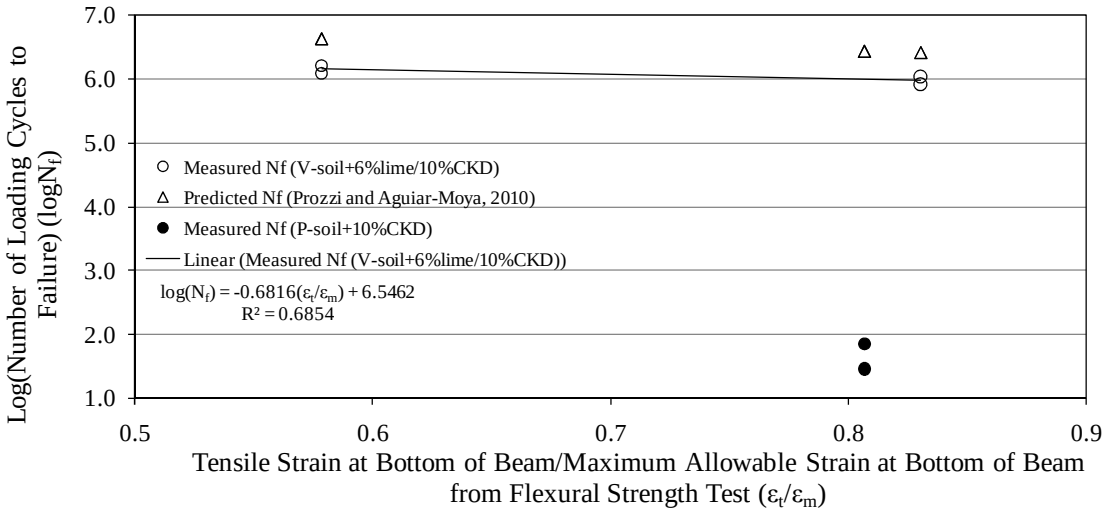

Figure 6.14 Strain-Based Model (Transfer Function) for Fatigue Life of 6% Lime- and 10% CKD-Stabilized P- and V-Soil Beams

CHAPTER 7

DESIGN OF SEMI-RIGID TYPE FLEXIBLE PAVEMENT

7.1 Introduction

The basis of the AASHTO 1993 flexible pavement design method was a landmark pavement performance test (AASHO Road Tests) conducted in the late 1950s near Ottawa, Illinois, at a cost of $27 million (1960 dollars) (Huang, 2004; Papagiannakis and Masad, 2007). This experiment consisting of 288 flexible pavements generated substantial database of pavement performance observations, which formed the basis for the pavement design methodology adopted by AASHTO. However, the new MEPDG adopted a mechanistic-empirical approach to the damage analysis of flexible pavements. The design process involves computing the pavement structural response to the load (i.e., stresses and strains), translating them into damage, and accumulating the damage into distresses, which reduce pavement performance over time (Papagiannakis and Masad, 2007).

Due to the effort towards implementation of the new MEPDG, several state agencies and researchers have evaluated flexible and rigid pavement sections using both empirical and mechanistic-empirical design methods (see e.g., Kim et al., 2005; Mulandi et al., 2006; Carvalho and Schwartz, 2006; Li et al., 2010). However, no studies to the author's knowledge compared design of *semi-rigid* type flexible pavements using both AASHTO 1993 and new MEPDG. Also, only a limited level of attention has been devoted to the MEPDG performance prediction capabilities of pavement systems involving stabilized layers (Saxena et al., 2010). Since the new MEPDG is intended to replace the previous AASHTO 1993 pavement design guide, which based primarily on

empirical methods, it is important to evaluate and compare *semi-rigid* pavement designs using both the AASHTO 1993 and the new MEPDG guides.

Consequently, the primary objective of the study presented herein is to develop design curves for performance prediction of stabilized layers and to compare *semi-rigid* flexible pavement designs between the empirical AASHTO 1993 and the mechanistic-empirical AASHTO 2002 pavement design methodologies. These comparisons span a range of different sections consisting of cementitious layers stabilized with different types and percentages of additives. Also, specific emphasis is devoted to the influence of stabilized subgrade layer properties and reliability levels on the comparisons. Further, cost comparisons of different sections stabilized with different additive types and contents were also pursued.

7.2 Semi-Rigid Type Flexible Pavement

Several classical books and references (e.g., AASHTO, 1993; Huang, 2004; AASHTO, 2004; Papagiannakis and Masad, 2007; Mallick and El-Korchi, 2008) are available that present the terms rigid or flexible to separate different possibilities of pavement structures. The term rigid refers to pavements with the top layer made of cement concrete material; the term flexible is associated with pavements with asphalt concrete (AC) layer on the top. The conventional flexible and rigid pavements differ in the way each structure distributes the vertical pressure over the subgrade. A rigid pavement tends to cause a dispersed spread of pressure over the lower layers. On the other hand, the response to loads on a flexible structure is more concentrated near the loaded area. Thus, considering the presence of a cementitiously stabilized layer on the subgrade of a flexible pavement, the pressure spread over the subgrade tends to become

more diffused compared to a conventional flexible pavement case. This behavior of flexible pavement having a cementitiously stabilized layer puts it into a new category called *semi-rigid* type flexible pavement (Balbo and Cintra, 1994). According to the new MEPDG, a pavement section having some type of chemically stabilized (pozzolanic) layer below the asphalt concrete layer is defined as a *semi-rigid* pavement (AASHTO, 2004).

7.3 Overview of the AASHTO 1993 and AASHTO 2002 MEPDG

7.3.1 AASHTO 1993 Design Guide

The AASHTO Guide for Design of Pavement Structures (AASHTO, 1993) is the primary document used to design new and rehabilitated pavements in the United States (Li, 2009). As noted earlier, AASHTO 1993 guide is primarily based on findings from the AASHO Road Test program conducted between October, 1958 and November, 1960. During the AASHO road tests, performance measurements of pavement sections were taken at regular interval. The performance data along with pavement material properties and traffic data was used to develop empirical models for pavement design.

7.3.1.1 Design Inputs

Following are the specific design inputs required for designing a pavement using AASHTO 1993 Design Guide (AASHTO, 1993):

1. Time Constraints: AASHTO categorized two types of time constraints namely, performance period and analysis period. Performance period is defined as the period of time that an initial pavement structure will last before it needs rehabilitation. On

the other hand, analysis period (or design life), refers to the period of time for which the analysis is conducted.

2. Traffic: The design procedure is based on number of Equivalent Single Axle Load (ESAL) applications. ESAL is defined as total number of applications of a standard axle (generally 80 kN, i.e., 18 kip single) required to produce the same damage or loss of serviceability as number of application of one or more different axle loads and/or configurations over life of pavement (Huang, 2004). It is a convenient way for converting mixed traffic data to a number of standard axles for design of a pavement.
3. Reliability: It is used for incorporating some degree of certainty into the design process to ensure that the various design alternatives will last the analysis period. Specifically, reliability accounts for variations in both traffic predictions and the performance prediction. Table 7.1 presents recommended levels of reliability for various functional classifications. For a given level of reliability, the reliability factor is defined by standard normal deviate (Z_R) and overall standard deviation (S_o). The recommended values of S_o for flexible and rigid pavements are 0.45 and 0.35, respectively (AASHTO, 1993).
4. Performance Criteria: Both functional and structural performances are considered in AASHTO 1993 design guide by using the concept of serviceability. The serviceability of a pavement is defined as its ability to serve the type of traffic which uses the facility. The primary objective measure of serviceability is the Present Serviceability Index (PSI) which ranges from 0 (impossible road) to 5 (perfect road). The difference in present serviceability index (ΔPSI) between construction/initial and end-of-life/terminal is the serviceability life.

5. Material Properties: The subgrade layer properties are incorporated in terms of effective resilient modulus. Other layer properties are accounted by using layer coefficients. The layer coefficients measure the relative ability of a unit thickness of a given material to function as structural component of the pavement. The AASHTO 1993 design guide provide correlations and charts between resilient modulus of material and layer coefficients (AASHTO, 1993). For example, following equation is recommended for granular base material:

$$a = 0.277 \log(M_r) - 0.839 \quad (7.1)$$

where, a = layer coefficient (in^{-1}) and M_r is in psi.

6. Drainage Characteristics: The level of drainage for a flexible pavement is accounted through the use of modified layer coefficient, i.e., a higher layer coefficient is used for improved drainage condition. The factor for modifying the layer coefficient to account for drainage effect is referred to as an 'm' value and depends on drainage quality and percent of time during the year pavement structure is normally exposed to moisture levels approaching saturation. The m value ranges between 0.40 for very slow draining layer and 1.40 for quick draining layer that never saturate.

7.3.1.2 Design Method

The AASHTO 1993 method utilizes the term Structural Number (SN) to quantify the structural strength of a pavement required for a given combination of pavement layer properties, total traffic, reliability, and serviceability level. The required SN is converted to actual thickness of surface, base and subbase, by means of appropriate layer coefficients representing the relative strength of the construction materials. The design equation used is as follows:

$$SN = a_1 D_1 + a_2 D_2 m_2 + a_3 D_3 m_3 \quad (7.2)$$

where, a_i = ith layer coefficient, D_i = ith layer thickness, and m_i = ith layer drainage coefficient. For a *semi-rigid* pavement, the subscripts 1, 2 and 3 refer to the asphalt concrete, stabilized subgrade and subbase layer (if applicable), respectively. The basic design equation for flexible pavements in the AASHTO 1993 design guide is as follows:

$$\log_{10}(W_{18}) = Z_R \times S_o + 9.36 \times \log_{10}(SN+1) - 0.20 + \frac{\log_{10}\left[\frac{\Delta PSI}{4.2-1.5}\right]}{0.40 + 1094/(SN+1)^{5.19}} + 2.32 \times \log_{10} M_r - 8.07 \quad (7.3)$$

where, W_{18} = predicted number of 80 kN (18 kip) ESAL applications. Eqn. 7.3 can be solved iteratively or by using nomographs for required SN value. The required design thickness of each layer is derived by using Eqn. 7.2 in combination with material properties of each layer.

7.3.2 AASHTO 2002 MEPDG

The AASHTO 2002 MEPDG developed in the NCHRP 1-37A study is a mechanistic-empirical (M-E) method for designing and evaluating pavement structures. The M-E design and analysis process, shown conceptually in Figure 7.1, integrates the environmental conditions and material properties of the asphalt concrete layer and underlying layers into the pavement structure. The responses of pavement structure to load (i.e., stresses and strains) are mechanistically calculated based on material properties, environmental conditions, and traffic characteristics. Thermal and moisture distributions are mechanistically determined using the Enhanced Integrated Climatic Model (EICM). These responses are then used as inputs in empirically derived distress models (or transfer functions), translating them into damage, and accumulating the

damage into distresses (e.g., permanent deformation, fatigue cracking, thermal cracking and roughness) that are responsible for reduced pavement performance over time (Priest and Timm, 2006; Papagiannakis and Masad, 2007). The damage for each condition is typically added together using Miner's hypothesis, shown in Eqn. 7.4, where the failure criteria is reached when the ratio approaches unity (Miner, 1959):

$$D = \sum_{i=1} \frac{n_i}{N_i} \tag{7.4}$$

where, D = total damage, n_i = number of load applications at condition i, N_i = number of load application at failure for condition i. The distress models were calibrated by using data from the Long Term Pavement Performance (LTPP) database for conditions representative of the entire United States (Li, 2009). Because the design process is modular, varying degrees of accuracy and sophistication can be used at each step depending on the needs of the design (Priest and Timm, 2006). This section further briefly describes the MEPDG design procedure and inputs.

7.3.2.1 Design Process

The MEPDG design process is not as straightforward as the 1993 AASHTO guide, in which the structure's thicknesses are obtained directly from the design equation (Li, 2009). In general, the design process consists of three major stages. Stage 1 of MEPDG design procedure involves development of input values. In this stage, the potential strategies for analysis are identified. The input data of pavement materials (as discussed later), traffic characterization and EICM model are developed. In Stage 2, performance analysis is conducted using an iterative process that begins with the selection of an initial trial design. If the trial design does not meet the performance

criteria, the design (thicknesses or material selection) must be modified and the calculations repeated until the design is acceptable. Stage 3 of the design process consists of the evaluation of structurally viable alternatives, such as an engineering analysis and life cycle cost analysis.

The MEPDG has a hierarchical approach for the design inputs, which provides designer with flexibility in obtaining the design inputs for a design project based on the availability of resources and the importance of the project (Von Quintus and Moulthrop, 2007). There are three levels:

Level 1 – This level provides most accurate designs with lowest level of uncertainty or error. Level 1 material inputs require laboratory measured material properties (e.g., dynamic modulus master curve for asphalt concrete, resilient modulus or modulus of elasticity for unbound and chemically stabilized materials) and project-specific traffic data (e.g., vehicle class, load distribution, axle configuration, monthly adjustments).

Level 2 – This level provides an intermediate design. Level 2 inputs are obtained through empirical correlations (e.g., resilient modulus estimated from soil and additive properties) or possibly from an agency database.

Level 3 – This level provides a design with lowest level of accuracy. Inputs are selected from a database of national or regional default values according to the material type or highway class (e.g., soil classification to determine the range of resilient modulus, highway class to determine vehicle class distribution). Level 3 is recommended for minor projects, usually low traffic roads. In addition, Level 3 may be appropriate for pavement management programs widely implemented in highway state agencies (AASHTO, 2004;

Schwartz and Carvalho, 2007). In this study, Level 3 was used throughout because (a) at present there are rarely all the Level 1 input data to be used on a consistent basis, and (b) the final version of the MEPDG software was calibrated using Level 3 (Schwartz and Carvalho, 2006). Also, Level 1 and 2 for stabilized subgrade layer are disabled in the MEPDG software.

7.3.2.2 Design Inputs

Following are the specific design inputs required for designing a pavement using MEPDG software (AASHTO, 2004):

1. General Information: This includes information regarding expected pavement design life, base/subgrade construction month, paving month, traffic opening month and pavement type. Information related to construction is used for establishing reference time for the EICM. On the other hand, selection of flexible or rigid pavement establishes the method of design and applicable performance models.
2. Site/Project Identification: Project site is identified using project ID, section ID and functional class of the pavement. The location of the project is provided in the form of latitude, longitude and height above sea level. This defines the climatic condition which is extracted from available database of nearly 800 weather stations throughout the United States, which allows the user to select a given station or to generate virtual weather stations for a project site under design.
3. Analysis Parameters: Analysis parameters are defined by initial International Roughness Index (IRI) and performance criteria. The typical initial IRI values range between 789 to 1,579 mm/km (i.e., 50 to 100 in/mile). For semi-rigid pavements, an initial IRI value of 1,026 mm/km (65 in/mile) is recommended by the new MEPDG.

The current MEPDG software Version 1.1 supports six different performance criteria namely, AC surface down cracking (longitudinal cracking), AC bottom up cracking (fatigue or alligator cracking), AC thermal cracking, fatigue cracking in chemically stabilized layer, permanent deformation, and terminal IRI. A designer may specify the desired level of reliability for each distress type and roughness. Table 7.2 provides values that are suggested for use in design by the new MEDPG. It is important to note here that the MEPDG is currently uncalibrated for *semi-rigid* pavements and is not recommended for analysis until it is globally calibrated (AASHTO, 2004; Saxena et al., 2010).

4. Traffic Characterization: The MEPDG requires the full axle-load spectrum traffic inputs for estimating the magnitude, configuration and frequency of the loads to accurately determine the axle loads that will be applied on the pavement in each time increment of the damage accumulation (AASHTO, 2004; Li, 2009). The traffic characterization information is provided through four separate modules namely, basic information, traffic volume adjustment factors, axle load distribution factors, and general traffic inputs. The basic information includes Annual Average Daily Truck Traffic (AADTT) for base year, directional distribution factor, lane distribution factor and operational speed of vehicles. The traffic volume adjustment is comprised of monthly adjustment factors, vehicle class distribution, hourly truck traffic distribution, and traffic growth factors. The general traffic inputs are used for calculating pavement response and includes mean wheel location (default value = 457 mm, i.e. 18 in), traffic wander standard deviation (default value = 254 mm, i.e. 10 in),

design lane width (default value = 3.66 m, i.e. 12 ft), number of axle types per truck class, axle configuration, and wheelbase.

5. Climate: The climatic inputs include hourly air temperature, precipitation, wind speed, percentage sunshine, and ambient relative humidity values over the design period. These data are used for considering the changes of temperature and moisture profiles in the pavement structure and subgrade over the design life of a pavement through the incorporation of the EICM model into the MEPDG design software. The EICM is a one-dimensional coupled heat and moisture flow program that simulates changes in the behavior and characteristics of pavement and subgrade materials in conjunction with climatic conditions (AASHTO, 2004).
6. Pavement Structure: This input data includes drainage/surface characteristics and layer properties. Further, the material parameters for each layer needed for the design process are classified into three major categories, namely, pavement response model material inputs, material related pavement distress criteria inputs, and other material properties. The pavement response model material inputs relate to the modulus and Poisson's ratio used to characterize layer behavior within the specific model (Li, 2009). Material parameters associated with pavement distress criteria are linked to some measure of material strength or to some manifestation of the actual distress effect (e.g., modulus of rupture, repeated load permanent deformation). The "other" category of material properties constitutes those associated with special properties such as thermal expansion and contraction coefficient of asphalt mixtures.

7.3.3 Conceptual Difference: AASHTO 1993 and AASHTO 2002 MEPDG

The main conceptual differences between AASHTO 1993 and the new MEPDG can be summarized as follows (AASHTO, 2004; Schwartz and Carvalho, 2007; Li, 2009):

1. The AASHTO 1993 guide designs pavements for a single performance criterion, the present serviceability index (PSI), whereas the MEPDG approach simultaneously considers multiple performance criteria (e.g., rutting, cracking, and roughness).
2. The AASHTO 1993 guide directly computes the layer thicknesses. On the other hand, MEPDG is an iterative procedure.
3. The MEPDG requires more input parameters such as environmental and material properties. It also employs a hierarchical concept in which designer may choose different quality levels.
4. The AASHTO 1993 was developed on the basis of limited field data from AASHO Road Test conducted at only one location. The seasonally adjusted subgrade resilient modulus and the layer drainage coefficients are the only variables for environmental condition. The new MEPDG utilizes a set of project-specific climate data (e.g., air temperature, precipitation, wind speed, and relative humidity) and the EICM to determine the material properties for different environmental conditions throughout the year
5. The AASHTO 1993 guide uses the concept of ESALs to define traffic levels, while the MEPDG adopts the more detailed load spectra concept. Pavement materials respond differently to traffic pattern, frequency and loading. Traffic loading in different seasons of the year also has different effects on the response of the pavement

structure. These factors can be most effectively considered using the load spectra concept.

7.4 Design Curves for Fatigue Life of Stabilized Subgrade Layer

7.4.1 Structural Model

The computer program KENLAYER (Huang, 2004), which is based on multi-layer elastic theory, was employed to calculate the structural response in terms of stresses, strains, and deflections in various layers of 25 hypothetical pavement sections (described in the next section).

7.4.2 Thickness and Material Properties

All 25 pavement sections contain a 101.6 mm (4 in) thick asphalt concrete surface course with a resilient modulus of 3,445 MPa (500,000 psi) and a Poisson's ratio of 0.35, and they are underlain by a V-soil subgrade having a design M_r value of 80 MPa (11,611 psi) and a Poisson's ratio of 0.4. Each section (except section P1) also has a stabilized subgrade layer with either different thickness or additive type (Poisson's ratio = 0.2 as recommended by MEPDG). All layers are assumed to be linear elastic. The pavements are designated as P1 through P25, and various combinations of thicknesses and resilient modulus values are shown in a design matrix in Table 7.3. Overall, twelve sections consider resilient modulus (M_r) in compression while the remaining twelve sections consider resilient modulus in tension (M_{rt}). As noted in Section 5.4.1, design M_r values were calculated at a deviatoric stress of 41.34 kPa (6.0 psi) and a confining pressure of 13.78 kPa (2.0 psi), as recommended by Jones and Witczak (1977) and Ping et al. (2001). On the other hand, M_{rt} were also calculated at a deviatoric stress of 41.34

kPa (6.0 psi) and effect of confinement on M_{rt} was neglected. As demonstrated in Section 2.7.4, M_r values of stabilized soil specimens showed low sensitivity towards low confining pressure (15 kPa, i.e., 2.2 psi). Similar behavior of low sensitivity of resilient modulus towards confining pressure is expected for stabilized soil specimens in tension. A schematic diagram of a pavement section showing all properties used is presented in Figure 7.2.

7.4.3 Traffic Load

As discussed in Section 7.3, AASHTO 1993 design uses 80 kN (18 kips) Equivalent Single Axle Loads (ESAL) while new MEPDG allows use of actual load distributions. Accordingly, pavement response is calculated due to application of a 40 kN (9 kips) wheel load on the surface layer. A tire pressure of 120 psi (default value recommended by MEPDG) is assumed to be the contact pressure applied to a circular area on the pavement surface.

7.4.4 Structural Response

The program KENLAYER treats the flexible pavement structure as an elastic multi-layer system under a circular loaded area (Huang, 2004). It analyze loading in axi-symmetric space and give outputs namely, stresses, strains, and vertical deflections, at user specified locations within the pavement system. For each pavement section, the maximum horizontal (radial) tensile strain at the bottom of the stabilized subgrade layer was obtained from the KENLAYER, and these outputs are presented in Table 7.4 and plotted in Figure 7.3. It is seen that, for the same resilient modulus value, the higher the thickness, the lower the tensile strain which is the expected trend. The curves tend to

flatten out for a stabilized subgrade layer thickness of more than 254 mm (10 in). Also, for the same thickness, lower tensile strain is induced in stabilized section having a higher resilient modulus, as expected, since increased resilient modulus corresponds to increased "rigidity" of the system (Sobhan, 1997; Huang, 2004). It is also clear from Figure 7.3 that for sections with same additives, M_r provides lower tensile strain compared to M_{rt}. This could be contributed to the fact that the magnitudes of M_r values are higher than the M_{rt} values, as discussed in Section 6.5.1.

7.4.5 Prediction of Stabilized Subgrade Layer Performance

The tensile strains reported in Table 7.4 were divided by the appropriate maximum allowable tensile strain from flexural strength tests to calculate the strain ratio (applied strain/maximum allowable tensile strain). Equation 6.18 and model proposed by Prozzi and Aguiar-Moya (2010) (see Table 6.3) were then employed to predict the allowable number of cycles beyond which fatigue failure occurs in each pavement; these values are presented in Tables 7.5 and 7.6 for Eqn. 6.18 and Prozzi and Aguiar-Moya (2010) model, respectively.

7.4.6 Thickness Design Curves

The variation in the predicted number of cycles to failure with the thickness of the stabilized subgrade layer is plotted in Figures 7.5 and 7.6 using Eqn. 6.8 and Prozzi and Aguiar-Moya (2010), respectively, for various values of the resilient modulus. For the given asphalt concrete course and subgrade properties, these charts provide the required minimum thickness of stabilized subgrade layer to prevent fatigue failure in the pavement. Similar charts can be prepared for other asphalt concrete and subgrade

properties. It is found that the curves representing different resilient modulus are almost parallel to each other. The location of the design curve for any other combination of soil and additive can be found by evaluating its resilient modulus and then interpolating its value on the chart.

7.4.6.1 Effect of Selection of Model

An examination of Tables 7.5 and 7.6 reveal that the model recommended by Prozzi and Aguiar-Moya (2010) provides higher fatigue life for all the stabilized sections. For example, Section P2 (V-soil stabilized with 6% lime) provided a fatigue life of 1,691,915 and 5,353,535 by using Eqn. 6.8 and model recommended by Prozzi and Aguiar-Moya (2010). It should be noted that the model recommended by Prozzi and Aguiar-Moya (2010) was calibrated by using the field data. The model provides allowance for a period of crack propagation from the time of crack initiation in stabilized layer to the time when the layer is extensively cracked. On the other hand, the model proposed in this study (Equation 6.8) is based on the laboratory data. The model assumes that fatigue failure is equal to the number of cycles required to reduce the initial stiffness by 50%. Fatigue life of stabilized subgrade layer in field is expected to be higher than laboratory due to several factors such as difference in stress state, traffic wander and material compaction (Al-qadi and Nassar, 2003). For example, fatigue laboratory testing applies the test control parameter, whether stress or strain, repetitively to the same exact location on the specimen. However, it is well recognized that traffic does not constrain itself to the same position on the wheel path.

7.4.6.2 Effect of Selection of Material Property

It is evident from Tables 7.5 and 7.6 that the selection of resilient modulus in compression or tension influences the fatigue life of the stabilized sections; sections utilizing M_r consistently showed higher fatigue life as compared to sections utilizing M_{rt}. For example, Section P4 (V-soil stabilized with 10% CKD) provided a fatigue life of 1,621,876, whereas Section P7 provided a fatigue life of 1,333,899. Thus, decrease in resilient modulus (compression to tension mode) value by approximately 42% reduced the fatigue life by approximately 18%. From the above discussion, it can be concluded that the selection of resilient modulus value is very important for predicting the fatigue life of *semi-rigid* pavement.

7.4.6.3 Effect of Additive Type

Since tension mode is more conservative and reasonable to use, it was decided to compare the additive performance for the sections utilizing M_{rt} values (i.e., P5 – P7, P11 – P13, P17 – P19, P23 – P25). Both Figures 7.4 and 7.5 illustrate that sections stabilized with 6% lime showed highest resistance towards fatigue failure followed by 10% CFA and 10% CKD. For example, the fatigue life of Section P11 (6% lime-stabilized) is 2,003,189, as compared to 1,934,128 and 1,717,592 for Sections P12 (10% CFA-stabilized) and P13 (10% CKD-stabilized), respectively (Table 7.5). Further, to illustrate the effect of additive type on fatigue life, the percentage increase in fatigue life of 6% lime- and 10% CFA-stabilized sections with respect to (w.r.t.) fatigue life of 10% CKD-stabilized specimens having similar thickness are plotted, as shown in Figure 7.6. It is interesting to note that the percent difference in the fatigue life of sections stabilized with different additives decreases with the increase in the thickness of stabilized layer. For

example, Sections P5 (6% lime-stabilized) and P6 (10% CFA-stabilized) having thickness of 101.6 mm (4 in) showed fatigue life of approximately 25% and 18% higher than fatigue life of Section P7 (10% CKD-stabilized). On the other hand, Sections P23 (6% lime-stabilized) and P24 (10% CFA-stabilized) having thickness of 254 mm (10 in) projected fatigue life approximately 8% and 7% higher than corresponding CFA-stabilized section, i.e., Section P25.

7.4.6.4 Overall Pavement Performance

To study the overall performance of pavement, fatigue life of asphalt concrete was also evaluated by using the fatigue cracking model recommended by the new MEPDG. This model is given by the following equation (AASHTO, 2004):

$$N_f = 0.00432 * k_1' C \left(\frac{1}{\varepsilon_{ta}}\right)^{3.9492} \left(\frac{1}{M_{ra}}\right)^{1.281} \quad (7.5)$$

$$C = 10^M = -0.0282 \quad (7.6)$$

$$M = 4.84\left(\frac{V_b}{V_a + V_b} - 0.69\right) = -1.55 \quad (7.7)$$

$$k_1' = \frac{1}{0.000398 + \frac{0.003602}{1 + e^{(11.02 - 3.49 * h_{ac})}}} = 262 \quad (7.8)$$

where, ε_{ta} = maximum tensile strain below the asphalt concrete layer (from KENLAYER), h_{ac} = thickness of AC layer (101.6 mm, i.e., 4 in), M_{ra} = resilient modulus of asphalt concrete layer (3,445 MPa, i.e., 500,000 psi), V_b = effective binder content (4.1%), and V_a = percent air voids (7%). The fatigue life of asphalt concrete layer for different sections computed by using Eqn. 7.8 is presented in Table 7.7. It is clear from Table 7.7 that at a particular thickness, section with stabilized subgrade layer having

highest resilient modulus showed maximum resistance towards fatigue failure of asphalt concrete. For example, among pavement Sections P20 through P25 having 254 mm thick stabilized subgrade layer, Section P22 having the highest resilient modulus value (1,575 MPa, i.e. 228,592 psi) produced the highest resistance towards fatigue failure of asphalt concrete (fatigue life = 48,618,672 cycles). On the other hand, among same aforementioned pavement sections, P23 having the lowest resilient modulus value (611 MPa, i.e., 88,679 psi) showed least resistance towards fatigue failure of asphalt concrete (fatigue life = 1,524,547 cycles). Thus, it can be concluded that 10% CKD providing higher resilient modulus value helped by increasing the number of cycles to failure of asphalt concrete. On the contrary, 6% lime producing the lowest resilient modulus values reduced the fatigue life of asphalt concrete layer.

Further, the fatigue life of stabilized subgrade layer (Tables 7.5 and 7.6) was compared with the fatigue life of asphalt concrete layer (Table 7.7). It is clear that Sections P4, P9, P10, P13, P15, P16, P18, P19, P21, P22, P24 and P25 showed fatigue life of stabilized subgrade layer lower than the fatigue life of asphalt concrete layer (Table 7.5). Similarly, using the Prozzi and Aguiar-Moya (2010), Sections P4, P10, P16 and P22 (10% CKD-stabilized) showed lower fatigue life of stabilized subgrade layer as compared to corresponding fatigue life of asphalt concrete layer (Table 7.6). Overall, improvement in the stiffness (M_r) of stabilized layer increased the fatigue life of asphalt concrete layer. Also, increase in the thickness of stabilized subgrade layer helped by increasing fatigue life of both stabilized subgrade and asphalt concrete layer.

7.5 AASHTO 1993 and AASHTO 2002 MEPDG Analysis

An attempt was made to compare AASHTO 1993 and AASHTO 2002 MEPDG design methods by analyzing 16 hypothetical pavement sections containing V-soil and K-soil stabilized layers. The objective is to predict the thickness of asphalt concrete layer for each pavement section using AASHTO 1993 and MEPDG and to compare the level of agreement between the two design methods. But before one can proceed with the design, there are several design parameters that need to be determined or assumed for AASHTO 1993 and MEPDG analysis (AASHTO, 1993; Huang, 2004; AASHTO, 2004). These design inputs are discussed briefly in the next section.

7.5.1 Design Parameters

It was decided to select common design inputs for both AASHTO 1993 and MEPDG analysis. However, as noted earlier, MEPDG requires more design inputs as compared to AASHTO 1993 Design Guide. In such cases Level 3 default design inputs were selected for MEPDG, as discussed below.

1. *Design Period*: The design period for the selected pavement sections is assumed to be 20 years.
2. *Traffic Characteristics*: A summary of design traffic used in the analysis is presented in Table 7.8. The initial two-way annual average daily traffic (AADT) for this design is assumed to as 11,378 with 3% of the traffic being heavy trucks (Yoder and Witczak, 1975; AASHTO, 1993; Huang, 2004). The ESAL is calculated from the information presented in Table 7.8. The ESAL for the present traffic and annual truck volume growth rate of 1.5% is found to be 3,138,596. Since it is customary to use 80 kN (18,000 lb) axle load in AASHTO 1993, it was decided to use axle load

distribution consisting of only 80 kN (18,000 lb) axle loads in MEPDG. For the ESAL simulation, the default vehicle class distribution was modified to include only class 9 vehicles. This class of vehicle has one single axle and two tandem axles; however, to represent the standard single axles load of 80 kN (18,000 lb) only single axle load of 80 kN (18,000 lb) are considered (Carvalho and Schwartz, 2007). The load distribution was also modified so that only a 80 kN (18,000 lb) load level was considered in the axle load distribution. These two modifications guaranteed only a standard single axle would be used as the traffic loading. Additional MEPDG inputs such as design lane width, traffic operation speed, tire pressure, mean wheel location and traffic wander standard deviation were taken as default value for Level 3 design, as presented in Table 7.8.

3. *Reliability and Performance Characteristics*: Table 7.9 presents the reliability and serviceability values used in this design application. These values are based on the recommendations by the AASHTO 1993 and MEPDG, as discussed in Section 7.3 Based on the AASHTO recommendation, a reliability level of 90% was selected as an input parameter (AASHTO, 1993; AASHTO, 2004). An overall standard deviation of 0.46 was used, as recommended by Oklahoma Department of Transportation. The initial and final serviceability values of the pavement are assumed as 4.2 and 3.0, respectively (AASHTO, 1993; Huang, 2004; Papagiannakis and Masad, 2007). For MEPDG, performance characteristics were assumed to be default values for a Level 3 design of a flexible pavement, as discussed in Section 7.3.
4. *Properties of Asphalt Concrete Layer*: As noted earlier, AASHTO 1993 requires layer coefficient (determined from resilient modulus) for asphalt concrete, whereas

MEPDG uses dynamic modulus and Superpave binder grading as input parameters. To use consistent properties of asphalt concrete in both AASHTO 1993 and MEPDG, it was decided to select a particular gradation of asphalt concrete mixture. Table 7.10 presents the gradation, binder and mix properties of the asphalt concrete used in the current study. The properties of the S3 mix are reproduced from Solanki et al. (2009c) which was used in the construction of an instrumented section on I-35 in the southbound lane. Further, details of the mix are given by Solanki et al. (2009c). The resilient modulus of the mix was determined by using the following correlations recommended by Navratnarajah (2006):

$$M_{ra} = (3048.96 - 23.12T - 148.36V_a - 280.39V_b + 443.04P_{200}) * (0.803 - 0.010T + 0.053V_a)^S \quad (7.9)$$

where, T = temperature (70°F, i.e., 21°C), S = stress ratio (0.030 – 0.375 from KENLAYER). On the other hand, dynamic modulus was computed by using Level 3 inputs in the MEPDG. The resultant master curve of dynamic modulus is presented in Figure 7.7. It is interesting to note that the dynamic modulus and resilient modulus value at a reference temperature of 70°F (21°C) (frequency = 10 Hz) are 3,149 MPa (457,039 psi) and 7,727 MPa (1,121,480 psi), respectively. Previous studies reported that the performance of pavements is affected by the choice of the asphalt concrete modulus (e.g., Loulizi et al., 2006; Lacroix et al., 2007).

5. *Stabilized Subgrade and Subgrade Properties*: The stabilized subgrade and subgrade properties were changed to examine the influence of additive and soil type on the design thickness. A summary of design matrix of 16 different pavement sections (S1 – S16) used in this study is presented in Table 7.12. A total of two different soils,

namely, V- and K-soil were evaluated. Sections S1 through S6 are underlain by a V-soil subgrade (design M_r value = 80 MPa, i.e., 11,611 psi), whereas Section S7 through S16 are underlain by raw K-soil subgrade (design M_r value = 56 MPa, i.e., 8,128 psi). Only Section S16 was assumed to have no stabilized soil layer. For AASHTO 1993 design, stabilized subgrade layer is counted as a subbase and assigned an appropriate structural layer coefficient (Qubain et al., 2000; Bin-Shafique et al., 2004). According to the AASHTO Design Guide (AASHTO, 1993), the relationship between the layer coefficient (a) of the subbase layer and its resilient modulus (in psi) is given by Eqn. 7.1. However, Eqn. 7.1 is valid for granular materials relating subbase layer coefficient to resilient modulus, but no such equation is available for the stabilized subgrade layer. Thus, in lieu of equation or charts specifically for the stabilized subgrade, the equation for granular subbase was assumed to apply to the stabilized subgrade layer to estimate the layer coefficient. This assumption was validated through field testing by other researchers (e.g., Bin-Shafique et al., 2004). The measured resilient modulus values for all the fifteen (S1 – S15) sections were used for calculating layer coefficients using Eqn. 7.1, as presented in Table 7.12. For MEPDG analysis, resilient modulus values were used directly for a Level 3 design.

7.5.2 Layer Thickness

Based on the design parameters selected, SN for AASHTO 1993 design is calculated using DARWin 3.1 – AASHTO 1993 Design Guide software (AASHTO, 1993). For the V- and K-soil subgrade, a SN of 3.87 (S1 – S6) and 4.48 (S7 – S16) is obtained, respectively. In order to convert the design SN to actual pavement thickness, a

semi-rigid type flexible pavement section which has an asphalt concrete layer on the top of 152.4 mm (6 in) stabilized subgrade layer is considered. Based on the AC layer coefficient (0.0176 mm^{-1}, i.e., 0.447 in^{-1}), the required asphalt concrete thickness can be determined by using specified thickness design method provided in DARWin 3.1 software. Table 7.12 presents the required AC thickness (D_E) for the calculated SN pertaining to Sections S1 through S16. The MEPDG analysis was conducted for all the sections (S1 through S16) by using the MEPDG software version 1.100 (AASHTO, 2004). The trial thickness of AC layer was selected from the AASHTO 1993 analysis results. If the section failed the criteria for the smoothness (IR) and other distresses, the thickness of AC layer was increased by 12.7 mm (one-half inch) and the analysis was redone. Analysis of each section took approximately 5 – 10 minutes on a Dell Inspiron 1501 laptop. This process was repeated until the section passed all the performance criteria. The AC thickness (D_M) that was eventually obtained was taken to be the equivalent MEPDG section as shown in Table 7.12. Also, KENLAYER (Huang, 2004) was used for analyzing the fatigue life of stabilized subgrade layer in Sections S1 through S6. The fatigue life of stabilized subgrade was computed in a similar manner as discussed in Section 7.4.5, except that the analyses were carried for only Eqn. 6.18. The minimum thickness of AC layer (D_K) required to prevent fatigue failure of stabilized subgrade layer in different pavement sections is presented in Table 7.12. A summary of required AC thicknesses for Sections S1 through S16 using both AASHTO 1993 and MEPDG is presented graphically in Figure 7.8.

7.5.2.1 Effect of Selection of Material Property

In the present study, both resilient modulus in compression (Sections S1 through S3) and tension (Sections S4 through S6) were considered for designing pavement sections. The required AC thicknesses computed using both AASHTO 1993 and MEPDG are presented in Table 7.12. It is evident from Table 7.12 that the selection of resilient modulus in compression or tension mode influences the design thickness of the stabilized sections. Sections utilizing M_r consistently showed lower design thickness as compared to corresponding stabilized section utilizing M_{rt}. For example, Section S1 (V-soil stabilized with 6% lime) provided an AASHTO 1993 design thickness of 117.9 mm (4.64 in), whereas Section S4 provided an AASHTO 1993 design thickness of approximately 122.9 mm (4.84 in). It is also clear that the influence of selection of resilient modulus in compression or tension mode is dependent on the selection of design method. For example, pavement Sections S4, S5 and S6 designed by AASHTO 1993 method showed an increase in AC thickness by approximately 5.0, 7.1 and 19.0 mm (i.e., 0.19, 0.28 and 0.75 in) with respect to AC thicknesses of S1, S2 and S3 sections, respectively. On the other hand, MEPDG showed an increase in AC thickness by approximately 7.5, 13.0 and 38.1 mm (i.e., 0.30, 0.51 and 1.50 in) between the similar aforementioned sections.

7.5.2.2 Effect of Soil and Additive Type

As noted earlier, V-soil was used in Sections S1 through S5 while K-soil was used in Section S7 through S16. Due to similar additive type and content, Sections S1 (V-soil stabilized with 6% lime), S2 (V-soil stabilized with 10% CFA) and S3 (V-soil stabilized with 10% CKD) were compared with Sections S8 (K-soil stabilized with 6% lime), S11 (K-soil stabilized with 10% CFA) and S14 (K-soil stabilized with 10% CKD),

respectively. It is clear that Sections S1, S2 and S3 consistently provided lower AASHTO 1993 AC design thickness as compared to Sections S8, S11 and S14, respectively. For example, the required AC design thickness of Sections S8, S11 and S14 were approximately 20.5, 41.1 and 47.0 mm (i.e., 0.81, 1.62 and 1.85 in) higher as compared to design thickness of S1, S2 and S3 sections, respectively (Figure 7.8). On the other hand, Sections S1 and S2 provided approximately 41.9 and 4.8 mm (i.e., 1.65 and 0.19 in) higher MEPDG AC design thickness as compared to Sections S8 and S11, respectively. Section S14 showed approximately 7.6 mm (0.30 in) higher MEPDG design thickness as compared to Section S3. The higher AASHTO 1993 design thicknesses of K-soil stabilized sections (S8, S11, S14) as compared to corresponding V-soil stabilized sections (S1, S2, S3) could be attributed to the fact that the design M_r value of K-soil (56 MPa, i.e., 8,128 psi) is lower than the design M_r value of V-soil (80 MPa, i.e., 11,611 psi). On the contrary, MEPDG design thicknesses showed a combined effect of both subgrade and stabilized subgrade layer. Although design M_r of V-soil is higher than the M_r of K-soil, M_r of K-soil stabilized with 6% lime (S8) is higher than the M_r of V-soil stabilized with 6% lime (S1).

Further, to evaluate the effect of additive type and content, the design thicknesses of Sections S8 through S15 were compared (Table 7.12). It is evident from Table 7.12 that increase in lime content showed a decrease in both AASHTO 1993 and MEPDG design thicknesses up to 6% of lime, followed by an increase in design thickness for 9% lime. On the other hand, CFA and CKD content in the stabilized subgrade layer helped by decreasing the design thickness of AC layer. For example, 6% lime (S8), 15% CFA (S12) and 15% CKD (S15) decreased the AASHTO 1993 design thickness of raw

subgrade soil (S16) by approximately 46%, 44% and 53%, respectively. The trend of design AC thickness is similar to the trend of M_r values of stabilized layer, as expected (Figure 7.8).

7.5.2.3 Overall Pavement Performance

It is clear from Figure 7.8 that for all the sections containing V-soil (S1 – S3), MEPDG consistently showed higher (approximately 50%) AC design thickness than the AASHTO 1993 thickness of corresponding sections. This behavior is consistent with the observations reported by other researchers for conventional flexible pavement without stabilized subgrade layer. For example, Carvalho and Schwartz (2006) concluded that the AASHTO 1993 over-estimates the performance of pavements (i.e., lower thickness) for pavements in warm locations. On the contrary, all the sections containing stabilized K-soil (S7 – S16) showed low percentage (< 10%) difference between the design thicknesses obtained from AASHTO 1993 and MEPDG methods. Additionally, Sections S7, S14, S15 and S16 provided higher AASHTO 1993 thickness than MEPDG design thickness. According to a study conducted by Mulandi et al. (2006) on lime-stabilized sections, the MEPDG procedure resulted in much thinner sections when compared to the sections obtained following the AASHTO 1993 design method.

The fatigue life prediction for Sections S1 through S6 showed that a comparatively thicker section is required for preventing fatigue failure of stabilized subgrade layer. For example, KENLAYER analysis showed that a design AC thickness of approximately 111%, 150%, 240%, 110%, 139% and 185% higher than MEPDG design thickness is required for Sections S1, S2, S3, S4, S5 and S6, respectively. However, it is important to note that the design thickness predicted by KENLAYER is

based on a model developed using limited laboratory data. The developed model may not be applicable directly in the field due to several factors such as difference in stress state, traffic wander and material compaction between laboratory and field (Al-qadi and Nassar, 2003).

7.5.3 Reliability Sensitivity

Three different reliability levels of 80%, 90% and 95% were considered for this study. Table 7.14 summarizes the effect of reliability level on the AASHTO 1993 and MEPDG design thickness of Sections S4, S13 and S16. Based on Table 7.14, it is clear that an improvement in the reliability from 80% to 95% resulted in an increase in the percent difference between pavement thicknesses (when using AASHTO 1993 design) by approximately 33%, 22% and 15% for Sections S4, S13 and S16, respectively. On the other hand, MEPDG showed comparatively less sensitiveness towards change in reliability level. For example, an increase in reliability level from 80% to 95% increased the required AC thickness (MEPDG) by approximately 23%, 16% and 12% for Sections S4, S13 and S16, respectively. According to Carvalho and Schwartz (2006), the performance predicted with the AASHTO 2002 MEPDG is relatively insensitive to the reliability level as compared to AASHTO 1993 designs.

7.6 Cost Comparisons

In addition to the reduction of thickness of AC layer achieved by utilizing cementitious additives in highway pavements, there is also a potential for economic savings. Also, selection of an additive depends on cost consideration of materials and hauling. Table 7.14 provides a comparison of costs associated with the delivery of lime,

CFA and CKD for the construction of a hypothetical pavement section in Norman, Oklahoma. Also, cost of a control section constructed using 152.4 mm (6 in) of ODOT Type A aggregate base (properties reproduced from Solanki et al., 2009c) is evaluated for comparison purposes. Cost figures shown in Table 7.14 were provided by the suppliers. Specifically, cost of hydrated lime was provided by the Texas Lime Company located in Cleburne, Texas. On the other hand, cost of CFA and CKD was provided by Lafarge North America located in Tulsa, Oklahoma. An aggregate base quarry located in Davis, Oklahoma (Dolese Bros Co.) provided material and freight cost of Type A aggregate base. Costs were calculated for aggregate base layer and Sections S7 through S15 by assuming a 305 m (1000 ft) wide stabilized subgrade layer stabilized to a depth of 152.4 mm (6 in). It is clear that Type A aggregate base provided highest cost. Further, cost comparisons indicate that the use of CKD was least expensive due to low material costs ($19/ton) and close proximity to the site. Sections stabilized with hydrated lime showed relatively high prices due to higher material cost ($123/ton). However, it is important to note that freight charges for lime may vary slightly depending on location in Oklahoma, but generally, lime prices are relatively insensitive to location within the State (Miller et al., 2003).

In Figure 7.9 a comparison of total aggregate base, lime, CFA and CKD costs is shown for different sections along with design M_r values. It is clear from Figure 7.9 that aggregate base layer provides most expensive section but with lowest design M_r value. Also, 15% CKD (S15) provides highest M_r values and lower costs as compared to 6% lime- (S9) and 15% CFA- (S12) stabilized sections. Further, costs were compared for different additive contents providing similar design M_r values. Sections S7 (3% lime),

S12 (15% CFA) and S14 (10% CKD) were selected for this purpose. It is evident from Figure 7.9 that the total additive cost of Sections S7 and S12 are approximately $3,566 and $7,265. On the other hand, Section S14 provided slightly higher M_r values and lower cost ($345 - $4,044 savings) as compared to Sections S8 and S12. Thus, based on material and hauling costs, CKD can be cheaper than hydrated lime and CFA. In addition, other factors should be considered in comparing the costs of lime-, CFA- and CKD-stabilized layers. For example, after capillary soaking CKD-stabilized soil appears to loose more strength as compared to lime- and CFA-stabilized specimens (see Section 3.5.4), which could result in more money for the maintenance of CKD-stabilized sections.

7.7 Concluding Remarks

In this study, design curves for fatigue performance prediction of stabilized layers were developed for different stabilized pavement sections. The effect of selection of fatigue model, soil type and additives on thickness of stabilized section was discussed. Further, *semi-rigid* flexible pavement designs of different sections between the empirical AASHTO 1993 and the mechanistic-empirical MEPDG pavement design methodology were compared and discussed. Specifically, comparisons spanning a range of different sections consisting of cementitious layers stabilized with different type and percentage of additives were discussed. Costs of different sections stabilized with different additive types and contents were also presented. The following points highlight the conclusions drawn from this study:

1. The selection of resilient modulus value is very important for predicting the fatigue life of *semi-rigid* pavement. It was found that sections utilizing M_r values consistently

showed a higher fatigue life as compared to corresponding sections utilizing M_{rt} values.

2. The sections stabilized with 6% lime showed highest resistance towards fatigue failure followed by 10% CFA and 10% CKD. However, the percent difference in the fatigue life of sections stabilized with different additives decreases with the increase in the thickness of stabilized layer.
3. Increase in the stiffness (M_r) of stabilized layer increased the fatigue life of asphalt concrete. Also, increase in the thickness of stabilized subgrade layer helped by increasing fatigue life of both stabilized subgrade and asphalt concrete layer.
4. The selection of resilient modulus in compression or tension mode influences the required AC design thickness. Sections utilizing M_r consistently showed lower design thickness as compared to corresponding stabilized sections utilizing M_{rt}.
5. The degree of influence of selection of resilient modulus in compression or tension mode is dependent on the design method (i.e., AASHTO 1993 and MEPDG).
6. The trend of the AC design thicknesses of different sections is similar to the trend of M_r values of stabilized layer.
7. The trend of AC design thicknesses predicted by using AASHTO 1993 and MEPDG were mixed. For the Sections S1 through S3 containing V-soil (design M_r = 80 MPa, i.e., 11,611 psi), MEPDG consistently showed higher (approximately 50%) AC design thicknesses than the AASHTO 1993 thickness of corresponding sections. On the contrary, Sections S7 through S16 containing K-soil (design M_r = 56 MPa, i.e., 8,128 psi) showed low percentage (< 10%) difference between the design thicknesses computed from AASHTO 1993 and MEPDG methods.

8. The fatigue life prediction for all the pavement sections showed that a relatively thicker AC section is required for preventing fatigue failure of stabilized subgrade layer.
9. MEPDG showed comparatively less sensitiveness towards change in reliability level as compared to AASHTO 1993 design methodology.
10. At a similar M_r level, CKD-stabilization provided economically low cost sections as compared to lime- and CFA-stabilized sections.

Table 7.1 Suggested Levels of Reliability by AASHTO 1993 (*Source: AASHTO, 1993*)

Functional Classification	Recommended Level of Reliability	
	Urban	Rural
Interstate and Other Freeways	85 – 99.9	80 – 99.9
Principal Arterials	80 – 99	75 – 95
Collector	80 – 95	75 – 95
Local	50 – 80	50 – 80

Table 7.2 Suggested Levels of Reliability by MEPDG (*Source: AASHTO, 2004*)

Functional Classification	Recommended Level of Reliability	
	Urban	Rural
Interstate and Other Freeways	95	95
Principal Arterials	90	85
Collector	80	75
Local	75	70

Table 7.3 Design Matrix Showing 25 Different Pavement Sections for Design Curves of Stabilized Subgrade Layer

Thickness of Stabilized Subgrade Layer (in)	Resilient Modulus in Compression, M_r (MPa)*				Resilient Modulus in Tension, M_{rt} (MPa)**		
	Raw V-soil (80)	V-soil + 6% Lime (715)	V-soil + 10% CFA (951)	V-soil +10% CKD (1,575)	V-soil + 6% Lime (611)	V-soil + 10% CFA (785)	V-soil + 10% CKD (916)
101.6	P1	P2	P3	P4	P5	P6	P7
152.4		P8	P9	P10	P11	P12	P13
203.2		P14	P15	P16	P17	P18	P19
254.0		P20	P21	P22	P23	P24	P25

*M_r value at p_a = 101.28 kPa, σ_3 = 13.78 kPa, σ_d = 41.34 kPa; ** M_{rt} value at σ_d = 41.34 kPa, σ_3 = 0 kPa

Table 7.4 Maximum Tensile Microstrain at Bottom of Stabilized Subgrade Layer Computed By KENLAYER

Thickness of Stabilized Subgrade Layer (mm)	Resilient Modulus in Compression, M_r (MPa)*				Resilient Modulus in Tension, M_{rt} (MPa)**		
	Raw V-soil (80)	V-soil + 6% Lime (715)	V-soil + 10% CFA (951)	V-soil +10% CKD (1,575)	V-soil + 6% Lime (611)	V-soil + 10% CFA (785)	V-soil + 10% CKD (916)
101.6	275 – 403	403	368	297	410	380	372
152.4		303	270	212	310	282	275
203.2		233	205	158	238	214	208
254.0		183	159	121	188	167	162

* M_r value at σ_3 = 13.78 kPa, σ_d = 41.34 kPa; **M_{rt} value at σ_d = 41.34 kPa, σ_3 = 0 kPa

Table 7.5 Prediction of Fatigue Life of Stabilized Subgrade Layer Using Equation 6.18

Thickness of Stabilized Subgrade Layer (mm)	Resilient Modulus in Compression, M_r (MPa)*				Resilient Modulus in Tension, M_{rt} (MPa)**		
	Raw V-soil (80)	V-soil + 6% Lime (715)	V-soil + 10% CFA (951)	V-soil +10% CKD (1,575)	V-soil + 6% Lime (611)	V-soil + 10% CFA (785)	V-soil + 10% CKD (916)
101.6	NA	1,691,915	1,611,689	1,621,876[1]	1,670,545	1,571,193	1,333,899
152.4		2,028,815	1,983,978[1]	2,024,097[1]	2,003,189	1,934,128	1,717,592[1]
203.2		2,303,813	2,277,195[1]	2,329,998[1]	2,282,990	2,234,145[1]	2,045,310[1]
254.0		2,522,778	2,510,528[1]	2,565,883[1]	2,499,976	2,468,296[1]	2,305,833[1]

*M_r value at σ_3 = 13.78 kPa, σ_d = 41.34 kPa; **M_{rt} value at σ_d = 41.34 kPa, σ_3 = 0 kPa; NA: Not Applicable; [1]Fatigue life lower than the fatigue life of asphalt concrete layer of same section

Table 7.6 Prediction of Fatigue Life of Stabilized Subgrade Layer Using Equation Recommended By Prozzi and Aguiar-Moya (2010)

Thickness of Stabilized Subgrade Layer (mm)	Resilient Modulus in Compression, M_r (MPa)*				Resilient Modulus in Tension, M_{rt} (MPa)**		
	Raw V-soil (80)	V-soil + 6% Lime (715)	V-soil + 10% CFA (951)	V-soil +10% CKD (1,575)	V-soil + 6% Lime (611)	V-soil + 10% CFA (785)	V-soil + 10% CKD (916)
101.6	NA	5,353,535	5,034,215	5,074,530[1]	5,268,073	4,874,616	3,962,050
152.4		6,737,235	6,549,294	6,717,408[1]	6,629,684	6,341,663	5,456,599
203.2		7,913,533	7,797,960	8,027,574[1]	7,823,091	7,611,802	6,806,655
254.0		8,877,505	8,822,964	9,069,967[1]	8,776,046	8,635,489	7,922,318

*M_r value at σ_3 = 13.78 kPa, σ_d = 41.34 kPa; **M_{rt} value at σ_d = 41.34 kPa, σ_3 = 0 kPa; NA: Not Applicable; [1]Fatigue life lower than the fatigue life of asphalt concrete layer of same section

Table 7.7 Prediction of Fatigue Life of Asphalt Concrete Layer Using MEPDG Transfer Function

Thickness of Stabilized Subgrade Layer (mm)	Resilient Modulus in Compression, M_r (MPa)*				Resilient Modulus in Tension, M_{rt} (MPa)**		
	Raw V-soil (80)	V-soil + 6% Lime (715)	V-soil + 10% CFA (951)	V-soil +10% CKD (1,575)	V-soil + 6% Lime (611)	V-soil + 10% CFA (785)	V-soil + 10% CKD (916)
101.6	NA	460,580	1,003,161	6,170,499	392,573	760,544	899,744
152.4		960,093	2,434,920	20,869,618	809,347	1,771,250	2,125,887
203.2		1,451,999	4,013,787	36,589,815	1,201,682	2,802,381	3,441,992
254.0		1,864,465	5,030,228	48,618,672	1,524,547	3,547,747	4,414,530

*M_r value at σ_3 = 13.78 kPa, σ_d = 41.34 kPa; **M_{rt} value at σ_d = 41.34 kPa, σ_3 = 0 kPa; NA: Not Applicable;
Note: Fatigue life: $N_f = 0.00432xk_1'xC(1/\varepsilon_{ta})^{3.9492}(1/M_{ra})^{1.281}$ where k_1' = 262, C = -1.55, ε_{ta}: tensile strain below asphalt concrete layer; M_{ra}: modulus of asphalt concrete layer (500,000 psi)

Table 7.8 Traffic Characteristics

Parameter	Value
Two-way annual average daily traffic AADT	11,378 (M,E)
Number of Lanes in Design Direction	2 (M,E)
Percent Heavy Trucks (of ADT) FHWA Class 4 or Higher*	3% (M,E)
Initial two-way AADTT	341 (M,E)
AADTT Vehicle Class Distribution (Class 9)	100% (M)
AADTT Vehicle Class Distribution (All Other Class)	0% (M)
Axle Load Distribution Factor (Class 9) 18,000 lbs	100% (M)
Axle Load Distribution Factor (Class 9) All Other	0% (M)
Design Lane Width	3.65 m (12 ft) (M)
Percent of All Trucks in Design Lane	80% (M,E)
Percent Trucks in Design Direction	50% (M,E)
Traffic Operation Speed	96 km/h (60 mph) (M)
Tire Pressure	827 kPa (120 psi) (M)
Mean Wheel Location	457.2 mm (18 in) (M)
Traffic Wander Standard Deviation	254 mm (10 in) (M)
Average Initial Truck Factor (ESALs/truck)	2.338 (E)
Annual Truck Volume Growth Rate (Compound Growth)	1.5% (M,E)
Total Calculated Cumulative ESALs	3,138,596 (E)

M: MEPDG Input; E: AASHTO 1993 Input; Only class 9 vehicles are considered

Table 7.9 Reliability and Serviceability

Parameter	Value
Reliability Level	90% (M,E)
Overall Standard Deviation	0.46 (E)
Initial Serviceability	4.2 (E)
Terminal Serviceability	3.0 (E)
Design Roadbed Resilient Modulus (MPa) (V-soil)	80 (E)
Drainage Factor for Layer Coefficient (Fair to Good)	1.0 (E)

M: MEPDG Input; E: AASHTO 1993 Input;

Table 7.10 Properties of Asphalt Concrete for Pavement Design

Parameter	Value
Mix Type	S3
Binder Type	PG 64-22 (M)
Binder Content (V_b)	4.1% (M)
Percent Passing 1 in Sieve	100% (M)
Percent Passing ¾ in Sieve	98% (M)
Percent Passing 3/8 in Sieve	80% (M)
Percent Passing No. 4 Sieve	58% (M)
Percent Passing No. 200 Sieve (P_{200})	2.9% (M)
Percent Air Voids (V_a)	7.0% (M)
Total Unit Weight	20.91 kN/m^3 (M)
Poisson's Ratio	0.35 (M)
Reference Temperature (T)	70 ^{o}F (M,E)
Tensile Strength	2,756 kPa
Applied Stress (Elastic Analysis of Pavement Configuration shown in Figure 7.1)	90 – 1,034 kPa
Stress Ratio (S)	0.030 – 0.375
Resilient Modulus in Indirect Tension (Navaratnarajah, 2006) at 70^{o}F (Frequency = 10 Hz) (M_{ra})*	2,746 – 3,552 MPa
Average Resilient Modulus in Indirect Tension (70^{o}F)	3,149 MPa (E)
Structural Layer Coefficient (Asphalt Concrete) mm^{-1}	0.0176 mm^{-1}(E)
Dynamic Modulus Master Curve from AASHTO 2002 MEPDG	See Figure 7.7 (M)
Dynamic Modulus Value (Frequency = 10 Hz)	7,727 MPa

*M_{ra} = (3048.96-23.12T-148.36V_a-280.39V_b+443.04P_{200}) x (0.803-0.010T+0.053V_a)^S; M: MEPDG Input; E: AASHTO 1993 Input

Table 7.11 Input Parameters for Stabilized Subgrade and Subgrade

Parameter	Value
Subgrade	
Design Roadbed Resilient Modulus (MPa) (V-soil)	80 MPa (M,E)
Drainage Factor for Layer Coefficient (Fair to Good)	1.0 (E)
Poisson's Ratio	0.4 (M)
Gradation, Atterberg Limits	See Table 2.2 (M)
Maximum Dry Unit Weight and Optimum Moisture Content	See Table 2.8 (M)
Stabilized Subgrade	
Design Resilient Modulus	See Table 7.12 (M,E)
Drainage Factor for Layer Coefficient (Fair to Good)	1.0 (E)
Structural Layer Coefficient, a*	See Table 7.12 (E)
Poisson's Ratio	0.2 (M)
Modulus of Rupture	See Table 6.7 (M)
Unit Weight	See Table 2.8 (M)

M: MEPDG Input; E: AASHTO 1993 Input; *a = 0.227log (M_r)-0.839 (where, M_r: psi, a: in^{-1})

Table 7.12 Pavement Design Matrix and Sections Using AASHTO 1993 and MEPDG Analysis

Section Number	**S1**	**S2**	**S3**	**S4**	**S5**	**S6**	**S7**	**S8**
Soil Type[1]	V-soil	V-soil	V-soil	V-soil	V-soil	V-soil	K-soil	K-soil
Additive Type	Lime	CFA	CKD	Lime	CFA	CKD	Lime	Lime
Percent	6	10	10	6	10	10	3	6
M_r or M_{rt}	M_r	M_r	M_r	M_{rt}	M_{rt}	M_{rt}	M_r	M_r
Design M_r (MPa)	715	951	1,575	611	785	916	1,017	1,081
a (mm^{-1})	0.0118	0.0129	0.0149	0.0112	0.0122	0.0128	0.0132	0.0134
SN	3.87	3.87	3.87	3.87	3.87	3.87	4.48	4.48
D_E $(mm)^2$	117.9	108.0	90.7	122.9	115.1	109.7	140.5	138.4
D_M $(mm)^2$	180.3	162.3	127.0	187.8	175.3	165.1	139.7	138.4
D_K $(mm)^2$	381.0	406.4	431.8	393.7	419.1	469.9	NA	NA
Section Number	**S9**	**S10**	**S11**	**S12**	**S13**	**S14**	**S15**	**S16**
Soil Type[1]	K-soil	K-soil	K-soil	K-soil	K-soil	K-soil	K-soil	K-soil
Additive Type	Lime	CFA	CFA	CFA	CKD	CKD	CKD	None
Percent	9	5	10	15	5	10	15	0
M_r or M_{rt}	M_r	M_r	M_r	M_r	M_r	M_r	M_r	M_r
Design M_r (MPa)	719	435	801	948	291	1,122	1,880	56
a (mm^{-1})	0.0118	0.0099	0.0122	0.0129	0.0083	0.0135	0.0155	NA
SN	4.48	4.48	4.48	4.48	4.48	4.48	4.48	4.48
D_E $(mm)^2$	152.4	169.4	149.1	142.7	182.4	137.7	119.9	254.8
D_M $(mm)^2$	165.1	182.9	157.5	147.32	195.6	134.6	73.7	228.6

M_r: Resilient Modulus in Compression; M_{rt}: Resilient Modulus in Tension; a: Structural Layer Coefficient; a = 0.227log (M_r)-0.839 (where, M_r: psi, a: in^{-1}); SN: Structural Number (for AASHTO 1993 Design); D_E: Required asphalt concrete thickness using AASHTO 1993 Design; D_M: Required asphalt concrete thickness using new MEPDG; D_K: Required asphalt concrete thickness using KENLAYER (Eqn. 6.18); NA: Not Applicable; [1]Roadbed soil is raw V-soil for Sections 1 through 6 and K-soil for Sections 7 through 16; [2]Thickness of stabilized subgrade layer = 152.4 mm

Table 7.13 Comparison of the Effect of Reliability Levels in Pavement Design on Sections S4, S13 and S16

Section Number	Reliability Level	Design Structural Number (SN)	Required AC Thickness (AASHTO 1993) (mm)	Required AC Thickness (MEPDG) (mm)
S4	80	3.54	104.1	165.1
	90	3.87	122.9	187.8
	95	4.15	138.4	203.2
S13	80	4.13	162.6	180.3
	90	4.48	182.4	195.6
	95	4.77	199.1	208.3
S16	80	4.13	235.0	213.4
	90	4.48	254.8	228.6
	95	4.77	271.3	238.8

AC: Asphalt Concrete; MEPDG: Mechanistic-Empirical Pavement Design Guide

Table 7.14 Cost Comparisons for Constructing Stabilized Subgrade Layer in Norman, OK

Section No.	Additive Type	Percent	Dry Density (kN/m^3)	Soil/Agg Weight (tons)	Additive Weight (tons)	Additive Cost ($ per tons)[1]	Freight Cost ($ per tons)[1]	Total Cost ($)
Type A Agg Base[2]	None	100	22.7	1,088	0	6.5	10.50	18,488
S7	Lime	3	17.0	813	24	123	23.20	3,566
S8	Lime	6	16.8	800	48	123	23.20	7,013
S9	Lime	9	16.3	779	70	123	23.20	10,244
S10	CFA	5	17.4	831	42	36	21.92	2,407
S11	CFA	10	17.4	833	83	36	21.92	4,822
S12	CFA	15	17.5	836	125	36	21.92	7,265
S13	CKD	5	17.3	827	41	19	20.55	1,634
S14	CKD	10	17.1	815	81	19	20.55	3,221
S15	CKD	15	16.9	809	121	19	20.55	4,796

Roadway width = 9.144 m (30 ft); Thickness of stabilized subgrade layer = 152.4 mm (6 in); Road length = 305 m (1000 ft); [1]Cost provided by Lafarge North America, Tulsa for CKD and CFA, Texas Lime Company for lime, and Dolese Bros Co, Davis for aggregate; [2]152.4 mm (6 in) thick ODOT Type A aggregate base (Solanki et al, 2009c); Agg: Aggregate

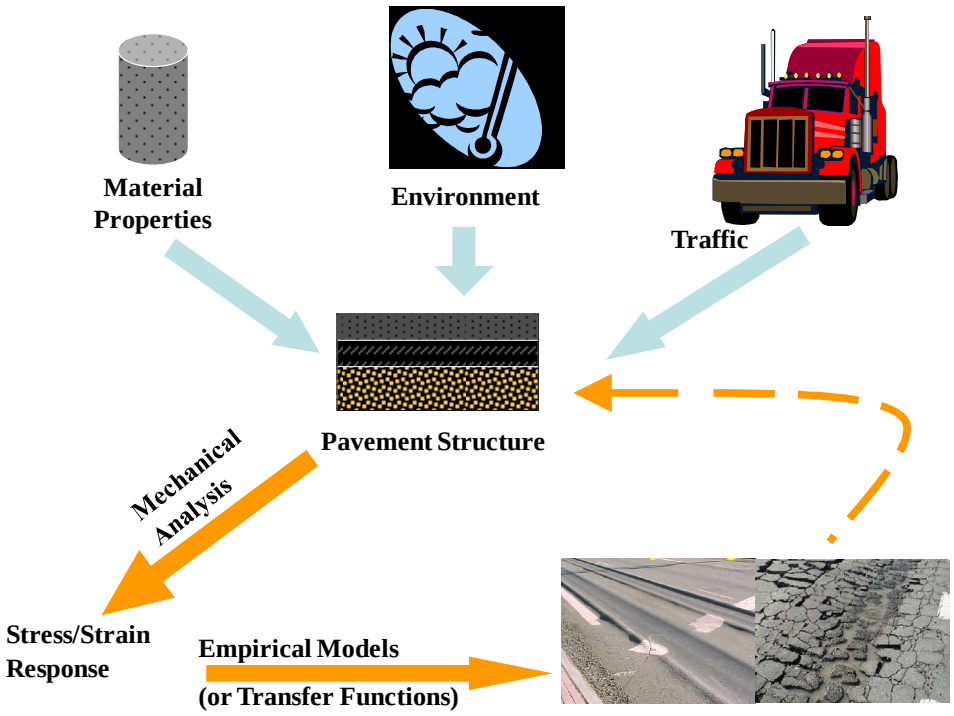

Figure 7.1 Schematic Summary of Mechanistic-Empirical Pavement Design

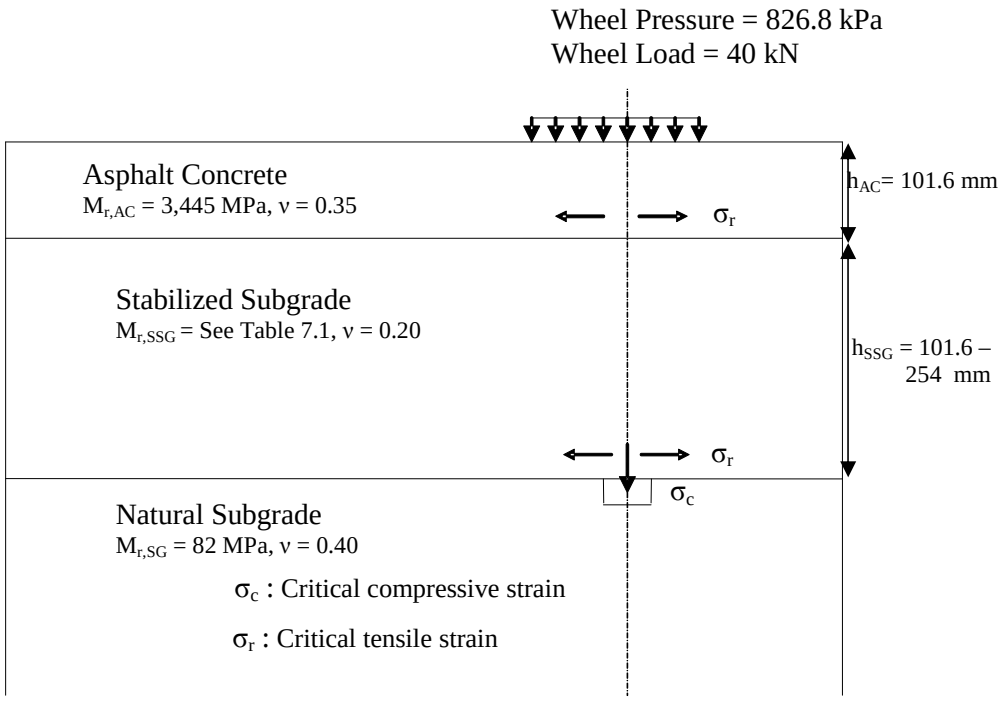

Figure 7.2 Pavement Configuration with Stabilized Subgrade Layer

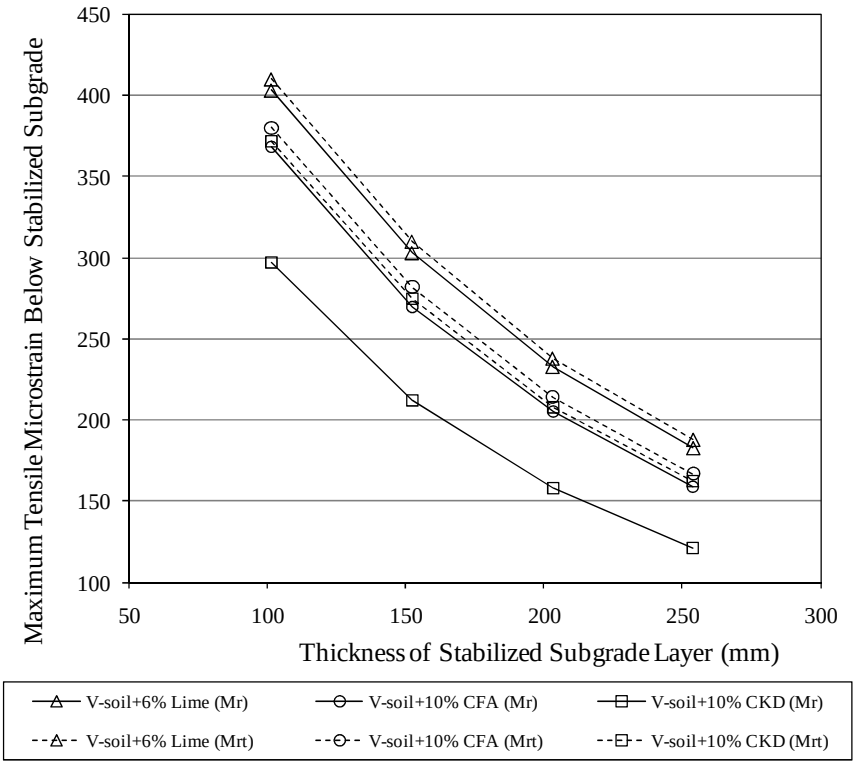

Figure 7.3 Variations in Tensile Strain Below Stabilized Subgrade Layer with Stabilized Subgrade Thickness

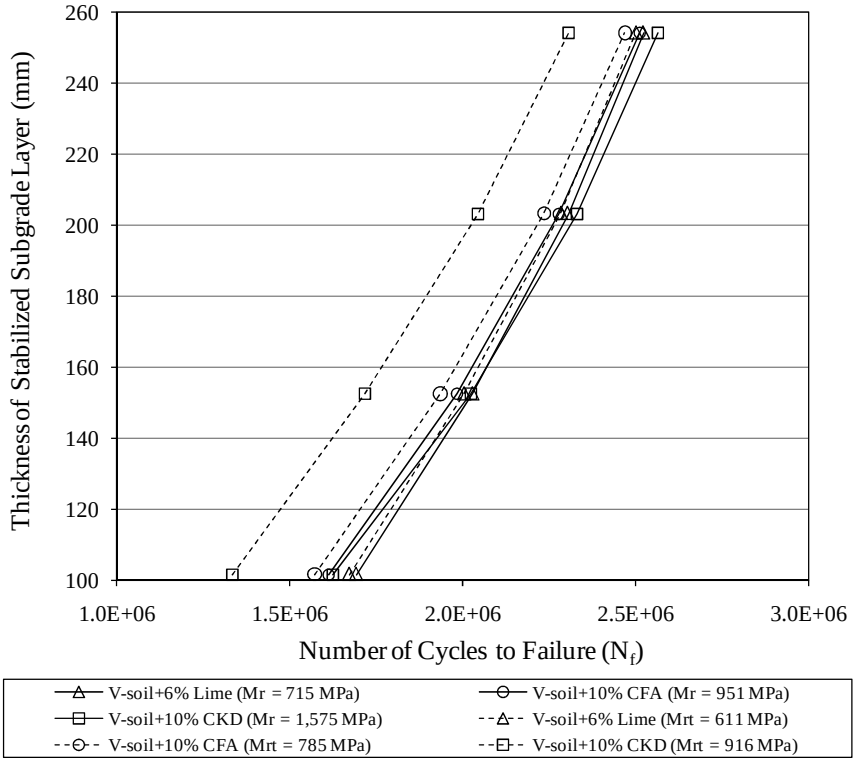

Figure 7.4 Thickness Design Curves for Stabilized Subgrade Layer Using Equation 6.18

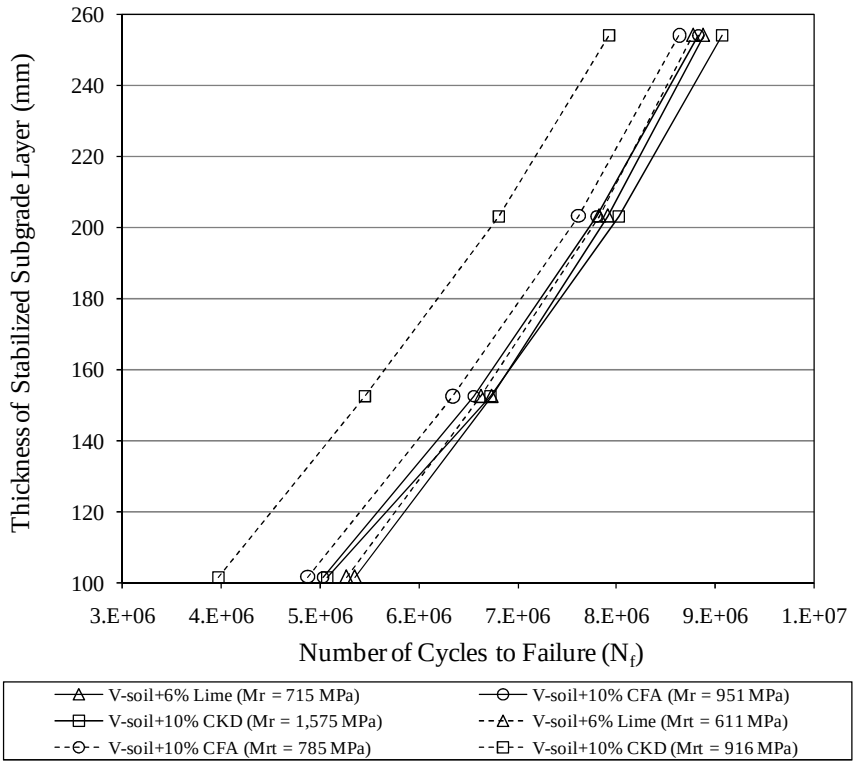

Figure 7.5 Thickness Design Curves for Stabilized Subgrade Layer Using Equation Recommended By Prozzi and Aguiar-Moya (2010)

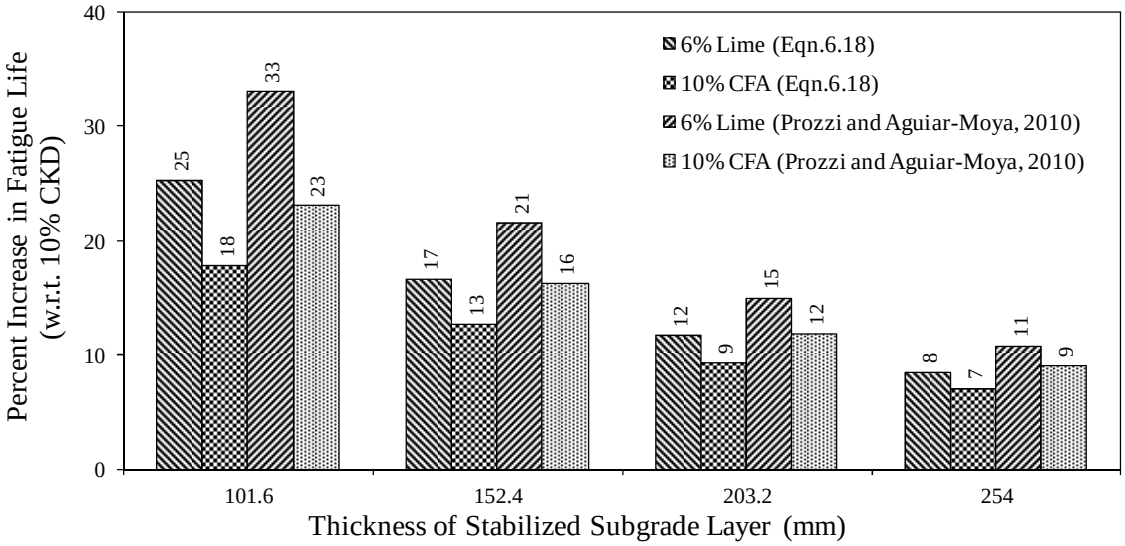

Figure 7.6 Percent Increase in Fatigue Life of 6% Lime- and 10% CFA-Stabilized Sections w.r.t Corresponding 10% CKD-Stabilized Sections

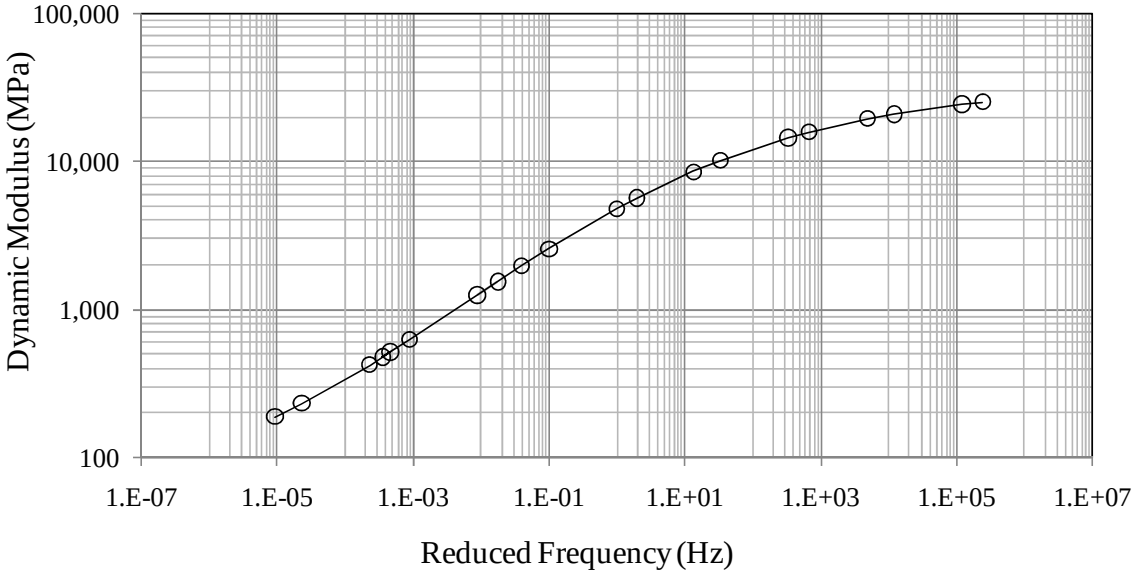

Figure 7.7 Dynamic Modulus Master Curve for Asphalt Concrete Mix from MEPDG

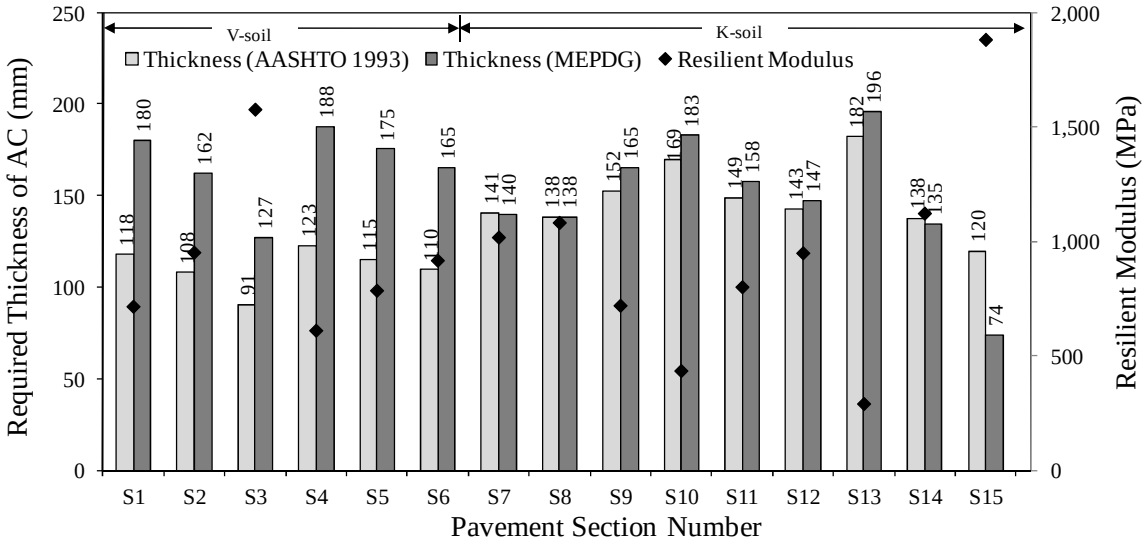

Figure 7.8 Required AC Thicknesses for Different Sections Using AASHTO 1993 and MEPDG

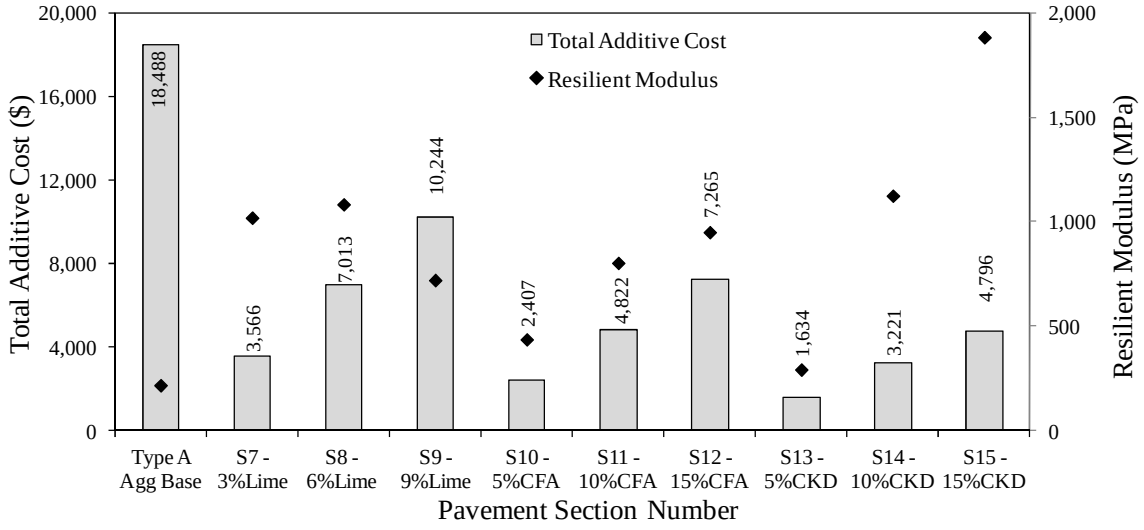

Figure 7.9 Total Additive Cost and Resilient Modulus of Different Sections

CHAPTER 8

SUMMARY AND RECOMMENDATIONS

8.1 Summary

The evaluation of engineering properties indicating short- and long-term performance of pavement is important for overall characterization of cementitiously stabilized subgrade soils. Variation in pavement performance with time indicates possible changes in the engineering properties of pavement materials.

In this study, the effect of type and amount of additive on the short-term performance in terms of material properties recommended by new MEPDG was examined. Four soils commonly encountered as subgrades in Oklahoma were utilized: (1) Port Series (P-soil); (2) Kingfisher Series (K-soil); (3) Vernon Series (V-soil); and (4) Carnasaw Series (C-soil). Cylindrical specimens stabilized with lime (3%, 6% and 9%), CFA (5%, 10% and 15%) and CKD (5%, 10% and 15%) were molded, cured for 28 days, and then subjected to different stress sequences to study the M_r followed by M_E and UCS test. Results showed that all the three additives improved the M_r, M_E and UCS values of P-, K-, V- and C-soil specimens; however, degree of improvement varied with the type of additive and soil. For CFA- and CKD-stabilization, the amount of improvement increases with increase in the additive content; however, a reduction in M_r, M_E and UCS values was observed beyond a certain percentage of lime content (between 6 – 9% for K- and C-soil, between 3 – 6% for V-soil). At lower application rates (3% to 6%), lime showed highest improvement in the M_r values. At higher application rates (> 10%), CKD provided maximum enhancements. The M_r values of stabilized soil specimens were found to have relatively low sensitivity towards change in stress level as compared to

untreated specimens. It was also found that the percentage of increase in M_r values correlate better with soil properties – cation exchange capacity; additive properties – free-lime content, alkali content, loss on ignition, percent passing No. 325 sieve, specific surface area, pH; and soil-additive mixture properties – silica sesquioxide ratio. Further, microscopic analysis confirmed the formation of reaction products such as C-S-H, C-A-S-H and ettringite which contributed to strength and stiffness development of stabilized soil specimens.

The long-term performance (or durability) of stabilized soil specimens was evaluated by conducting freeze-thaw (F-T) cycling, vacuum saturation and tube suction tests on 7-day cured P-, K- and C-soil specimens stabilized with 6% lime, 10% CFA and 10% CKD. Also, specimens were capillary-soaked for 60 days and tested for M_r, as an additional indicator for evaluating long-term performance. This study is motivated by the fact that during the service life of pavement stabilized layers are subjected to F-T cycles and moisture variations. Results showed that UCS values of all the specimens decreased with increase in the number of F-T cycles. Such a decrease could be explained by the increase in moisture absorbed by specimen during the thawing portion of the cycle and pore structure of the stabilized specimen. For the different percentages and types of additives used in this study, results showed that lime offers highest resistance against F-T cycles for lean clay (K-soil) and fat clay (C-soil). On the other hand, CKD-stabilization is more effective with silty clay (P-soil) against damage caused by F-T cycles. A similar qualitative trend of behavior was observed for retained UCS after vacuum saturation test. It was also found that the 12 F-T cycles are more severe than the vacuum saturation test for the particular soils used in this study. A strong correlation was observed between

UCS values retained after vacuum saturation and F-T cycles. The final dielectric constant values (DV) measured by conducting tube suction test are influenced by the method of specimen preparation. Stabilization with 10% CFA is more effective in reducing the DV of silty clay specimens followed by 6% lime. However, 6% lime proved more effective in reducing DV of lean clay and fat clay specimens. On the contrary, 10% CKD was found to show no significant improvement in DVs for the soils used in this study. After capillary soaking, 6% lime-stabilization of lean clay and fat clay showed the best performance by providing highest M_r values. With silty clay, the degree of effectiveness after capillary soaking was found more for 10% CFA-stabilized specimens than corresponding 6% lime-stabilized specimens. Contrary to short-term performance, CKD-stabilized specimens showed the worst long-term performance after 60-day capillary soaking. Also, the different test procedures employed in this study are expected to benefit future studies in this area.

The long-term performance of natural sulfate bearing lean clay (V-soil) specimens stabilized with high (lime), low (CFA), and moderate (CKD) calcium-based additives were evaluated by subjecting specimens to 120 days of capillary soaking. During soaking, specimens were tested for 3-D swell to compare the effect of additive type on the phenomenon of sulfate-induced heave. After 120 days of capillary soaking, specimens were further tested for M_r, M_E, and UCS. It was found that after 120 days of capillary soaking, raw and all stabilized specimens showed reduction in M_r, UCS, and M_E values. For example, M_E and UCS values of lime-, CFA- and CKD-stabilized specimens showed decrease ranging between approximately 86 – 89%, 31 – 92%, and 77 – 95% due to 120 days of capillary soaking. Overall, the 15% CKD-stabilized specimen (moderate

calcium-based additive) showed the highest improvement after 28 days of curing, while the 15% CFA-stabilized specimen (low calcium-based additive) showed the highest M_r, UCS, and M_E values after 120 days of capillary soaking. For CFA-stabilization, the amount of improvement after capillary soaking increased with increase in the additive content; however, a reduction in M_r, M_E and UCS values was observed beyond a certain percentage of lime or CKD content (between 3 – 6% for lime, between 10 – 15% for CKD). Three-dimensional swelling test showed an increase in volume for lime- (22.3% for 9% lime) and CKD-stabilized (6.4% for 15% CKD) specimens, while a reduction in volume for the CFA-stabilized specimen, as compared to raw sulfate bearing clay specimens. This increase in volume is attributed to sulfate-induced heaving which results in the formation of expansive mineral ettringite. Further, the presence of ettringite was verified using SEM/EDS tests in conjunction with XRD analyses. Also, pH value greater than 10.0 (or calcium content) and availability of moisture were verified as two dominant factors required for sulfate-induced heaving.

For Level 2 design of pavements, a total of four stress-based statistical models and two feed-forward-type ANN models, were evaluated to correlate resilient modulus with specimen characteristics and soil/additive properties. The M_r data of stabilized P-, V- and C-soil was used for evaluation/development of different models, whereas M_r data of K-soil was used for the validation of the models. Specifically, one semi-log (σ_3, σ_d) and three log-log (θ, σ_d; σ_3, σ_d; θ, τ_{oct}) stress-based statistical models were evaluated. The log-log model recommended by AASHTO 2002 Design Guide (θ, τ_{oct}) for unbound materials was found to show the least acceptable performance. Further, all three stress-based statistical models were validated by using additional M_r data of stabilized K-soil

specimens. Overall, a semi-log (σ_3, σ_d) model was found to show best acceptable performance with the highest R^2 value (0.98) and lowest average S_e/S_y value of 0.48. From the correlations of best performing statistical model (Model 3), it appears that the model constants for 28-day M_r were mainly governed by compacted specimen characteristics – UCS, molding moisture content, molding dry unit weight, percentage of additive, silica sesquoxide ratio of soil-additive mixture; soil properties –clay content, pH, cationic exchange capacity; and additive properties – silica content, calcium oxide, magnesium oxide content, loss on ignition. For the RBFN model, with one hidden layer, the R^2 value for the development/evaluation dataset showed worst performance (0.62) among all the statistical and ANN models used in this study. The R^2 value of the MLPN model with one hidden layer was found to be 0.99 for evaluation/development dataset. Overall, the MLPN model was found to be the best model for the present development/evaluation and validation datasets. This model as well as the other models could be refined using an enriched database.

Further, the effect of type of additive on indirect tensile and fatigue characteristics of stabilized P- and V-soil was evaluated. This study is based on the fact that stabilized layer is subjected to tensile stresses under wheel loading. Cylindrical specimens stabilized with 6% lime, 10% CFA and 10% CKD were molded using a Superpave gyratory compactor, cured for 28 days and subjected to different stress sequences in indirect tension to study the M_{rt}. On the other hand, 6% lime-, 10% CFA- and 10% CKD-stabilized beam specimens were compacted using a Linear Kneading Compactor and subjected to repeated cycles of reloading-unloading after 28 days of curing in a four-point beam fatigue apparatus for evaluating fatigue life and flexural stiffness. It was found that

all three additives improved the M_{rt}, σ_t and MOR values of P- and V-soil specimens; however, degree of improvement varied with the type of additive and soil. Overall, specimens stabilized with 10% CKD provided highest M_{rt} values with both silty (P-soil) and lean clay (V-soil). The test results suggested that the M_{rt} depends on the applied load. Based on the test results, the M_{rt} decreased with increases in stress ratio. The magnitude of resilient modulus in tension is lower than it is in compression, consistent with the studies conducted by other researchers on cementitiously stabilized materials. For both silty clay and lean clay specimens, 10% CKD provided highest increase in tensile strength values followed by 10% CFA and 6% lime. Correlations developed between indirect tensile strength, MOR and UCS suggest that σ_t can be estimated as approximately 16% of UCS. On the other hand, MOR is approximately 41% of UCS. The beams stabilized with 10% CKD exhibited greater initial stiffness value, but its stiffness reduced more rapidly than 6% lime-stabilized beams under repeated load. The fatigue life tests conducted on beam specimens showed that the mean fatigue life of P-soil beams stabilized with 6% lime is greater than 2 million cycles. On the other hand, beams of silty clay stabilized with 6% lime failed at relatively a low N_f value (approximately 50). The 6% lime- and 10% CKD-stabilized beams of lean clay exhibited mean fatigue life of 1,430,000 and 965,000, respectively. A strain-based model was proposed for predicting fatigue life of cementitiously stabilized soil and comparisons were made with the existing model in the literature. This model could be refined using an enriched database. Although CKD-stabilized specimens showed best performance in enhancing the indirect tensile characteristics (M_{rt}, σ_t) and MOR, worst performance was observed in the fatigue life tests.

In order to illustrate the application of the evaluated engineering properties, the design curves for fatigue performance prediction of stabilized layers were developed for different stabilized pavement sections. Further, *semi-rigid* flexible pavement designs of different sections between the empirical AASHTO 1993 and the mechanistic-empirical MEPDG pavement design methodology were compared. It was found that the selection of resilient modulus value is very important for predicting the fatigue life of *semi-rigid* pavement. The sections utilizing M_r values consistently showed higher fatigue life as compared to sections utilizing M_{rt} values. The sections stabilized with 6% lime showed highest resistance towards fatigue failure followed by 10% CFA and 10% CKD. Increase in the stiffness (M_r) of stabilized layer increased the fatigue life of asphalt concrete layer. The degree of influence of selection of resilient modulus in compression or tension mode is dependent on the design method (i.e., AASHTO 1993 and MEPDG). The fatigue life prediction for all the pavement sections showed that a relatively thicker AC section is required for preventing fatigue failure of stabilized subgrade layer. The new MEPDG showed comparatively less sensitiveness towards change in reliability level as compared to AASHTO 1993 design methodology. At similar M_r level, CKD-stabilization provided economically low cost sections as compared to lime- and CFA-stabilization.

8.2 Recommendations

Based on the observations from this study, the following recommendations are made for future studies:

1. As indicated in this study, only short-term properties such as strength (UCS) and stiffness (M_r, M_E) alone can be misleading. In the present study, for example, CKD showed highest acceptable short-term performance but poor long-term performance.

It is also worth noticing that properties of CKD can vary significantly from plant to plant depending on the raw materials and type of collection process used (Miller and Zaman, 2000). Similarly, fly ash properties may be unique to same source while it may differ from ashes obtained from other sources (Ferguson and Levorson, 1999). These differences in physical and chemical properties can lead to different short- and long-term performances of stabilized soil specimens. Hence, it is recommended that a proper mix design be done with locally available traditional stabilizers considering all the short- and long-term performance parameters. Such designs, including the type and amount of additive, will ensure compatibility and satisfactory shot- and long-term performance.

2. Although CKD might help by increasing properties such as M_r and UCS, it can negatively influence the fatigue life of stabilized subgrade and hence performance and the service life of the pavement. Therefore, it is recommended that future studies be conducted focusing on the evaluation of fatigue parameters for different soil types stabilized with different percentage and types of cementitious additives. Also, field studies should be conducted for comparing performance of stabilized subgrade layer in laboratory and field.
3. This study projected relatively low calcium-based additive, CFA, showing best acceptable performance with sulfate bearing soil. However, this study was limited to only one soil (V-soil) from northwestern Oklahoma. Further, short- and long-term performance of CFA should be evaluated with other sulfate bearing soils. Also, full-scale test sections should be built to test this hypothesis in the field.

4. The combined development and evaluation dataset in this study consisted of 160 soil specimens consisting of four soils stabilized with three additives namely, lime, CFA and CKD. It is recommended that these datasets be enriched by adding additional sites from throughout Oklahoma. It is suggested that different geological features be considered in selecting additional sites. Training the statistical and ANN models using an enriched dataset is likely to improve the predictive capabilities of these models. Also, as the datasets include more soils from different locations, the models will become more representative of diversity in Oklahoma soils.
5. It is recommended to develop a field testing program to measure pavement distresses at the selected representative *semi-rigid* type flexible pavement sites and compare field data to MEPDG distress predictions. The field data in combination with laboratory data will be essential for eventual calibration of the MEPDG for *semi-rigid* pavements.

REFERENCES

AASHTO (1986). *Guide for Design of Pavement Structures*, Transportation Research Board, National Research Council, Washington, DC.

AASHTO (1993). *Guide for Design of Pavement Structures*, Transportation Research Board, National Research Council, Washington, DC.

AASHTO (2004). "Guide for Mechanistic-Empirical Design of New and Rehabilitated Pavement Structures," *Final Report prepared for National Cooperative Highway Research Program (NCHRP) 1-37A*, Transportation Research Board, National Research Council, Washington DC.

AASHTO (2009). *Rough Road Ahead: Fix Them Now or Pay For It Later*, Transportation Research Board, National Research Council, Washington, DC.

Achampong, F. (1996). "Evaluation of Resilient Modulus for Lime and Cement Stabilized Synthetic Cohesive Soils," PhD Thesis, Wayne State University, Detroit, MI.

Achampong, F., Usmen, M., and Kagawat, T. (1997). "Evaluation of Resilient Modulus for Lime- and Cement-Stabilized Synthetic Cohesive Soils," *Transportation Research Record: Journal of the Transportation Research Board*, Vol. 1589, pp. 70 – 75.

Adams, A. G. (2008). "Sulfate Induced Heave in Lime-Stabilized Soils," MS Thesis, University of Oklahoma, Norman, OK.

Adaska, W. S., and Luhr, D. R. (2004). "Control of Reflective Cracking in Cement Stabilized Pavements," *Proceedings of 5th International RILEM Conference on Cracking in Pavements: Mitigation, Risk Assessment and Prevention*, Limognes, France.

Adek (2007). *Operating Instructions and Technical Data*, Percometer v.7, Estonia.

Agostinacchio, M. L., Ciampa, D. and Olita, S. (2008). "Cracking Response and Service Life Prediction of Flexible and Semi-Rigid Road Pavements Implementing M-E PDG 2002 code," *Proceedings of 6th RILEM International Conference on Cracking in Pavements*, Chicago, IL, pp. 201 – 210.

Air Force Manual (AFJMAN) (1994). "Soil Stabilization for Pavements," *Technical Manual No. 5-822-14*, Departments of the Army and Air Force, Washington, DC.

Ali, F. H. (1992). "Stabilization of a Residual Soil," *Soils and Foundations*, Vol. 32, No. 4, pp. 178 – 185.

Al-qadi, I. and Nassar, W. N. (2003). "Fatigue Shift Factors to predict HMA Performance," *International Journal of Pavement Engineering*, Vol. 4, No. 2, pp. 69 – 76.

Al-Rawas, A. A., Taha, R., Nelson, J. D., Al-Shab, T. B., and Al-Siyabi, H. (2002). "A Comparative Evaluation of Various Additives Used in the Stabilization of Expansive Soils," *ASTM Geotechnical Testing Journal*, Vol. 25, No. 2, pp. 199 – 209.

Al-Shamrani, M. A., and Al-Mhaidib, A. (2000). "Swelling Behavior under Oedometric and Triaxial Loading Conditions," *Geotechnical Special Publication*, Vol. 99, pp. 344-360.

Andrei, D., Witczak, M. W., Schwartz, C. W. and Uzan, J. (2004). "Harmonized Resilient Modulus Test Method for Unbound Pavement Materials," *Transportation Research Record: Journal of the Transportation Research Board*, Vol. 1874, pp. 29 – 37.

Arellano, D., and Thompson, M. R. (1998). "Stabilized Base Properties (Strength, Modulus, Fatigue) for Mechanistic-Based Airport Pavement Design," *Final Report, COE Report No. 4*, Center of Excellence for Airport Pavement Research, University of Illinois, Urbana, IL.

Arora, S., and Aydilek, A. H. (2005). "Class F Fly-Ash-Amended Soils as Highway Base Materials." *ASCE Journal of Materials in Civil Engineering*, Vol. 17, No. 6, pp. 640 – 649.

Baghdadi, Z. A. (1990). "Utilization of Kiln Dust in Clay Stabilization," *J. King Abdulaziz Univ.: Eng Sci*, Vol. 2, pp. 53 – 163.

Baghdadi, Z. A., and Rahman, M. A. (1990). "The Potential of Cement Kiln Dust for the Stabilization of Dune Sand in Highway Construction," *Building and Environment*, Vol. 25, No. 4, pp. 285 – 289.

Baghdadi, Z. A., Fatani, M. N., and Sabban, N. A. (1995). "Soil Modification by Cement Kiln Dust," *ASCE Journal of Materials in Civil Engineering*, Vol. 7, No. 4, pp. 218 – 222.

Balbo, J. T., and Cintra, J. P. (1994). "Fatigue Verification Criteria for Semi-rigid Pavements," http://www.ptr.usp.br/lmp/download/fatcri.PDF, Last accessed: Nov., 2007.

Barbu, B. G. and Scullion, T. (2005). "Repeatability and Reproducibility Study for Tube Suction Test," *Report 5-4114-01*, Final report submitted to Texas Transportation Institute, College Station, TX.

Barbu, B., and McManis, K. (2005). "Study of Problematic Silts Stabilization," *Transportation Research Board 84th Annual Meeting*, CD-ROM Publication, Transportation Research Board, Washington, DC.

Barbu, B., McManis, K. and Nataraj, M. (2004). "Study of Silts Moisture Susceptibility Using the Tube Suction Test," *Transportation Research Board 83rd Annual Meeting*, CD-ROM Publication, Transportation Research Board, Washington, DC.

Barksdale, R. D., Alba, J., Khosla, N. P., Kim, R., Lambe, P. C., and Rahman, M. S. (1997). "Laboratory Determination of Resilient Modulus for Flexible Pavement Design," *Final Report Prepared for NCHRP Project 1-28*, National Cooperative Highway Research Program, Transportation Research Record, National Research Council, Washington, DC.

Bhattacharya, P. G. and Pandey, B. B. (1986). "Flexural Fatigue Strength of Lime-Laterite Soil Mixtures," *Transportation Research Record: Journal of the Transportation Research Board*, Vol. 1089, pp. 86 – 92.

Bhatty, J. I., Bhattacharja, S., and Todres, H. A. (1996). "Use of Cement Kiln Dust in Stabilizing Clay Soils," Portland Cement Association, Skokie, IL.

Bin-Shafique, S., Edil, T., and Benson, C. (2004). "Incorporating a Fly Ash Stabilized Layer into Pavement Design Case Study," *Geotechnical Engineering*, Vol. 157, No. 4, pp. 239 – 249.

Bishop C (1995). *Neural Networks for Pattern Recognition*, University Press, Oxford, United Kingdom.

Camargo, F. F., Edil, T. B., and Benson, C. H. (2009). "Strength and Stiffness of Recycled Base Materials Blended with Fly Ash," *Transportation Research Board 88th Annual Meeting*, CD-ROM Publication, Transportation Research Board, Washington, DC.

Canakci, H., and Pala, M. (2007). "Tensile Strength of Basalt from a Neural Network," *Engineering Geology*, Vol. 94, pp. 10 – 18.

Carvalho, R. L., and Schwartz, C. W. (2006). "Comparisons of Flexible Pavement Designs AASHTO Emprical Versus NCHRP Project 1-37A Mechanistic-Empirical," *Transportation Research Record: Journal of the Transportation Research Board*, Vol. 1947, pp. 167 – 174.

Cerato, A. B., and Lutenegger, A. J. (2002). "Determination of surface are of fine-grained soils by the ethylene glycol monoethyl ether (EGME) method," *ASTM Geotechnical Testing Journal*, Vol. 25, No. 3, pp. 1 – 7.

Chang, D.T. (1995). "Resilient Properties and Microstructure of Modified Fly Ash-stabilized Fine Grained Soils." *Transportation Research Record: Journal of the Transportation Research Board*, Vol. 1486, pp. 88 – 96.

Chapman, H. D. (1965). "Cation Exchange Capacity," *Methods of Soil Analysis*, American Society of Soil Agronomy, C. A. Black et al., Eds., Madison, WI, pp. 891 – 901.

Chaunsali, P., and Peethamparan, S. (2010). "Microstructural and Mineralogical Characterization of Cement Kiln Dust Activated Fly Ash Binder," *Transportation Research Board 89th Annual Meeting*, CD-ROM Publication, National Research Council, Washington, DC.

Choquette, M., Berube, M. –A., and Locat, J. (1987). "Mineralogical and Microtextural Changes Associated with Lime Stabilization of Marine Clays from Eastern Canada," *Applied Clay Science*, Vol. 2, pp. 215 – 232.

Collins, R. J., and Emery, J. J. (1983). "Kiln Dust/Fly Ash Systems for Highway Bases and Subbases," U.S. Department of Transportation – Department of Energy Report, FHWA/RD-82/167.

Consoli, N. C., Lopes, L. S., and Heineck, K. S. (2009). "Key Parameters for the Strength Control of Lime Stabilized Soils," *ASCE Journal of Materials in Civil Engineering*, Vol. 21, No. 5, pp. 210 – 216.

Cordon, W. A. (1962). "Resistance of Soil-Cement Exposed to Sulfates," *Highway Research Board Bulletin*, Transportation Research Board, Washington, DC.

Dai, S., and Zollars, J. (2002). "Resilient Modulus of Minnesota Road Research Project Subgrade Soil," *Transportation Research Record: Journal of the Transportation Research Board*, Vol. 1786, pp. 20 – 28.

Das, B. M., and Dass, R. N. (1995). "Lightly Cemented Sand in Tension and Compression," *Geotechnical and Geological Engineering*, Vol. 13, No. 3, pp. 169 – 177.

Dempsey, B. J., and Thompson, M. R. (1973). "Vacuum Saturation Method for Predicting Freeze-Thaw Durability of Stabilized Materials," *Highway Research Record*, Vol. 442, Highway Research Board, Washington, DC.

Diamond, S., and Kinter, E. B. (1964). "Mechanisms of Soil-Lime Stabilization," *Highway Research Record*, Vol. 92, pp. 83 – 96.

Drumm, E. C., Boateng-Poku, Y., Pierce, T. J. (1990). "Estimation of Subgrade Resilient Modulus from Standard Tests," *ASCE Journal of Geotechnical Engineering*, Vol. 116, No. 5, pp. 774 – 789.

Drumm, E. C., Reeves, J. S., Madgett, M. R., and Trolinger, W. D. (1997). "Subgrade Resilient Modulus Correction for Saturation Effects," *ASCE Journal of Geotechnical and Geoenvironmental Engineering*, Vol.123, No.7, pp. 663 – 670.

Dunlap, W. S. (1963). "A Report on a Mathematical Model Describing the Deformation Characteristics of Granular Materials," Technical Report 1, Project 2-8-62-27, TTI, Texas A&M University, TX.

Eades, J. (1962). "Reactions of $Ca(OH)_2$ with Clay Minerals in Soil Stabilization," PhD Thesis, University of Illinois, Urbana, IL.

El-Basyouny, M. M., and Witczak, M., (2005). "Development of the Fatigue Cracking Models for the 2002 Design Guide," *Transportation Research Board 84th Annual Meeting*, CD-ROM Publication, National Research Council, Washington, DC.

Elias, M. B. and Titi, H. H. (2006). "Evaluation of Resilient Modulus Model Parameter for Mechanistic-Empirical Pavement Design," *Transportation Research Record: Journal of the Transportation Research Board*, Vol. 1967, pp. 89 – 100.

Elliot, R. P., and Thornton, S. I. (1988). "Simplification of subgrade resilient modulus testing," *Transportation Research Record: Journal of the Transportation Research Board*, Vol. 1192, pp. 1 – 7.

Evangelos, S. (2006). "A Solution to the Problem of Predicting the Suitability of Silty-Clayey Materials for Cement-Stabilization," *Geotechnical and Geological Engineering*, Vol. 24, No. 2, pp. 379 – 398.

Fang H. Y. (1997). *Introduction to Environmental Geotechnology*, CRC Press, NY.

Far, M. S. S., Underwood, B. S., Ranjithan, S. R., Kim, Y. R., and Jackson, N. (2009). "The Application of Artificial Neural Networks for Estimating the Dynamic Modulus of Asphalt Concrete," *Transportation Research Board 2009 Annual Meeting*, CD-ROM Publication, Washington, DC

Far, M. S. S., Underwood, B. S., Kim, Y. R., Puccinelli, J. and Jackson, N. (2010). "Development of Artificial Neural Network Predictive Models for Populating the Dynamic Moduli of LTPP Sections," *Transportation Research Board 89th Annual Meeting*, CD-ROM Publication, Transportation Research Board, Washington, DC.

Farrar, M. J., and Turner, J. P. (1991). "Resilient modulus of Wyoming Subgrade Soils Mountain Plains," *Consortium Report No. 91-1*, The University of Wyoming, Laramie, WY.

Fausett, L. V. (1994). *Fundamentals neural networks: Architecture, Algorithms and Applications*, Prentice-Hall, Inc, Englewood Cliffs, NJ.

Federal Highway Administration (FHWA) (2009). http://www.tfhrc.gov/hnr20/recycle/waste/app5.htm, Last accessed: May, 2009.

Ferguson, G., and Levorson, S. M. (1999). "Soil and Pavement Base Stabilization with Self-Cementing Coal Fly Ash," Final Report for American Coal Ash Association, Alexandria, VA.

Foley, G., and Australian Stabilisation Expert Group (2001). "Mechanistic Design Issues for Stabilized Pavement Materials," *Contract report*, AUSTROADS, Rc91022-3.

Gabrisova, A., Havlica, J., and Sahu, S. (1991). "Stability of Calcium Sulphoaluminate Hydrates in Water Solutions with Various pH Values," *Cement and Concrete Research*, Vol. 21, No. 6, pp. 1023 – 1027.

George, K. P. (1992). "Resilient Testing of Soils using Gyratory Testing Machine," *Transportation Research Record: Journal of the Transportation Research Board*, Vol. 1369, pp. 63 – 72.

Ghosh, A., and Subbarao, C. (2001). "Microstructural Development in Fly Ash Modified with Lime and Gypsum," *ASCE Journal of Materials in Civil Engineering*, Vol. 13, No. 1, pp. 65 – 70.

Gnanendran, C. T., and Piratheepan, J. (2008). "Characterisation of a Lightly Stabilised Granular Material by Indirect Diametrical Tensile Testing," *International Journal of Pavement Engineering*, Vol. 9, No. 6, pp. 445 – 456.

Gomes, A. C., and Gillett, S. (1996). *Flexible Pavement: Resilient Behavior of Soils*. Balkema, Rotterdam, ISBN 90 54 10 5232.

Gomez, J. D. P. (2009). "Influence of Curing Time on the Resilient Modulus of Chemically Stabilized Soils," MS Thesis, University of Oklahoma, Norman, OK.

Guthrie, W. S., and Scullion, T. (2003). "Interlaboratory Study of the Tube Suction Test," *Research Report 0-4114-2,* Texas Transportation Institute, College Station, TX.

Guthrie, W. S., and Hermansson, A. (2003). "Frost Heave of Variably Saturated Aggregate Base Materials," *Transportation Research Record: Journal of the Transportation Research Board,* Vol. 1821, pp. 13 – 19.

Guthrie, W. S., and Scullion, T. (2000). "Assessing Aggregate Strength and Frost Susceptibility Characteristics with the Tube Suction Test," *Proceedings of the Texas Section Fall Meeting*, American Society of Civil Engineers, El Paso, TX, pp. 197 – 206.

Guthrie, W. S., P. M. Ellis, and Scullion, T. (2001). "Repeatability and Reliability of the Tube Suction Test," *Transportation Research Record: Journal of the Transportation Research Board*, Vol. 1772, pp. 151 – 157.

Guthrie, W. S., Roper, M. B. and Eggett, D. L. (2008). "Evaluation of Laboratory Durability Tests for Stabilized Aggregate Base Materials," *Transportation Research Board 87th Annual Meeting*, CD-ROM Publication, Transportation Research Board, National Research Council, Washington, DC.

Guthrie, W. S., Sebesta, S., and Scullion, T. (2002). "Selecting Optimum Cement Contents for Stabilizing Aggregate Base Materials," *Report 7-4920-2*, Texas Transportation Institute, College Station, TX.

Harris, P., Holdt, J. V., Sebesta, S., and Scullion, T. (2006). "Recommendations for Stabilization of High-Sulfate Soils in Texas," *Report 0-4240-3*, Texas Transportation Institute, College Station, TX.

Harrris, P., Sebsesta, S., and Scullion, T. (2004). "Hydrated Lime Stabilization of Sulfate-Bearing Vertisols in Texas," *Transportation Research Board 83rd Annual Meeting*, CD-ROM Publication, Transportation Research Board, Washington, DC.

Haston, J.S., and Wohlgemuth, S.K. (1985). "Experiences in the Selection of the Optimum Lime Content for Soil Stabilization." *Texas Civil Engineer*, November 1985, pp.17 – 20.

Haykin, W. L. (1994). *Neural Networks: A Comprehensive Foundation*. Macmillan College Publishing, NY.

Hibbeler, R. C. (2008). *Mechanics of Materials*, Seventh Edition, Prentice Hall, Upper Saddle River, NJ.

Hill, T., and Lewicki, P. (2006). *STATISTICS Methods and Applications*. StatSoft, Tulsa, OK.

Hillbrich, S. L. and Scullion, T. (2010). "Stabilizing Sulfate-Rich Soils Using Traditional Stabilizers and Non-Traditional Construction Methods: A Case Study of State Highway 289 in Grayson County, Texas," *Transportation Research Board 89th Annual Meeting*, CD-ROM Publication, Transportation Research Board, Washington, DC.

Hillbrich, S. L., and Scullion, T. (2006). "A Rapid Alternative for Laboratory Determination of Resilient Modulus Input Values on Stabilized Materials for the AASHTO M-E Design Guide," *Transportation Research Board 86th Annual Meeting*, CD-ROM Publication, Transportation Research Board, Washington, DC.

Hopkins TC, Beckham TL, Sun L, Pfalzer B. (2004). "Kentucky Geotechnical Database," *Publication KTC-03-06/SPR-177-98-1F*, University of Kentucky Transportation Center, College of Engineering, Lexington, KY.

Hossain, M. S. (2009). "Estimation of Subgrade Resilient Modulus for Virginia Soil," *Transportation Research Board 88th Annual Meeting*, CD-ROM Publication, Transportation Research Board, Washington, DC.

Huang, Y.H. (2004). *Pavement Analysis and Design*, 2nd edition, Prentice Hall, Inc. Englewood Cliffs, NJ.

Hunter, D. (1988). "Lime-induced Heave in Sulfate-bearing Clay Soils," *Journal of Geotechnical Engineering*, Vol.114, No.2, pp.150 – 167.

Intharasombat, N. (2003). "Ettringite Formation in Lime Treated Sulfate Soils: Verification by Mineralogical and Swell Testing," MS Thesis, University of Texas, Arlington, TX

Indian Road Congress (IRC) (2000). "State of the Art: Lime-Soil Stabilization," *Special Report*, IRC Highway Research Board, New Delhi, India.

Jade (1999). *Materials Data Manual*, MDI, Livermore, CA, 94550.

Jones, M. P., and Witczak, M. W. (1977). "Subgrade Modulus on the San Diego Test Road," *Transportation Research Record: Journal of the Transportation Research Board*, Vol. 641, pp. 1 – 6.

Kavak, A., and Akyarh, A. (2007). "A field Application for Lime Stabilization," *Environmental Geology*, Vol. 51, pp. 987 – 997.

Kenai, S., Bahar, R., and Benazzoug, M. (2006). "Experimental Analysis of the Effect of Some Compaction Methods on Mechanical Properties and Durability of Cement Stabilized Soil," *Journal of Materials Science*, Vol. 41, No. 21, pp. 6956 – 6964.

Kennedy, T. W., Moore, R. K., and Anagnos, J. N. (1971). "Estimations of Indirect-Tensile Strengths for Cement-Treated Materials," *Highway Research Record*, Vol. 351, pp. 112 – 114.

Khattak, M., and Alrashidi, M. (2006). "Durability and Mechanistic Characteristics of Fiber Reinforced Soil–cement Mixtures," *International Journal of Pavement Engineering*, Vol. 7, No. 1, pp. 53 – 62.

Khazanovich, L., Celauro, B., Chabourn, B., and Zollars, J. (2006). "Evaluation of Subgrade Resilient Modulus Predictive Model for Use in Mechanistic-Empirical Pavement Design Guide," *Transportation Research Record: Journal of the Transportation Research Board*, Vol. 1947, pp. 155 – 166.

Khoury, N. N. (2005). "Durability of Cementitiously Stabilized Aggregate Bases for Pavement Application," PhD Thesis, University of Oklahoma, Norman, OK.

Khoury, N., and Zaman, M. M. (2007). "Durability of Stabilized Base Courses Subjected to Wet-Dry Cycles," *International Journal of Pavement Engineering*, Vol. 8, No. 4, pp. 265 – 276.

Kim, D., and Stokoe, II K., H. (1992). "Characterization of Resilient Modulus of Compacted Subgrade Soils using Resonant Column and Torsional Shear Tests," *Transportation Research Record: Journal of the Transportation Research Board*, Vol. 1369, pp. 83 – 91.

Kim, D., and Siddiki, N. (2004). "Lime Kiln Dust and Lime – A Comparative Study in Indiana," *Transportation Research Board 83rd Annual Meeting*, CD-ROM Publication, Transportation Research Board, Washington, DC.

Kim, D., Kweon, G., and Lee, K. (1997). "Alternative Method of Determining Resilient Modulus of Compacted Subgrade Soils Using Free-Free Resonant Column Test,"

Transportation Research Record: Journal of the Transportation Research Board, Vol. 1577, pp. 62 – 69.

Kim, S., Ceylan, H., and Heitzman, M. (2005). "Sensitivity Study of Design Input Parameters for Two-Flexible Pavement Systems Using the Mechanistic-Empirical Design Guide," *Proceedings of the 2005 Mid-Continent Transportation Research Symposium*, Ames, IA.

Kota, P. B. V. S., Hazlett, D., and Perrin, L. (1996). "Sulfate-Bearing Soils: Problems with Calcium-based Additives," *Transportation Research Record: Journal of the Transportation Research Board*, Vol. 1546, pp. 62 – 69.

Kuennen, T., (2006). "For Long-Lived Roads, Understand your Soils," *Better Roads*, Vol. 76, No. 6, pp. 22 – 32.

Lacroix, A., Khandan, A. A. M., and Kim, Y. R. (2007). "Predicting the Resilient Modulus of Asphalt Concrete from the Dynamic Modulus," *Transportation Research Record: Journal of the Transportation Research Board*, Vol. 2001, pp. 132– 140.

Laguros, J. G. (1965). "Lime-Stabilized Soil Properties and the Beam Action Hypothesis," *Highway Research Record*, Vol. 92, pp. 12 – 20.

Laguros, J. G. and Keshwarz, M. S. (1987). "Construction and Performance of the Stabilized Base Course on U. S. 77 Ponca City, Kay County," *Report No. FHWA/OK 87(7)*, Oklahoma DOT Item Number 2128, Oklahoma City, OK.

Larsen, T. J., and Nussbaum, P. J. (1967). "Fatigue of Soil Cement," *Bulletin D 119*, Portland Cement Association, Skokie, IL.

Lav, A. H., and Lav, M. A. (2000). "Microstructural Development of Stabilized Fly Ash as Pavement Base Material," *ASCE Journal of Materials in Civil Engineering*, Vol. 12, No. 2, pp. 157 – 163.

Lav, A. H., Lave, M. A., and Goktepe, A. B. (2006). "Analysis and Design of a Stabilized Fly Ash as Pavement Base Material," *Fuel*, Vol. 85, pp. 2359 – 2370.

Lee, W., Bohra, N.C., Altschaeffl, A. G. and White, T. D. (1998). "Resilient Modulus of Cohesive Soils," *ASCE Journal of Geotechnical and Geoenvironmental Engineering*, Vol. 123, No. 2, pp. 131 – 135.

Li, J., Uhlmeyer, J. S., Mahoney, J. P., and Muench, S. T. (2010). "Use of the AASHTO 1993 Guide, MEPDG and Historical Performance to Update the WSDOT Pavement Design Catalog," *Transportation Research Board 89th Annual Meeting*, CD-ROM Publication, Transportation Research Board, Washington, DC.

Li, L., Edil, T. B., and Benson, C. H. (2009). "Properties of Pavement Geomaterials Stabilized with Fly Ash," *Proceedings of 2009 World of Coal Ash Conference*, Lexington, KY.

Li, Q. (2009). "Database Support and Modeling for the Mechanistic Empirical Pavement Design Guide (MEPDG)," PhD Thesis, University of Arkansas, AR.

Ling, J., Xie, H., and Guo, R. (2008). "A Method to Predict Resilient Modulus of Lime and Lime-Cement Stabilized Soils Used in Highway Subgrade," *Transportation Research Board 87th Annual Meeting*, CD-ROM Publication, Transportation Research Board, Washington, DC.

Little, D. L. (1995). *Handbook for Stabilization of Pavement Subgrades and Base Courses with Lime*, Kendall/Hunt Publishing Company, IA.

Little, D. N. (2000). "Evaluation of Structural Properties of Lime Stabilized Soils and Aggregates," *Mixture Design and Testing Protocol for Lime Stabilized Soils*, Vol. 3, National Lime Association report, http://www.lime.org/SOIL3.PDF, Last Accessed: Jan., 2007.

Little, D. N. and Nair, S. (2009). "Recommended Practice for Stabilization of Subgrade Soils and Base Materials," *NCHRP Web-Only Document 144*, Contractor's Final Task Report for NCHRP Project 20-07, Transportation Research Board, National Research Council, Washington, DC.

Little, D. N., and Petry, T. M. (1992). "Recent Developments in Sulfate-Induced Heave in Treated Expansive Clays," *Proceedings of 2nd Interagency Symposium on Stabilization of Soils and Other Materials*, LA.

Little, D. N., Males, E. H., Prusinski, J. R., and Stewart, B. (2000). "Cementitious Stabilization," *79th Millenium Rep. Series*, Transportation Research Board, Washington, DC.

Little, D. N., Nair, S., and Herbert, B. (2010). "Addressing Sulfate-Induced Heave in Lime Treated Soils," *ASCE Journal of Geotechnical and Geoenvironmental Engineering*, Vol. 136, No. 1, pp. 110 – 118

Locat, J., Tremblay, H., and Leroueil, S. (1996). "Mechanical and Hydraulic Behavior of a Soft Inorganic Clay Treated with Lime," *Canadian Geotechnical Journal*, Vol. 33, pp. 654 – 669.

Loulizi, A., Al-Qadi, I. L., and Elseifi, M., (2006). "Difference between In Situ Flexible Pavement Measured and Calculated Stresses and Strains," *ASCE Journal of Transportation Engineering*, Vol. 132, No. 7, pp. 574 – 579.

Loulizi, A., Flintsch, G. W., Al-Qadi, I. L., and Mokarem, D. (2006). "Comparing Resilient Modulus and Dynamic Modulus of Hot-Mix Asphalt as Material Properties for Flexible Pavement Design," *Transportation Research Record: Journal of the Transportation Research Board*, Vol. 1970, pp. 161 – 170.

Luo, R., and Prozzi, J. A. (2008). "Benefit of Lime Treatment for Controlling Longitudinal Pavement Cracking Due to Expansive Subgrade," *Transportation*

Research Board 87th Annual Meeting, CD-ROM Publication, Transportation Research Board, Washington, DC.

Malla, R. B., Joshi, S. (2008). "Subgrade Resilient Modulus Prediction Models for Coarse and Fine-grained Soils based on Long-term Pavement Performance Data," *International Journal of Pavement Engineering*, Vol. 9, No. 6, pp. 431 – 444

Mallela, J., Quintus, H. V., and Smith, K. L. (2004). "Consideration of Lime-Stabilized Layers in Mechanistic-Empirical Pavement Design," F*inal Report submitted to the National Lime Association*, Arlington, VA.

Mallick, R. B., and El-Korchi, T. (2008). *Pavement Engineering*, CRC Press, NY.

May, R. W., and Witczak, M. W. (1981). "Effective Granular Modulus to Model Pavement Response," *Transportation Research Record: Journal of the Transportation Research Board*, Vol. 810, pp. 1 – 9.

McCallister, L. D. and Petry, T. M. (1991). "Physical Properties Changes in a Lime-Treated Expansive Clay Caused by Leaching," *Transportation Research Record: Journal of the Transportation Research Board*, Vol. 1295, pp. 37 – 44.

McCallister, L. D. and Petry, T. M. (1992). "Leach Tests on Lime-Treated Clay," *ASTM Geotechnical Testing Journal*, Vol. 15, No. 2, pp. 106 – 114.

McCallister, L. D. and Petry, T. M. (1990). "Property Changes in Lime-Treated Expansive Clay under Continuous Leaching," *Report No. GL-90-17*, Final Report to Department of Army, U S Army Corps of Engineers, Washington, DC.

McCoy, W. J., and Kriner, R. W. (1971). "Use of Waste Kiln Dust for Soil Consolidation," Lehigh Portland Cement Co., Allentown, PA.

McManis, K. L., and Arman, A. (1989). "Class C Fly Ash as a Full or Partial Replacement for Portland Cement or Lime," *Transportation Research Record: Journal of the Transportation Research Board*, Vol. 1219, pp. 68 – 61.

Mehrotra, K., Mohan, C. K., Ranka, S. (1996). *Elements of Artificial Neural Networks*. MIT Press, Cambridge, MA.

Meier R. W., Alexander, D., and Freeman, R. B. (1996). "Using Artificial Neural Networks as a Forward Approach to Backcalculation," *Transportation Research Record: Journal of the Transportation Research Board*, Vol. 1570, pp. 126 – 133.

Miller, G. A. and Zaman, M. (2000). "Field and Laboratory Evaluation of Cement Kiln Dust as a Soil Stabilizer," *Transportation Research Record: Journal of the Transportation Research Board*, Vol. 1714, pp. 25 – 32.

Miller, G. A., Zaman, M. M., Rahman, J., and Tan, N. K. (2003). "Laboratory and Field Evaluation of Soil Stabilization Using Cement Kiln Dust," *Final Report Item No. 2144*, Oklahoma Department of Transportation, Oklahoma City, OK.

Miller, G.A. and Azad, S. (2000). "Influence of Soil Type on Stabilization with Cement Kiln Dust." *Construction and Building Materials*, Vol. 14, pp. 89 – 97.

Miller, G.A. and Zaman, M. (2000). "Field and Laboratory Evaluation of Cement Kiln Dust as a Soil Stabilizer," *Transportation Research Record: Journal of the Transportation Research Board*, Vol. 1714, pp. 25 – 32.

Miner, M. A. (1959). "Estimation of Fatigue Life with Particular Emphasis on Cumulative Damage." *Metal Fatigue*, Edited by Sines and Waisman, McGraw Hill, pp. 278-89.

Mir, B.A. (2004). "Effect of Fly Ash on Geotechnical Properties of Soils," *Proceedings of National Symposium on Advances in Geotechnical Engineering*, Indian Institute of Science, Bangalore, India.

Misra, A. (1998). "Stabilization Characteristics of Clays Using Class C Fly Ash," *Transportation Research Record: Journal of the Transportation Research Board*, Vol. 1611, pp. 46 – 54.

Mitchell, J. K. (1986). "Practical Problems from Surprising Soil Behavior," *Journal of Geotechnical Engineering*, Vol. 112, No. 3, pp. 255 – 289

Mitchell, J. K., and Dermatas, D. (1990). "Clay Soil Heave Caused by Lime-Sulfate Reactions," *ASTM Special Technical Publication*, Vol. 1135, pp. 41 – 64.

Mitchell, J. K., and Dermatas, D. (1992). "Clay Soil Heave Caused by Lime-Sulfate Reactions," *ASTM STP 1135: Innovations and Uses for Lime*, Philadelphia, PA.

Mitchell, J.K. (1993). *Fundamentals of Soil Behavior*. 2nd Edition. John Wiley & Sons, NY.

Mohammad, L. N., Huang, B., Puppala, A. J. and Allen, A. (1999). "Regression Model for Resilient Modulus of Subgrade Soils," *Transportation Research Record: Journal of the Transportation Research Board*, Vol. 1687, pp. 47 – 54.

Mohammad, L. N., Nazzal, M. D., Abu-Farsakh, M. Y. and Alshibli, K. (2009). "Estimation of Subgrade Soils Resilient Modulus from In-situ Devices Test Results," *ASTM Journal of Testing and Evaluation*, Vol. 37, No. 3, pp. 1 – 9.

Mohammad, L.N., Raghavandra, A. and Huang, B. (2000), "Laboratory Performance of Cement-stabilized Soil Base Mixtures", *Transportation Research Record: Journal of the Transportation Research Board*, Vol. 1721, pp. 19 – 28.

Molenaar, A. A. A., and Pu, B. (2008). "Prediction of Fatigue Cracking in Cement Treated Base Courses," *Proceedings of 6th RILEM International Conference on Cracking in Pavements*, Chicago, IL, pp. 191 – 199.

Montgomery, D. C., Peck, E. A., and Vining, G. G. (2006). *Introduction to Linear Regression Analyses*. Wiley Series in Probability and Statistics, John Wiley and Sons, Inc, NJ.

Moon, D. H., Grubb, D. G., and Reilly, T. L. (2009). "Stabilization/Solidification of Selenium-Impacted Soils Using Portland Cement and Cement Kiln Dust," *Journal of Hazardous Materials*, Vol. 168, pp. 944 – 951.

Moon, H. M., Dermatas, D., Wazne, M., Sanchez, A. M., Chrysochoou, M., and Grubb, D. G. (2007), "Swelling Related to Ettringite Crystal Formation in Chromite Ore Processing Residue," *Environmental Geochem. Healts*, Vol. 29, No. 4, pp. 289 – 294.

Mooney, M. A. and Toohey, N. M. (2010). "Accelerated Curing and Strength-Modulus Correlation for Lime-Stabilized Soils," *Final Repot No. CDOT-2010-1*, Colorado Department of Transportation, Denver, CO.

Moossazadeh, J. M., and Witczak, M. W. (1981). "Prediction of Subgrade Moduli for Soil that exhibits Nonlinear Behavior," *Transportation Research Record: Journal of the Transportation Research Board*, Vol. 810, pp. 9 – 17.

Mulandi, J., Khanum, T., Hossain, M., and Schieber, G. (2006). "Comparison of Pavement Design Using AASHTO 1993 and NCHRP Mechanistic-Empirical Pavement Design Guides," *Proceedings of Airfield and Highway Pavements: Meeting Today's Challenges with Emerging Technologies*, pp. 912 – 923.

Myers, R. H., Montgomery, D. C., and Vining, G. G. (2001). *Generalized Linear Models: With Applications in Engineering and the Sciences*, John Wiley and Sons, Inc, NJ.

Nagaraj, T. S. (1964). "Discussion on "Soil-lime Research at Iowa State University," *ASCE Journal of the Soil Mechanics and Foundations Division*, Vol. 90, No. 6, pp. 225 – 226.

Najjar, Y. M., Basheer, I. A., Ali H. E., and McReynolds, R. L. (2000). "Swelling Potential of Kansas Soils: Modeling and Validation Using Artificial Neural Network Reliability Approach," *Transportation Research Record: Journal of the Transportation Research Board*, Vol. 1736, pp. 141 – 147.

Nalbantoglu, Z. (2004). "Effectiveness of Class C Fly Ash as an Expansive Soil Stabilizer," *Construction and Building Materials*, Vol. 18, pp. 377 – 381.

Nalbantoglu, Z. (2006). "Lime Stabilization of Expansive Clay," *Expansive Soils*, Part 7, Vol. 1, pp. 341 – 348.

Nalbantoglu, Z. and Tuncer, E. R. (2001). "Compressibility and Hydraulic Conductivity of a Chemically Treated Expansive Clay," *Canadian Geotechnical Journal*, Vol. 38, pp. 154 – 160.

Narayan, S. (2002). "Using Genetic Algorithms to Adapt Neuron Functional Forms," *Proceedings Artificial Intelligence and Soft Computing*, Banff, Canada.

National Cooperative Highway Research Report (NCHRP) (1976). "Lime-Fly Ash-Stabilized Bases and Subbases," Transportation Research Board, National Council, Washington, DC.

NCHRP (1997). "Laboratory Determination of Resilient Modulus for Flexible Pavement Design," *NCHRP Web Document 14 for Project 1-28*, Transportation Research Board, Washington, DC.

Navratnarajah, S. K. (2006). "Performance Characteristics of Selected Asphalt Mixes: A Laboratory and Field Study," MS Thesis, University of Oklahoma, Norman, OK.

NCHRP (2003). "Procedure for Resilient Modulus of Unstabilized Aggregate Base and Subgrade Materials," *Project 1-28A*, Transportation Research Board, Washington DC.

Nevels, J. B., and Laguros, J. G. (2005). "Discussion of "Studies of Sulfate-Resistant Cement Stabilization Methods to Address Sulfate-Induced Soil Heave," by Anand J. Puppala, Julie Ann Griffin, Laureano R. Hoyos, and Suppakit Chomtid, *ASCE Journal of Geotechnical and Geoenvironmental Engineering*, Vol. 131, No. 11, pp. 1439 – 1440.

Oklahoma Department of Transportation (ODOT) (2006). OHD L-50, Soil Stabilization Mix Design Procedure, Material and Testing e-Guide, *Department Test Methods (OHDL)*, http://www.okladot.state.ok.us/materials/ohdllst.htm, Last Accessed: July, 2006.

Oklahoma Department of Transportation (ODOT) (2007). "Conditions and Performance of Pavements on the National Highway System in Oklahoma," *Final Report prepared by Oklahoma Department of Transportation*, Pavement Management Branch, Oklahoma City, OK.

Ooi, P. S., Archilla, R. and Sandefur, K. G. (2004). "Resilient Modulus Model for Compacted Cohesive Soils," *Transportation Research Record: Journal of the Transportation Research Board*, Vol. 1874, pp. 115 – 124.

Osinubi, K. J., Soni, E. J., and Ijimdiya, T. S. (2010). "Lime and Slag Admixture Improvement of Tropical Black Clay Road Foundation," *Transportation Research Board 89th Annual Meeting*, CD-ROM Publication, Transportation Research Board, Washington, DC.

Osinubi, K. J., and Nwaiwu, C. M. O. (2006). "Compaction Delay Effects on Properties of Lime-Treated Soil," *ASCE Journal of Materials in Civil Engineering*, Vol. 19, No.2, pp. 250 – 258.

Papagiannakis, A. T., and Masad, E. A. (2007). *Pavement Design and Materials*, John Wiley and Sons, Inc., NJ.

Parker, J. W. (2008). "Evaluation of Laboratory Durability Tests for Stabilized Subgrade Soils," MS Thesis, Brigham Young University, Provo, UT.

Parsons, R. L., and Milburn, J. P. (2003). "Engineering Behavior of Stabilized Soils," *Transportation Research Record: Journal of the Transportation Research Board*, Vol. 1837, pp. 20 – 29.

Parsons, R.L. and E. Kneebone. (2004). "Use of Cement Kiln Dust for the Stabilization of Soils," *Proceedings of Geo-Trans 2004*, Los Angeles, California, No. 1, pp. 1124 – 1131.

Parsons, R.L., Kneebone, E. and Milburn, J.P. (2004). "Use of Cement Kiln Dust for Subgrade Stabilization." *Final Report No. KS-04-03*, Kansas Department of Transportation, Topeka, KS.

Paute, J. L., and Hornych, P. (1996). *Flexible Pavement: Influence of Water Content on the Cyclic Behavior of a Silty Sand*, Balkema, Rotterdam, ISBN 90 54 10 5232.

Peethamparan, S. and Olek, J. (2008). "Study of the Effectiveness of Cement Kiln Dusts in Stabilizing Na-montmorillonite Clays," *ASCE Journal of Materials in Civil Engineering*,Vol. 20 No.2, pp.137 – 146.

Peethamparan, S., Olek, J. and Diamond, S. (2008). "Physicochemical Behavior of Cement Kiln Dust-Treated Kaolinite Clay," *Transportation Research Record: Journal of the Transportation Research Board*, Vol. 2059, pp. 80 – 88.

Peethamparan, S., Olek, J., and Diamond, S. (2009). "Mechanism of Stabilization of Na-montmorillonite Clay with Cement Kiln Dust," *Cement and Concrete Research*, Vol. 39, pp. 580 – 589.

Petry, T. and Wohlgemuth, S. K. (1988). "The Effects of Pulverization on the Strength and Durability of Highly Active Clay Soil Stabilized with Lime and Portland Cement," *Transportation Research Record: Journal of the Transportation Research Board*, Vol. 1190, pp. 38 – 45.

Petry, T. M. (1995). "Studies of Factors Causing and Influencing Localized Heave of Lime Treated Clay Soils (Sulfate Induced Heave)," *Final Report to U. S. Army Engineers Waterways Experiment Station*, Vicksburg, MS.

Petry, T. M., and Little, D. N. (1992). "Update on Sulfate Induced Heave in Treated Clays: Problematic Sulfate Levels," *Transportation Research Record: Journal of the Transportation Research Board*, Vol. 1362, pp. 51 – 55.

Petry, T. M., and Sobhan, K. (2005). "Evaluation of Chemical Stabilizers," *Transportation Research Circular E- C086*, Transportation Research Board, National Research Council, Washington, D.C., http://onlinepubs.trb.org/onlinepubs/circulars/ec086.pdf, Last Accessed: Sep., 2008.

Phanikumar, B. R., and Sharma, R. S. (2004). "Effect of Fly Ash on Engineering Properties of Expansive Soils," *ASCE Journal of Geotechnical and Geoenvironmental Engineering*, Vol. 130, No. 7, pp. 764 – 767.

Ping, W. V., Y. Zenghai, Chunshui, L., and Bruce, D. (2001). "Measuring Resilient Modulus of Granular Materials in Flexible Pavements," *Transportation Research Record: Journal of the Transportation Research Board*, Vol. 1778, pp. 81 – 90.

Portland Cement Association. (PCA). (1992). *Soil-Cement Laboratory Handbook*. EB052, Skokie, IL, 1992

Prabakar, J., Dndorkar, N. and Morchhale, R. K. (2004). "Influence of Fly Ash on Strength Behavior of Typical Soils," *Construction and Building Materials*, Vol. 18, pp. 263 – 267.

Priest, A. L., and D. H. Timm. (2006). "Methodology and Calibration of Fatigue Transfer Functions for Mechanistic-Empirical Flexible Pavement Design," *Publication NCAT Report 06-03*, National Center for Asphalt Technology, Auburn University, AL.

Prozzi, J., and Aguiar-Moya, J. (2010). "Design, Response, and Performance of Cement-Treated Materials," *Transportation Research Board 89th Annual Meeting*, CD-ROM Publication, National Research Council, Washington, DC.

Prusinski, J. R., and Bhattacharia, S. (1999). "Effectiveness of Portland cement and lime in stabilizing clay soils," *Transportation Research Record: Journal of the Transportation Research Board*, Vol. 1632, pp. 215 – 227.

Puppala, A. J., E. Wattanasanticharoen, and A. Porbaha. (2006). "Expansive soils: Recent advances in characterization and treatment, A. Combined lime and polypropylene fiber stabilization for modification of expansive soils," Chapter 24, Taylor and Francis, NY.

Puppala, A. J., Griffin, J. A., Hoyos, L. R. and Chomtid, S. (2004). "Studies of Sulfate-Resistant Cement Stabilization Methods to Address Sulfate-Induced Soil Heave," *ASCE Journal of Geotechnical and GeoEnvironmental Engineering*, Vol.130, No.4, pp.391 – 402.

Puppala, A. J., Intharasombat, N., and Vempati, R. K. (2005). "Experimental Studies on Ettringite-Induced Heaving in Soils," *ASCE Journal of Geotechnical and Geoenvironmental Engineering*, Vol. 131, No. 3, pp. 325 – 337.

Puppala, A. J., Mohammad and Allen, A., (1996). "Engineering Behavior of Lime-Treated Louisiana Subgrade Soil," *Transportation Research Record: Journal of the Transportation Research Board*, Vol. 1548, pp. 24 – 31.

Puppala, A. J., Suppakit, C., Viyanant, C., and Perrin, L. (2001). "Sulfate heaving problems in stabilized soils: observations from a few case studies," *2nd International Conference on Engineering Materials*, San Jose, California, pp. 16–19.

Puppala, A. J., Viyanant, C., Kruzic, A., and Perrin, L. (2002). "Evaluation of a modified sulfate determination method for cohesive soils," *Geotechnical Testing Journal*, Vol. 25, No. 1, pp. 85 – 94.

Puppala, A. J., Wattanasanticharoen, E., Intharasombat, N., and Hoyos, L. R. (2003). "Studies to Understand Soil Compositional and Environmental Variables on Sulfate Heave Problems," *Proceedings of Soil Rock America: 12th Pan American Conference on Soil Mechanics and Geotechnical Engineering*, Boston, MA.

Qubain, B. S., Seksinsky, E. J., and Li, J. (2000). "Incorporating Subgrade Lime Stabilization into Pavement Design," *Transportation Research Record: Journal of the Transportation Research Board*, Vol. 1721, pp. 3 – 8.

Raad L., Minassian, G. H., Gartin S. (1992). "Characterization of Saturated Granular Bases Under Repeated Loads," *Transportation Research Record: Journal of the Transportation Research Board*, Vol. 1369, pp. 73 – 82.

Raad, L. (1976). "Design Criteria for Soil-Cement Bases," PhD Dissertation, Department of Civil Engineering, University of California, Berkeley, CA.

Raad, L. (1985). "Behavior of Stabilized Layers Under Repeated Loads," *Transportation Research Record: Journal of the Transportation Research Board*, Vol. 1022, pp. 72 – 79.

Rada C., Witczak W. M. (1981). "Comprehensive Evaluation of Laboratory Resilient Moduli Results for Granular Material," *Transportation Research Record: Journal of the Transportation Research Board*, Vol. 810, pp. 23 – 33.

Rahim, A. M., and George, K. P. (2004). "Subgrade Soil Index Properties to Estimate Resilient Modulus," *Transportation Research Board 83rd Annual Meeting*, CD-ROM Publication, Transportation Research Board, Washington, DC.

Rajendran, D., and Lytton, R. L. (1997). "Reduction of Sulfate Swell in Expansive clay Subgrades in the Dallas district," *Texas Transportation Institute Report No. TX-98/3929-1*, Bryan, TX

Ramakrishna, A. M. (2002). "Evaluation of Resilient Moduli Characteristics of Chemically Treated Soil from North Texas," MS Thesis, University of Texas, Arlington, TX.

Rankine, R. M., and Sivakugan, N. (2005). "Prediction of Paste Backfill Performance Using Artificial Neural Networks," *Proceedings of the 16th ISSMGE*, Vol. 2, Osaka, Canada.

Rao, S. M., and Shivananda, P. (2005). "Impact of Sulfate Contamination on Swelling Behavior of Lime-Stabilized Clays," *Journal of ASTM International*, Vol. 2, No. 6, pp. 1-10

Ripley, B. D. (1996). *Pattern Recognition and Neural Networks*, Cambridge University Press, Cambridge, UK.

Rollings, R. S., Burkes, J. P., and Rollings, M. P. (1999). "Sulfate Attack on Cement-stabilized Sand," *ASCE Journal of Geotechnical and Geoenvironmental Engineering*, Vol. 125, No. 5, pp. 364–372.

Roy, A., Wang, L., Seals, R. K., and Metacalf, J. B. (2003). "Stabilization Techniques for Reactive Aggregate in Soil-Cement Base Course," *Final Report submitted to Louisiana Transportation Research Center*, FHWA/LA.03/366, Baton Rouge, LA.

Rumelhart, D. E., and McClelland, J. (1986). *Parallel Distributed Processing*. Vol. 1, MIT Press, Cambridge, MA.

Saaed, A., Hall, J. W. Jr., and Barker, W. (2003). "Performance-Related Tests of Aggregates for Use in Unbound Layers," *NCHRP Report No. 453*, Transportation Research Board, National Research Council, Washington, DC.

Saarenketo, T. (2006). "Electrical Properties of Road Materials and Subgrade Soils and the Use of Ground Penetrating Radar in Traffic Infrastructure Surveys," PhD Thesis, University of Oulu, Finland.

Saarenketo, T., and Scullion, T. (1996). "Using Electrical Properties to Classify the Strength Properties of Base Course Aggregates," *Research Report 1341-2*. Texas Transportation Institute, Texas A&M University System, College Station, TX.

Saarenketo, T., Kolisoja, P., Vuorimies, N., and Ylitapio, S. (2001). "Suction and Deformation Properties of Base Course Aggregates," *Final Report 10/2001*, Finnish National Road Administration, Helsinki, Finland.

Saarenketo, T., Scullion, T., and Kolisoja, P. (1998). "Moisture Susceptibility and Electrical Properties of Base Course Aggregates," *Proceedings of the Fifth International Conference on the Bearing Capacity of Roads and Airfields*, Trondheim, Norway, Vol. 1998, pp. 1401 – 1410.

Saxena, P., Tompkins, D., Khazanovich, L., and Balbo, J. (2010). "Evaluation of Characterization and Performance Modeling of Cementitiously Stabilized Layers in the MEPDG," *Transportation Research Board 89th Annual Meeting*, CD-ROM Publication, Transportation Research Board, Washington, DC.

Sayah, A. I. (1993). "Stabilization of a Highly Expansive Clay Using Cement Kiln Dust," MS Thesis, University of Oklahoma, Norman, OK.

Schwartz, C. W., and Carvalho, R. L. (2007). "Implementation of the NCHRP 1-37A Design Guide," Volume2: Implementation of Mechanistic-Empirical Design Procedure, *Final Report UMD FRS No. 430572*, University of Maryland, College Park, MD.

Scullion, T. (2002). "Field Investigation: Pre-Cracking of Soil-Cement Bases to Reduce Reflection Cracking," *Transportation Research Board 81st Annual Meeting*, CD-ROM Publication, Transportation Research Board, Washington, DC.

Scullion, T., and Saarenketo, T. (1997). "Using Suction and Dielectric Measurements as Performance Indicators for Aggregate Base Materials," *Transportation Research Record: Journal of the Transportation Research Board*, Vol. 1577, pp. 37 – 44.

Sear, L.K.A. (2001). *Properties and Use of Coal Fly Ash – A Valuable Industrial By-Product*, Thomas Telford, Reston, VA.

Seed, H. B., Mitry, F. G., Monosmith C. L., and Chan, C. K. (1967). "Prediction of Pavement Deflection from Laboratory Repeated Load Tests," *NCHRP Report 35*, Transportation Research Board, Washington, DC.

Senol, A., Bin-Shafique, Md. S., Edil, T. B. and Benson, C. H. (2002). "Use of Class C Fly Ash for Stabilization of Soft Subgrade," *Proceedings of 5th International Congress on Advances in Civil Engineering*, Istanbul Technical University, Turkey.

Sezer, A., Inan, G., Yilmaz, R. and Ramyar, K. (2006). "Utilization of a Very High Lime Fly Ash for Improvement of Lzmir Clay," *Building and Environment*, Vol. 41, No. 2, pp. 150 – 155.

Shahin M. A., Jaksa, M. B., and Maier, H. R. (2001). "Artificial Neural Network Applications in Geotechnical Engineering." *Australian Geomechanics*, Vol. 36, No. 1, pp. 49 – 62.

Shahin, M. A., Maier, H. R., and Jaksa, M. B. (2004). "Data Division for Developing Neural Networks Applied to Geotechnical Engineering," *Journal of Computing in Civil Engineering*, Vol. 18, No. 2, pp. 105 – 114.

Sharma S., and Das, A. (2008). "Backcalculation of Pavement Layer Moduli from Falling Weight Deflectometer Data Using an Artificial Neural Network," *Canadian Journal of Civil Engineering*, Vol. 35, No. 1, pp. 57 – 66.

Sherwood, P. T. (1958). "Effect of Sulfates on Cement-Stabilized Clay," *Highway Research Board Bulletin*, Vol. 193, pp. 45 – 54.

Sherwood, P. T. (1962). "Effect of Sulfates on Cement and Lime-Stabilized Soils," *Highway Research Board Bulletin*, Vol. 353, pp. 98-107.

Shihata, S. A., and Baghdadi, Z. A. (2001). "Simplified Method to Assess Freeze-Thaw Durability of Soil Cement," *ASCE Journal of Materials in Civil Engineering*, Vol. 13, No. 4, pp. 243 – 247.

Si, Z., and Herrera, C. H. (2007). "Laboratory and Field Evaluation of Base Stabilization using Cement Kiln Dust," *Transportation Research Record: Journal of the Transportation Research Board*, Vol. 1989, pp. 42 – 49.

Skapura, D. M. (1996). *Building Neural Networks*. ACM Press, NY.

Sobhan, K. (1997). "Stabilized Fiber-Reinforced Pavement Base Course With Recycled Aggregates," PhD Thesis, Northwestern University, Evanston, IL.

Sobhan, K., and Das, B. M. (2007). "Durability of Soil-Cements against Fatigue Fracture," *ASCE Journal of Materials in Civil Engineering*, Vol. 19, No. 1, pp. 26 – 32.

Sobhan, K., and Mashnad, M., (2003a). "Fatigue Behavior of a Pavement Foundation with Recycled Aggregate and Waste HDPE Strips," *ASCE Journal of Geotechnical and Geoenvironmental Engineering*, Vol. 129, No. 7, pp. 630 – 638.

Sobhan, K., and Mashnad, M., (2003b). "Mechanical Stabilization of Cemented Soil-Fly Ash Mixtures with Recycled Plastic Strips," *ASCE Journal of Environmental Engineering*, Vol. 129, No. 10, pp. 943 – 947.

Solanki, P., and Zaman, M. M. (2010). "Laboratory Performance Evaluation of Subgrade Soils Stabilized with Sulfate-Bearing Cementitious Additives," *ASTM Journal of Testing and Evaluation*, Vol. 38, No. 1, pp. 1 – 12.

Solanki, P., and Zaman, M. M. (2010). "Effects of Lime and Cement Kiln Dust on the Performance of Lean Clays," *International Journal of Geotechnical Engineering*, Vol. 3, No. 4, pp. 455 – 465.

Solanki, P., Ebrahimi, A., and Zaman, M. M. (2008). "Statistical Models for Determination of the Resilient Modulus of Subgrade Soils," *International Journal of Pavement Research and Technology*, Vol. 1, No. 3, pp. 85 – 93.

Solanki, P., Khoury, N., and Zaman, M. M. (2009a). "A Comparative Evaluation of Various Additives Used in the Stabilization of Sulfate Bearing Soil," *Journal of ASTM International*, Vol. 6, No. 8, pp. 50 – 67.

Solanki, P., Khoury, N., and Zaman, M. M. (2009b). "Engineering Properties and Moisture Susceptibility of Silty Clay Stabilized with Lime, Class C Fly Ash and Cement Kiln Dust," *ASCE Journal of Materials in Civil Engineering*, Vol. 21, No. 12, pp. 749 – 757.

Solanki, P., Zaman, M., and Dean, J. (2010). "Resilient Modulus of Clay Subgrades Stabilized with Lime, Class C Fly Ash and Cement Kiln Dust for Pavement Design," *Transportation Research Record: Journal of the Transportation Research Board* (in press).

Solanki, P., Zaman, M., Muraleetharan, K. K., and Timm, D. (2009c). "Evaluation of Resilient Moduli of Pavement Layers at an Instrumented Section on I-35 in Oklahoma," *Road Materials and Pavement Design*, Vol. 10, Special Issue (ICAM), pp. 167 – 188.

Sreekrishnavilasam, A., Rahardja, S., Kmetz, R. and Santagata, M. (2007). "Soil Treatment Using Fresh and Landfilled Cement Kiln Dust," *Construction and Building Materials*, Vol. 21, pp. 318 – 327.

StatSoft Inc. (2006). *Electronic Statistics Textbook*. Tulsa, OK.

Strategic Highway Research Program (SHRP). (1989). "Resilient Modulus of Unbound Granular Base/Subbase Materials and Subgrade Soils," *Report SHRP Protocol P-46*, UG07, SS07, Washington, DC.

Syed, I., Scullion, T. and Harris, J. P. (1999). "Durability of Recycled and Stabilized Pavement Materials," *Geotechnical Special Publication*, Vol. 89, pp. 25 – 36.

Syed, I., Scullion, T. and Smith, R. E. (2003). "Recent Developments in Characterizing Durability of Stabilized Materials." *Transportation Research Board 82nd Annual Meeting*, CD-ROM Publication, Transportation Research Board, Washington, DC.

Syed, I., Scullion, T., and Randolph, R. B. (2000). "Tube Suction Test for Evaluating Aggregate Base Materials in Frost- and Moisture – Susceptible Environments," *Transportation Research Record: Journal of the Transportation Research Board*, Vol. 1709, pp. 78 – 90.

Tarefder R. A., White L., and Zaman, M. (2005). "Neural Network Model for Asphalt Concrete Permeability," *ASCE Journal of Materials in Civil Engineering*, Vol. 17, No. 1, pp. 19 – 27.

Tarefder, R. A. (2005). "Laboratory and Model Prediction of Rutting in Asphalt Concrete," PhD Thesis, University of Oklahoma, Norman, OK.

Thompson, M. R., Robnett, Q. L. (1976). "Resilient Properties of Subgrade Soils," *Final report FHWA-IL-UI-160*, University of Illinois, Urbana, IL.

Thompson, M. R. (1966). "Shear Strength and Elastic Properties of Lime-Soil Mixtures," *Highway Research Record No. 139*, Transportation Research Board, Washington, DC.

Thompson, M. R. (1986). "Mechanistic Design Concepts for Stabilized Base Pavements," Civil Engineering Studies, *Transportation Engineering Series No. 46*, Illinois Cooperative Highway and Transportation Series No. 214, University of Illinois, Urbana, IL.

Thompson, M. R. (1994). "High-Strength Stabilized Base Thickness Design Procedure," *Transportation Research Record: Journal of the Transportation Research Board*, Vol. 1440, pp. 1 – 7.

Transportation Research Board (TRB) (1999). "Use of Artificial Neural Networks in Geomechanical and Pavement Systems," *Transportation research circular number E-C012*, Transportation Research Board, National Research Council, Washington, DC.

Uzan, J. (1985). "Characterization of granular material," *Transportation Research Record: Journal of the Transportation Research Board*, Vol. 1022, pp. 52 – 59.

Verstraeten, J., Veverka, V., and Francken, L. (1982). "Rational and Practical Design of Asphalt Pavements to Avoid Cracking and Rutting," *5th International Conference on Structural Design of AsphaltPavements*, Delft University of Technology, Netherlands.

Von Quintus, H. L. and Killingsworth, B. M. (1997). "Design Pamphlet for the Determination of Design Subgrade in Support of the 1993 AASHTO Guide for the Design of Pavement Structures," *FHWA-RD-97-083*, FHWA, McLean, VA.

Von Quintus, H. L., and Moulthrop, J. S. (2007). "Mechanistic-Empirical Pavement Design Guide Flexible Pavement Performance Prediction Models for Montana," Vol. III, *Calibration and User's Guide for the Mechanistic-Empirical Pavement Design Guide*, Montana Department of Transportation, Helena, MT.

Wang, L. (2002). "Cementitious Stabilization of Soils in the Presence of Sulfate," PhD Thesis, Louisiana State University, Baton Rouge, LA.

White, G. W., and Gnanendran, C. T. (2005). "The Influence of Compaction Method and Density on the Strength and Modulus of Cementitiously Stabilised Pavement Materials," *International Journal of Pavement Engineering*, Vol. 6, No. 2, pp. 97 – 110.

Wild, S. (1996). "Effects of Ground Granulated Blast-furnace Slag on the Strength and Swelling Properties of Lime Stabilized Kaolinite in the Presence of Sulfates," *Clay Minerals*, Vol. 31, pp. 423 – 433.

Wild, S. (1998). "Effects of Partial Substitution of Lime with Ground Granulated Blast Furnace Slag (GGBS) on the Strength Properties of Lime-stabilized Sulfate-bearing Clay Soils," *Engineering Geology*, Vol. 51, pp. 37 – 53.

Williams, R. I. T. (1986). *Cement-Treated Pavements: Materials, Design and Construction*, Elsevier Applied Science Publishers Ltd., London.

Winterkorn, H. F., and Baver, L. D. (1934). "Sorption of Liquids by Soil Colloids, I: Liquid Intake and Swelling by Soil Colloidal Materials," *Soil Science*, Vol. 38, No. 4, pp. 291 – 298.

Xiao, F. (2006). "Development of Fatigue Predictive Models of Rubberized Asphalt Concrete RAC Containing Reclaimed Asphalt Pavement (RAP) Mixtures," PhD Thesis, Clemson University, Clemson, SC.

Yau A., and Von Quintus H. L. (2002). "Study of LTPP Laboratory Resilient Modulus Test Data and Response Characteristics," *Final report FHWA-RD-02-051*, USDOT, FHWA, Washington, DC.

Yeh, I. C. (1998). "Modeling of Strength of HPC Using NN," *Cement and Concrete Research*, Vol. 28, pp. 1797 – 1808.

Yilmaz, I. and Yuksek, A. G. (2007). "An Example of Artificial Neural Network (ANN) Application for Indirect Estimation of Rock Parameters," *Rock Mechanics and Rock Engineering*, Vol. 41, No. 5, pp. 781 – 795.

Yoder, E. J. and Witczak, M. W. (1975). *Principles of Pavement Design*, 2nd Edition, John Wiley & Son, Inc., NY.

Zaman, M. M., Chen, D. H, and Laguros, J. G. (1994). "Resilient Moduli of Granular Materials and Their Correlations with Other Engineering Properties," *ASCE Journal of Transportation Engineering*, Vol. 120, No. 6, pp. 967 – 988.

Zaman, M., Laguros, J. G., and Sayah, A. I. (1992). "Soil Stabilization using Cement Kiln Dust," *Proceeding of the 7th International Conference on Expansive Soils*, Dallas, TX, pp. 1 – 5.

Zaman, M., Laguros, J., Tian, P., Zhu, J, and Pandey, K. (1998). "Resilient Moduli of Raw and Stabilized Aggregate Bases and Evaluations of Layer Coefficients for AASHTO Flexible Pavement Design." *ORA 125-4262*, Item 2199, Department of Transportation, Oklahoma City, OK.

Zaman, M., Solanki, P., Ebrahimi, A., and White, L. (2010). "Neural Network Modeling of Resilient Modulus Using Routine Subgrade Soil Properties," *ASCE International Journal of Geomechanics*, Vol. 10, No. 1, pp. 1 – 12.

Zhang, Z. and Tao, M. (2006). "Durability of Cement Stabilized Low Plastic Soils," *Transportation Research Board 85th Annual Meeting*, CD-ROM Publication, Transportation Research Board, Washington, DC.

Zhang, Z., and Tao, M. (2008). "Durability of Cement Stabilized Low Plasticity Soils," *ASCE Journal of Geotechnical and Geoenvironmental Engineering*," Vol. 134, No. 2, pp. 203 – 213.

Zheng, J. and Qin, W. (2003). "Performance Characteristics of Soil-Cement from Industry Waste Binder," *ASCE Journal of Materials in Civil Engineering*, Vol. 15, No. 6, pp. 616 – 618.

Zia, N., and Fox, P. J. (2000). "Engineering Properties of Loess-Fly Ash Mixtures for Roadbase Construction," *Transportation Research Record: Journal of the Transportation Research Board*, Vol. 1714, pp. 49 – 56.

Zurada, J. M. (1992). *Introduction to Artificial Neural Systems*, West St. Paul, MN.

DISCLAIMER

Neither the developers of this work nor the University of Oklahoma assume any legal liability or responsibility for the accuracy, completeness, or usefulness of any information, product or process disclosed in this dissertation.

LIST OF SYMBOLS AND ABBREVIATIONS

LIST OF SYMBOLS

η	Constant
γ_d	Dry Density
γ_w	Unit Weight of Water
b	Average Width of Beam
D	Diameter of Cylindrical Specimen
D_g	Distance Between LVDTs measuring Deformation
h	Average Height of Beam
h_{ac}	Thickness of Asphalt Concrete Layer
LL	Liquid Limit
M_E	Modulus of Elasticity
M_r	Resilient Modulus of Raw or Stabilized Soil in Compression
M_{ra}	Resilient Modulus of Asphalt Concrete in Indirect Tension
M_{rf}	Flexural Stiffness
M_{rt}	Resilient Modulus of Raw or Stabilized Soil in Indirect Tension
N_f	Number of Cycles to Fatigue Failure
NM_r	Normal Percent Increase in Resilient Modulus
P	Applied Maximum Load
P_{200}	Percent Passing No. 200 Sieve
P_{325}	Percent Passing No. 325 Sieve
P_a	Atmospheric Pressure
PL	Plastic Limit

Q_i	Constant Bias Term
R^2	Coefficient of Regression
S	Stress Ratio
S_e	Standard Deviation of Errors
S_j	Weighted Sum of the j^{th} Neuron
S_o	Overall Standard Deviation
S_y	Standard Deviation of Sample
T	Temperature
t	Thickness of Cylindrical Specimen
V_a	Percent Air Voids
V_b	Binder Content
W_{ij}	Weight Between the j^{th} Neuron and the i^{th} Neuron in the Preceding Layer
Z_R	Standard Normal Deviate
α	Significance Level
δ	Beam deflection in Neutral Axis
ΔH_T	Total Recoverable Horizontal Deformation
ΔV_T	Total Recoverable Vertical Deformation
ε_f	Tensile Strain at the Bottom of Beam
ε_m	Maximum Tensile Strain at the Bottom of Beam from Flexural Strength Tests
ε_r	Resilient Strain
ε_t	Tensile Strain at the Bottom of Beam
ε_{ta}	Tensile Strain at the Bottom of Asphalt Concrete Layer

θ	Bulk Stress
σ_3	Confining Stress
σ_d	Deviatoric Stress
σ_f	Tensile Stress at the Bottom of Beam
σ_t	Indirect Tensile Strength
τ_{oct}	Octahedral Shear Stress
υ	Poisson's Ratio

LIST OF ABBREVIATIONS

1-D	One-Dimensional
3-D	Three-Dimensional
AADTT	Annual Average Daily Truck Traffic
AASHTO	American Association of State Highway and Transportation Officials
AC	Asphalt Concrete
ACA	Alkali Content of Additive
ACAA	American Coal Ash Association
ANN	Artificial Neural Network
ASCE	American Society for Civil Engineers
ASTM	American Society for Testing of Materials
C-A-S-H	Calcium-Alumino-Silicate-Hydrate
CBR	California Bearing Ratio
CC	Clay Content
CEC	Cationic Exchange Capacity

CFA	Class C Fly Ash
CKD	Cement Kiln Dust
C-S-H	Calcium-Silicate-Hydrate
CSM	Cementitiously Stabilized Material
C-soil	Carnasaw Series Soil
CV	Coefficient of Variation
DI	De-Ionized
DOT	Department of Transportation
DUW	Molding Dry Unit Weight
DV	Dielectric Constant Value
EDS	Energy Dispersive Spectroscopy
EGME	Ethylene Glycol Monoethyl Ether
EICM	Enhanced Integrated Climatic Model
EPA	Environmental Protection Agency
ESAL	Equivalent Single Axle Load
FA	Fly Ash
FHWA	Federal Highway Administration
FL	Free-Lime Content
F-T	Freeze-Thaw
FWD	Falling Weight Deflectometer
HDPE	High Density Polyethylene
IRC	Indian Road Congress
IRI	International Roughness Index

K-soil	Kingfisher Series Soil
LKD	Lime Kiln Dust
LMO	Lime Modification Optimum
LOI	Loss on Ignition
LSO	Lime Stabilization Optimum
LTPP	Long-Term Pavement Performance
LVDT	Linear Variable Differential Transformer
MC	Molding Moisture Content
MDD	Maximum Dry Density
M-E	Mechanistic-Empirical
MEPDG	Mechanistic-Empirical Pavement Design Guide
MLPN	Multi-Layer Perceptrons Network
MOR	Modulus of Rupture
MTS	Material Testing System
NA	Not Applicable
ODOT	Oklahoma Department of Transportation
OHD	Oklahoma Highway Department
OMC	Optimum Moisture Content
PA	Percentage of Additive
PC	Portland Cement
PDG	Pavement Design Guide
PI	Plasticity Index
PSI	Present Serviceability Index

P-soil	Port Series Soil
RBFN	Radial Basis Function Network
RLTT	Repeated Load Triaxial Test
SD	Standard Deviation
SEM	Scanning Electron Microscopy
SHRP	Strategic Highway Research Program
SN	Structural Number
SSA	Specific Surface Area
SSR	Silica Sesquoxide Ratio
TRB	Transportation Research Board
TST	Tube Suction Test
UCS	Unconfined Compressive Strength
USCS	Unified Soil Classification System
V-soil	Vernon Series Soil
W-D	Wet-Dry
XRD	X-Ray Diffraction
XRF	X-Ray Fluorescence